DTU Library

Exploring novel catalytic transformations of bioalcohols and mechanistic studies using Ru-PNP complexes

Ni, Zhenwei

Publication date:
2022

Document Version
Publisher's PDF, also known as Version of record

[Link back to DTU Orbit](#)

Exploring novel catalytic transformations of bioalcohols and mechanistic studies using Ru-PNP complexes

PhD thesis

Author

Zhenwei Ni (倪振威)

Supervisors

Martin Nielsen

Susanne Lis Mossin

Kgs.Lyngby, September 2022

献给：

倪蚕林和孙爱凤

Preface

One of the major concepts of sustainable human development is the harmony between human beings and nature. With the growth of population and the innovation of industrial technology, the old world energy sources led by fossil fuels (heavy pollution and low energy efficiency) are greatly used and therefore deviate from this concept to some extent. It was at this time that the idea of upgrading biomass-related alcohols was gradually transformed into reality under the leadership of the scientific community. The sources of such substances are stable, non-polluting, reliable, cheap, and mostly derived directly from living beings. The upgraded product has a higher energy density and is greener.

Catalysis, as a downstream application of chemistry as a discipline, is closely related to human life and has led to the prosperity of the world economy due to its accelerated reaction course. Homogeneous catalysis, a branch of this field, is capable of performing reactions under more moderate conditions. And as this field develops, more homogeneous catalytic results can be used directly in industrial applications.

In this work, I mostly take advantage of organometallic complexes for exploring novel catalytic transformations of bioalcohols, involving important reactions such as hydrogenation and dehydrogenation. As a hope, more efficient and convenient green reaction pathways can be developed and applied.

This PhD thesis represents my academic output from September 1, 2019 to August 31, 2022. As an abbreviated version of a precious academic journey, the work was instructed by Assoc. Prof. Martin Nielsen and Assoc. Prof. Susanne Lis Mossin at the Department of Chemistry, Technical University of Denmark.

Kgs. Lyngby, September

Zhenwei Ni

v

Acknowledgments

During my three years of study in the fairy tale kingdom of Denmark, I have met many people, some of whom have inspired me to create academically, some of whom have brought me joy in my daily life, and some of whom have given me warmth to protect me from the cold of Scandinavia.

First and foremost, I would like to thank my supervisor Assoc. Prof. Martin Nielsen for taking me to the colorful field of organometallic catalysis. He is a very demanding person in terms of scientific research, very meticulous and rigorous. Martin Nielsen has his own unique style of management, and under his guidance, I have been allowed to expand my knowledge not only at the organometallic chemistry level but also to qualitatively improve my presentation skills, academic writing, and social ability. In the meantime, He often buys equipment to support my analysis, provides useful theoretical courses, and encourages me to participate in international conferences to show my output. I also would like to thank my co-supervisor Assoc. Prof. Susanne Lis Mossin, who inspired me in half-year report meetings and offer glovebox usage.

I am grateful for the financial support from the China Scholarship Council, without whose sponsorship I would not have been able to carry out my PhD research, and who gave me this precious opportunity to explore the boundaries of science.

In terms of research, Senior researcher Rosa Maria Padilla Paz is someone I am very thankful for on this dark path. She introduced me to the theory and basic operations in the field of organometallics, and her continuous help continued until the end of my PhD. She is also the person I interact with most academically besides my supervisor. She would take the initiative to schedule meetings to communicate the progress of my topics. Also, Thanks to Nicklas Garnæs Vagner to translate this abstract into the Danish version.

There is a sincere thanks to my parents. They are not only the backup for my PhD study but also the support for my future work and study. Whenever I have a setback, they would always call to comfort me and encourage me. This trust and affirmation from them is also an indispensable source of energy for my PhD journey.

Abstract

The large-scale development and supply of renewable, clean, and green energy to fulfill the needs of our society is an important task in the context of a green transition. The study of biomass-related alcohols plays an essential role in new energy exploration. In this thesis, three projects on the transformations of bioalcohols by using homogeneous catalyzed processes in presence of pincer PNP complexes, which are both valuable in academia and industry, are discussed.

Of these results, I disclosed an unprecedented reaction pathway for ethanol upgrading that leads to the production of secondary alcohols rather than the typical primary alcohols, employing Ru-PNP complexes as the catalyst under mild reaction conditions. Interestingly, the selectivity of the reaction pathway between secondary and primary alcohols was modulated by simply tuning the bulkiness of peripheral ligand substituents on the ancillary phosphine units. The novelty of the findings will open new horizons in ethanol valorization to deliver innovative catalytic solutions and new technologies under mild conditions.

Continuing my ethanol journey, I studied the effect of solvents with different polarities on the acceptorless dehydrogenative coupling of ethanol, achieving high conversion and yield. Experimental guidelines were given for the selection of such dual-organic phase catalytic systems in acceptorless dehydrogenation.

The last inspiration was gained in the alcohol transfer hydrogenation project that I initially worked on as a collaborator. I applied this idea to glycerol, which possesses three hydroxyl groups and can make more chemical changes, and the transfer hydrogenation or dehydrogenation performed by it has not been much studied in academia, thus leaving me more room for manipulation.

In conclusion, this thesis contributes to enlarging current knowledge about catalytic processes for ethanol and glycerol valorization, explaining relevant parameters for their conversions, and presenting new routes for the optimization of the homogeneous catalytic system.

x

Resumé

Stor-skala udvikling og tilgængelighed af grøn energi til brug i samfundet er en vigtig opgave i konteksten af den grønne omstilling. Forskning i biomasse-relaterede alkoholer spiller en vigtig rolle i opdagelsen af nye metoder til udvinding af energi. I denne afhandling præsenteres tre projekter omhandlende transformationer af bio-alkoholer ved brug af homogent katalyserede processer i tilstedeværelsen af pincer PNP komplekser, hvilke er både værdifulde inden for akademisk forskning og industrielle applikationer.

Fra disse resultater har jeg fundet en ny reaktionsvej for opgradering af ethanol som producerer sekundære alkoholer i stedet for de typiske primære alkoholer, ved brug af Ru-PNP komplekser som katalysatorer under milde reaktionsforhold. Interessant nok så er selektiviteten af reaktionsvejen mellem sekundære og primære alkoholer styret ved at ændre størrelsen af PNP-substituenterne på fosfor enhederne. Disse nye fund ser lovende ud og forventes at hæve værdien af innovative katalytiske løsninger og nye teknologier under milde forhold.

Som fortsættelse på min ethanol rejse studerede jeg effekterne af solvent med forskellige polariteter på acceptorløs dehydrogenativ coupling af ethanol, hvor jeg opnåede høj omdannelse, samt udbytte. Der blev givet eksperimentelle retningslinjer for udvælgelse af sådanne katalytiske systemer med dobbelt-organisk fase i acceptorløs dehydrogenering.

Den afsluttende inspiration var fundet i det initielle transfer hydrogenerings projekt som jeg arbejde på som en kollaboratør. Jeg anvendte denne ide med glycerol, hvilket indeholder tre hydroxylgrupper og kan undergå flere kemiske ændringer, og transfer hydrogeneringen eller dehydrogeneringen udført er ikke velkendt i litteraturen hvilket gav mig flere muligheder for nye opdagelser.

Som konklusion, denne afhandling bidrager til at udvide den nuværende viden omkring katalytiske processer for grøn omdannelse af ethanol og glycerol. Den forklarer de relevante parametre for omdannelserne og præsenterer nye måder at optimere det homogene katalytiske system.

List of publications

1) **Zhenwei Ni**, Rosa Padilla, Lucas dos Santos Mello, and Martin Nielsen, Low-temperature selective ethanol upgrading to primary or secondary alcohols by homogeneous catalysis, *Nat. Commun.*, submitted.

2) **Zhenwei Ni**, Rosa Padilla, and Martin Nielsen, Effect of organic solvents on ethanol dehydrogenation to ethyl acetate with PNP complexes, manuscript in preparation.

3) Rosa Padilla, **Zhenwei Ni**, and Martin Nielsen, Catalytic base-free transfer hydrogenation of biomass derived furanic aldehydes with bioalcohols and PNP pincer complexes, *ChemCatChem*, revision.

Dissemination Activities

Poster presentation

> 4 November 2021: PhD Symposium, DTU Department of Chemistry, Comwell Borupgaard, Snekkersten.

> 28 June 2022: XXXVIII Biennial Meeting, Spanish Royal Society of Chemistry (RSEQ), Granada Convention Center, Granada.

Oral presentation

> 25 March 2022: 26970 course, DTU Department of Chemistry, DTU, Lyngby.

> 25 November 2022: 26970 course, DTU Department of Chemistry, DTU, Lyngby.

Awards

Otto Mønsteds Fond, conference participation abroad: RSEQ in Spain.

Abbreviations

AcOEt = Ethyl acetate

ADC = Acceptorless dehydrogenative coupling

DCM = Dichloromethane

DHMF = 2,5-Di(hydroxymethyl)furan

DMSO = Dimethyl sulfoxide

EtOH = Ethanol

FID = Flame ionization detector

GC = Gas chromatography

HMF = 5-Hydroxymethylfurfural

IR = Infrared spectroscopy

$LiBF_4$ = Lithium tetrafluoroborate

NaOAc = Sodium acetate

NaOEt = Sodium ethoxide

NaOtBu = Sodium *tert*-butoxide

NMR = Nuclear magnetic resonance

MEK = Methyl ethyl ketone

MLC = Metal-ligand cooperation

MON = Motor octane number

MS = Mass spectrometry

MVK = Methyl vinyl ketone

RON = Research octane number

TCD = Thermal conductivity detector

TH = Transfer hydrogenation

THF = Tetrahydrofuran

TMS = Tetramethylsilane

Contents

List of Figures

xxii

xxiii

List of Tables

List of Schemes

xxx

Chapter 1

1 General introduction

This chapter will provide general information about this thesis including the fundamental introduction to organometallic complexes and the corresponding catalysis through them, to mitigate current macro issues such as climate change, energy crisis, energy transition, etc. For the three basic directions of chemistry, namely, synthesis, catalysis, and application, although the author has attempted synthetic work during his PhD career, this thesis will mainly focus on the latter two directions. Hence, the main content will be in order as follows:

1) A very macroscopic view of the current problems faced by the chemical community;

2) Description of biomass as renewable energy and conversion of biomass-related alcohols;

3) A general introduction to pincer complexes and some important concepts;

4) A basic understanding and some typical reactions of organometallic homogeneous catalysis;

5) Practical applications of PNP complexes in transformations of bioalcohols (like ethanol, glycerol).

In the actual narrative, entries 1, 3, and 4 are given in chapters 1.1, 1.3, and 1.4, respectively, and entry 5 is a subset of entry 2, both of which are grouped in chapter 1.2. Chapter 2 is a detailed description of the PNP complex, in other words, a more specific account of one of the complexes that is an important catalyst for the overall work. Chapter 3 is an expansion of entries 2, and 5 and will specifically delve into the experimental part of the chemistry.

1.1 Climate change and energy crisis

An important reason for the survival of human civilization is that humans must be kind to the environment they inhabit, namely the Earth.[1-4] Although the past three industrial revolutions have left a strong mark on the progress of human civilization,[5,6] coal, gas, electronics, nuclear, and the internet gradually were used in people's daily life, just as there are two sides to the coin, it is true that the process of industrialization has to some extent harmed the earth's environment and damaged the ecosphere. Now, the 4th revolution related to renewable energy is on the rise.[7,8]
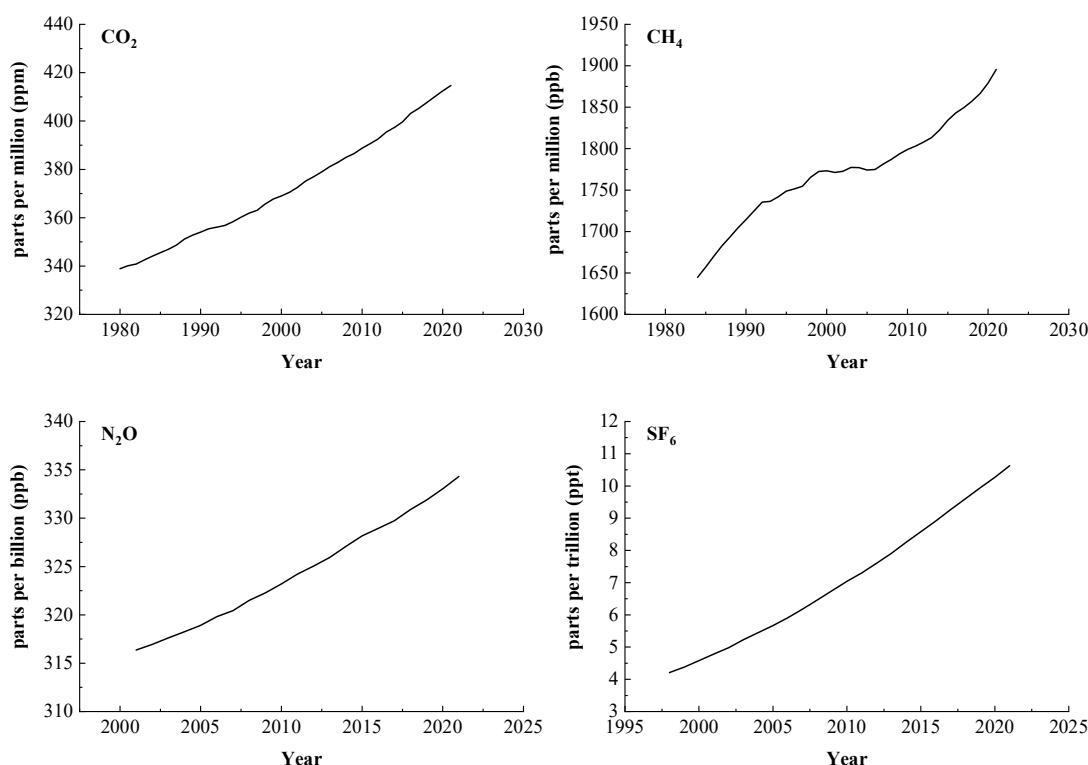
Figure 1.1: Globally-averaged, annual mean atmospheric four greenhouse gases abundance over 40 years.[*]

To visualize how humans have polluted the environment in recent decades, giving data on greenhouse gas emissions is a good way to illustrate the situation. Some research institutes are measuring the pollution in the atmosphere all year round. Figure 1.1 gives the change in the

---

[*] Global Monitoring Laboratory - Carbon Cycle Greenhouse Gases. *Gml.noaa.gov* (2022). at <https://gml.noaa.gov/ccgg/trends/>

abundance of four greenhouse gases, carbon dioxide, methane, nitrous oxide, and sulfur hexafluoride, over the last 40 years determined from marine surface sites. All of them become more concentrated over time.

Because of this increasing abundance of greenhouse gases in the atmosphere, the global mean temperature will likely go up by 2 °C over these decades, which for sure will cause many disasters, such as sea-level rise, melting glaciers, reduced biodiversity, and an increased number of extreme weather events.[9–11]

In addition to the grand proposition of climate change, which is often talked about, how to deal with the energy crisis is also a question that many scientists, politicians, and economists are thinking or have thought about.[12] The emergence of the energy crisis is also closely related to the process of human industrialization. Despite the development driven by technology, however, current and even foreseeable future, human civilization still needs to consume fossil fuels to drive.[13]
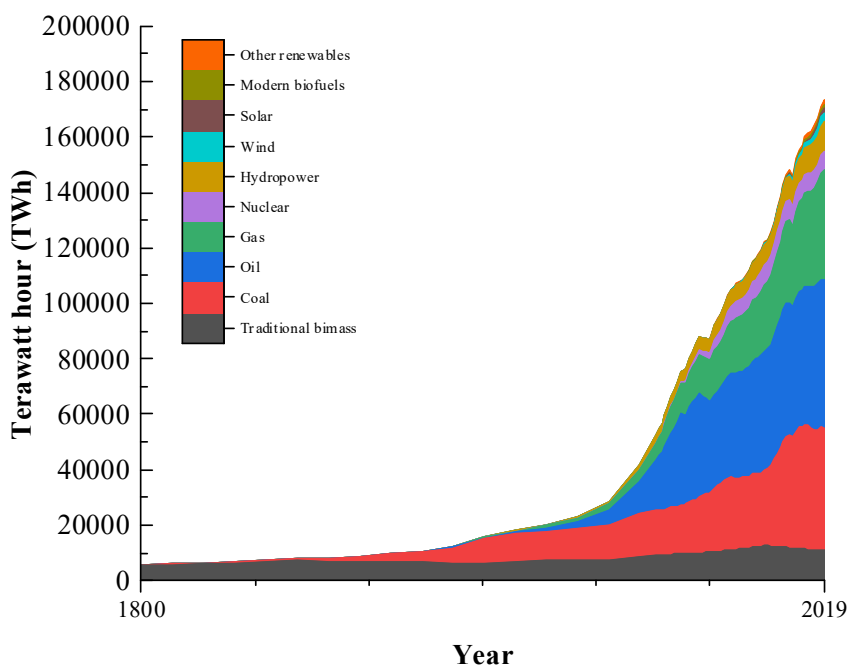
Figure 1.2: Global primary energy consumption by source.[†]

According to BP's (British Petroleum) Statistical Review of World Energy and combined with Vaclav Smil's[‡] estimates, Figure 1.2 demonstrates the reliability of this conclusion. Between the years 1800 and 2019, from the point of view of energy consumption, fossil fuel (coal, oil, natural gas) is still the irrefutable primary energy source, fossil energy still occupies nearly 80% of global energy consumption. This is one of the reasons why greenhouse gas emissions continue to increase and is a problem that we urgently need to address. At the same time, it is not difficult to notice that the proportion of fossil energy in total energy consumption is not a significant downward trend. The fundamental reason is that the production and consumption of fossil energy have formed a mature system, and this system is difficult to subvert in a short period. In stark contrast, the utilization of so-called new energy sources (nuclear, wind, solar) is still very limited.

In addition to the low and unstable utilization of these new energy sources, just as you cannot put all your eggs in one basket, the search for alternative sustainable energy sources cannot be limited to nuclear, wind, and solar power.

[‡] Canadian economic analyst

1.2 Biomass energy and bioalcohols conversion

The term 'biomass' refers to any organic materials produced from non-fossil biological sources, commonly including plants, wood, and waste, and broadly speaking, ethanol produced from corn or sugarcane and methane captured from landfills are also on the list.[14–16] In terms of the current energy consumption from biomass, Figure 1.2 in Chapter 1.1 already unveils that besides fossil fuel, biomass accounts for about one-third of the remaining, which is an important part of the energy supply. The environmental and scientific communities have an optimistic attitude towards the use of biomass because the carbon dioxide produced in biomass waste is originally absorbed from the air and is therefore neutral at the level of greenhouse gas emissions.[17,18]

Biomass as energy is widely and frequently used for industrial heat.[19–22] However, especially considering that ethanol as a more environmentally friendly biomass has a higher research octane number (RON) and automotive octane number (MON) than gasoline.[23–25] This has led to more attention being paid to liquid transportation fuels. Some countries have added ethanol to automobile fuels, such as Brazil, the United States, China, etc., to reduce the dependence on fossil fuels.[26–29] In fact, in the field of transportation, electricity, and hydrogen are also considered the energy provider, nevertheless, electricity and hydrogen can only be used for light-duty vehicles and short-distance transportation because of lacking high volumetric and gravimetric density,[30–33] while medium and heavy-duty vehicles accounted for around 270 million tons CO_2 emissions only in 2014.[34] This part of the carbon emissions can be reduced through the use of biomass energy. If we take advantage of these energy-dense liquid fuels from biomass (like ethanol) and integrate them into a net-zero emissions energy system, shown in Figure 1.3 (**I** and **M**),[34] it will be extremely beneficial to both human development and the future of the Earth's environment.
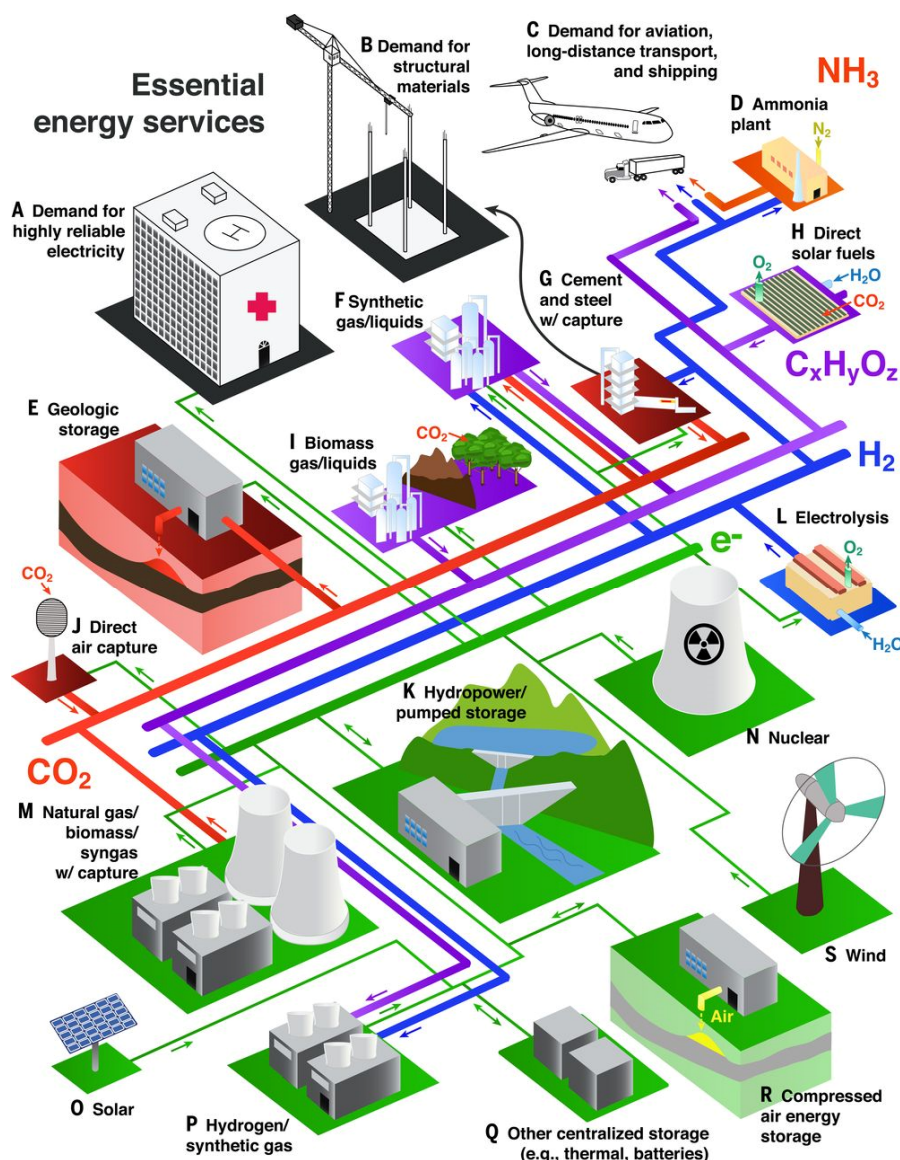
Figure 1.3: Schematic of an integrated system that can provide essential energy services without adding any CO_2 to the atmosphere.[34]

At present, liquid biofuels stand for about 4.2% of total energy consumption by the transport sector worldwide.[35,36] Biofuels from biomass conversion are the most cost-effective way and one of them is bulk production of ethanol from grain and sugar cane, which is still challenged for its life-cycle carbon emissions, cost, and scalability.[37] In addition, upgrade of biomass obtained by fermentation to value-added chemicals, and these products may have more energy density so that they can be applied to the industry. The major work presented in this thesis is upgrading bioalcohols,[38,39] as one of the more promising biomasses. In the next chapters, ethanol and glycerol

will be treated as two typical substrates to conduct upgrading/valorization tests with homogeneous catalysis. Even though the so-called biomass used in the laboratory is pure chemicals, bio-graded ethanol and glycerol can also work in the same system. It is worth mentioning that the system of biomass-related alcohols transformation perspective provided in this thesis can get not only the upgraded products but also the value-added products such as hydrogen and hydrocarbon at the same time. According to the essential energy service figure envisioned in Figure 1.3, the product applications will be deployed in several aspects such as **C**, **I**, **M**, and **P**. Overall, with the relevant research going deep, it is highly likable that clean energy provided by biomass shortly would play a significant role in the carbon-neutral system.

1.2.1 Overview of homogeneous ethanol upgrading

Current research within sustainable chemistry aims for solutions that provide renewable carbon sources as well as clean and green energy alternatives.[37] The substitution of conventional fossil fuels is necessary to reduce greenhouse gas emissions in the transportation sector and industrial heating.[40–42] Hence, alternative and benign fuels derived from biomass conversion represent promising sustainable options.[43] As mentioned earlier, biomass has a broad and promising future as a biofuel,[44–48] and it brings up the topic of ethanol upgrading. Advanced chemicals upgraded from ethanol are also not limited to the application of automotive fuel. An integrated process will be like, firstly, through fermentation of corn, potatoes, grain (wheat, barley, and rye), sugar beet, sugar cane, and vegetable residues, to get bioethanol, as the starting substrate.[49–51] The capital cost of this step is very low and can be produced in large quantities locally. Then, the fermented ethanol may be upgraded to higher value-added alcohols, one of the most direct products is four-carbon 1-butanol. Scheme 1.1 vividly describes this procedure.
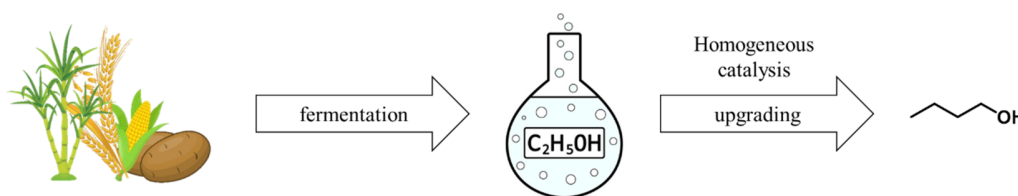
Scheme 1.1: Typical ethanol upgrading way to primary alcohols.

In terms of being a biofuel, 1-butanol indeed has more advantages than ethanol. Since ethanol is of low energy density (70% of that of gasoline),[52] high water solubility,[53] and corrosion effects on the engine,[54] while 1-butanol arises not only as a more favorable alternative than ethanol but also as less susceptible to phase separation and is more hydrophobic.[55] Moreover, Table 1-1 concludes the properties between gasoline, ethanol, and 1-butanol. it is clearly shown that the octane number of 1-butanol is closer to gasoline and it owns a higher energy density than ethanol, which leads 1-butanol to a more suitable biofuel candidate.

Table 1-1: Properties of gasoline, ethanol, and 1-butanol.[§]

Properties	gasoline	ethanol	1-butanol
Boiling point	200	78	117
Flashpoint	-43	13	34
Research octane number (RON)	91 - 99	120 - 135	94 - 96
Motor octane number (MON)	81 - 89	100 - 106	78 - 81
Energy Density (MJ/L)	32	21	29.2
Self-ignition temperature (°C)	247 - 280	365 - 423	343
Explosive limits (%)	1.4 - 7.6	4 - 19	1.4 - 11.2
Solubility in water (wt%)	Not soluble	Fully miscible	7.7

In the homogeneous field, professor Duncan F. Wass firstly reported a catalytic system of ethanol upgrading to 1-butanol in 2013,[56] which is followed by a typical Guerbet reaction.[57] Scheme 1.2 shows the base-driven Guerbet reaction with starting product ethanol as an example, the general steps are like that: 1) Ethanol dehydrogenation affords acetaldehyde; 2) Two molecules of acetaldehyde undergo aldol condensation to generate crotonaldehyde; 3) Hydrogenation of crotonaldehyde produces 1-butanol.

[§] AMF. *Iea-amf.org* (2022). at <https://iea-amf.org/content/fuel_information/butanol/properties>
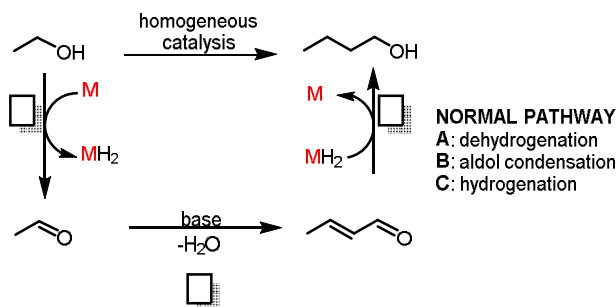
Scheme 1.2: The typical Guerbet reaction.

Due to the highly attractive interest in this ethanol upgrading field, more research groups followed up on this study, also including professor Duncan F. Wass himself. Research in this area has been ongoing, as only some early classical examples[53,58–61] are given here.
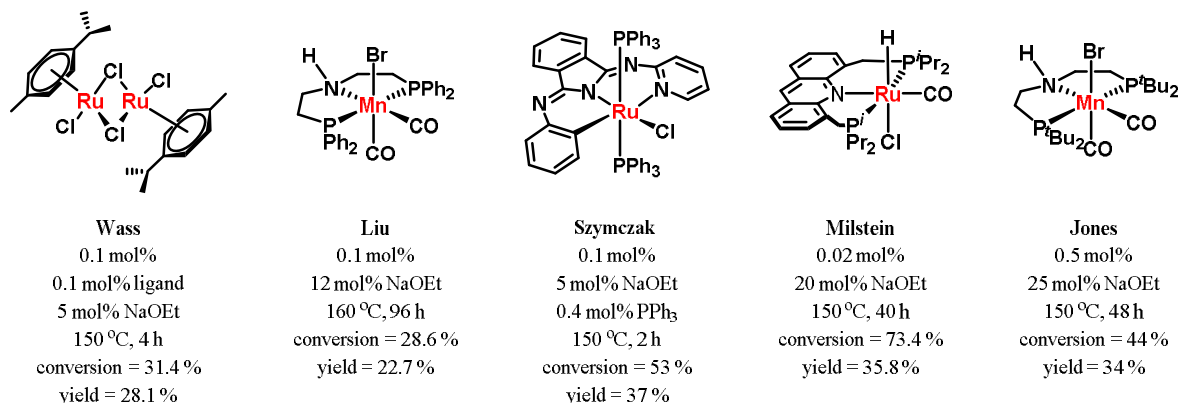
Scheme 1.3: Some typical examples of ethanol upgrading.

Scheme 1.3 summarizes some ethanol upgrading work with reaction conditions. These efforts were the inspiration for the novel ethanol upgrade and for exploring the mechanisms of product selectivity in the nature of the different complexes.

In this thesis, using ethanol upgrading as a starting point, I revisited the Guerbet reaction and succeeded not only in producing large amounts of primary alcohols at low temperatures and with low catalyst introduction. At the same time, a new reaction mechanism was discovered, capable of producing secondary alcohols and even hydrocarbons.

1.2.2 Overview of solvent effects on acceptorless dehydrogenative coupling of ethanol

Acceptorless dehydrogenative coupling abbreviated as ADC, is an efficient reaction that requires no stoichiometric oxidant, and nonpolluting activation of substrates. It is atom economic and only produces water and (or) H_2 as the byproducts.[62,63] In terms of these advantages, some research work related to alcohols to the corresponding esters has been conducted, and when it comes to a base-free homogeneous system, their main focus is alcohols with three or more carbons (polycarbonate aliphatic and aromatic alcohols). Even though a few research tried to improve ethanol conversion but failed, Scheme 1.4 introduces three typical acceptorless dehydrogenative coupling of ethanol examples.[64-66]

Beller	Gauvin	Szymczak
500 ppm	6000 ppm	10000 ppm
90 °C, 6 h	110 °C, 72 h	110 °C, 24 h
NaOEt	yield = 3%	Toluene
yield = 81%		yield = 9%
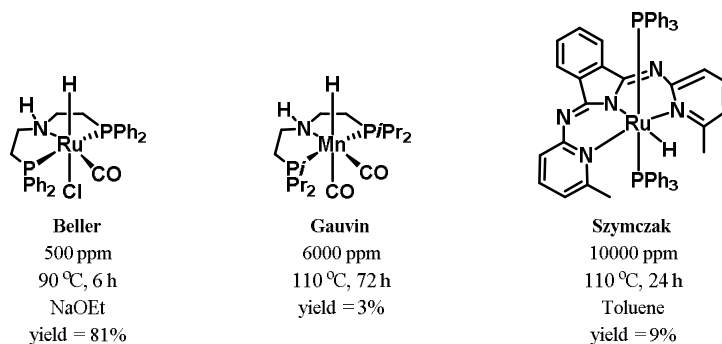
Scheme 1.4: Typical examples for acceptorless dehydrogenative coupling of ethanol.

It is clearly shown that in terms of a base-free system, the dehydrogenation of ethanol will give a low boiling point of acetaldehyde, and without a perfect capture of it, the reaction results will be greatly compromised. This is an obvious reason why ethanol is harder to be converted compared to other higher alcohols. To fix this kind of issue, usually, a cooling system will be introduced. Moreover, most of the organometallic complexes have poor solubility in pure ethanol (or organic compounds, depending on the compound structure),[67,68] and this is why researchers always add an extra co-solvent. A co-solvent does not only play a big role in dissolving the catalysts and advancing the reaction activity. And for a deeper reason, which is precisely the gap left by today's academia. In the author's work, successfully converting ethanol to ethyl acetate without an extra base (even no co-solvent) is just one aspect, the other aspect is that the corresponding explanations

will be given, from the perspectives, such as the polarity, boiling point, energy, and etc. With these deep studies, it is more understandable how to choose a better homogeneous catalytic system.

To study the ADC catalytic cycle with pincer ligands, both outer- and inner-sphere mechanisms would be considered.[69,70,71–74] Beller[75] has established a concerted metal-ligand cooperative pathway using aliphatic pincer-type PNP ligands, which was generally accepted in academia (Scheme 1.5). While in a practical ADC reaction, two molecules of aldehyde can also go through a Tishchenok-type disproportionation,[76,77] therefore, the other possible catalytic cycle -- stepwise mechanism, was suggested by Gusev[78–80] (Scheme 1.6).
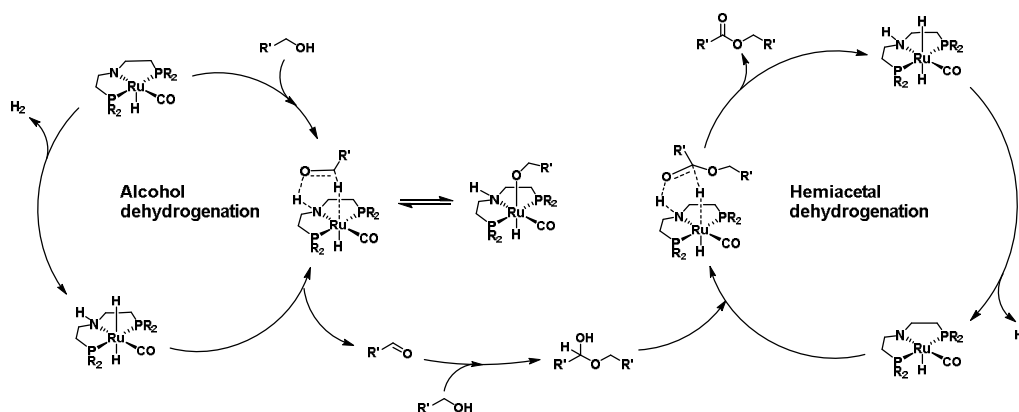
Scheme 1.5: Simplified catalytic cycle for alcohol ADC reaction (Concerted mechanism).
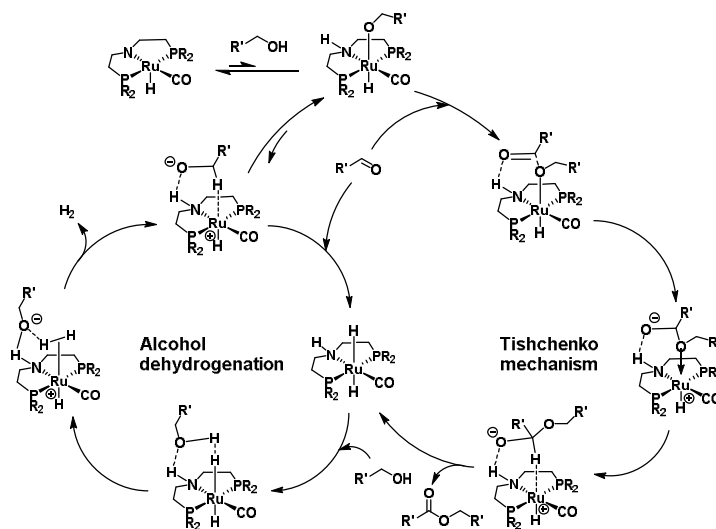
Scheme 1.6: Simplified catalytic cycle for alcohol ADC reaction (Stepwise mechanism).

In 2018, Gauvin et al.[81] re-examined the base-free, acceptorless dehydrogenative coupling of ethanol to ethyl acetate catalyzed by Ru-aliphatic PNP systems in-depth. Evidence confirmed ester production via aldehyde as intermediate species, and in terms of the first step of ADC reaction, a stepwise mechanism seems to be more plausible than a converted one, for the second phase step, a Tishchenko-like reaction is an operative, involving the reaction of an aldehyde with alkoxide ruthenium. Moreover, the catalyst deactivation could be related to water, which leads to inactive carboxylato Ru complexes and hinders further reactions.

In this thesis, a base-free, one-step ethanol ADC system would be proposed and the effects of different co-solvents would be discussed.

1.2.3 Investigations on glycerol valorization

Another biomass feedstock, glycerol, is mainly a by-product of the biodiesel *trans*-esterification process.[82,83] Since it contains three hydroxyl groups, which would make more chemical changes compared to other non-polyols. Moreover, like ethanol, it is cheap, non-toxic, and can be found in all-natural fats and oils.[84,85] Around 10% glycerol will form for each tone of biodiesel and its annual production worldwide is increasing rapidly.[84,86] Therefore, it is necessary to use glycerol to obtain higher value-added chemicals or to act as intermediates for some reactions.

In this thesis, glycerol acts as a hydrogen donor in transfer hydrogenation and dehydrogenates to produce lactic acid, these two specific chemical processes will be discussed in detail.

Transfer hydrogenation of glycerol is not well studied in academia,[87–89] and the classic examples all need an extra base, which is likely on the one hand, to activate the complex itself, on the other hand, to assist in proton dissociation from the hydroxyl group of the alcohol. Some previous catalytic systems are concluded in

Table 1-2. It is clear to see that the NHC ligand is a preference in glycerol transfer hydrogenation, the reason may be because it has a strong electron donor, which could enhance the reactivity of interacting with the electrophilic carbonyl substrate.[90,91] Another notable point is that besides the traditional oil bath heating, microwave and ultrasound systems are also applied in this kind of

reaction to speed up the reaction and improve reactivity. However, some catalysts will decompose faster under microwaves.[91]

Table 1-2: Summary of literature on transfer hydrogenation of glycerol.

Catalysts	Conditions	References
Ir and Ru N-heterocyclic carbine complexes	2.5 mol% catalyst, 0.5 mmol substrate, 0.5 mmol KOH, 80 - 120 °C, 0.8 mL glycerol	Peris[90]
Ir and Ru half-sandwich piano-stool complexes	1 mol% catalyst, 2 mmol substrate, 3 mmol KOH, 120 °C, in air, 8 mL glycerol	Singh[92]
Ir(I) and Ir(III) N-heterocyclic carbine complexes	2.5 mol% catalyst, 0.5 mmol substrate, 0.5 mmol KOH, 80 - 120 °C, 0.4 - 0.8 mL glycerol	Colacino[91]
Ru(II) and Ir(III) N-heterocyclic carbene complexes	2 mol% catalyst, 0.5 mmol substrate, 0.25 mmol KOH, 120 - 140 °C, 2 mL glycerol	Voutchkova-Kostal[93]

Another topic, the production of lactic acid by glycerol dehydrogenation, has also attracted academic interest. Besides benefiting from the excellent physical and chemical properties of glycerol as mentioned above, the product lactic acid plays an important role in the food industry, especially in the production of yogurt and cheese,[94,95] which is estimated to be around 260,000 tons according to the literature of the year 2012.[96]

Professor Crabtree took the lead in developing a homogeneous catalytic system with Ir complexes and achieved over 90% conversion in 2014.[97] This study has inspired other researchers and the topic has continued to be expanded in the following years. Some of the famous examples are summarized in Scheme 1.7.[97-102]

Crabtree
360 ppm
KOH, H$_2$O
115 °C, 24 h
conversion = 94 %
yield = 91 %

Beller
2.5 ppm
NaOH, H$_2$O, NMP
140 °C, 24 h
conversion = 100 %
yield = 67 %

Hazari
2000 ppm
NaOH, H$_2$O, NMP
140 °C, 6 h
conversion = 39 %
yield = 34 %

Williams
140 ppm
NaOH, H$_2$O
145 °C, 7 d
conversion = 90 %
yield = 61.2 %

Voutchkova-Kostal
12 ppm
KOH, H$_2$O
150 °C, 24 h
conversion = 92 %
yield = 92 %

Kumar
300 ppm
KOH, ethanol
140 °C, 48 h, open Ar
conversion = 92 %
yield = 90 %
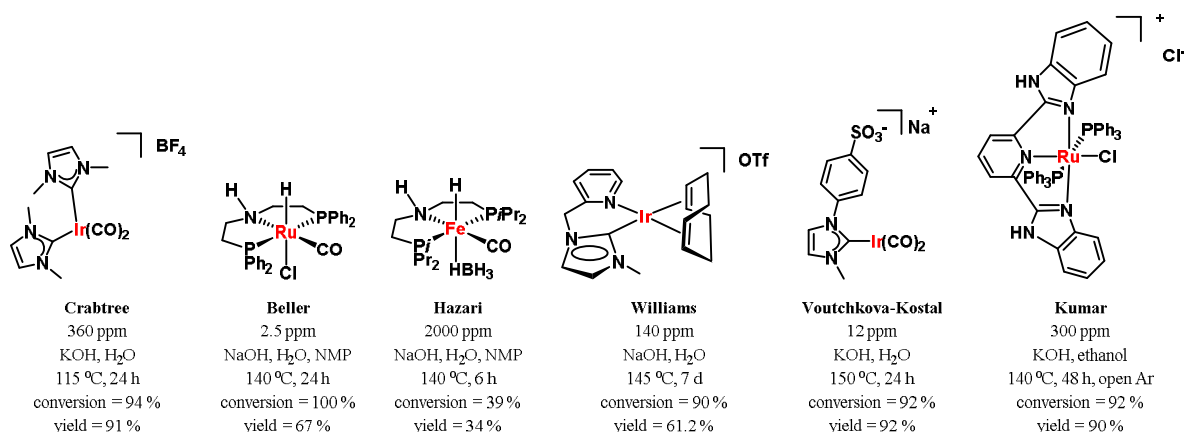
Scheme 1.7: Previous examples of glycerol to lactic acid.

The same with the transfer hydrogenation, glycerol dehydrogenation also needs an extra base for now in academia. Some of them require extra solvent, and it seems that they cannot make a balance between, catalyst loading, catalyst stability, temperature, time, and additives. In this thesis, a base-free, additive-free system would be proposed and it will be shown and talked about in detail afterward.

1.3 Pincer complex and metal-ligand cooperation

Bernard Leslie Shaw[103–109] published some pioneering reports in the mid-1970s, and this created the 'pincer complex chemistry'. A pincer complex is a figurative term for a certain type of organometallic compound, with the general formula $[2,6\text{-}(ECH_2)_2C_6H_3]^-$ (ECE). E is a neutral two-electron donor (amine, phosphine, sulfide, etc.) and C stands for the anionic aryl carbon atom connecting the 2,6-disubstituted phenyl ring.[110] It usually has a core of transition metals, such as manganese, iron, ruthenium, iridium, etc, and attaches with phosphines the most of time. The synthesis and catalysis work of the pincer complex can trace back to the mid-1970s and with the rapid development of this field, the coordination 'ECE' (E = N, P) modes have been extended to ENE (E =C, S, Se, P), PCN and YNX (Y = C, N, O; X = N, O, S).[111–119] PR$_3$ and PR$_2$, due to their strong ability to stabilize metal centers in high and low oxidation states, have been widely used as donor atoms in organometallic chemistry.[120] Further, if another 'E' in the *cis* position is amine or amino, then, naturally, this leads to the so-called PNP ligands, which as a subclass of pincer ligands, are the focus, and the primary complex used in the catalytic systems of this thesis. Scheme 1.8 gave a generic structure of a six coordination Ru(II)-PNP complex. R usually stands for phenyl, *i*-propyl, cyclohexyl, *t*-butyl, etc. X means an X-type ligand with a formal charge of -1, such as H, Cl, BH$_4$, etc. Likewise, L means an L-type ligand with a formal charge of 0, and the most common one is the CO ligand. There are also some NO ligands from the Nielsen group that are under development.**
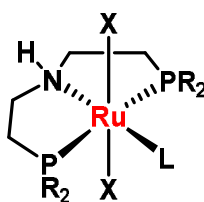
Scheme 1.8: A generic structure of a Ru(II)-PNP complex.

PNP complexes are proved to be super-efficient for (de)hydrogenation catalysis and indeed have been applied in various chemical reactions. In 2004, Milstein designed a novel Ru-PNP complex

---

for dehydrogenation of primary alcohols to esters.[121] Further, Beller focused on the dehydrogenation of aqueous-phase methanol to H_2 and CO_2.[122] Based on *in situ* NMR, they proposed an outer-sphere mechanism, which is described in Scheme 1.9.
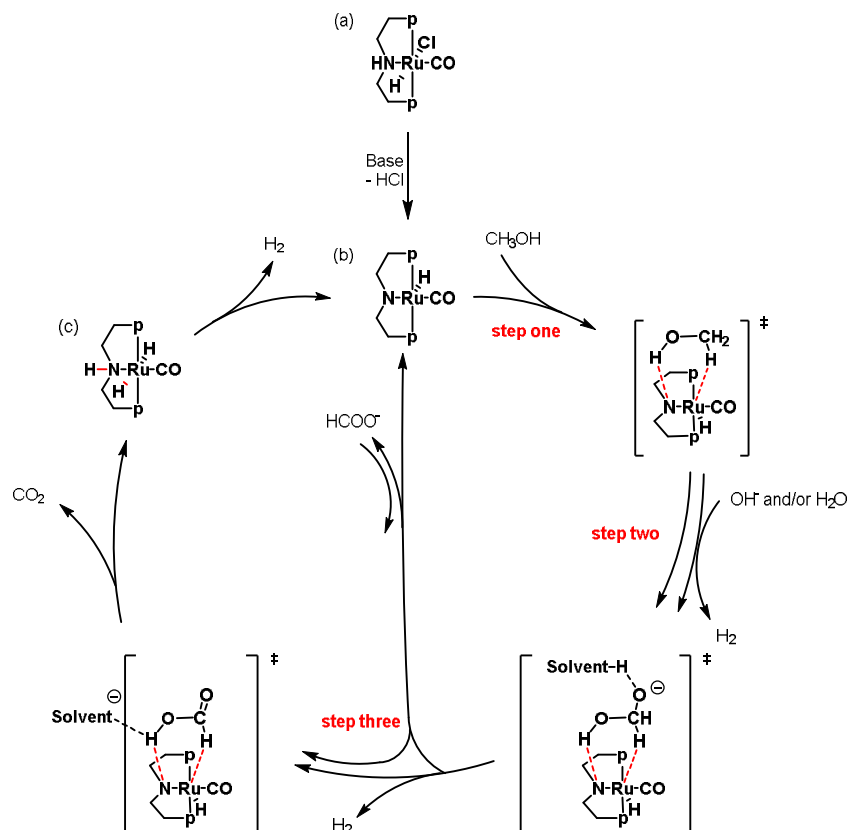
Scheme 1.9: Proposed catalytic cycle for Ru-promoted aqueous-phase methanol dehydrogenation, presented by Beller.

In the beginning, complex (**a**) as a pre-catalyst, is activated by the base while losing one molecule of HCl, then the main catalytic produce goes through three steps. In step one, through an outer-sphere[††] concerted process (methanol does not directly coordinate with the metal), one molecule of H_2 is released; In step two, one molecule of hydroxide from the solvent attaches with the intermediate complex, to give the *gem*-diol(ate), in the meantime, another molecule of H_2 and

---

[††] Outer-sphere reactions are those that take place without breaking any bonds between a metal and a group such as water or hydroxide ion bound to it.

16

formate are produced. In step three, the intermediate would finish the final cycle, releasing CO_2. For a complete diagram and explanation of the catalytic mechanism see the original manuscript.

Overall, pincer complexes are getting more and more attention in modern chemistry owing to their potential to achieve well-defined and tunable systems, which is an ultimate goal of inorganic and organometallic chemistry.[110,120] To understand more deeply the catalytic behavior of the pincer complexes used in this thesis, it is necessary to elucidate a concept here. It is called metal-ligand cooperation.

In traditional homogeneous catalysis, transformations, like oxidative addition, reductive elimination, β-hydride elimination, etc. only happen at the metal center while the ligands keep unchanged during the whole course of the reaction. A bond activation process that involves metal-ligand cooperation, where both the metal and the ligand undergo chemical changes (Scheme 1.10).[69]
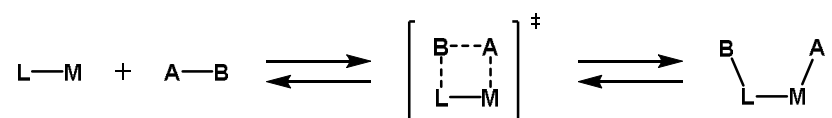
Scheme 1.10: Bond activation by metal-ligand-cooperation.

In 1997, when Noyori[123–127] conducted transfer hydrogenation experiments on ketones, he and his co-workers found, as their research progressed, that additives of diamines or ethanolamine containing at least one NH group have a huge effect on the experiment results with Ru complexes. This impact has been summarized as 'metal-nitrogen bond cooperation', which shows that H–H and H–heteroatom bonds are activated by metal amide/amine systems. The core mechanism component of this type of catalyst is a metal center coordinated with an N-H group. Most of the catalysts used in this thesis, including Ru-MACHO-BH, belong to the so-called Noyori-class of catalysts. It is worth mentioning that its analogous 'Ru-MACHO', could be considered a very typical prototype of M/N–H bifunctional complexes. Besides the precious metal, Ru, researchers are dedicated to exploring other earth-abundant metals, such as Mn, Fe, Co, and Ni and progress have been made.[128–131]

As mentioned before the pincer complex, also known as the tridentate complex intensified scientists' knowledge of the role of metal ligands in catalysis. Mechanistically speaking, complexes

consisting of NH groups as well as metal-hydride can undergo both outer and inner sphere mechanisms in the actual reaction. For example, Gusev[132] presented some complexes, which are beneficial for hydrogenation of esters to alcohols and the reverse reactions, also, due to the potentially hemilabile pyridine arm, both the Noyori-type outer-sphere and the classical inner-sphere hydrogenation mechanisms are possible (Scheme 1.11).
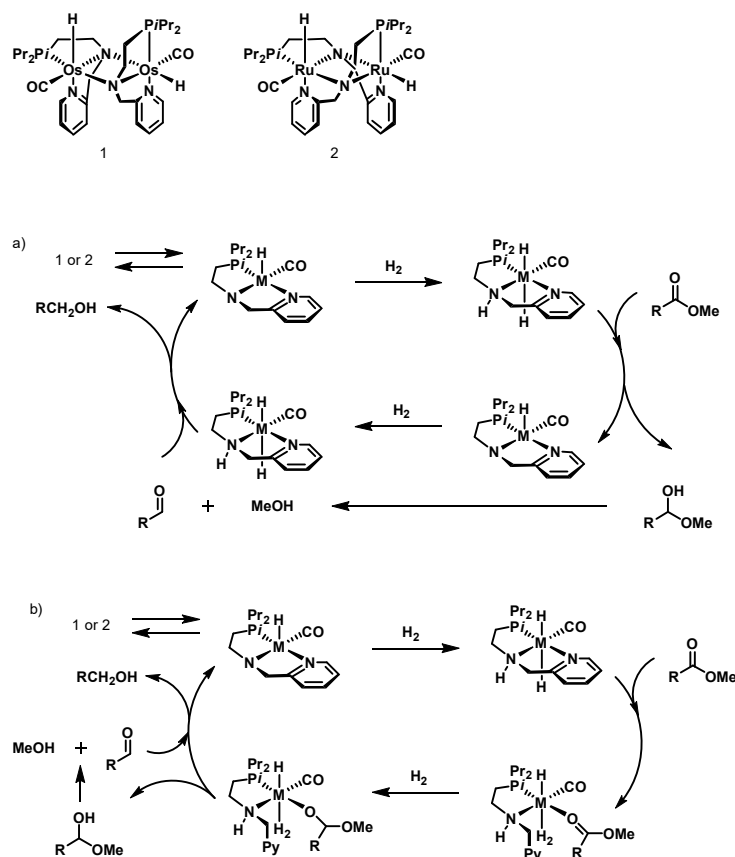
Scheme 1.11: Outer-sphere (a) and inner-sphere (b) hydrogenation by Gusev.

MLC would accurate the catalytic procedure and most of the time, more catalyst loading is needed in absence of MLC in the system. For instance, Gauvin[133] and Möller[134] research groups respectively studied the oxidation of alcohols to carboxylic acids in water, and it turned out that the catalytic system that triggers the MLC is much better than the other systems.

In this thesis, the catalytic effects in transformations of bioalcohols with over five pincer Noyori-type complexes will be talked and Ru-MACHO-BH will be mainly introduced as an excellent (de)hydrogenation catalyst.

1.4 Organometallic homogeneous catalysis

Catalysis is indispensable in both academia and industry.[135–137] The Swedish chemist Berzelius invented the term '*catalysis*' but a proper definition, 'Catalysis is the acceleration of a slow chemical process by the presence of a foreign material' was formally proposed by Baltic German chemist Ostwald in 1894.[138] A non-catalysis reaction has higher activation energy (Figure 1.4) than its corresponding reaction in the presence of catalysts. The catalyst will participate in the substrate reaction, exchanging with the molecules in the reaction while accelerating the forward and reverse reaction processes, allowing the reaction to reach equilibrium faster, but with the equilibrium position unchanged. An efficient catalyst would also limit or hinder undesirable side reactions.[139]
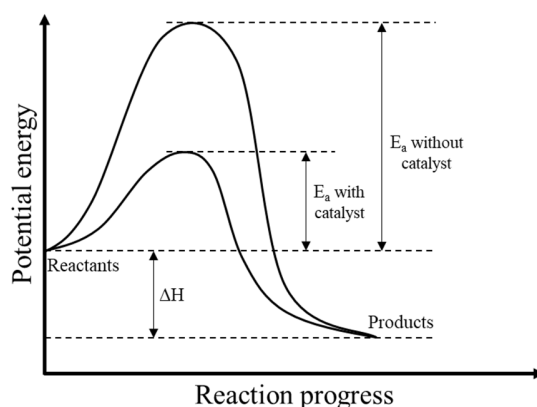
Figure 1.4: A typical energy diagram profile with/without catalysts.

In chemistry, catalysis mainly can be divided into heterogeneous catalysis, where the reactants or products are in different phases from the catalyst, and homogeneous catalysis, where the mixture exists in the same phase. Thanks to the advantages of higher selectivity, relatively mild reaction conditions, and more easily explored mechanisms, homogeneous catalysis occupies an important place in the whole field of catalysis. Moreover, The shortcoming of homogeneous catalysis, which has been criticized, namely the inability to industrialize well, is slowly improving.[135] Organometallic complexes are widely used in homogeneous catalysis, and act as multifunctional (pre)catalysts.[140,141] Some reasons have been concluded for why these complexes can speed up the break and form of chemical bonds without being consumed in the course of reactions:[142] 1) When

molecules with a functional group are coordinated with a metal center, the reactivity of the former will be greatly activated; 2) Highly reactive species can be well stabilized (e.g. chelated structures of pincer ligands) for subsequent reactions; 3) The two molecules can coordinate to the same metal center, increasing the probability of the reaction by proximity; 4) Different ligands can effectively modulate the selectivity of the reaction (e.g. auxiliary phosphorous ligands).

As described in Chapter 1.3, the pincer complex can be well used as an organometallic catalyst in homogeneous catalysis. And this chapter would mainly talk about two classic reactions, dehydrogenation and hydrogenation, which are related to the author's work as well as provide some typical examples.

1.4.1 Dehydrogenation of alcohols and alkanes

A modern and atomic economy approach for dehydrogenation of alcohols is under acceptorless conditions without sacrificial hydrogen acceptors. This kind of reaction format can be traced back to 1975, two of Robinson's leading efforts opened up this field.[143,144] Despite being a pioneer in this field, the results of the reaction did not yield very satisfactory results at the catalytic level. It was not until 2004 that Milstein et al.[145] used ruthenium PNP complexes for the dehydrogenation of secondary alcohols and achieved satisfactory results (Scheme 1.12).
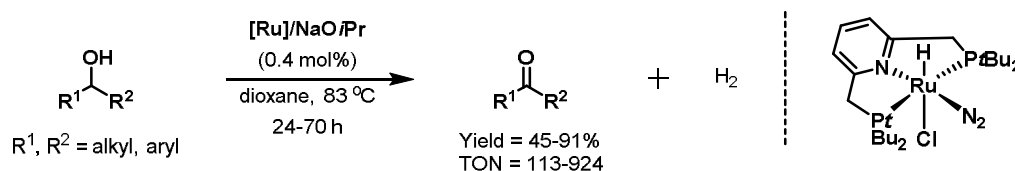
Scheme 1.12: Acceptorless dehydrogenation of secondary alcohols by Milstein.

With the excessive consumption of fossil fuels, the dehydrogenation of biomass-related alcohols, such as bioethanol, is gaining attention, and the conversion of these primary alcohols is more difficult than that of aromatic alcohols, and academic interest is gradually moving in this direction.[146,147] Beller[148] developed the first example of acceptorless dehydrogenation of isopropyl as well as biorelevant ethanol, under mind and natural conditions (< 100 ºC). Moreover, the same research group attempted an aqueous methanol-reforming process as mentioned in Chapter 1.3, and to remove the additional base, recently, they explored a bi-catalytic system using Ru-

MACHO-BH and $Ru(H)_2(dppe)_2$ for the base-free dehydrogenation of methanol to H_2 and CO_2.[149] Subsequently, Milstein proposed an efficient reusable homogeneous catalytic system for hydrogen production from aqueous methanol, giving around 1 month continuous running, without any decrease in activity.[150]

Through one-step dehydrogenation of primary alcohols to get the corresponding aldehydes and further reacting with the alcohol to form hemiacetals and at the same time, releasing H_2, this self-coupling of alcohols to esters formation has been widely exploited in the past decades (Scheme 1.13).[75,132,151–154]
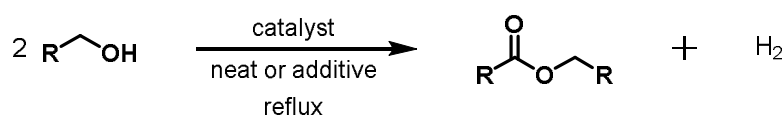
Scheme 1.13: Self-coupling of primary alcohols to esters.

Early catalytic systems generally required the addition of additional bases, for example, Milstein[151] reported dehydrogenation of primary alcohols to esters and H_2 with KOH and got 99% conversion and 99% yield. The production of ethyl acetate is highly relevant in the industry. This basic short-chain ester is widely used in the synthesis of biodiesel, paints, adhesives, herbicides, and resins.[155] Therefore, it is necessary to develop an efficient way of ethanol dehydrogenation to produce ethyl acetate, and details about this part will be given in Chapter 3 and the work of the author.

Unlike alcohols, it is more difficult to carry out the dehydrogenation of alkanes with homogeneous catalysis. Some organometallic catalysts have very poor catalytic effects or even do not survive at high temperatures, which are required for alkane dehydrogenation. Roddick published the first ruthenium PCP pincer complex system for cyclooctane dehydrogenation in 2011.[156] With the complex, 1:1 mixtures of cyclooctane and *tert*-butylethylene at 150 and 200 °C resulted in initial rates of 180 and 1000 turnovers h^{-1} of cyclooctene, respectively (Scheme 1.14).
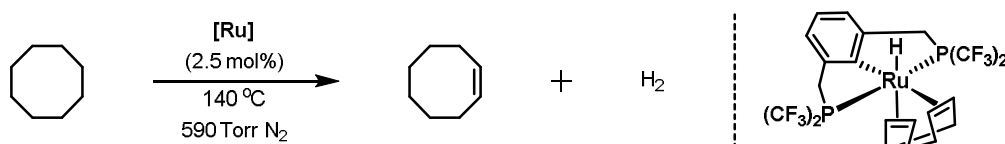
Scheme 1.14: Acceptorless dehydrogenation of Alkanes by Roddick.

The development of more thermally stable catalysts can better solve the problems in alkane dehydrogenation, in short, there is a long way to go regarding this piece of catalysis.

1.4.2 Hydrogenation of aldehydes, ketones, and esters

Homogeneous catalysis of hydrogenation of aldehydes, ketones, and esters by transition metal complexes was developed in the last few decades.[157–159] With the understanding and exploration of metal-ligand cooperation (MLC),[69] numerous pincer complexes provided much-required breakthroughs and have been exploited for hydrogenation under mild conditions.[160] Noyori[161] reported practical chemo- and stereoselective hydrogenation of achiral and chiral ketones using ruthenium complexes. In 2011, Milstein[162] reported the first example of hydrogenation of aromatic and heterocycle ketones to alcohols using the non-precious iron pincer complex (Scheme 1.15) and proposed a dearomatized hydrogenation mechanism, which was shown in Scheme 1.16.
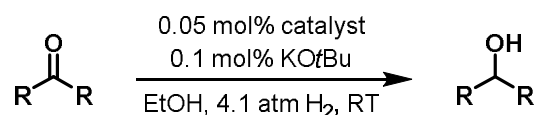
Scheme 1.15: Hydrogenation of ketones by Milstein.

Complex **1** is activated by the base to form **A**, ketone coordinates to **A** followed by isomerization to **B**, then the H in the Fe-H bond reacts with the coordinated ketone species to form **C**. The pentacoordinate unstable intermediate **C** reacts with H_2 to get **D**, after releasing the alcohol, to finish one cycle.
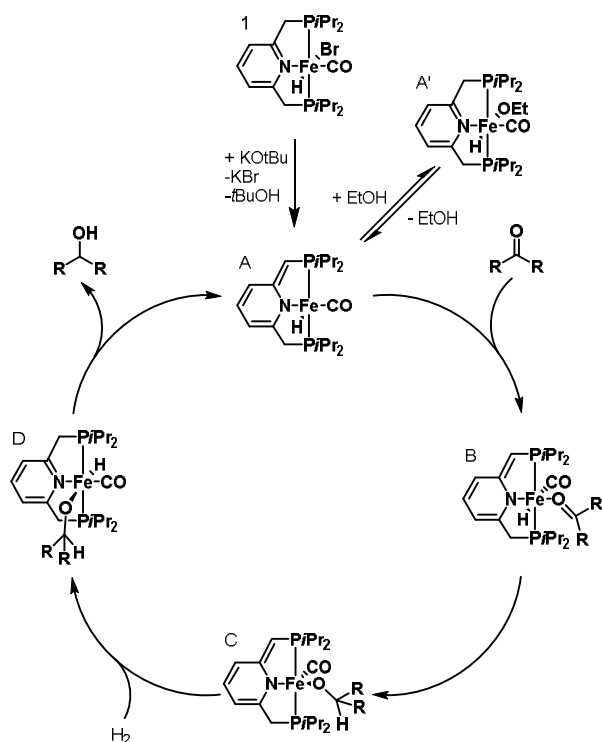
Scheme 1.16: Proposed mechanism for the hydrogenation of ketones by Milstein.

Subsequently, the same research group[163] launched a general approach for the hydrogenation of aldehydes to alcohols with iron complex, [(iPr-PNP)Fe(H)(CO)(Br)] was proved as an efficient precatalyst for catalyzing secondary and tertiary aliphatic aldehydes and aryl aldehydes. Almost at about the same time, Kircher et al.[164] developed a new class of Fe-PNP pincer hydride complexes chemoselectively hydrogenating ketones and aldehydes to alcohols. With additional solvents for a short time, at room temperature, up to 99% yield and 770 TON were achieved (Scheme 1.17).
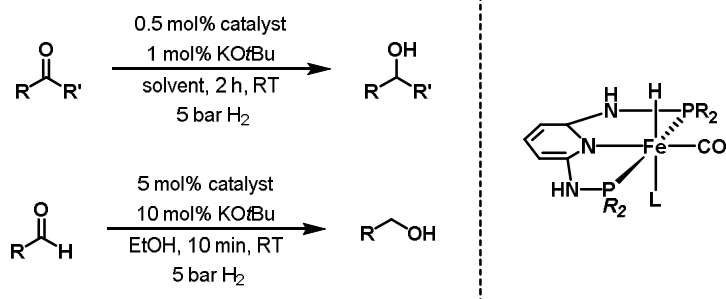
Scheme 1.17: Iron-catalyzed hydrogenation of ketones (up) and aldehydes (down) by Kircher.

Hydrogenation of carbonic acid derivates, like esters, is luring research but it is more difficult than that of ketones and aldehydes.[70,165,166] A pioneering and innovative work published by Milstein[167] using PNN ruthenium hydride complexes in 2006, although it seemed relatively crude at the time, it did influence the development of the field. A large number of different transition metal complexes have been studied in this way, including Ru-CNN,[168–170] Ru-PNN,[170] Ir-PNP,[171] Fe-PNP,[172–174] OS-PNP,[175] Co/triphos,[176] etc. The pincer ligand named 'MACHO' is very versatile, Beller[171] explored the use of Ir-MACHO complex, in the presence of a base and high pressure of H_2, and up to 98% yield was achieved. In fact, one year later, instead of the phosphorus group, Gusev[177] tested sulfur substituted $HN(C_2H_4SEt)_2$ ligand for hydrogenation of esters, and got up to 100% conversion (Scheme 1.18).

X = Cl, H.

X, R = Cl, PPh₃; H, PPh₃;
Cl, AsPh₃; H, CO.
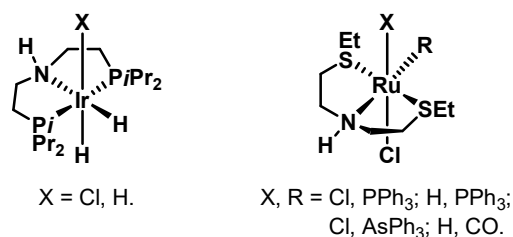
Scheme 1.18: Ir-PNP and Ru-SNS complexes for hydrogenation of esters by Beller (left) and Gusev (right).

Beller[174] reported a non-precious iron transition metal example with 'MACHO' ligand for hydrogenation a variety of aromatic and aliphatic esters, replacement of different auxiliary ligands with *i*-Pr, Cy, and Et, up tp 99% yield was got.

1.5 Summary and outlook

This concludes this section.

Chapter 1.1 discusses climate change and the energy crisis at a macro level, and the range of issues arising from them is a pressing academic concern. Chapter 1.2 firstly, the concept of biomass is given, and it is explained that value-added biomass-related alcohols are a good way to deal with the current environmental pollution and energy crisis. Then, three sub-chapters are given. These talked about the state-of-the-art related to the author's work, which more or less inspired the author to conduct his research. Nevertheless, most of the work is innovative not just adding or polishing pioneer's studies. The specific work will be focused on in Chapter 3. Chapter 1.3 gives the concept of the pincer complex, which is the main complex used by the authors for their catalytic work as well as the modern organometallic concept of 'metal-ligand cooperation'. Chapter 1.4 describes classic examples of organometallic homogeneous catalysis for dehydrogenation and hydrogenation reactions.

Chapter 2

2 Introduction of Ru-MACHO-BH and its latest catalysis

Ru(II)-MACHO-BH, which consists of a tridentate ligand that contains two phosphino groups, an NH group, and a carbonyl ligand, was formally patented by Takasago International Corporation in 2013.[‡‡] In the original invention, it was described as an excellent catalyst for reducing ketones, esters, and lactones to alcohols. Scheme 2.1 briefly shows the standard synthesis procedure of Ru-MACHO-BH, and it is quite convenient and intuitive. The product is stable and therefore suitable for catalysis and industrial applications. Please visit the patent file for more detailed synthesis information.
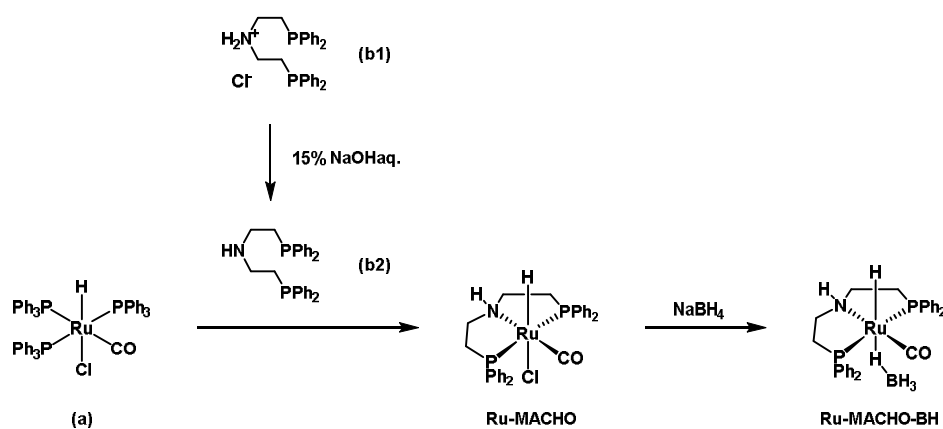
Scheme 2.1: The standard synthesis procedure of Ru-MACHO-BH.

The big advantage over its 'predecessor', Ru-MACHO, is that it is already an 'activated' complex, able to catalyze reactions without additional acid/base additives. The highly reactive BH_3 ligand is easily lost at a certain temperature and thus directly activated. A common mechanism is that

---

[‡‡] Takasago, 2013, US 8471,048 B2

after the BH_3 ligand loses, one H directly connecting with the metal combines with the other H in the NH group releasing H_2 (Scheme 2.2).
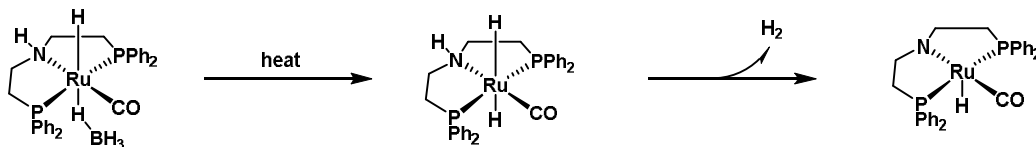
Scheme 2.2: A common mechanism of activation of Ru-MACHO-BH.

Although Ru-MACHO-BH was initially labeled as a hydrogenated ketone and ester by Takasago et al, more chemical catalytic potentials have been reported due to the frequent in-depth studies of this complex in academia and its unique advantages, the more famous ones being CO_2 hydrogenation,[178,179–181] reversible CO_2 hydrogenation/formate dehydrogenation,[182] CO hydrogenation,[183] methanol dehydrogenation,[184] base-free dehydrogenative coupling of alcohols,[185] etc. According to the current understanding, the ionic BH_4^- ligand always pass through bridging hydrogen atoms and the coordination mode is monodentate (η^1-HBH_3).[186] Since the patenting of this complex, it has been developed over the years and is now being explored by the academic community in a whole new way, some of its unexpected potentials have been or are being tapped, with several new examples being discussed in detail here.

Integrated catalytic technology for carbon capture is an attractive research direction.[187–189] In particular, homogeneous catalysis is introduced into the carbon cycle economy. Recently, Bert Sels[190] explored a viable approach 'suppression of stationary state species', Ru-MACHO-BH in the presence of amine additives was evaluated with ZnO, to advance CO_2 hydrogenation to methanol. Speaking of methanol, it can be produced from renewable sources,[191] such as the direct CO_2 hydrogenation as mentioned just right now, also, it is easy to store, transport, and distribute. Therefore, methanol as an energy storage medium is considered an important role in energy and chemistry.[192–194] Leitner research group,[195] presented the first homogeneous catalysis example for dehydrogenation of methanol to CO and H_2 with Ru-MACHO-BH. Once again, the catalytic potential of this complex was verified. Up to 3150 TON for CO and 9230 TON for H_2 at 150 ºC were achieved by carrying out Ru-MACHO-BH, with the help of NMR, IR, MS analysis, previous reports, and performing some control experiments, a plausible mechanism for methanol dehydrogenation was launched (Scheme 2.3). This mechanism integrates part of the old

mechanism of Ru-MACHO-BH as well as pioneering part of the new mechanism that will deepen the reader's understanding of the catalytic properties of the complex.

Like the other organometallic catalysis, metal-ligand-cooperation is involved,[69,196,197] Ru-MACHO-BH loses BH$_3$ ligand as well as a portion of hydrogen when subjected to heat, to form active species complex **I** comprising the cooperative M-N site.[198] The process of generating **II** from **I** under the attack of alcohol has been well shown in previous literature.[199,200] The first step of the dehydrogenation process is completed by the removal of formaldehyde from complex **II** to form dihydride complex **III**. After the completion of one hydrogen liberation process from complex **III**, complex **I** is generated again. Ru-complex **IV** undergoes a one-step decarbonylation reaction to form CO and form Ru-dihydride complex **III**. This series of processes is discussed in cycle 1.

The formaldehyde released from complex **II** can also react directly with the methanol in the system to form methoxymethanol, which reacts with complex **I** to form **V** while releasing methyl formate. Like the complex **IV**, **VI** can also go through a decarbonylation process with methyl formate and produce CO. This series of processes is discussed in cycle 2.
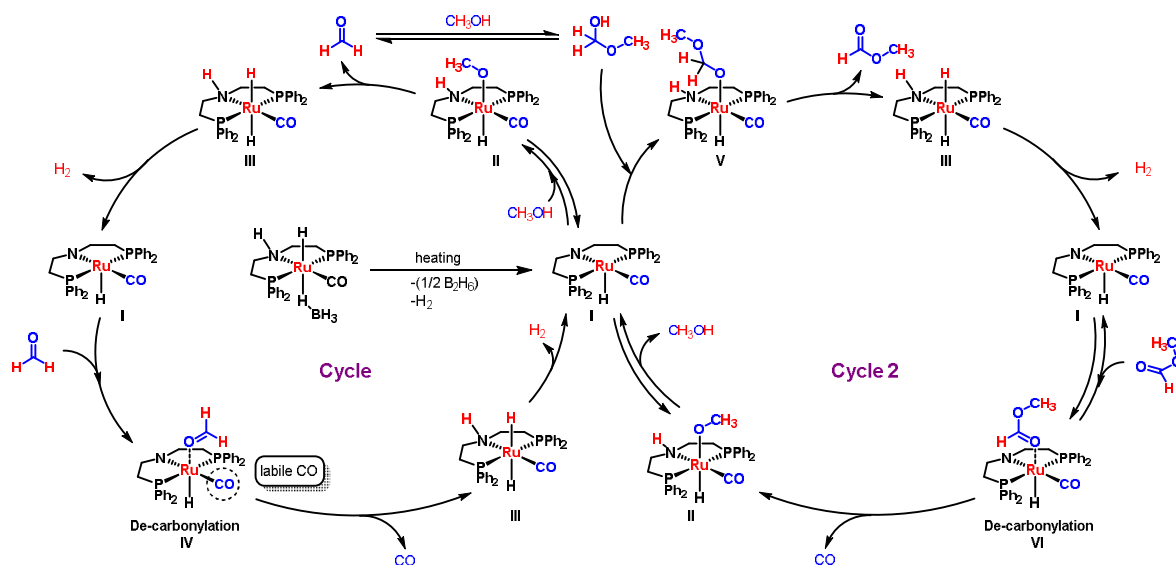
Scheme 2.3: Plausible mechanism for methanol dehydrogenation to CO and H$_2$ by Leitner.

Ru-MACHO-BH has also been proved that with less bulky phenyl substituted phosphines, it would catalyze ethanol to novel secondary alcohols, which is a recent innovative discovery by the author. The discussion would be in chapter 3. Figure 2.1 shows the ball and stick model of the

optimized Ru-MACHO-BH structure (its real crystal structure remains unknown). For most of the practical work, the complex is usually in the form of a benchmark catalyst.
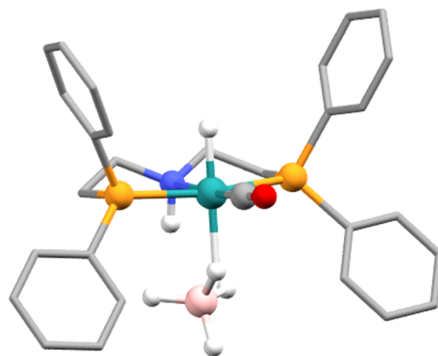
Figure 2.1: Model structure of Ru-MACHO-BH.

Different from BH_4^- ligand Ru-MACHO-BH, other PNP complexes with chloride always need a basic environment to do the activation. After adding a base, the chloride and hydride connecting to the amide group will lose with the HCl format. Scheme 2.4 shows the mechanism and these PNP complexes are other pre-catalysts for the authors' catalytic work.
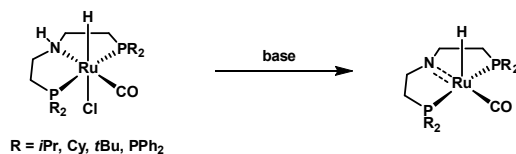
Scheme 2.4: A common mechanism of other PNP complexes.

The next chapter will conduct experiments with Ru-MACHO-BH as the baseline catalyst and reveal its unique catalytic properties, such as the ability to convert ethanol to secondary alcohols, and efficient base-free dehydrogenation of ethanol or glycerol to produce ethyl acetate or lactic acid, etc.

Chapter 3

3 Organometallic catalytic bioalcohols conversion for sustainability

The catalytic work performed by the author is classified as Chapter 3 and further divided into three subchapters that discuss in detail.

Most of the reactions in Chapter 3.1, are conducted in either high-pressure reactors which are made by the workshop department at DTU chemistry and placed on the aluminum heating module panel or digital high-pressure reactors which are purchased from Parr.

Most of the reactions in Chapter 3.2, are conducted in an open reflux system with a cooling system and placed in an oil bath.

Most of the reactions in Chapter 3.3, are conducted in 15 mL pressure tubes and placed in an oil bath.

3.1 Low-temperature novel ethanol upgrading

3.1.1 General information

In this Chapter, I will formally discuss the first project, which is 'low-temperature novel ethanol upgrading'. More specifically, low-temperature selective ethanol upgrading to primary or secondary alcohols by homogeneous catalysis. Herein, the word 'novel' is the core of this project. It means that we can get different isomers of higher alcohols by changing the auxiliary ligands of PNP complexes. And in the previous talk, we already knew that all of the current homogeneous research is based on the Guerbet reaction, and in other words, these studies are limited by the classic pathway. However, this project will broaden the boundaries of response.

First, Scheme 3.1 listed the five catalysts that I used for this project, and from left to right, the bulkiness of auxiliary ligands increases. **Ru-1 - Ru-5** are commercially available and used without further purification.
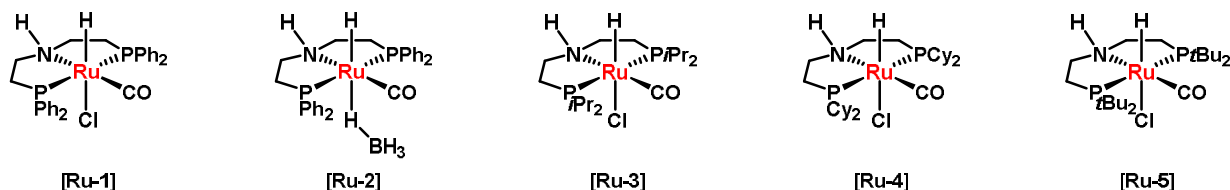
Scheme 3.1: Used catalysts for novel ethanol upgrading.

As described in Chapter 1, all five complexes belong to the Noyori type. Scheme 3.2 provided a table of content of this project to give readers a general impression. In this study, the choice of the auxiliary ligand will lead to the reaction to a different route, resulting in traditional primary alcohol, as well as new secondary alcohol. After fully exploring the spatial effects of the auxiliary ligands, such catalysis will no longer be a 'spray and pray' type in the traditional sense but will become more targeted. The efficiency of academic research or industrialization will be greatly accelerated.
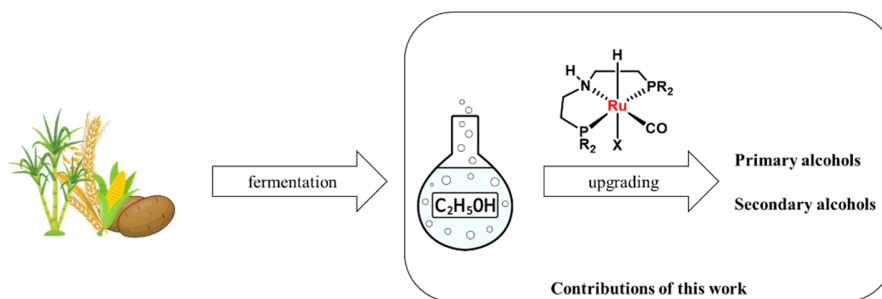
Scheme 3.2: Novel ethanol upgrading pathway to primary or secondary alcohols.

Although the upgraded secondary alcohols are not as common as primary alcohols for gasoline additive applications, the data on 2-butanol is still shown in Table 3-1 for the reader to review.

Table 3-1: Properties of gasoline, ethanol, 1-butanol, and 2-butanol.

Properties	gasoline	ethanol	1-butanol	2-butanol
Boiling point	200	78	117	100
Flashpoint	-43	13	34	31
Research octane number (RON)	91 - 99	120 - 135	94 - 96	101
Motor octane number (MON)	81 - 89	100 - 106	78 - 81	91
Energy Density (MJ/L)	32	21	29.2	32
Self-ignition temperature (°C)	247 - 280	365 - 423	343	380 - 406
Explosive limits (%)	1.4 - 7.6	4 - 19	1.4 - 11.2	1.7 - 9.8
Solubility in water (wt%)	Not soluble	Fully miscible	7.7	12.5

Moreover, in industry, the production of 2-butanol exceeds 800,000 tons per year,[201] and is manufactured from glucose by fermentation.[202,203] 2-butanol is also widely used as a pharmaceutical standard,[204] an organic solvent,[205] as a crucial intermediate for producing 1-butene, 2-butene,[206] butyl acetate,[207,208] *sec*-butyl acetate,[207] and methyl ethyl ketone (MEK).[209]

The direct production of alkenes/alkanes from ethanol represents a potentially more economic route to jet- and diesel-range hydrocarbon fuels relative to the state-of-the-art technology.[210,211] Thus, the selective production of 2-butenes from renewable feedstock is considered a critical challenge for the eco-nomically viable production of jet fuels and diesel.[212–214] The molecules are also essential feedstock for the production of high-value-added products, such as rubbers, polymers,
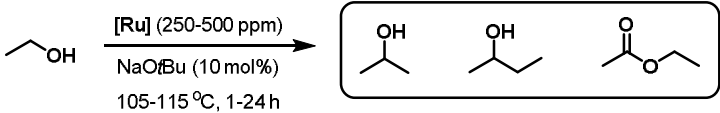
and synthetic oils.[215,216] Indeed, recently the production of butenes from bioethanol is attracting more attention in sustainability research fields, with yields exceeding 60% at reaction temperatures between 300-400 ºC.[210,217] As a significant component of liquefied petroleum gases (LP gases), butane is industrially derived from natural gas and crude oil.[218] It may alternatively be obtained from ethanol using heterogeneous catalysis at reaction temperatures between 200-300 ºC, typically resulting in low yields of linear butane (<5%) and higher yields of the branched isomers (up to 85%).[219,220] However, the use of homogeneous catalytic systems and mild conditions for all the transformations of ethanol to 2-butanol, 2-butenes, or butane remains undisclosed.

In this novel ethanol upgrading, 2-butanol was further converted to 2-butenes and butane. We speculate that 2-butanol dehydrates to the 2-butenes under this reaction conditions[221,206] and hydrogenates to butane. A more detailed discussion will be developed in the experimental section.

3.1.2 Experimental results and discussion

Some blank or additive-free experiments were carried out at the beginning (Table 3-2). As we can see, for **Ru-1**, ethanol would be converted only in the presence of both catalyst and base, and the main products were secondary alcohols (Entry 3). For **Ru-2**, even if without base, the reaction will also happen, while the main product was ethyl acetate (Entry 4). In the subsequent experiments, for **Ru-2**, the addition of base also generated secondary alcohols. These two catalysts belong to the same category containing less bulky and aryl-based phenyl substituted phosphines. They are robust catalysts for a wide range of sustainable chemical transformations under mild reaction conditions.[122,64,98,222–224]

Table 3-2: Control experiments and model reactions for ethanol upgrading.

Entry	Catalyst (ppm)	Base (mol%)	EtOH (mL)	T [ºC]	t [h]	Conversion [%][a]	Yields [%][a]			
							2-propanol	2-butanol	ethyl acetate	H$_2$
1	-	NaOtBu, 10	2.5	105	1	0	-	-	-	-

2	**Ru-1**, 500	-	2.5	105	1	0	-	-	-	-
3	**Ru-1**, 500	NaOtBu, 10	5	105	1	3	0.2	0.9	-	-
4	**Ru-2**, 250	-	5	115	24	16	-	-	5.4	1.6

Reaction conditions: 2.5-5 mL EtOH, 250-500 ppm catalyst, 10mol% NaOtBu, 105-115 °C, 1-24 h, high-pressure reactor, 600 rpm.

[a] Determined by GC-FID (liquid phase products), GC-MS (liquid phase products), and Micro-GC (H₂).

I firstly tested a set of different time-based reactions with 1000 ppm of **Ru-1** and 20 mol% NaOtBu (Table 3-3, Entries 1 - 5). Ethanol was converted stably until 72 h to reach a plateau of 57%, extending time to 96 h, ethanol conversion kept unchanged but yields of products still increased, and at the end, 22.3% total C3 - C7 secondary alcohols were achieved plus 3% 1-butanol. More experiments indicated that higher base loading (25 mol%) would make the reaction turn non-homogeneous, and cause reactor burden and potential reaction hazards. The yields of secondary were also reduced (Entry 6). These results indicated that **Ru-1** was not suitable for the production of primary alcohols, but on the contrary, it was friendly for secondary alcohols. So, I tried to use the classical base,[225,58,60] NaOEt, used as the Guerbet reaction for the reactions afterward. I also found that there was a little overflow of catalyst at 1000 ppm, hence, decreasing to 250 ppm with NaOEt, still could get 9.6% 2-butanol and 16.6% total secondary alcohols (Entry 7). It turned out that the catalyst itself determines the course of the reaction rather than the base.

Table 3-3: Low temperature, time-based ethanol upgrading with **Ru-1**.

| Entry | t [h] | Conv. [%][a] | | | Yields [%][a] | | | |

			2a	2b	2c	2d	2e	Total 2	1	3	4
1	4	23	1.3	5.3	0.4	1.2	-[d]	8.2	1.9	-	0.25
2	19	40	0.8	7.5	0.4	3.0	0.1	11.8	2.7	-	-
3	48	43	1.6	7.5	0.9	2.6	<0.1	12.6	1.9	-	0.09
4	72	57	2.3	10.3	1.5	4.6	0.2	18.9	2.4	-	0.08
5	96	57	2.7	11.5	2.0	5.8	0.3	22.3	3.0	-	0.16
6[b]	96	53	0.9	5.4	0.7	2.3	<0.1	9.3	1.6	-	-
7[c]	96	57	2.0	9.6	1.3	3.6	0.1	16.6	3.0	0.8	-

Reaction conditions: 5 mL EtOH in a high-pressure reactor at 115 °C, 250-1000 ppm **Ru-1**, 20-25 mol% base, 4-96 h, 600 rpm.

[a] Determined by GC-TCD (H_2), GC-FID (liquid phase products), GC-MS (liquid phase products, organic gases), and Micro-GC (H_2 and organic gases). [b] 25 mol% NaO*t*Bu. [c] 250 ppm **Ru-1**. 20 mol% NaOEt. [d] <0.1% yield.

Immediately after the preliminary results above, time-based ethanol upgrading reactions of 250 ppm **Ru-2** with 20 mol% NaOEt were tested. Moreover, besides the liquid-phase products, gas-phase, and solid-phase products were investigated too. Often, NaOAc is observed as a side product in traditional ethanol upgrading.[57] The Cannizzaro or Tishchenko mechanisms[58] or the dehydrogenative pathway[226] could be responsible for its formation. Indeed, I also detected NaOAc. It precipitated under the reaction conditions, and after 96 h, NaOAc was observed with a yield of 11% when using **Ru-2** (Table 3-4, Entry 5). It is worth mentioning that the formation of NaOAc started in the early stage of the reaction, indicating that water formation, likely from the Aldol condensation, also occurs swiftly. Moreover, the results in Table 3-4 suggest a different, and less straightforward, relationship between catalyst structure and NaOAc selectivity than what was observed for alcohol production. H_2 is the source of most of the pressure, with yields of less than 5% for *trans*, *cis*-2-butene, and butane.

Table 3-4: Low temperature, time-based ethanol upgrading with **Ru-2**.

Entry	t [h]	Conv. [%][a]	Yields [%][a]										
			2a	2b	2c	2d	2e	Total 2	1	3	4	H$_2$	NaOAc
1	4	16	-[b]	2.4	0.2	0.5	-	3.1	1.2	-	-	[c]	
2	24	40	1.2	5.8	0.5	1.5	-	9	2.1	-	0.15	15.6	
3	48	41	1.3	6.7	0.5	1.7	-	10.2	1.9	-	0.12	18.7	
4	72	44	2.0	11.1	1.3	4.2	0.1	18.7	2.8	-	-		
5	96	55	0.6	12.3	1.4	3.9	-	18.2	2.5	-	-	25.1	10.6

Reaction conditions: 5 mL EtOH in a high-pressure reactor at 115 °C, 250 ppm **Ru-2**, 20 mol% base, 4-96 h, 600 rpm.

[a] Determined by NMR (NaOAc), GC-TCD (H$_2$), GC-FID (liquid phase products), GC-MS (liquid phase products, organic gases), and Micro-GC (H$_2$ and organic gases). [b] <0.1% yield. [c] not determined.

Figure 3.1 depicts the time-dependent conversion of ethanol and production of 2-butanol as well as all combined secondary alcohols with 250 ppm **Ru-2** (Table 3-4, Entries 1 – 5). It shows a steady increase in the formation of secondary alcohols, with 2-butanol as the major product in solution, until it reaches a plateau after approximately 72 h. Likewise, ethanol is steadily converted, and its conversion is at all times higher than the amount of formed liquid-phase products. In addition, it continues to be converted after 72 h. Apart from the main secondary alcohols produced, small amounts of ethyl acetate, diethoxymethane, ketones, C5-C7 branched alcohols, and C9+ secondary alcohols and even some aromatics were produced and for the gas phase, the trace of methane and/or ethane were also observed, depending on the reaction conditions.
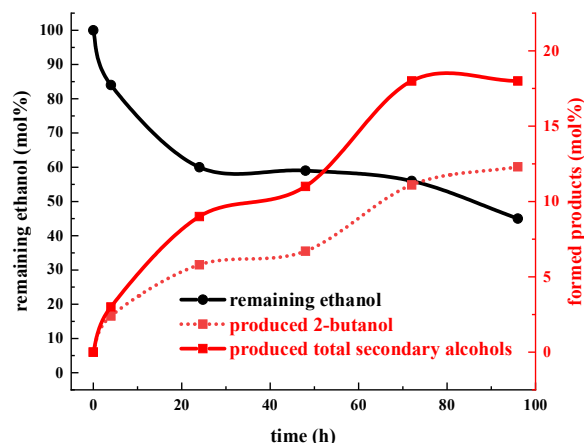
Figure 3.1: Ethanol conversion and production of 2-butanol and other secondary alcohols over time.

The catalysts **Ru-3** and **Ru-4** containing semi-bulky and alkyl-based *i*-propyl and cyclohexyl *P*-substituents, **Ru-5** containing the bulky alkyl-based *t*-butyl *P*-substituents were investigated under optimal conditions mentioned before. We can clearly know, that after changing the auxiliary ligands, the alcohol products became unselective with **Ru-3** and **Ru-4**, while **Ru-5** gave almost exclusively primary alcohols (Table 3-5, Entries 1 - 3).

Table 3-5: Low temperature, ethanol upgrading with **Ru-3 – 5**.
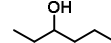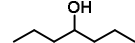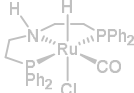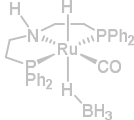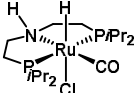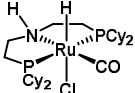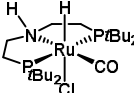
Entry	Cat.	Conv. [%][a]	Yields [%][a]										
			2a	**2b**	**2c**	**2d**	**2e**	**Total 2**	**1**	**3**	**4**	**H$_2$**	**NaOAc**
1	**Ru-3**	27	0.6	3.0	0.3	1.0	–[b]	4.9	5.2	-	-	17.5	4.0

2	Ru-4	26	0.7	3.8	0.4	1.5	-	6.4	5.3	-	-	22.3	8.9
3[c]	Ru-5	42	-	-	-	-	-	-	12.9	-	-	12.8	[d]

Reaction conditions: 5 mL EtOH in a high-pressure reactor at 115 °C, 250 ppm [Ru], 20 mol% base, 96 h, 600 rpm.

[a] Determined by NMR (NaOAc), GC-TCD (H²), GC-FID (liquid phase products), GC-MS (liquid phase products, organic gases), and Micro-GC (H₂ and organic gases). [b] <0.1% yield. [c] 0.4 % of 2-ethyl-1-butanol and 0.9 % of 1-hexanol were also determined. [d] not determined.

Along with the results above, Ru-PNP complexes with less bulky and aryl-based phenyl substituted phosphines are proved to tend to produce novel secondary alcohols and potential hydrocarbons, while bulky alkyl-based *t*-butyl *P*-substituents are proved to exclusively produce traditional primary alcohols, hence, around with **Ru-2** and **Ru-5**, I conducted a set of temperature enhancement experiments, which were shown in Table 3-6.

Table 3-6: Ethanol upgrading with **Ru-1**, **2**, and **5** at 130 °C.

Entry	Cat.	t [h]	Conv. [%][a]	Yields [%][a]											
				2a	2b	2c	2d	2e	Total 2	1	3	4	H₂	NaOAc	butane
1[b]	Ru-1	96	60	1.2	5.8	0.7	2.0	-[c]	9.7	3.0	-	-	22.2	[d]	
2[b]	Ru-2	96	86	0.9	4.1	0.8	2.3	-	8.1	4.1	-	-	31.1		4.7
3	Ru-2	96	68	1.4	7.1	0.3	1.2	-	10.0	2.6	-	-	26.0	15.9	2.7
4[e]	Ru-5	168	32	0.3	0.8	0.2	0.4	-	1.7	7.8	-	-	11.5	4.6	
5[f]	Ru-5	24	33	-	0.9	-	-	-	0.9	17.6	-	-	12.5	5.2	2.4
6[g]	Ru-5	96	49	-	1.0	-	-	-	1	22.1	-	-	20.4		

Reaction conditions: 2.5 mL EtOH in a high-pressure Parr reactor at 130 ℃ and 160 ℃, 8.3-250 ppm [**Ru**], 20 mol% base, 24-168 h, 600 rpm.

[a] Determined by NMR (NaOAc), GC-TCD (H_2), GC-FID (liquid phase products), GC-MS (liquid phase products, organic gases), and Micro-GC (H_2 and organic gases). [b] reaction temperature, 160 ℃. [c] <0.1% yield. [d] not determined. [e] 8.3 ppm **Ru-2**. [f] 0.6 % of 2-ethyl-1-butanol and 2.2 % of 1-hexanol were also determined. [g] 0.9 % of 2-ethyl-1-butanol and 3.0 % of 1-hexanol were also determined.

The results turned out that at 130 ℃, butenes were fully hydrogenated and only butane was observed, again, H_2 was the major component of the gas phase. Interestingly, increasing the reaction temperature to 130 ℃ or 160 ℃ led to a decrease in longer-chain secondary alcohol production (Entries 1 - 3). Extending the reaction time to 168 h gave 32% conversion, with 7.8% 1-butanol yield (Entry 4) and with the observation of hexane, albeit not quantified (Appendix A). For **Ru-5**, from 24 to 96 h, 1-butanol yield increased from 17.6 to 22.1% (Entries 5 and 6).
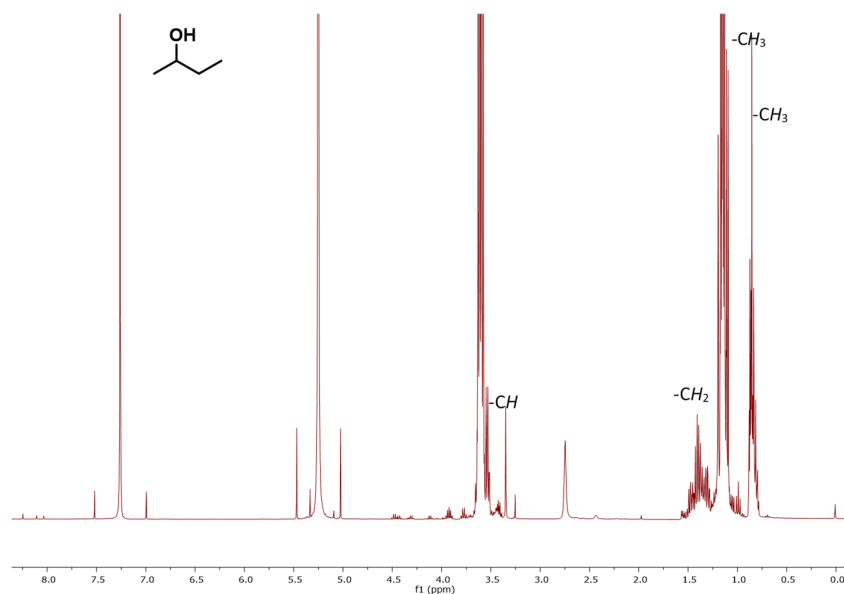
Figure 3.2: ^{1}H NMR of the reaction mixture (400 MHz, CDCl$_3$ at 25 ℃, Table 3-4, Entry 5).

Figure 3.3: ^{13}C NMR of the reaction mixture (100.62 MHz, CDCl$_3$ at 25 °C, Table 3-4, Entry 5).
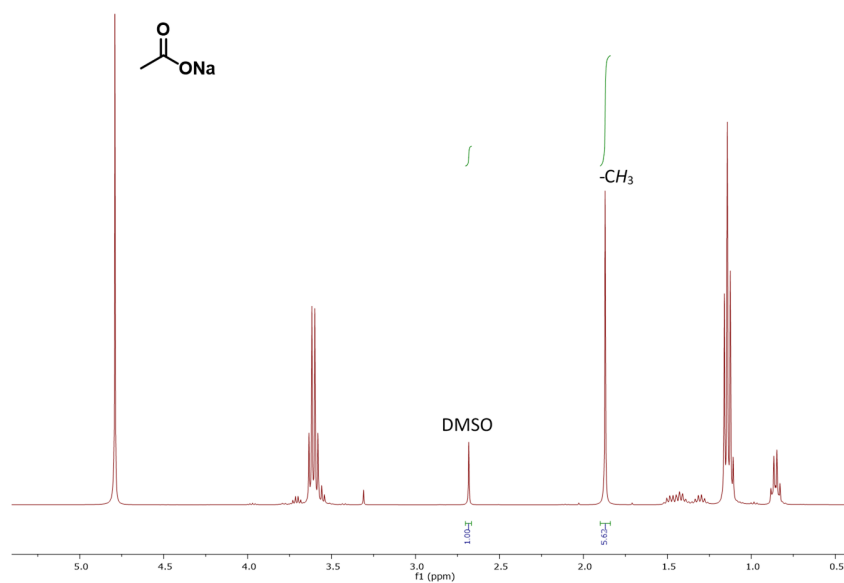
Figure 3.4: ^{1}H NMR of sodium acetate quantification (DMSO as internal standard, 400 MHz, D$_2$O at 25 °C, Table 3-6, Entry 3).
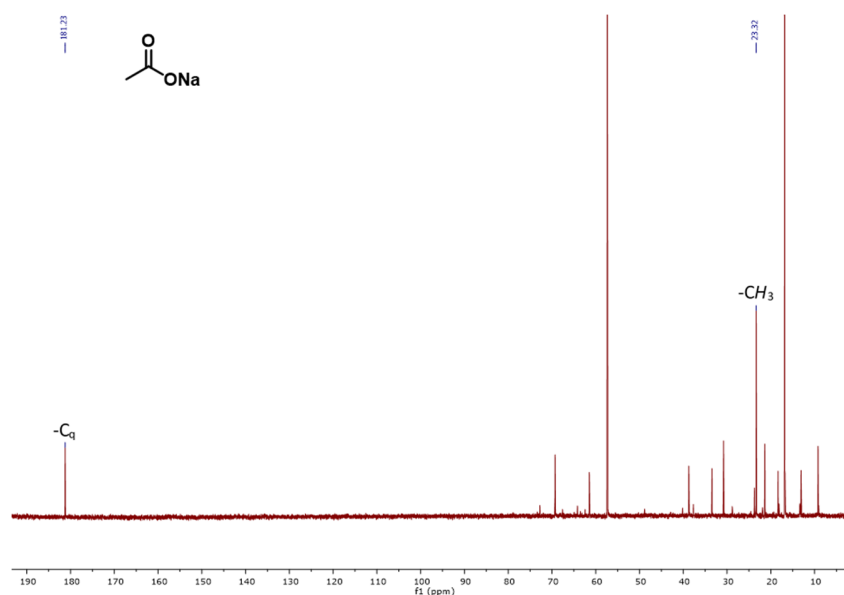
Figure 3.5: ^{13}C NMR of sodium acetate quantification (100.62 MHz, D$_2$O at 25 °C, Table 3-6, Entry 3).

3.1.3 Mechanistic studies

After the experimental section was done, a related mechanistic study was necessary. Before that, the selectivity between primary (1°) and secondary (2°) alcohols have been introduced. The specific calculation method is: from the same reaction, the selectivity of primary and secondary alcohols are obtained separately, and then their summation values are used as the denominator, and the respective selectivity is used as the denominator, and then the final result in the calculation, as shown in Equations 3.1 and 3.2.

$$selectivity\ (1°) = \frac{yield\ (1°)/_{conversion}}{yield\ (1°)/_{conversion} + yield\ (2°)/_{conversion}} \tag{3.1}$$

$$selectivity\ (2°) = \frac{yield\ (2°)/_{conversion}}{yield\ (1°)/_{conversion} + yield\ (2°)/_{conversion}} \tag{3.2}$$

As Figure 3.6 shows, the selectivity between 1° and 2° alcohols changes drastically depending on the choice of catalyst. For example, the catalysts **Ru-1** and **Ru-2** containing less bulky phenyl (Ph) substituted phosphines afford mainly secondary alcohols, whereas **Ru-3** and **Ru-4** containing semi-bulky i-propyl (-iPr) and cyclohexyl (-Cy) P-substituents, respectively, provide practically

43

no selectivity. Finally, **Ru-5** containing the bulky *t*-butyl (-*t*Bu) *P*-substituents gives almost exclusively primary alcohols.
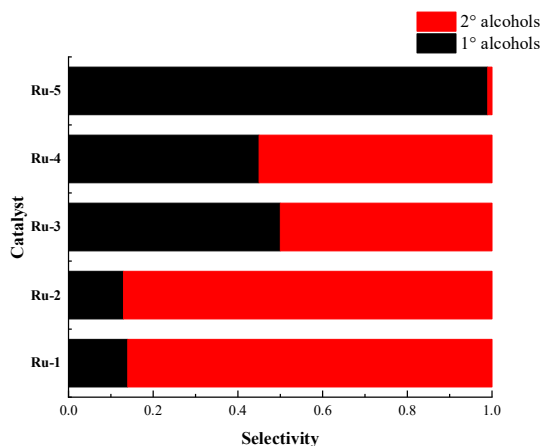
Figure 3.6: Distribution of 1º and 2º alcohols using **Ru-1** to **Ru-5** under optimal conditions in each reaction.

As in the typical Guerbet-type ethanol upgrading, this system also relies on generating acetaldol by the Aldol reaction of two acetaldehyde molecules, initially formed by ethanol dehydrogenation (Scheme 3.3). Typically acetaldol then proceeds to dehydrate to crotonaldehyde and water followed by hydrogenation to 1-butanol (grey-colored route). However, here we observe a competing reaction that likely involves a dehydrogenation/hydrogenation process to the novel key intermediate 4-hydroxy-2-butanone. This intermediate then undergoes dehydration to yield MVK and water, and hydrogenation of MVK yields 2-butanol. We suggest that the given reaction conditions are, to some extent, capable of inducing dehydration of 2-butanol to 2-butenes, which are then finally hydrogenated to butane. The water is likely responsible for the observation of NaOAc, which also provides the necessary excess of H_2 for hydrogenating the 2-butenes to butane.
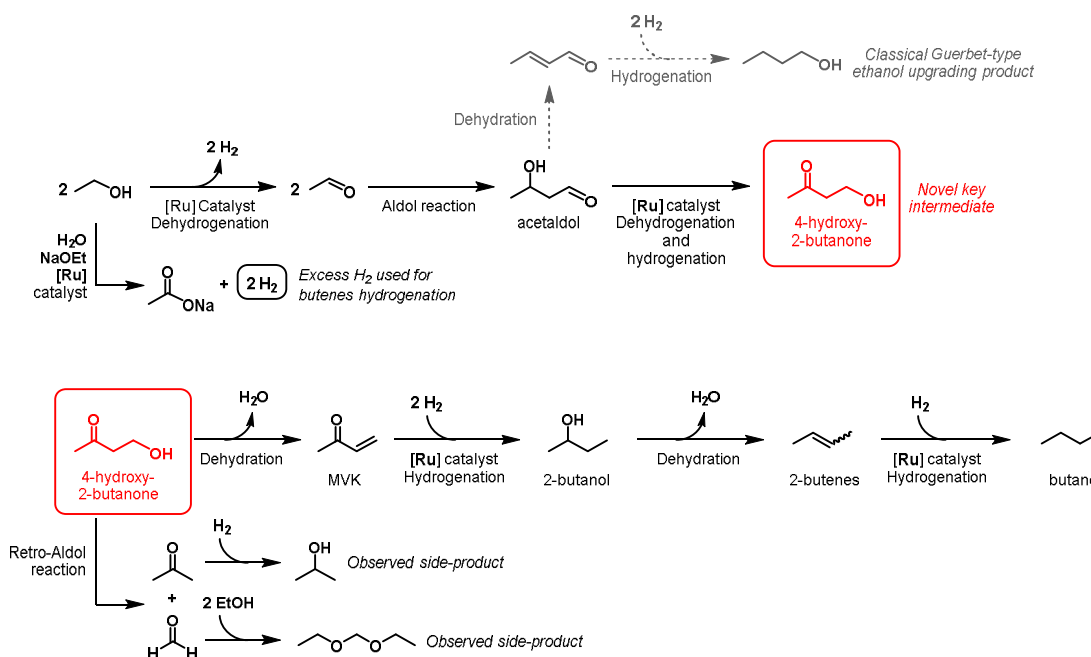
Scheme 3.3: Proposed mechanism for the novel transformation of ethanol to 2-butanol, 2-butenes, and butane.

To further validate our hypothesis of 4-hydroxy-2-butanone comprising a novel key intermediate towards secondary alcohols and hydrocarbons, some qualitative test reactions were performed with this compound as substrate and **Ru-2** as the catalyst at 115 ℃ in the presence of 22 bar of H_2 (Table 3-7). Using an excess of 4-hydroxy-2-butanone to H_2 led to the formation of MVK and a minor amount of 2-butanol along with almost complete consumption of H_2 (Entry 1). There was a large amount of 4-hydroxy-2-butanone remaining, and 2-butanone and acetone were also observed. As a note, several different long-carbon products were observed as well. On the contrary, when H_2 is in excess, 2-butanol and 1,3-butanediol were produced as two main products, and trace amounts of butenes/butane were found in the gas phase (Entry 2). Moreover, there was still H_2 left at the end of the reaction (7 bar pressure). Finally, the addition of 20 mol% NaOAc was also tested (Entry 3). Acetone, 2-butanone, and 2-butanol were produced and almost no H_2 pressure was left while some 4-hydroxy-2-butanone remained. These results corroborate the hypothesis that 4-hydroxy 2 butanone is the key intermediate towards 2-butanol or butenes/butane.

Table 3-7: Mechanistic tests with 4-hydroxy-2-butanone as substrate.

Entry	Additive (mol%)	4-hydroxy-2-butanone [mL]	GC-MS observed products[a]					
			acetone	methyl vinyl ketone	2-butanone	2-butanol	1,3-butanediol	butenes /butane
1	/	5	√	√	√	√	×	×
2	/	2.5	×	×	×	√	√	√
3	NaOAc (20)	2.5	√	×	√	√	×	×

Reaction conditions: 2.5-5mL 4-hydroxy-2-butanone, 250 ppm **Ru-2**, with or without 20 mol% NaOAc, 115 ºC, 24 h, high-pressure reactor, 600 rpm. [a] Determined by GC-MS. See appendix for more products.

3.1.4 Summary

In conclusion, I present significant differences in the selectivity of different auxiliary ligands for ethanol upgrading. Hence, I disclose fundamentally new insights into the carbon chain growth of ethanol upgrading, providing a novel pathway leading to highly valuable secondary alcohols and even hydrocarbons. I demonstrate that low catalyst loading of **Ru-2** (250 ppm) with NaOEt (20 mol%) at 115 ºC is suitable for the production of 2-butanol. Up to 12% of 2-butanol (TON of 480), 4% of 3-hexanol (TON of 160) and a combined 18% of all secondary alcohols (TON of 720) can be achieved. In addition to 2-butanol and 3-hexanol, 2-butenes/butane and NaOAc comprise the main products. Catalyst **Ru-5** primarily follows the traditional Guerbet reaction and produces 22% of 1-butanol. This work represents the first example of a homogeneous catalytic system to produce 2-butanol as well as higher secondary alcohols and hydrocarbons from ethanol. Finally, a new mechanism for the selective production of these novel products from ethanol upgrading is suggested.

3.2 Solvent effects on acceptorless dehydrogenative coupling of ethanol

3.2.1 General information

In this Chapter, I will formally conduct a discussion of solvent effects on the acceptorless dehydrogenative coupling of ethanol. Herein, consistent with what has been mentioned before, around Ru-MACHO-BH (**Ru-1**), the remaining five ruthenium-based (**Ru-2 - 6**) compounds and one iridium-based (**Ir-1**) compound were introduced to test ethanol dehydrogenation properties (Scheme 3.4).
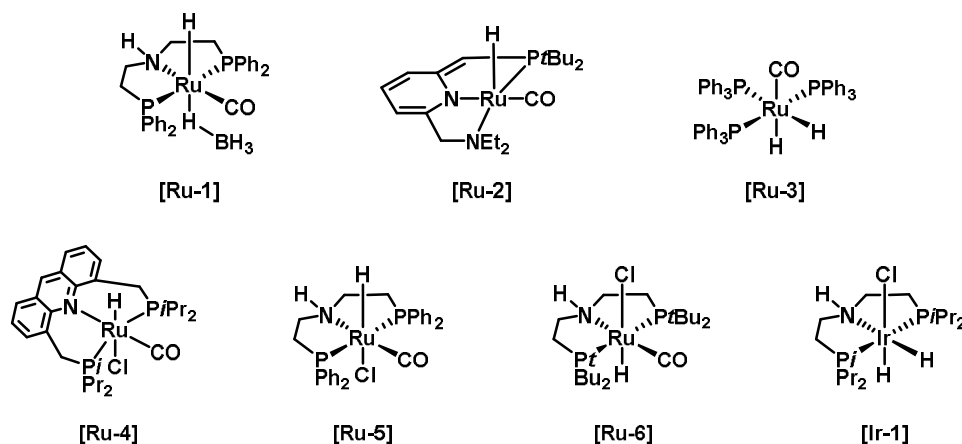
Scheme 3.4: Used catalysts for acceptorless dehydrogenative coupling of ethanol.

Sixteen cyclic compounds were added as co-solvents to improve both solubilities of the catalyst and conversion rate, including aromatics, halo-aromatics, cycloalkanes, ethers, and heterocyclic. (Figure 3.7). These compounds with decent boiling points cover the range from highly polar to nonpolar and are useful for the study of dehydrogenation of ethanol systems.
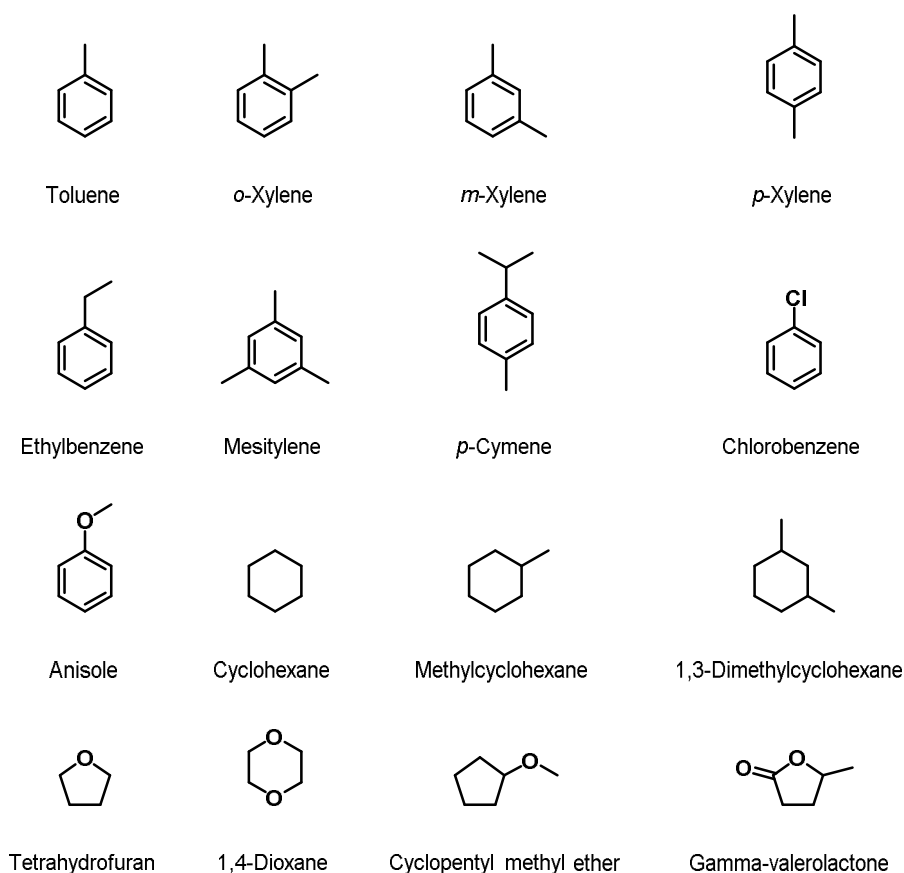
Figure 3.7: Used co-solvents for acceptorless dehydrogenative coupling of ethanol.

Table 3-8 concluded the properties of different solvents, including boiling point and dielectric constant. It was arranged according to the dielectric constant from smallest to largest, which means that the polarity of the solvent gets stronger as you go down the list.

Table 3-8: Properties of different solvents.[§§]

Solvent	Boiling point (^{o}C)	Dielectric constant (20 ^{o}C)
cyclohexane	80.8	2.02
methylcyclohexane	101	2.02
1,3-dimethylcyclohexane	120-125	/

[§§] Liquids - Dielectric Constants. *Engineeringtoolbox.com* (2022). at <https://www.engineeringtoolbox.com/liquid-dielectric-constants-d_1263.html>

Frontier, A. Reagents & Solvents. *Chem.rochester.edu* (2022). at <https://www.chem.rochester.edu/notvoodoo/pages/reagents.php?page=solvent_polarity>

p-xylene	138.4	2.27
p-cymene	177	2.3
toluene	110.6	2.4
1,4-dioxane	101	2.2 (25 °C)
m-xylene	139	2.36
ethylbenzene	136	2.5
o-xylene	144	2.56
mesitylene	164.7	2.4-3.4
anisole	153.8	4.3
cyclopentyl methyl ether	106	4.76 (25 °C)
chlorobenzene	132	5.6 (25 °C)
tetrahydrofuran	66	7.58 (25 °C)
acetaldehyde	20.2	21.8 (18 °C)
ethanol	78.4	24.5
γ-valerolactone	207	36.47 (25 °C)

As one of the acid derivates, ester occupies an important place in the field of chemical research. In the homogeneous catalytic field, alkoxycarbonylation/carbonylation processes under CO/CO_2 pressure,[227–229] and acceptorless dehydrogenative coupling of alcohols[121,153,132] are two main modern production methods. However, considering environmentally benign, low cost, and safe production, ADC is attracting huge interest both in industry and academia. ADC-based reactions involve dehydrogenation, with the generation of hydrogen gas and water[230] followed by coupling of the dehydrogenated intermediate with another substrate to generate value-added products.[231]

This kind of reaction is the foundation for efficient, atom economic, sustainable, and environmentally benign synthetic methodology to construct carbon-carbon and carbon-heteroatom bonds.[232] The low-cost and non-toxic ethanol (EtOH) availability has offered the opportunity to develop useful chemical processes for the production of different chemicals such as ethylene,[233] diethyl ether,[234] acetaldehyde,[235] and ethyl acetate using ethanol as raw material. With the excessive consumption of fossil fuels, the dehydrogenation of biomass-related alcohols, such as

bioethanol, is gaining attention, and the conversion of these primary alcohols is more difficult than that of aromatic alcohols, and academic interest is gradually moving in this direction. In this sense, the production of ethyl acetate is highly relevant in the industry with an estimated annual 1.7 million tons produced worldwide in 2013.[155] This basic short-chain ester is widely used in the synthesis of biodiesel, paints, adhesives, herbicides, and resins.[236,237] Conventionally, ethyl acetate is produced by Fischer–Speier esterification, refluxing acetic acid, and ethanol in the presence of concentrated sulfuric acid.[155] However, the addition of concentrated sulfuric acid generates toxic waste, representing an environmental issue. The process is thermodynamically reversible with slow reaction rates.[238]

The order of the discussion in this Chapter is such that the experimental part is given first as well as an explanation of the mechanisms behind the possible causes of these results.

3.2.2 Experimental results and discussion

The study started with the benchmark reaction for the ADC of ethanol (2 mL) to ethyl acetate with **Ru-1** (0.05 mol%) complex and without any co-solvent (Table 3-9). After 24 h at 120 ℃, the reaction afforded moderate conversion of 43% and 34% yield (Entry 1). Interestingly, the conversion remained similar when extending the reaction time to 48 h. This type of experiment without additional solvent will have a large amount of catalyst spillage, meaning that the results obtained depend on how much catalyst is actually involved in the reaction, which is why there is float. This point is related to the fact that the previously mentioned organometallic complexes have limited solubility in pure organic liquids.

Table 3-9: Initial attempts for ethanol conversion to ethyl acetate with **Ru-1**.

Entry	Solvent	Time [h]	Conversion [%][a]	Yield [%][a]	Selectivity [%]
1	/	24	43	34	79
2	/	48	42	31	74

[a] determined by NMR, dimethyl sulfoxide is an internal standard.

Hence, a co-solvent was added to improve both solubilities of the catalyst and conversion. We firstly introduced toluene as a co-solvent since it has a suitable boiling point (110 $^{\circ}$C) for this process. Then the addition of 10 mL toluene led to the stable conversion (43%, Appendix B). Our observations suggest that the polarity and boiling point of the co-solvent could affect the ethanol dehydrogenation process and the conversion rate. During the course of the reaction, the formation of the intermediates and their solubility differs dramatically with the different boiling points of the solvents.

I enlarged **Ru-1** loading to 0.01 mol%, Table 3-10 concluded ethanol conversion results by adding 10 mL of different co-solvents at 120 $^{\circ}$C for 24 h.

Table 3-10: Screening of different organic solvents in ethanol conversion with **Ru-1**.

$$2 \diagup\diagdown_{OH} \xrightarrow[\substack{\text{0.1 mol\% \textbf{Ru-1}} \\ \text{v(ethanol:co-solvent) = 1:5}}]{\text{24 h, 120 °C}} \text{(ethyl acetate)} + 2\,H_2$$

Entry	Solvent	Conversion [%][a]	Yield [%][a]	Selectivity [%]
1	cyclohexane	52	50	96
2	methylcyclohexane	55	50	91
3	1,3-dimethylcyclohexane	51	46	90
4	*p*-xylene	40	27	68
5	*p*-cymene	66	53	80
6	toluene	63	46	73
7	1,4-dioxane	53	41	77
8	*m*-xylene	87	79	91
9	ethylbenzene	68	55	81
10	*o*-xylene	58	51	88
11	mesitylene	30	15	50
12	anisole	61	49	80
13	cyclopentyl methyl ether	52	46	88
14	chlorobenzene	10	5	50

| 15 | tetrahydrofuran | 22 | 20 | 91 |
| 16 | γ-valerolactone | 12 | 7 | 58 |

[a] determined by NMR, dimethyl sulfoxide is an internal standard.

Among them, high polarity seemed to be unfavorable for the reactions. For example, haloaromatic solvents such as chlorobenzene showed only 10% conversion and 5% yield (Entry 14) under the actual reaction conditions. Followed by γ-valerolactone (Entry 16, 12% conversion, 7% yield) and tetrahydrofuran (Entry 15, 22% conversion, 20% yield). 1,4-dioxane (Entry 7, two lactones, 53% conversion, 41% yield) or cyclopentyl methyl ether (Entry 13, ectone compound, 52% conversion, 46% yield) provided similar results. Moreover, extending the reaction time to 48 h, except for the still elevated yield in the presence of tetrahydrofuran, the rest of the results did not differ from those at 24 h, showing that the reaction had stopped (Appendix B).

For cycloalkanes and their derivatives, with non-polar backgrounds, the number of methyls would not affect the conversion according to the investigations. Cyclohexane (Entry 1, 52% conversion, 50% yield, 96% selectivity), methylcyclohexane (Entry 2, 55% conversion, 50% yield, 91% selectivity), 1,3-dimethylcyclohexane (Entry 3, 51% conversion, 46% yield, 90% selectivity) almost showed the same results with high selectivity. It is worth mentioning that 0.1 mol% **Ru-1** overflowed in the above three solvents. This point is a good entry point to explore the factor of low catalyst introduction, and more relevant experiments will be given.

For aromatics, toluene as a basic solvent with a proper boiling point provided 63% conversion and 46% yield (Entry 6). After adding another methyl group directly to the benzene ring, *m*-xylene (Entry 8, 87% conversion, 79% yield, 91% selectivity) was the best compared to *o*-xylene (Entry 10, 58% conversion, 51% yield) and *p*-xylene (Entry 4, 40% conversion, 27% yield). Instead of methyl groups, anisole showed 61% conversion and 49% yield (Entry 12). Moreover, compared to polarity, basic functional groups have little effect on the conversion. Mesitylene (three methyl groups), ethylbenzene (ethyl group), or *p*-cymene (a more complicated combination) showed 30% conversion & 15% yield (Entry 11), 68% conversion & 55% yield (Entry 9), 66% conversion & 53% yield (Entry 5), respectively.

On basis of the excellent output with the addition of some co-solvents, a group of experiments in extending time have been performed and shown in Table 3-11. For cyclohexanes and their derivatives, considering they have the same properties, after getting the 48 h reaction results of cyclohexane, which turned out that the reaction has stopped compared to that for 24 h (Entry 1). It indicated that for them, it was a catalyst loading-dependent system. Likewise, 1,4-dioxane, ethylbenzene, and cyclopentyl methyl ether showed the same results for 48 h compared to 24 h (Entries 4, 6, and 8). The conversion and yield continuously were improved with toluene as a co-solvent and got 92% and 86% for 72 h (Entries 2 and 3). *m*-xylene was an excellent co-solvent based on the previous results and extending time to 48 h, 95% conversion and 76% yield were achieved (Entry 5), it was noteworthy that there was a large loss between conversion and yield. With anisole for 48 h, the conversion and yield increased a little bit to 73% and 57% (Entry 7) while with toluene under the same conditions, the output drastically went up to 63% and 58% (Entry 9), further extending to 72 h, the results kept unchanged (Entry 10). These results turned out that some of the co-solvent catalytic systems would rely on the catalyst, once the catalyst amount was not sufficient or the catalytic cycle was off then the reaction just stopped.

Table 3-11: Long-time tests of ADC of ethanol with **Ru-1**.

Entry	Solvent	Time [h]	Conversion [%][a]	Yield [%][a]	Selectivity [%]
1	cyclohexane	48	51	34	67
2	toluene	48	72	52	72
3	toluene	72	92	86	93
4	1,4-dioxane	48	59	43	73
5	*m*-xylene	48	95	76	80
6	ethylbenzene	48	72	55	76
7	anisole	48	73	57	78
8	cyclopentyl methyl ether	48	56	45	80
9	tetrahydrofuran	48	63	58	92

| 10 | tetrahydrofuran | 72 | 65 | 63 | 97 |

[a] determined by NMR, dimethyl sulfoxide is an internal standard.

According to the results above, we proposed a plausible reason to explain them. Numerous **Ru-1** will stay in the solid phase and will not contact the substrate since the limited solubility in pure ethanol. More **Ru-1** can enter the liquid phase when solvents with less polarity are added to the catalytic system due to the increasing solubility. Even if ethanol is more polarized and solvents are less polar, the exchange rating of **Ru-1** is faster than that of **Ru-1** in the solid phase to pure ethanol. Hence, more **Ru-1** will react with ethanol. If solvents with high polarity are added to the system, the more polar, the more difficult it is for **Ru-1** to enter the liquid phase (first step), and the less contact between **Ru-1** and ethanol.

After finishing the two rounds of discussion, for co-solvents that can potentially be further optimized (according to the conversion, yield, selectivity, etc. they give), the actual results are studied by varying the temperature profile, the amount of catalyst introduced, and the amount of co-solvent added (to adjust the boiling point of the mixture, which changes the intensity of the reaction.). Therefore, toluene and cyclohexane were used as excellent co-solvents for further optimization (Table 3-12).

Table 3-12: Optimization of ADC of ethanol.

Entry	Solvent	Ratio	**Ru-1** [mol%]	Time [h]	Conversion [%][a]	Yield [%][a]	Selectivity [%]
1	toluene	1.25	0.1	24	98	92	94
2	toluene	2.5	0.1	24	91	87	96
3	toluene	5	0.1	24	63	46	73
4	toluene	7.5	0.1	24	53	52	98
5[b]	toluene	1.25	0.1	24	37	34	92
6	toluene	1.25	0.05	24	47	43	91
7	toluene	1.25	0.1	18	89	84	94

8	cyclohexane	5	0.05	24	25	25	100
9	cyclohexane	5	0.1	24	52	50	96
10	cyclohexane	5	0.1	48	51	34	67

[a] Determined by NMR, dimethyl sulfoxide is an internal standard. [b] temperature, 100 ºC.

For the analysis of the results of toluene volume addition, it can be seen that at 24 h, the best volume ratio between ethanol and toluene was 1.25 (Entry 1, 98% conversion, 92% yield), compared to other ratios (Entries 2 - 4). It was worth mentioning that the catalyst could not completely be dissolved under 1.25 ratio conditions. In this case, a low-temperature 100 ºC reaction was performed (Entry 5), but it turned out that only 37% conversion was achieved, likely since the solubility also decreased with the temperature. In addition, lowering **Ru-1** to 0.05 mol% (still not fully dissolved) caused a halving of conversion and yield (Entry 6). Continually decreasing reaction time to 18 h with 0.1 mol% **Ru-1**, the conversion and yield showed a downtrend to 89% and 84% (Entry 7).

For cyclohexane series compounds, 0.1 mol% of them could not fully be soluble in the reaction, but they can provide decent results as mentioned above. Hence, it is necessary to further study this co-solvent. I decreased **Ru-1** loading to 0.05 mol% (Entry 8), unfortunately, the corresponding conversion and yield fell in equal proportion compared to 0.1 mol% (Entry 9). While extending the reaction time to 48 h (Entry 10), like most other co-solvents, the results remained the same. This result again demonstrates the critical importance of the amount of catalyst introduction in this system.

In terms of co-solvent, toluene, Figure 3.8, Figure 3.9, and Figure 3.10 offered conversion of ethanol and the corresponding yield and selectivity of ethyl acetate under the different chemical environments with toluene. The first two pictures showed that using 10 mL co-solvent, **Ru-1** loading was important and even though over 90% conversion was achieved, a long reaction time (72 h) was indispensable. After adjusting the volume ratio between ethanol and toluene to 1.25, the conversion rate drastically went up, and the addition of more toluene was not beneficial to the catalytic system.
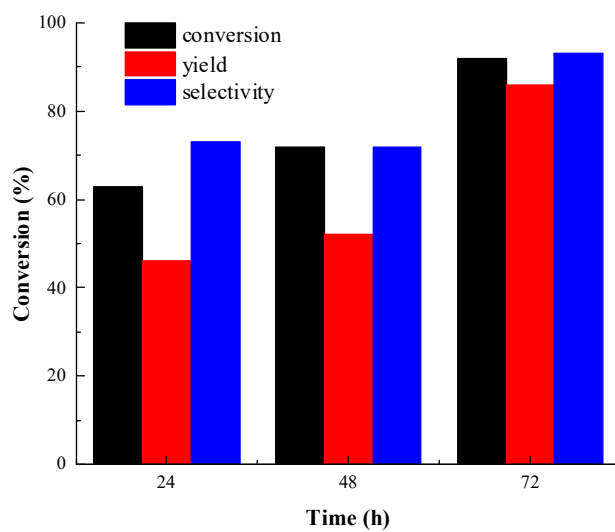
Figure 3.8: Time-based ADC of ethanol (Reacton conditions: 2 mL EtOH, 10 mL toluene, 0.1 mol% **Ru-1**, 120 °C).
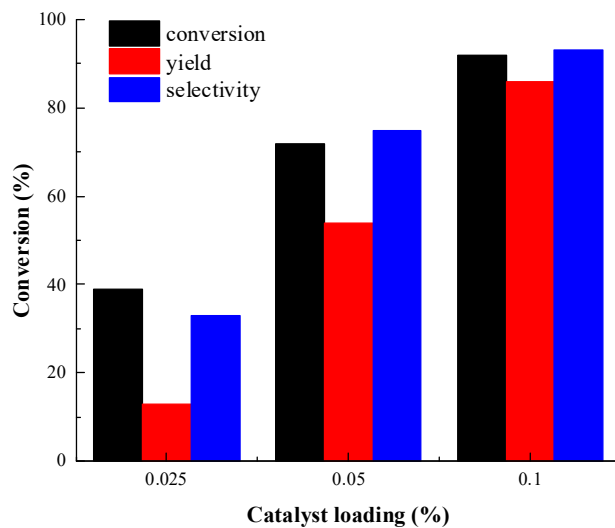
Figure 3.9: **Ru-1** loading-based ADC of ethanol (Reacton conditions: 2 mL EtOH, 10 mL toluene, 120 °C, 72 h).
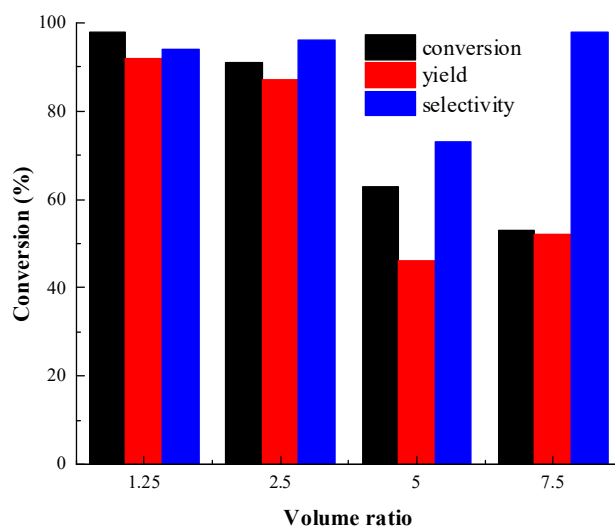
Figure 3.10: Volume ratio-based ADC of ethanol (Reacton conditions: 2 mL EtOH, 2.5 - 15 mL toluene, 0.1 mol% **Ru-1**, 120 °C, 24 h).

Again, the ratio value 1.25 and 24 h was proved to be the optimal condition. Based on these findings, Figure 3.11 and Figure 3.12 gave the NMR spectra under optimal conditions.
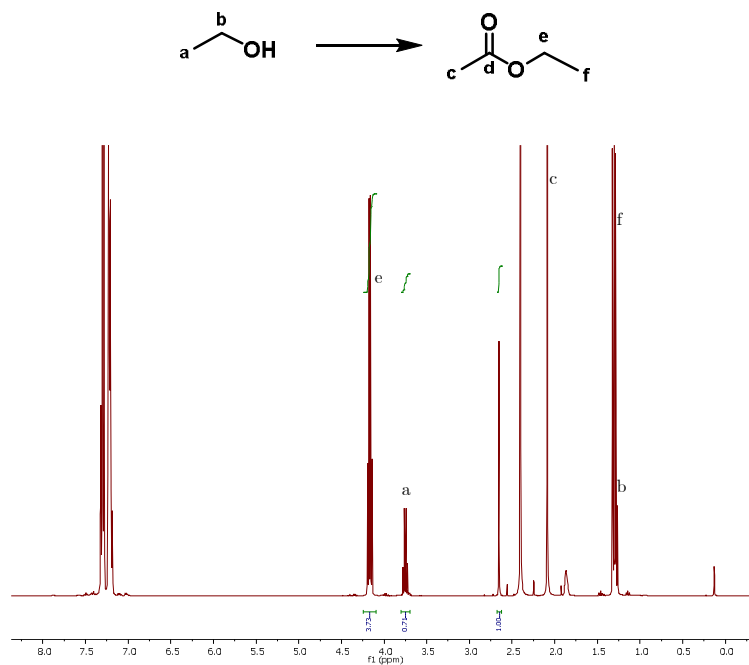
Figure 3.11: ^{1}H NMR of acceptorless dehydrogenation of ethanol to ethyl acetate with toluene (CDCl$_3$, 25 °C, 400 MHz, Table 3-11, Entry 1).
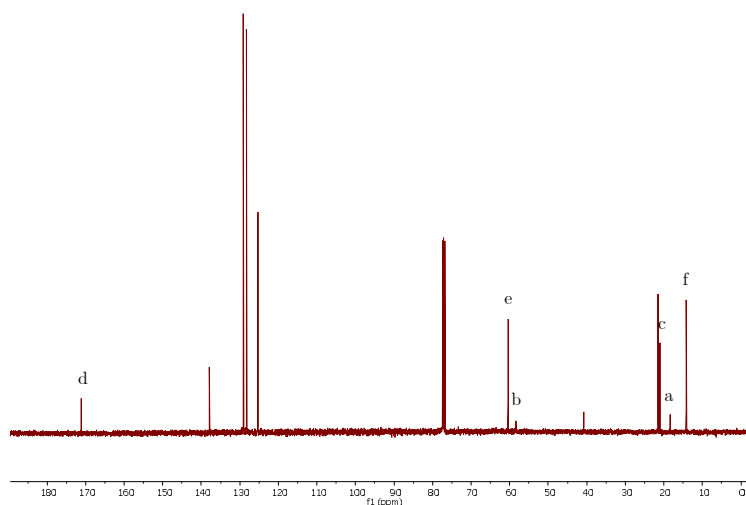
Figure 3.12: ^{13}C NMR of acceptorless dehydrogenation of ethanol to ethyl acetate with toluene (CDCl$_3$, 25 ºC, 100.62 MHz, Table 3-11, Entry 1).

In the last stage of the experimental part, I investigated other catalysts in ethanol conversion with toluene, which is the best co-solvent according to the screening. Appendix B showed the results, and most of them need an extra base or acid to activate the catalysts themselves. **Ru-2** is an activated catalyst, giving a limited conversion mainly because it needs a higher reaction temperature.[239]

3.2.3 Additional tests

Here, some additional tests and results will be given that are different from the acceptorless dehydrogenation of ethanol to produce ethyl acetate. They are not so-called failed experiments, but simply because my focus was shifted or for some other reason did not go further. Therefore, these studies will also help other researchers to gain inspiration. In addition, I provide some advice during the narrative. Under reflux, without a cooling system, using both 1-butanol and ethanol with proper LiBF$_4$ would get acetal (Table 3-13). The mechanism was shown in Scheme 3.5.

Table 3-13: Coupling of alcohols to acetal with Lewis acid.

Substrate (mmol)	**Ru-1** [mol%]	Additive (mg)	Temperature (°C)	Time (h)	Comment
1-butanol, 55	0.03	LiBF$_4$, 94	130	3	Oil bath, glass vessel, reflux
ethanol, 85	0.03	LiBF$_4$, 94	90	5	Oil bath, glass vessel, reflux
ethanol, 85	0.03	LiBF$_4$, 94	90	24	Oil bath, glass vessel, reflux

In the first two steps, consistent with ADC reaction, alcohol firstly is dehydrogenated to aldehyde, which couples to another alcohol, and then, for ADC reaction, the intermediate is hydrogenated to ester while 'acetal' reaction continuously introduces another alcohol. Hence, the catalytic system would produce water, if considering higher yield, water removal would be a good suggestion. Moreover, even acetal was also observed with ethanol as the substrate but to catch the low boiling point substance, acetaldehyde, a cooling system is necessary.
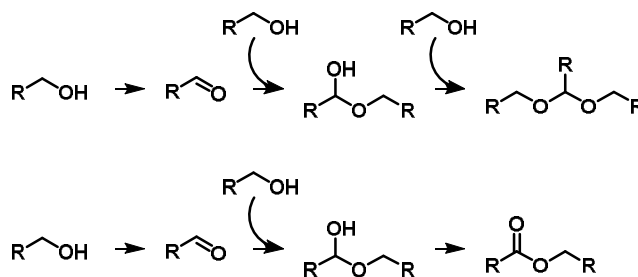
Scheme 3.5: Mechanism of acceptorless, coupling of alcohols to acetal with Lewis acid (up) and ADC of alcohols to esters (down).

Figure 3.13 and Figure 3.14 respectively gave the ^{1}H and ^{13}C NMR of base-free, acceptorless, one-step coupling 1-butanol to acetal with LiBF$_4$.
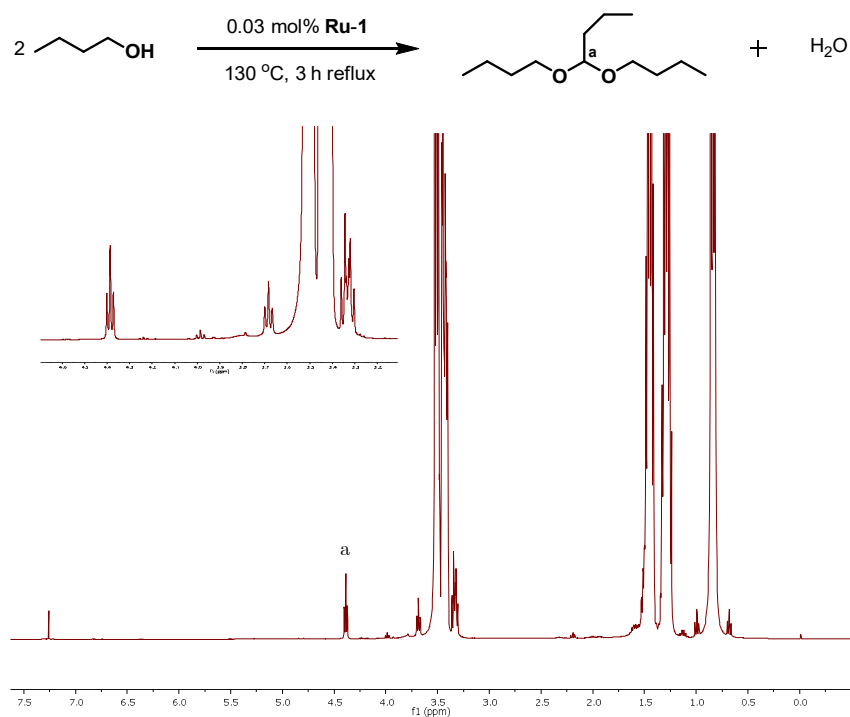
Figure 3.13: ^{1}H NMR of Coupling of 1-butanol to acetal with LiBF$_4$ (CDCl$_3$, 25 ^{o}C, 400 MHz).
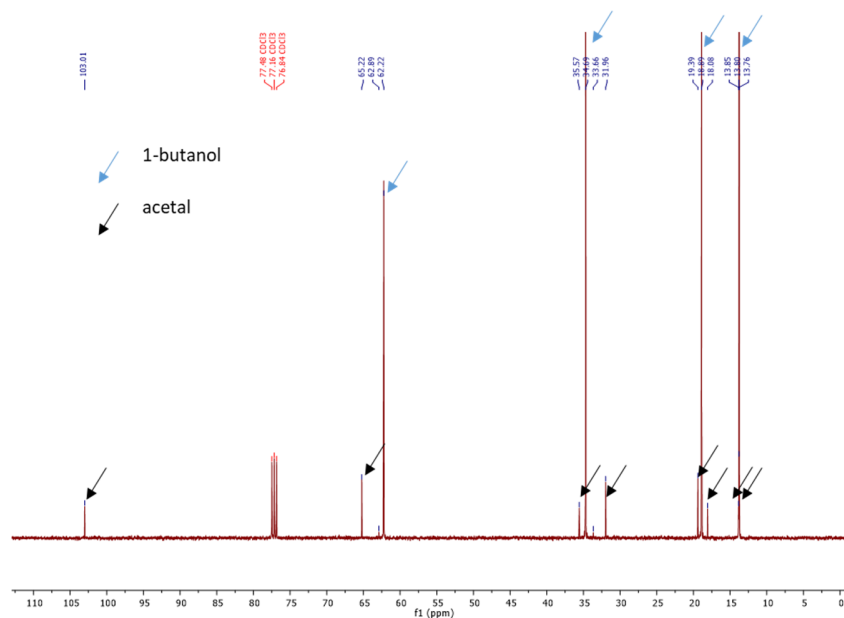
Figure 3.14: ^{13}C NMR of Coupling of 1-butanol to acetal with LiBF$_4$ (CDCl$_3$, 25 ^{o}C, 100.62 MHz).

3.2.4 Summary

In conclusion, I present solvent effects on ADC of ethanol, sixteen cyclic compounds with relatively good boiling points were selected, including aromatics, halo-aromatics, cycloalkanes, ethers, and heterocyclic. According to the polarity difference, these compounds as co-solvents were tested sequentially and in the initial screening, using a volume ratio between ethanol and compound of 1:5 at 120 °C for 24 h with 0.1 mol% **Ru-1**, complexes with dielectric constant around 2.4 are considered to be the most suitable choice, such as toluene and *m*-xylene. Extending reaction time to 48 h, most of them were highly dependent on the loading of catalyst, which means that their results are similar to those at 24 h. On balance, toluene was considered to be the optimal co-solvent and therefore continued to be optimized. Employing 0.1 mol% **Ru-1** at 120 °C for 24 h, with only 1:1.25 volume ratio between ethanol and toluene achieved 98% conversion, 92% yield with 94% selectivity, incomplete conversion of the intermediate product acetaldehyde is thought to be responsible for the slight loss of yield.
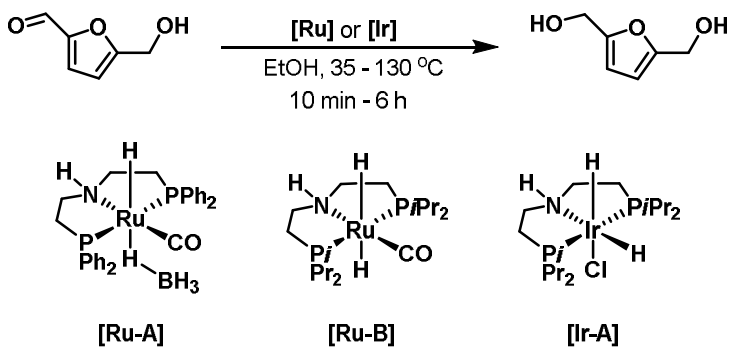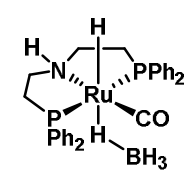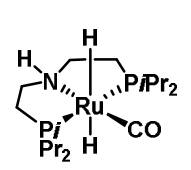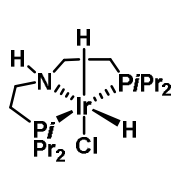
3.3 Transfer hydrogenation and dehydrogenation of glycerol

3.3.1 General information

In this Chapter, I will formally discuss 'transfer hydrogenation and dehydrogenation of glycerol'. This work is still in its initial stages and only certain initial experimental results are available, which will be more or less enlightening for the researchers.

Alcohols like methanol,[240–243] ethanol,[244–248] and 2-propanol[249–251] are acted as hydrogen donors in a typical TH reaction. When it comes to ethanol, my preferred substrate for research, in a project, spearheaded by Senior researcher Rosa Padilla in Nielsen's group, performed lots of ethanol as hydrogen donor experiments with PNP complexes. I am only a co-worker of this work, the selected results only represent a small piece of her work.

Table 3-14: Selected results from the transfer hydrogenation of HMF to DHMF with EtOH.

Entry	Catalyst (mol%)	Temperature [ºC]	Time [h]	Conversion [%][a]
1	**Ru-A** (1.0)	35	6	≥ 99
2	**Ru-A** (1.0)	50	1	≥ 99
3	**Ru-A** (0.6)	50	2	≥ 99
4	**Ru-A** (0.6)	80	10 min	≥ 99
5	**Ru-B** (0.6)	50	2	≥ 99
6	**Ir-A** (0.1)	130	0.5	≥ 99

[a] Determined by NMR.

As Table 3-14 described, Ru- and Ir-PNP complexes were used to study HMF transfer hydrogenation reaction with ethanol as hydrogen donor. After optimization, from a low-temperature perspective, employing 1.0 mol% **Ru-A**, at 35 °C for 6 h, NMR analysis suggested ⩾ 99 conversion (Entry 1). Interestingly, slightly improving temperature to 50 °C only within 1 h, full conversion still was got (Entry 2). Then, decreasing **Ru-A** loading to 0.6 mol%, just double reaction time based on Entry 2, HMF was again completely converted (Entry 3). From a short-time or low-catalyst loading perspective, employing 0.6 mol% **Ru-A**, at 80 °C for 10 min, or 0.1 mol% **Ir-A**, at 130 °C for 0.5 h, both could offer 100% conversion (Entry 5 and 6).

Indeed, an efficient and rapid catalytic HMF transfer hydrogenation would succeed using ethanol as a hydrogen donor. Glycerol, another non-toxic, cheap, and readily available biomass has not been particularly exhaustively used in base-free TH reactions. In session one, six ketones and aldehydes have been investigated, some basic information related to these substrates is shown in Table 3-15. The versatile Ru-MACHO-BH complex continues playing the role of catalyst.

Table 3-15: Substrates for transfer hydrogenation of glycerol.

Substrate	Molar mass (g/mol)	Density (g/cm³)	Boiling point (°C)	Comment
benzaldehyde	106.12	1.04	178	soluble in: Water
acetophenone	120.15	1.03	202	solubility in water: 5.5 g/L at 25 °C; 12.2 g/L at 80 °C
2-hexanone	100.161	0.81	128	solubility in water: 1.4% (14 g/L)
benzophenone	182.217	1.11	305	solid, insoluble in water
2-acetylfuran	110.112	1.1	169	low melting solid
4'-Methylacetophenone	134.17	1.0	226	water solubility: 0.37 mg/mL at 15 °C

In session two, several tests of glycerol dehydrogenation to lactic acid were performed under different conditions. Again, Ru-MACHO-BH was used to catalyze these systems.

3.3.2 Experimental results and discussion

For session one, a typical experiment setup would be like that: 0.5 mmol chosen substrates plus 2 mL glycerol as the hydrogen donor, with 1 mol% Ru-MACHO-BH at 120 °C for 24 h in an oil

bath (Scheme 3.6). After the reaction, ketones or aldehydes would be converted to the corresponding alcohols and glycerol probably would also be transformed to dehydrogenation products or even lactic acid.

$$\text{Substrate} + \text{Glycerol} \xrightarrow[120\ ^{\circ}C,\ 24\ h]{1\ \text{mol\% cat.}} \text{Products}$$
$$0.5\ \text{mmol} \qquad 2\ \text{mL}$$
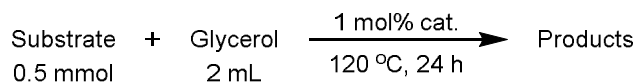
Scheme 3.6: A typical reaction of transfer hydrogenation of glycerol.

For benzaldehyde, substrate peaks remain but product peaks are more intense, which shows effective conversions. For acetophenone, the situation is almost the same. And using DMSO (0.025 mL) as an internal standard with CD_3OD and D_2O, respectively, a detailed quantitative study (Table 3-16) showed that taking CD_3OD results as an example, a total of 0.5 mmol acetophenone was converted to 0.267503 mmol 1-phenylethanol and 0.028158198 mmol was left, so, 94.4% conversion and 53.5% yield was achieved, meanwhile, a total of 27.3634 mmol glycerol was converted to 0.070395495 mmol lactic acid and 18.533122 mmol was left, so, 32.3% conversion and 0.3 % yield was achieved. Some intermediates from glycerol conversion, like, dihydroxyacetone, 2,3-dihydroxypropanal, l methylglyoxal, etc. may explain some loss of conversion.

Table 3-16: A typical quantitive study of TH.

	Total DMSO (mmol)	Total acetophenone (mmol)	1-phenylethanol (mmol)	Left acetophenone (mmol)	Conversion, yield (%)
CD_3OD		0.5	0.267503	0.028158198	94.4, 53.5
	0.351977	Total glycerol (mmol)	lactic acid (mmol)	Left glycerol (mmol)	Conversion, yield (%)
		27.3634	0.070395495	18.533122	32.3, 0.3
	Total DMSO (mmol)	Total acetophenone (mmol)	1-phenylethanol (mmol)	Left acetophenone (mmol)	Conversion, yield (%)
D_2O		0.5	0.330859	0.035197747	93.0, 66.2
	0.351977	Total glycerol (mmol)	lactic acid (mmol)	Left glycerol (mmol)	Conversion, yield (%)

| 27.3634 | 0.077435044 | 21.722642 | 20.6, 0.3 |

For 2-hexanone, and 4'-methylacetophenone at 120 °C, after 24 h, the conversion is not over and there are small substrate peaks remaining, while, for benzopheone and 2-acetylfuran, the substrate peaks completely disappear, which shows 100% NMR conversion rate. Overall, under these kind of reaction conditions, all six substrates could be converted well.
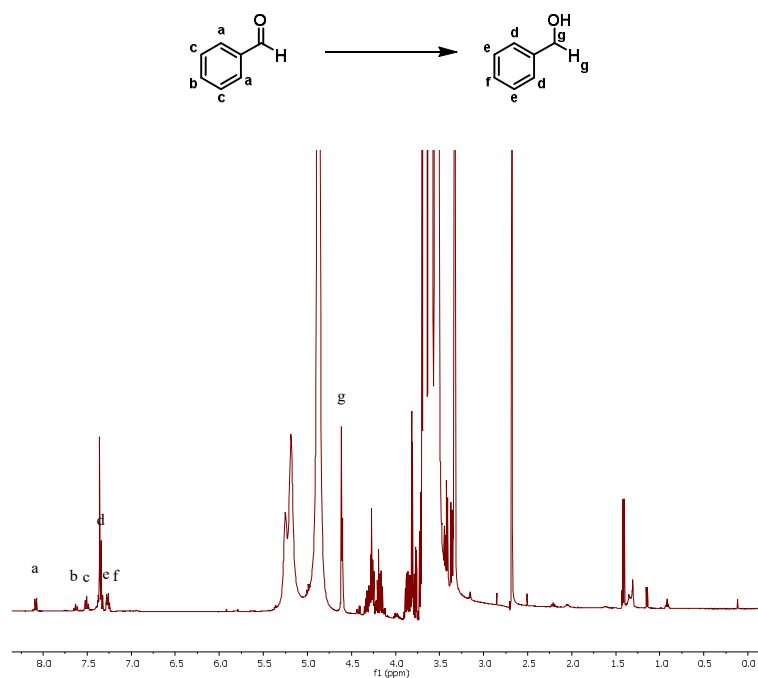
Figure 3.15: ^{1}H NMR of transfer hydrogenation with benzaldehyde (CD$_3$OD, 25 °C, 400 MHz).
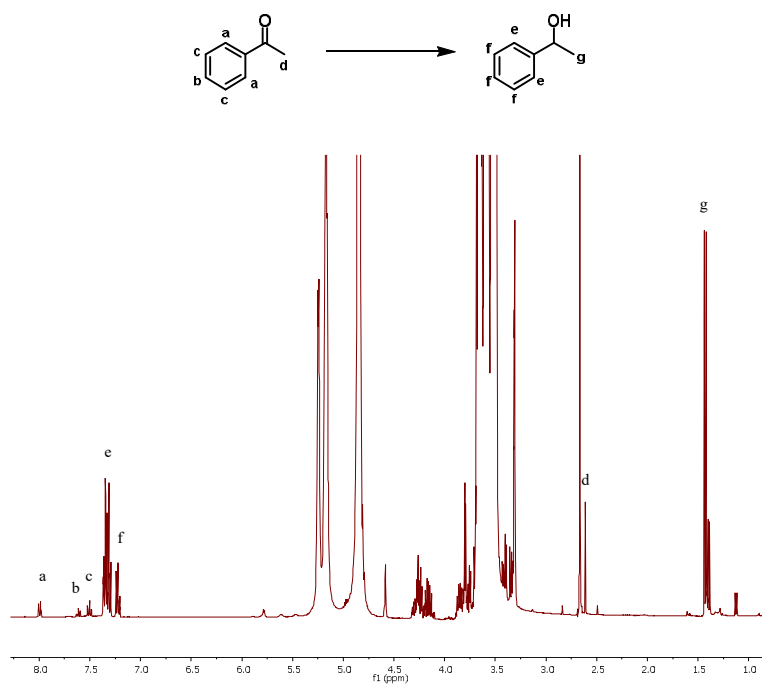
Figure 3.16: ^{1}H NMR of transfer hydrogenation with acetophenone (CD$_3$OD, 25 ^{o}C, 400 MHz).
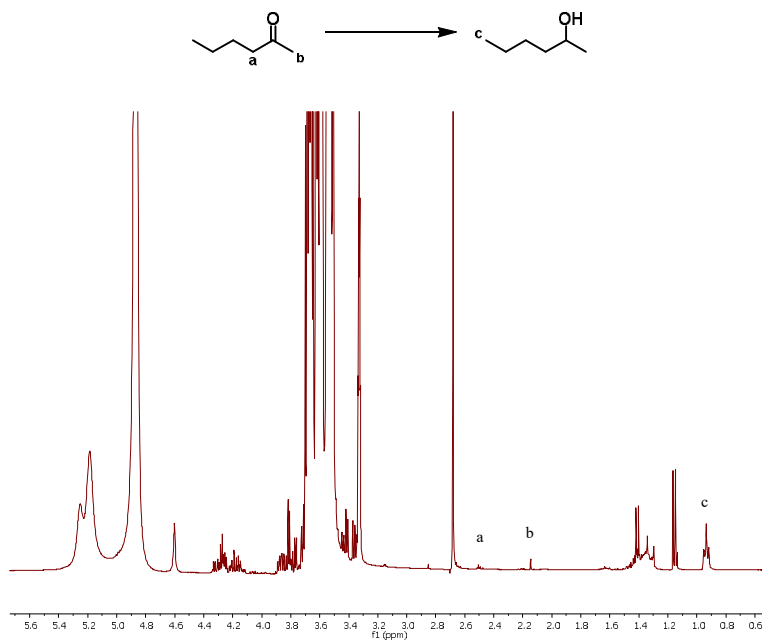
Figure 3.17: ^{1}H NMR of transfer hydrogenation with 2-hexanone (CD$_3$OD, 25 ^{o}C, 400 MHz).

66
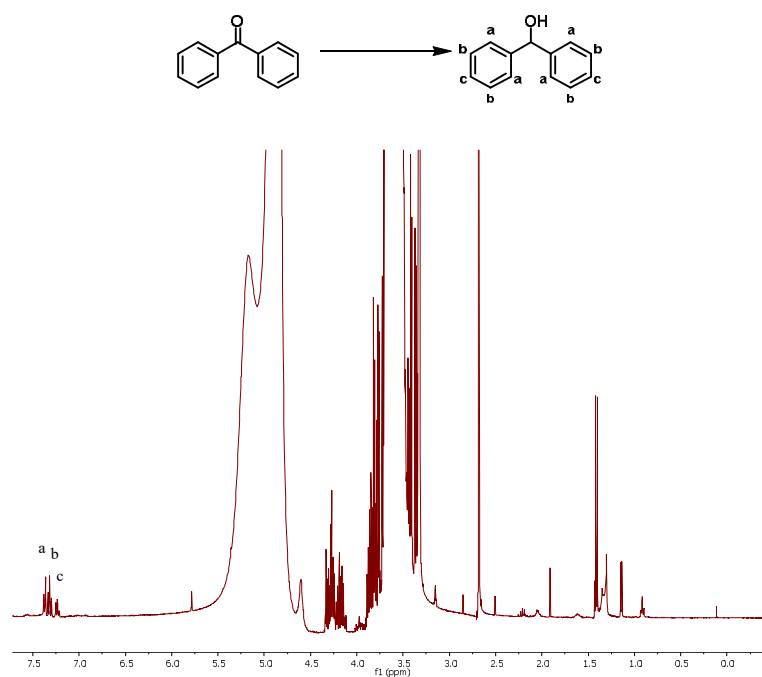
Figure 3.18: ^{1}H NMR of transfer hydrogenation with benzophenone (CD$_3$OD, 25 ^{o}C, 400 MHz).
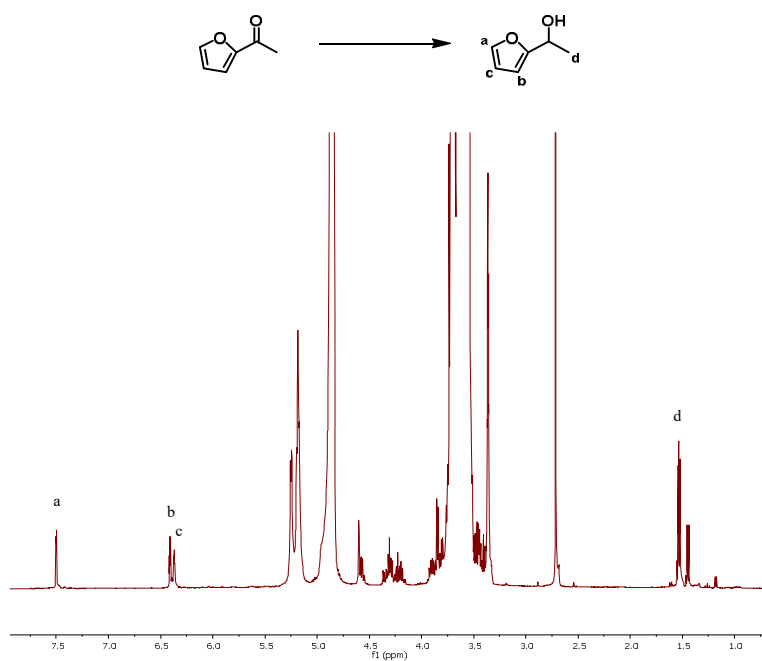
Figure 3.19: ^{1}H NMR of transfer hydrogenation with 2-acetylfuran (CD$_3$OD, 25 ^{o}C, 400 MHz).

67
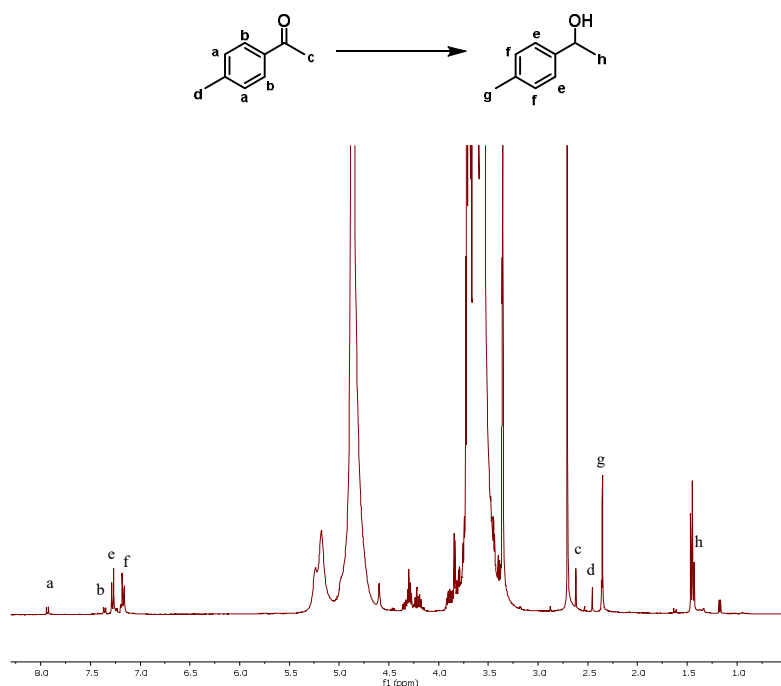
Figure 3.20: ^{1}H NMR of transfer hydrogenation with 4'-methylacetophenone (CD$_3$OD, 25 ^{o}C, 400 MHz).

For session two, three conditions have been applied (Table 3-17). In the first try, 2 mL ethanol was added to improve glycerol dissolution in the system, however, it turned out to be failed because numerous red solids appeared and the liquid became yellow and muddy when dissolved in D$_2$O, it is presumed that the catalyst is deactivated and the open system should be replaced by a reflux system. When shifting to the second try, lactic acid peaks showed up and to get better results, the third test was performed, it is noteworthy that hydrogen in the closed system is not good for the reaction, according to NMR analysis (Figure 3.21 and Figure 3.22), lactic acid as the main product was formed. So far, the preliminary data have been presented, to give an experience for the later research, that during the course of the reaction, some formed acid intermediate would 'kill' the catalyst (As far as we know, Ru-MACHO-BH will die in an acidic environment), nither the sealed nor the opened reflux system would not achieve high yield of lactic acid. Some other novel methods should be proposed.

Table 3-17: Dehydrogenation of glycerol to lactic acid.

Substrate (mmol)	Catalyst (mol%)	Additive (mL)	Temperature (°C)	Time (h)	Comment
Glycerol, 6.8	0.1	Ethanol, 2	110	24	Oil bath, pressure tube, open air
Glycerol, 6.8	0.1	/	120	6	Oil bath, pressure tube
Glycerol, 6.8	0.1	/	150	24	Parr system
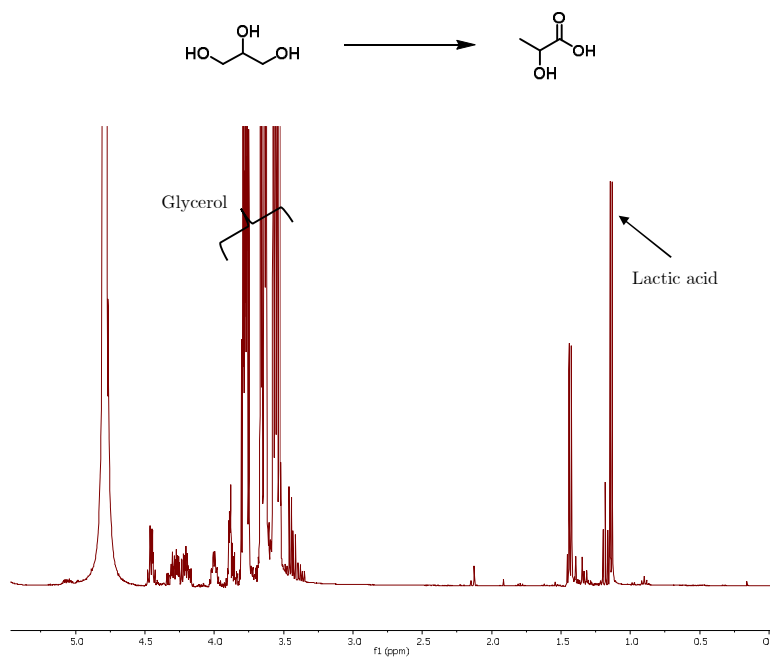
Figure 3.21: ^{1}H NMR of dehydrogenation of glycerol to lactic acid (D$_2$O, 25 °C, 400 MHz).
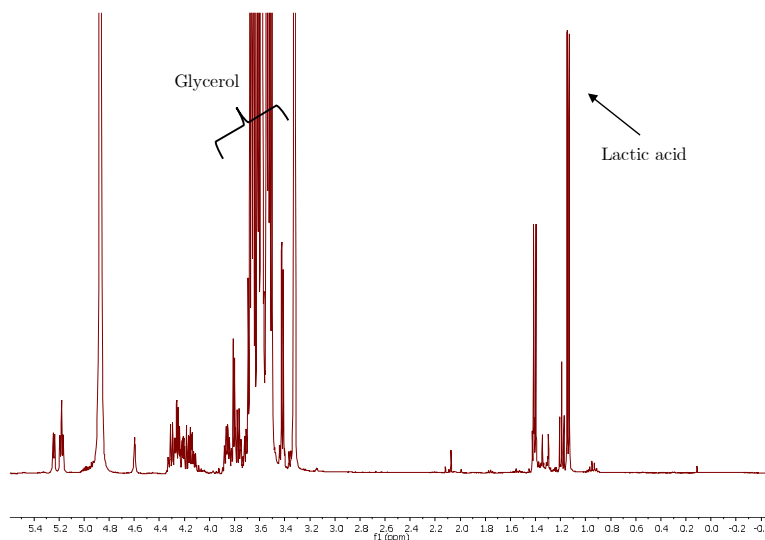
Figure 3.22: ^{1}H NMR of dehydrogenation of glycerol to lactic acid (CD$_3$OD, 25 ^{o}C, 400 MHz).

3.3.3 Summary

In conclusion, on the one hand, I have demonstrated that glycerol can be a good hydrogen donor in transfer hydrogenation reactions, using 1 mol% Ru-MACHO-BH at 120 ^{o}C for 24 h, some typical aromatic aldehydes, aromatic ketones and aliphatic ketones have been shown high conversion and yield. Among them, 2-hexanone, and 4'-methylacetophenone are shown 100% conversion by NMR analysis. These preliminary reaction conditions could be polished/optimized in the near future, especially the catalyst loading.

On the other hand, it is proved that lactic acid can be directly got through glycerol dehydrogenation without an external base/an extra intermediate step, which is simpler than that reported in current research. Using 0.1 mol% Ru-MACHO-BH, at 150 ^{o}C for 24 h in a sealed reactor, lactic acid as the dominant product was produced. It is noteworthy that produced hydrogen is not beneficial for glycerol conversion, and most catalysts can deactivate in an acidic environment, which launched a challenge toward one-step direct glycerol to lactic acid reaction with high yield.

Chapter 4

4 General conclusions and perspectives

In conclusion, the author has demonstrated catalytic transformations of bioalcohols with PNP complexes were efficient.

In Chapter 3.1, the author has explored a novel carbon-chain growth using Ru-pincer complexes with phenyl substituted phosphines, different from the typical Guerbet reaction, which is used for primary alcohol production, this kind of mechanism is the coupling of aldehydes and ketones to form secondary alcohols. The methodology unveils the potential for using bulk bio-alcohols to selectively produce primary or secondary alcohols and hydrocarbons under mild conditions. Moreover, as the selectivity of the auxiliary ligands for the reaction products is revealed, more ligands or metal centers could be used for testing in future work on alcohol upgrading.

On the catalytic side, employing [(^{Ph}PNP)RuH(Cl)CO] (**Ru-1**, 1000 ppm) as a catalyst in ethanol, containing 20 mol% of NaOtBu, at 115 ºC leads to 89% selective production of secondary alcohols over primary alcohols. A yield of 12% of 2-butanol, and in total 22% of secondary alcohols, was achieved. Employing more active [(^{Ph}PNP)RuH(HBH$_3$)CO] (**Ru-2**, 250 ppm) under the same reaction conditions, Up to 12% of 2-butanol (TON of 480), 4% of 3-hexanol (TON of 160) and a combined 18% of all secondary alcohols (TON of 720) can be achieved. In addition, minor amounts of 2 butenes/butane (≤5%) were observed in the gas phase. When temperate went up to 130 ºC, butenes were fully hydrogenated to butane.

Whereas [(^{i}PrPNP)RuH(Cl)CO] (**Ru-3)** and [(^{Cy}PNP)RuH(Cl)CO] (**Ru-4)** containing semi-bulky i-propyl (-iPr) and cyclohexyl (-Cy) P-substituents, respectively, provide practically no selectivity. Employing [(^{t}BuPNP)RuH(Cl)CO] (**Ru-5**) containing the bulky t-butyl (-tBu) P-substituents under the same optimal reaction conditions, leading to >99% selectivity of 1-butanol (13% yield) over secondary alcohols. In fact, the catalytic system is highly competitive for producing 1-butanol

with 22% yield plus 3% of 1-hexanol obtained at 130 ⁰C, a temperature significantly lower than previously reported systems.

In terms of mechanistic research, 4-hydroxy-2-butanone was proved as the novel key intermediate to produce secondary alcohols, after acetaldol is formed, in fact, there are two competing reactions depending on the auxiliary ligands of the complex, i.e. the overall spatial structure. For **Ru-1** or **Ru-2** involved catalysis, instead of dehydration of acetadol, with the intervention of the catalyst, the system directly goes through dehydrogenation and hydrogenation to form 4-hydroxy-2-butanone. A series of mechanistic tests were performed, and it turns out 4-hydroxy-2-butanone plays an important role in secondary alcohol production. Some related retro-aldol products, like acetone, etc., were observed.

Hopefully, the low-temperature novel ethanol upgrading project would give the field a shot in the arm and lead more scientists to pay attention to the importance of this field. Enabling ethanol, or a single primary alcohol upgrade, to no longer be limited to primary alcohols, but to diversify and achieve multi-product selection by adjusting the spatial bulkiness of the ancillary ligands.

Low-temperature novel ethanol upgrading

Complexes

[Ru-1] [Ru-2] [Ru-3] [Ru-4] [Ru-5]

less bulky phenyl substituted phosphines | semi-bulky *i*-propyl and cyclohexyl *P*-substituents | bulky *t*-butyl *P*-substituents

Catalysis

Secondary alcohols

Liquid phase

Primary alcohols

Liquid phase

Solid phase

Gas phase

Mechanism

Typical Guerbet-type ethanol upgrading product

acetaldol

4-hydroxy-2-butanone *Novel key intermediate*

This work pathway

4-hydroxy-2-butanone — Dehydration — MVK — [Ru] catalyst Hydrogenation — 2-butanol — Dehydration — 2-butenes — [Ru] catalyst Hydrogenation — butane

Retro-Aldol reaction

Observed side-product

Observed side-product

In Chapter 3.2, firstly, a base-free, solvent-free, one-step, acceptorless dehydrogenative coupling of ethanol to ethyl acetate was demonstrated. Due to the limited solubility of **Ru-1** in pure ethanol, this kind of reaction was unstable at the chemical level. Based on this, second, sixteen cyclic compounds with decent boiling points and variable polarities were added as co-solvents to improve both solubilities of the catalyst and conversion rate, including aromatics, halo-aromatics, cycloalkanes, ethers, and heterocyclic. Medium polarity compounds were considered to be more suitable for this catalytic system. Most of the compounds involved in the catalytic system were catalyst-dependent. After optimization, employing 0.1 mol% **Ru-1** at 120 ℃ for 24 h, with only 1:1.25 volume ratio between ethanol and toluene achieved 98% conversion, 92% yield with 94% selectivity. Third, another six catalysts were tested but either the temperature is insufficient to obtain good results, or there is a lack of activators, such as a base. In a practical application scenario, toluene can be easily separated from ethanol and recycled.

Besides, some additional tests were also performed to show how acetal would be produced. $LiBF_4$ was used as the necessary additive, to change the reaction pathway. In practice, water removal operation was essential to get a higher yield and a cooling system was still critical to catching up with some low boiling point intermediates. The formation of acetal was considered to be of great potential academic research value.

This work firstly demonstrated the AD reaction of ethanol in presence of different co-solvents with various boiling points and polarities. Experimental guidelines are given for the selection of such dual organic phase catalytic systems. Hopefully, After separating the co-solvent, this catalytic system is able to directly obtain ethyl acetate and continue recycling the co-solvent.

Solvent effects on acceptorless dehydrogenative coupling of ethanol

Complexes

[Ru-1]   [Ru-2]   [Ru-3]   [Ru-4]   [Ru-5]   [Ru-6]   [Ir-1]

Solvents

High polarity

Ethylbenzene   *o*-Xylene   Mesitylene   Anisole   Cyclopentyl methyl ether   Chlorobenzene   Tetrahydrofuran   Gamma-valerolactone

Cyclohexane   Methylcyclohexane   1,3-Dimethylcyclohexane   *p*-Xylene   *p*-Cymene   Toluene   1,4-Dioxane   *m*-Xylene

Low polarity

Low polarity   High polarity
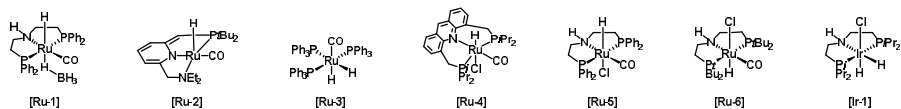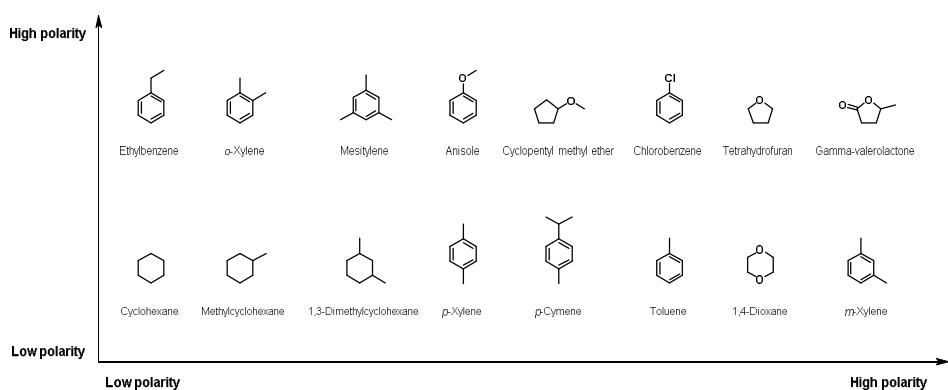
Catalysis
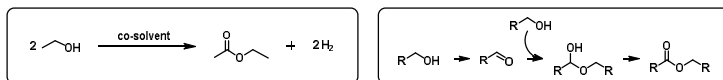
Additional acetal production
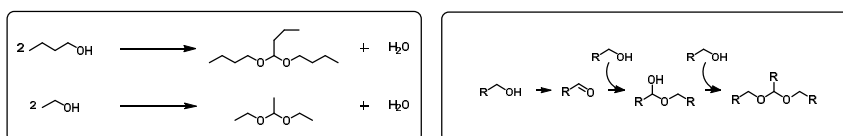
In Chapter 3.3, two kinds of different chemical reactions have been investigated.

First, glycerol as a hydrogen donor was tested in a typical transfer hydrogenation reaction. Usually, some low-carbon alcohols, like methanol, ethanol, or 2-propanol would act as hydrogen donors, but glycerol is also a cheap, highly-available, non-toxic biomass (bioalcohol), research in this area is relatively scarce, and this work is also acid to fill some gaps. Six typical substrates, including aromatic aldehydes, aromatic ketones, and aliphatic ketones were used in this catalytic system. Employing preferenced multifunctional complex Ru-MACHO-BH (1 mol%) at 120 °C for 24 h, it turned out that 2-hexanone, and 4'-methylacetophenone were shown 100% conversion by NMR analysis, as well as over 90% conversion for other substrates. These results indicated that Ru-MACHO-BH and glycerol are suitable for this base-free, one-step transfer hydrogenation reaction but deeper optimizations are waiting to be implemented.

Then, dehydrogenation of glycerol directly to lactic acid was performed, and it is noteworthy that this catalytic system is still improving. Employing 0.1 mol% Ru-MACHO-BH, at 150 °C for 24 h in a sealed reactor, lactic acid as the dominant product was produced. Considering that hydrogen removal is beneficial for the reaction itself, a reflux system would be a good choice to advance the yield, however, during the course of the reaction, some acidic substances form, which will 'kill' Ru-MACHO-BH somehow (hinder further reactions). Hence, developing a good 'activated' (no need additive to activate it) complex with strong survival ability in an acidic environment is very critical.

Transfer hydrogenation and dehydrogenation of glycerol

Transfer hydrogention
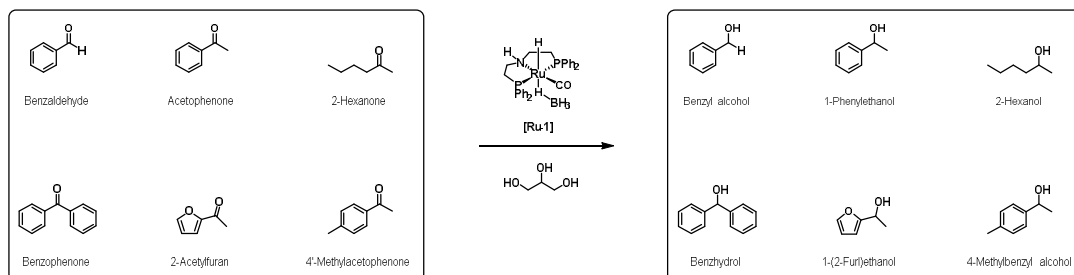
Dehydrogenation
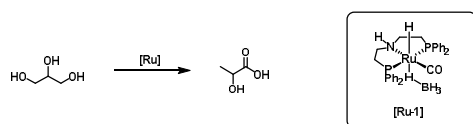
Transfer hydrogenation of HMF to DHMF with EtOH (as a co-worker)
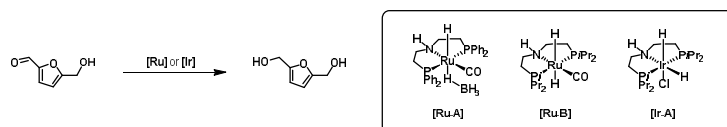
A large proportion of the catalytic work carried out by the author has actually been shelved or canceled due to poor results or failure to achieve the desired outcome. For example, the author has tried to create a system of mixing ethanol and water in an acidic environment to produce acetic acid in one step. However, after extensive testing and adjustment, the experiment was ultimately unsuccessful. I have also tried to synthesize catalysts, as described at the beginning of Chapter 1. In addition to this, the global pandemic of the corona led me to fail to make a successful external stay. Overall, projects 1 and 2 are relatively complete, but project 3 has very many areas that deserve optimization.

It is sincerely hoped that these works will bring enlightenment to the academic community, especially in the area of homogeneous bioalcohols conversion.

Chapter 5

5 A General instrumentation

NMR

Bruker Avance III 400 MHz spectrometer

GC-MS

Agilent Technologies 6890 Network GC System with 5973 inent Mass Selective Detector

Agilent Technologies 7890A Network GC System with 5975C VL MSD with Tripe-Axis Detector

GC-FID

Agilent Technologies 6890N Network GC System with Agile with 7683B Series Injector

GC-TCD

Agilent Technologies 6890N Network GC System (G1540N)

Micro-GC

Agilent Technologies 490 Network GC System

NMR, GC-MS, GC-FID, GC-TCD, and Micro-GC were used for Project 1 and NMR was used for Projects 2 and 3.

Bibliography

[1]   Vlachogianni, T.; Valavanidis, A. *Am. J. Educ. Res.* **2013**, *1* (3), 68–78.

[2]   Falkowski, P.; Scholes, R. J.; Boyle, E.; Canadell, J.; Canfield, D.; Elser, J.; Gruber, N.; Hibbard, K. *Science (80-.).* **2000**, *290*, 291–297.

[3]   Foster, J. B.; Foster, J. B. *Int .Crit.Theor.* **2017**, *7*, 439–458.

[4]   Baum, S. D.; Armstrong, S.; Ekenstedt, T.; Häggström, O.; Hanson, R.; Kuhlemann, K.; Maas, M. M.; Miller, J. D.; Salmela, M.; Sandberg, A.; Sotala, K.; Torres, P.; Turchin, A.; Yampolskiy, R. V. *Foresight* **2019**, *21* (1), 53–83.

[5]   Singh, B. J.; Sharma, A.; Singh, B. J. *IJITEE* **2022**, *9*.

[6]   Overview, P. P.; Groumpos, P. P.; Peter, P. *IFAC Pap.* **2021**, *54* (13), 464–471.

[7]   Dogaru, L. *Procedia Manuf.* **2020**, *46*, 397–401.

[8]   Nuvolari, A. *Environ. Innov. Soc.* **2019**, *32* (July 2017), 33–44.

[9]   Thomas, C. D. *Divers* **2010**, *16* (3), 488–495.

[10]   Le Quéré, C.; Mayot, N. *Science (80-.).* **2022**, *375* (6585), 1091–1092.

[11]   Ricke, K. L.; Caldeira, K. *Nat. Clim. Chang.* **2014**, *4* (5), 333–338.

[12]   Pathak, S. *Int. J. Eng. Res. Appl.* **2014**, *4* (3), 845–851.

[13]   Ghosh, S. *GJES* **2020**, *5* (2), 1–5.

[14]   Field, C. B.; Campbell, J. E.; Lobell, D. B. *Trends Ecol. Evol.* **2007**, *23* (2), 65–72.

[15]   Li, M.; Luo, N.; Lu, Y. *Sustainability* **2017**, *9*, 567.

[16]   Patzek, T. W.; Patzek, T. W. *CRC Crit. Rev. Plant Sci.* **2010**, *23* (6), 519–567.

[17]   Lin, M. Y.; Tanaka, S. *Appl .Microbiol. Biotechnol.* **2006**, *69*, 627–642.

[18]   Kemper, J. *Int. J. Greenh. Gas Control.* **2015**, *40*, 401–430.

[19]   Farlat, J.; Blok, K.; Schipper, L. *Energy Polic.* **1997**, *25* (97), 745–758.

Bibliography

[20]   Bajwa, D. S.; Peterson, T.; Sharma, N.; Shojaeiarani, J.; Bajwa, S. G. *Renew. Sust. Energ. Rev.* **2018**, *96*, 296–305.

[21]   Ã, M. P. *Biomass Bioenergy* **2004**, *27*, 613–620.

[22]   Lenz, V.; Szarka, N.; Jordan, M. *Chem. Eng. Technol.* **2020**, *43* (8), 1469–1484.

[23]   Hoang, L. V.; Nguyen, D. C.; Truong, T. H.; Le, H. C.; Nguyen, M. N. *Int. J. Renew. Energy Dev.* **2022**, *11* (1), 237–254.

[24]   Niven, R. K. *Renew. Sust. Energ. Rev.* **2005**, *9*, 535–555.

[25]   Anderson, S. T. *J. Environ. Econ. Manag.* **2012**, *63* (2), 151–168.

[26]   Cavalett, O.; Chagas, M. F.; Junqueira, T. L.; Watanabe, M. D. B.; Bonomi, A. *Ind. Crop. Prod.* **2017**, *106*, 31–39.

[27]   Nu, H. M.; Onal, H. *Agric. Econ.* **2022**, *44* (2013), 487–499.

[28]   Wu, B.; Wang, Y.; Dai, Y.; Song, C.; Zhu, Q.; Qin, H.; Tan, F.; Chen, H.; Dai, L.; Hu, G.; He, M. *Renew. Sust. Energ. Rev.* **2021**, *145*, 111079.

[29]   Access, O. *Environ. Res. Lett.* **2006**, *1*, 014008.

[30]   Fulton, L. M.; Körner, A.; Agency, I. E. *Biofuels, Bioprod. Bioref.* **2015**, *9*, 476–483.

[31]   Ball, M.; Weeda, M. *Int. J. Hydrog. Energy* **2015**, *40* (25), 7903–7919.

[32]   Mazloomi, K.; Gomes, C. *Renew. Sust. Energ. Rev.* **2012**, *16* (5), 3024–3033.

[33]   Winter, C. *Int. J. Hydrog. Energy* **2010**, *34* (2009), 1–52.

[34]   Davis, S. J.; Lewis, N. S.; Shaner, M.; Aggarwal, S.; Arent, D.; Azevedo, I. L.; Benson, S. M.; Bradley, T.; Brouwer, J.; Chiang, Y.; Clack, C. T. M.; Cohen, A.; Doig, S.; Edmonds, J.; Fennell, P.; Field, C. B.; Hannegan, B.; Hodge, B.; Hoffert, M. I.; Ingersoll, E.; Jaramillo, P.; Lackner, K. S.; Mach, K. J.; Mastrandrea, M.; Ogden, J.; Peterson, P. F.; Sanchez, D. L.; Sperling, D.; Stagner, J.; Trancik, J. E.; Yang, C.; Caldeira, K. *Science (80-.).* **2018**, *360*, 1419.

[35]   Bilgen, S. *Renew. Sust. Energ. Rev.* **2014**, *38*, 890–902.

85

[36] Lamers, P.; Hamelinck, C.; Junginger, M.; Faaij, A. *Renew. Sust. Energ. Rev.* **2011**, *15* (6), 2655–2676.

[37] Tilman, D.; Socolow, R.; Foley, J. A.; Hill, J.; Larson, E.; Lynd, L.; Pacala, S.; Reilly, J.; Searchinger, T.; Somerville, C.; Williams, R. *Science (80-.).* **2009**, *325*, 270–272.

[38] Shah, Y. R.; Sen, D. J. *Int. J. Cur. Sci. Res.* **2011**, *1* (2), 57–62.

[39] Han, G. B.; Jang, J. H.; Ahn, M. H. In *Alcohol Fuels - Current Technologies and Future Prospect*; 2019; pp 1–14.

[40] Pasel, J.; Häusler, J.; Schmitt, D.; Valencia, H.; Meledina, M.; Mayer, J.; Peters, R. *Catalysts.* 2020, p 1151.

[41] Kalair, A.; Abas, N.; Saleem, M. S.; Kalair, A. R.; Khan, N. *Energy storage* **2020**, *3*.

[42] Dasappa, S.; Sridhar, H. V; Sridhar, G.; Paul, P. J.; Mukunda, H. S. *Biomass Bioenergy* **2003**, *25*, 637–649.

[43] Díaz-Pérez, M. A.; Serrano-Ruiz, J. C. *Molecules* **2020**, *25* (4), 802.

[44] Voloshin, R. A.; Rodionova, M. V; Zharmukhamedov, S. K.; Veziroglu, T. N. *Int. J. Hydrog. Energy* **2016**, *41* (39), 17257–17273.

[45] Yue, D.; You, F.; Snyder, S. W. *Comput. Chem. Eng.* **2014**, *66*, 36–56.

[46] Lin, T.; Rodríguez, L. F.; Shastri, Y. N.; Hansen, A. C.; Ting, K. C. *Bioresour. Technol.* **2014**, *156*, 256–266.

[47] Demirbas, A. *Energy Convers. Manag.* **2008**, *49*, 2106–2116.

[48] Simmons, B. A.; Loque, D.; Blanch, H. W. *Genome Biol.* **2008**, *9* (12).

[49] Hajar, S.; Azhar, M.; Abdulla, R.; Jambo, S. A.; Marbawi, H.; Azlan, J.; Azifa, A.; Faik, M.; Francis, K. *BB Reports* **2017**, *10*, 52–61.

[50] Talebnia, F.; Karakashev, D.; Angelidaki, I. *Bioresour. Technol.* **2010**, *101* (13), 4744–4753.

[51] Casabar, J. T.; Unpaprom, Y.; Ramaraj, R. *Biomass Convers. Biorefin.* **2019**, *9*, 761–765.

Bibliography

[52]   Veza, I.; Said, M. F. M.; Latiff, Z. A. *Int. J. Automot. Mech. Eng.* 2020, pp 7648–7666.

[53]   Tseng, K. N. T.; Lin, S.; Kampf, J. W.; Szymczak, N. K. *Chem. Commun.* **2016**, *52* (14), 2901–2904.

[54]   Liu, Q.; Xu, G.; Wang, X.; Mu, X. *Green Chem.* **2016**, *18* (9), 2811–2818.

[55]   Zuo, C.; Hindley, J.; Ding, X.; Gronnow, M.; Xing, W.; Ke, X. *J. Memb. Sci.* **2021**, *638*, 119702.

[56]   Dowson, G. R. M.; Haddow, M. F.; Lee, J.; Wingad, R. L.; Wass, D. F. *Angew. Chem. Int. Ed.* **2013**, *52*, 9005–9008.

[57]   O'Lenick, A. J. *J. Surfactants Deterg.* **2001**, *4* (3), 311–315.

[58]   Wingad, R. L.; Gates, P. J.; Street, S. T. G.; Wass, D. F. *ACS Catal.* **2015**, *5* (10), 5822–5826.

[59]   Fu, S.; Shao, Z.; Wang, Y.; Liu, Q. *J. Am. Chem. Soc.* **2017**, *139* (34), 11941–11948.

[60]   Xie, Y.; Ben-David, Y.; Shimon, L. J. W.; Milstein, D. *J. Am. Chem. Soc.* **2016**, *138* (29), 9077–9080.

[61]   Kulkarni, N. V.; Brennessel, W. W.; Jones, W. D. *ACS Catal.* **2018**, *8* (2), 997–1002.

[62]   Subaramanian, M.; Sivakumar, G.; Balaraman, E. *Chem. Rec.* **2021**, *21*, 3839–3871.

[63]   Friedrich, A.; Schneider, S. *ChemCatChem* **2009**, *1*, 72–73.

[64]   Nielsen, M.; Junge, H.; Kammer, A.; Beller, M. *Angew. Chemie* **2012**, *124* (23), 5809–5811.

[65]   Nguyen, D. H.; Trivelli, X.; Capet, F.; Paul, J. F.; Dumeignil, F.; Gauvin, R. M. *ACS Catal.* **2017**, *7* (3), 2022–2032.

[66]   Tseng, K. N. T.; Kampf, J. W.; Szymczak, N. K. *Organometallics* **2013**, *32* (7), 2046–2049.

[67]   Wang, Y.; Ma, X.; Ding, Y.; Wang, J.; Yang, Z. *J. Mol. Liq.* **2019**, *293*, 111541.

[68]   Jespersen, D.; Keen, B.; Day, J. I.; Singh, A.; Briles, J.; Mullins, D.; Weaver, J. D. *Org. Process Res. Dev.* **2019**, *23*, 1087–1095.

[69]   Khusnutdinova, J. R.; Milstein, D. *Angew. Chem. Int. Ed.* **2015**, *54*, 12236–12273.

[70] Gunanathan, C.; Milstein, D. *Chem. Rev.* **2014**, *114*, 12024–12087.

[71] Werkmeister, S.; Neumann, J.; Junge, K.; Beller, M. *Chem. Eur. J.* **2015**, *21*, 12226 –12250.

[72] Srimani, D.; Balaraman, E.; Gnanaprakasam, B.; Ben-David, Y.; Milsteina, D. *Adv. Synth. Catal.* **2012**, *354*, 2403–2406.

[73] Gnanaprakasam, B.; Ben-david, Y.; Milstein, D. *Adv. Synth. Catal.* **2010**, *352*, 3169–3173.

[74] Spasyuk, D.; Vicent, C.; Gusev, D. G. *J. Am. Chem. Soc.* **2015**, *137*, 3743–3746.

[75] Nielsen, M.; Junge, H.; Kammer, A.; Beller, M. *Angew. Chem. Int. Ed.* **2012**, *51*, 5711–5713.

[76] Sorkau, A.; Schwarzer, K.; Wagner, C.; Poetsch, E.; Steinborn, D. *J. Mol. Catal. A. Chem.* **2004**, *224*, 105–109.

[77] Simon, M.; Darses, S. *Adv. Synth. Catal.* **2010**, *352*, 305–308.

[78] Gusev, D. G. *ACS Catal.* **2016**, *6*, 6967– 6981.

[79] Morris, S. A.; Gusev, D. G. *Angew. Chem. Int. Ed.* **2017**, *56*, 6228–6231.

[80] Gusev, D. G. *ACS Catal.* **2017**, *7*, 6656– 6662.

[81] Nguyen, D. H.; Trivelli, X.; Capet, F.; Swesi, Y.; Favre-Réguillon, A.; Vanoye, L.; Dumeignil, F.; Gauvin, R. M. *ACS Catal.* **2018**, *8* (5), 4719–4734.

[82] Th, F.; Simao, F.; Rafael, I.; Falc, D. A.; Saraiva, L.; Junior, D. M.; Sousa, S.; Guimaraes, T.; Cristiane, M.; Souza, M. De; S, C. *Fuel* **2021**, *288*, 119577.

[83] Veljkovi, V. B.; Biberd, M. O.; Bankovi, I. B.; Djalovi, I. G.; Tasi, M. B.; Nje, Z. B.; Stamenkovi, O. S. *Renew. Sust. Energ. Rev.* **2018**, *91*, 531–548.

[84] Hristoph, R. A. L. F. C.; Gmbh, C. D. *Ullmann's encycl. ind. chem.* **1998**, *17*.

[85] Tan, H. W.; Aziz, A. R. A.; Aroua, M. K. *Renew. Sust. Energ. Rev.* **2013**, *27*, 118–127.

[86] Quispe, C. A. G.; Coronado, C. J. R.; Carvalho, J. A. *Renew. Sust. Energ. Rev.* **2013**, *27*, 475–493.

[87] Wang, D.; Astruc, D. *Chem. Rev.* **2015**, *115*, 6621– 6686.

[88]   Brieger, G.; Nestrick, T. J. *Chem. Rev.* **1974**, *74*, 567–580.

[89]   Ito, J.; Nishiyama, H. *Tetrahedron Lett.* **2014**, *55* (20), 3133–3146.

[90]   Azua, A.; Mata, J. A.; Peris, E.; I, U. J. **2011**, *2* (1), 5532–5536.

[91]   Azua, A.; Mata, J. A.; Peris, E.; Lamaty, F.; Martinez, J.; Colacino, E. *Organometallics* **2012**, *31* (10), 3911–3919.

[92]   Prakash, O.; Sharma, K. N.; Joshi, H.; Gupta, P. L.; Singh, A. K. *Organometallics* **2014**, *33* (10), 2535–2543.

[93]   Azua, A.; Finn, M.; Yi, H.; Beatriz Dantas, A.; Voutchkova-Kostal, A. *ACS Sustain. Chem. Eng.* **2017**, *5* (5), 3963–3972.

[94]   Vijayakumar, J.; Aravindan, R.; Viruthagiri, T. *Chem. Biochem. Eng. Q.* **2008**, *2*, 245–264.

[95]   Rodrigues, C.; Vandenberghe, L. P. S.; Woiciechowski, A. L. *Biotechnol. Bioeng.* **2017**, *24*, 543–556.

[96]   Andres, F.; Martinez, C.; Marcos, E.; Dom, M.; Souza, R. P. De. **2013**, *30*, 70–83.

[97]   Sharninghausen, L. S.; Campos, J.; Manas, M. G.; Crabtree, R. H. *Nat. Commun.* **2014**, *5*, 1–9.

[98]   Li, Y.; Nielsen, M.; Li, B.; Dixneuf, P. H.; Junge, H.; Beller, M. *Green Chem.* **2015**, *17* (1), 193–198.

[99]   Sharninghausen, L. S.; Mercado, B. Q.; Crabtree, R. H.; Hazari, N. *Chem. Commun.* **2015**, *51* (90), 16201–16204.

[100]   Lu, Z.; Demianets, I.; Hamze, R.; Terrile, N. J.; Williams, T. J. *ACS Catal.* **2017**, *6*, 2015–2018.

[101]   Finn, M.; Ridenour, J. A.; Heltzel, J.; Cahill, C.; Voutchkova-Kostal, A. *Organometallics* **2018**, *37* (9), 1400–1409.

[102]   Dutta, M.; Das, K.; Prathapa, S. J.; Srivastava, H. K.; Kumar, A. *Chem. Commun.* **2020**,

56 (68), 9886–9889.

[103] Moulton, B. C. J.; Shaw, B. L. *J.C.S. Dalt.* **1975**, No. 1020, 1020–1024.

[104] Shaw, L. *J.C.S. Chem. Comm.* **1977**, *006* (3), 96–97.

[105] Medium-chain, S.; Crocker, C.; Errington, R. J.; Markham, R.; Moulton, C. J.; Odell, K. J.; Shaw, B. L. *J. Am. Chem. Soc.* **1980**, *18*, 4373–4379.

[106] Clocker, B. C.; Errington, R. J.; Markham, R.; Moulton, C. J.; Shaw, L. *J.C.S. Dalt.* **1982**, 387–395.

[107] Trans, D.; Crocker, B. C.; Empsall, H. D.; Errington, R. J.; Hyde, E. M.; Mcdonald, W. S.; Markham, R.; Norton, M. C.; Shaw, B. L.; Weeks, B. *J. Chem. Soc. Dalt. Trans.* **1982**, *4*, 1217–1224.

[108] Trans, D.; Briggs, B. J. R.; Constable, A. G.; Mcdonald, W. S.; Shaw, L. *J. Chem. Soc. Dalt. Trans.* **1982**, *1982* (3), 1–6.

[109] Errington, R. J.; Mcdonald, W. S.; Shaw, B. L. *J. Chem. Soc. Dalt. Trans.* **1982**, *2*, 1829–1835.

[110] Albrecht, M., Van Koten, G. *Angew. Chem. Int. Ed.* **2001**, *40*, 3750–3781.

[111] Lu, Z.; White, C.; Rheingold, A. L.; Crabtree, R. H. *Inorg. Chem.* **1993**, *32* (19), 3991–3994.

[112] Suárez, A.; Fernández, J. J.; Fernández, A.; López-torres, M.; Adams, H. *J. Chem. Soc. Dalt. Trans.* **1999**, 4193–4201.

[113] Wang, L.; Pan, H.-R.; Yang, Q.; Fu, H.-Y.; Chen, H.; Li, R.-X. *Inorg. Chem. Commun.* **2011**, *14* (9), 1422–1427.

[114] Lawrence, M. A. W.; Jackson, Y. A.; Mulder, W. H.; Björemark, P. M.; Håkansson, M. *Aust. J. Chem.* **2015**, *68* (5), 731–741.

[115] Bakir, M.; Lawrence, M. A. W.; Singh-Wilmot, M. *J. Coord. Chem.* **2007**, *60* (22), 2385–2399.

Bibliography

[116] Arashiba, K.; Miyake, Y.; Nishibayashi, Y. *Nat. Chem.* **2011**, *3* (2), 120–125.

[117] Peris, E.; Loch, J. A.; Mata, J.; Crabtree, R. H. *Chem. Commun.* **2001**, No. 2, 201–202.

[118] Teratani, T.; Koizumi, T.; Yamamoto, T.; Tanaka, K.; Kanbara, T. *Dalt. Trans.* **2011**, *40* (35), 8879–8886.

[119] Charette, B. J.; Ritch, J. S. *Inorg. Chem.* **2016**, *55* (12), 6344–6350.

[120] Lawrence, M. A. W.; Green, K. A.; Nelson, P. N.; Lorraine, S. C. *Polyhedron* **2018**, *143*, 11–27.

[121] Zhang, J.; Leitus, G.; Ben-David, Y.; Milstein, D. *J. Am. Chem. Soc.* **2005**, *127* (31), 10840–10841.

[122] Nielsen, M.; Alberico, E.; Baumann, W.; Drexler, H. J.; Junge, H.; Gladiali, S.; Beller, M. *Nature* **2013**, *495* (7439), 85–89.

[123] Noyori, R.; Hashiguchi, S. *Acc. Chem. Res.* **1997**, *30* (2), 97–102.

[124] Noyori, R.; Ohkuma, T. *Angew. Chem. Int. Ed.* **2001**, *40*, 40–73.

[125] Noyori, R.; Ohkuma, T. *Angew. Chem.* **2001**, *113*, 40–75.

[126] Noyori, R.; Koizumi, M.; Ishii, D.; Ohkuma, T. *Pure Appl. Chem.* **2001**, *73* (2), 227–232.

[127] Noyori, R.; Kitamura, M.; Ohkuma, T. *PNAS* **2004**, *101* (15), 5356–5362.

[128] Zell, T.; Langer, R. *ChemCatChem* **2018**, *10*, 1930–1940.

[129] Filonenko, G. A.; Putten, R. Van; Pidko, E. A.; Elizovo, G. F. *Chem. Soc. Rev.* **2018**, *47*, 1459–1483.

[130] Morris, R. H. *Chem. Rec.* **2016**, *16*, 2644–2658.

[131] Bullock, R. M.; Helm, M. L. *Acc. Chem. Res.* **2017**, *48*, 2017–2026.

[132] Spasyuk, D.; Smith, S.; Gusev, D. G. *Angew. Chem. Int. Ed.* **2012**, *51*, 2772–2775.

[133] Zhang, L.; Nguyen, H.; Raffa, G.; Trivelli, X.; Capet, F. *ChemSusChem* **2016**, *9*, 1413–1423.

Bibliography

[134] Malineni, J.; Keul, H.; Möller, M. *Dalt. Trans.* **2015**, *44*, 17409–17414.

[135] Cole-hamilton, D. J. *Science (80-.).* **2003**, *299*, 1702–1707.

[136] Schlçgl, R. *Angew. Chem. Int. Ed.* **2015**, *54* (150), 3465–3520.

[137] Benkovic, S. J.; Hammes-schiffer, S. *Science (80-.).* **2003**, *301*, 1196–1203.

[138] Ostwald, W.; Ertl, G. *Angew. Chem. Int. Ed.* **2009**, *48*, 6600–6606.

[139] George W. Parshall. *Science (80-.).* **1980**, *208* (4449), 1221–1224.

[140] Harder, S. *Alkaline-Earth Metal Compounds*; 2012.

[141] Copÿret, C.; Chabanas, M.; Saint-arroman, R. P.; Basset, J. *Angew. Chem. Int. Ed.* **2003**, *42* (2), 156–181.

[142] Blaser, H.; Indolese, A.; Schnyder, A. *Curr. Sci.* **2000**, *78* (11), 1336–1344.

[143] AlanDobscn, S. D. R. *J. Organomet. Chem.* **1975**, *7*, 52–53.

[144] Deeming, A. J.; Shaw, B. L.; A, J. C. S.; Dobson, A.; Robinson, S. D.; Dobson, A.; Robinson, S. D. *Inorg. Chem.* **1977**, *16* (1), 137–142.

[145] Zhang, J.; Gandelman, M.; Shimon, L. J. W.; Rozenberg, H.; Milstein, D. *Organometallics* **2004**, *23* (11), 4026–4033.

[146] Rass-hansen, J.; Falsig, H.; Jørgensen, B.; Christensen, C. H. *J. Chem. Technol. Biotechnol.* **2007**, *82*, 329–333.

[147] Balat, M.; Balat, H.; O¨z, C. *Prog. Energy Combust. Sci.* **2008**, *34*, 551–573.

[148] Nielsen, M.; Kammer, A.; Cozzula, D.; Junge, H.; Gladiali, S.; Beller, M. *Angew. Chem. Int. Ed.* **2011**, *50*, 9593–9597.

[149] Barsch, E.; Sponholz, P.; Junge, H.; Ludwig, R.; Beller, M. *Chem. Commun.* **2014**, *50*, 707–709.

[150] Hu, P.; Diskin-posner, Y.; Ben-david, Y.; Milstein, D. *ACS Catal.* **2014**, *4*, 2649– 2652.

[151] Zhang, J.; Leitus, G.; Ben-david, Y.; Milstein, D.; Reho, V. *J. Am. Chem. Soc.* **2005**, *127*, 10840–10841.

92

[152] Murahashi, S.; Naota, T.; Ito, K.; Maeda, Y.; Taki, H. *J. Org. Chem.* **1987**, *19*, 4319–4327.

[153] Gunanathan, C.; Shimon, L. J. W.; Milstein, D. *J. Am. Chem. Soc.* **2009**, *131*, 3146–3147.

[154] Spasyuk, D.; Gusev, D. G. *Organometallics* **2012**, *31*, 5239–5242.

[155] Löser, C.; Urit, T.; Bley, T. *Appl. Microbiol. Biotechnol.* **2014**, *98* (12), 5397–5415.

[156] Brian C. Gruver, Jeramie J. Adams, Seth J. Warner, Navamoney Arulsamy, and D. M. R. *Organometallics* **2011**, *30*, 5133–5140.

[157] Chakraborty, S.; Bhattacharya, P.; Dai, H.; Guan, H. *Acc. Chem. Res.* **2015**, *48* (2), 1995–2003.

[158] Ø, H. V.; Garc, A.; Canseco-gonzalez, D.; Morales-, D. *ChemCatChem* **2018**, *10*, 3136–3172.

[159] Beller, M.; Beller, M. *Chem. Commun* **2011**, *47*, 4849–4859.

[160] Dub, P. A.; Ikariya, T. *ACS Catal.* **2012**, *2*, 1718–1741.

[161] Noyori, R.; Takeshi Ohkuma. *Angew. Chem. Int. Ed.* **2001**, *40*, 40–73.

[162] Langer, R.; Leitus, G.; Ben-david, Y.; Milstein, D. *Angew. Chem. Int. Ed.* **2011**, *50*, 2120–2124.

[163] Zell, T.; Ben-david, Y.; Milstein, D. *Catal. Sci. Technol.* **2015**, *5*, 822–826.

[164] Gorgas, N.; Stöger, B.; Veiros, L. F.; Pittenauer, E.; Allmaier, G.; Kirchner, K. *Organometallics* **2014**, *33*, 6905–6914.

[165] Zhu, S.; Zhou, Q. *Acc. Chem. Res.* **2017**, *50*, 988–1001.

[166] Clarke, M. L. *Catal. Sci. Technol.* **2012**, *2*, 2418–2423.

[167] Zhang, J.; Leitus, G.; Ben-david, Y.; Milstein, D. *Angew. Chem. Int. Ed.* **2006**, *45*, 1113–1115.

[168] Sun, Y.; Koehler, C.; Tan, R.; Annibale, V. T.; Song, D. *Chem. Commun.* **2011**, *47*, 8349–8351.

[169] Fogler, E.; Balaraman, E.; Ben-david, Y.; Leitus, G.; Shimon, J. W.; Milstein, D. *Organometallics* **2011**, *30*, 3826–3833.

Bibliography

[170] Balaraman, E.; Fogler, E.; Milstein, D. *Chem. Commun.* **2012**, *48*, 1111–1113.

[171] Junge, K.; Wendt, B.; Jiao, H.; Beller, M. *ChemCatChem* **2014**, *6*, 2810–2814.

[172] Zell, T.; Ben-david, Y.; Milstein, D. *Angew. Chem. Int. Ed* **2014**, *53*, 4685–4689.

[173] Werkmeister, S.; Junge, K.; Wendt, B.; Alberico, E.; Jiao, H.; Baumann, W.; Junge, H.; Gallou, F.; Beller, M. *Angew. Chem. Int. Ed* **2014**, *53*, 8722–8726.

[174] Elangovan, S.; Wendt, B.; Topf, C.; Bachmann, S.; Scalone, M.; Spannenberg, A.; Jiao, H.; Baumann, W.; Junge, K.; Beller, M. *Adv.Synth. Catal.* **2016**, *358*, 820–825.

[175] Links, D. A.; Acosta-ramirez, A.; Bertoli, M.; Gusev, D. G.; Schlaf, M. *Green Chem.* **2012**, *14*, 1178–1188.

[176] Korstanje, T. J.; Vlugt, J. I. Van Der; Elsevier, C. J.; Bruin, B. De. *Science (80-.).* **2015**, *350* (6258).

[177] Spasyuk, D.; Smith, S.; Gusev, D. G. *Angew. Chem. Int. Ed.* **2013**, *52*, 2538–2542.

[178] Rezayee, N. M.; Hu, C. A.; Sanford, M. S. *J. Am. Chem. Soc.* **2015**, *137*, 1028‒1031.

[179] Kothandaraman, J.; Goeppert, A.; Czaun, M.; Olah, G. A.; Prakash, G. K. S. *J. Am. Chem. Soc.* **2016**, *138*, 778‒781.

[180] Kar, S.; Sen, R.; Goeppert, A.; Prakash, G. K. S. *J. Am. Chem. Soc.* **2018**, *140*, 1580‒1583.

[181] Kar, S.; Goeppert, A.; Prakash, G. K. S. *ChemSusChem* **2019**, *12*, 3172–3177.

[182] Kothandaraman, J.; Czaun, M.; Goeppert, A.; Haiges, R.; Jones, J.; May, R. B.; Prakash, G. K. S.; Olah, G. A. *ChemSusChem* **2015**, *8*, 1442–1451.

[183] Kar, S.; Goeppert, A.; Prakash, G. K. S. *J. Am. Chem. Soc.* **2019**, *141*, 12518–12521.

[184] Monney, A.; Barsch, E.; Sponholz, P.; Junge, H.; Ludwig, R.; Beller, M. *Chem. Commun.* **2014**, *50* (6), 707–709.

[185] Nguyen, D. H.; Merel, D.; Merle, N.; Trivelli, X.; Capet, F.; Gauvin, R. M. *Dalt. Trans.* **2021**, *50*, 10067–10081.

[186] Chang, J.; Ding, M.; Kang, J.; Zhang, J.; Chen, X. **2022**, No. Chart 1, 11507–11514.

[187] Dowell, N. Mac; Fennell, P. S.; Shah, N.; Maitland, G. C. *Nat. Clim. Chang.* **2017**, *7*, 243–249.

[188] Tackett, B. M.; Gomez, E.; Chen, J. G. *Nat. Catal.* **2019**, *2*, 381–386.

[189] Stuardi, F. M.; Macpherson, F. *Curr. Opin. Green Sustain.* **2019**, *16*, 71–76.

[190] Bai, S.; Zhou, C.; Wu, X.; Sun, R.; Sels, B. *ACS Catal.* **2021**, *11*, 12682–12691.

[191] Olah, G. A.; Goeppert, A.; Prakash, G. K. S. *J. Org. Chem.* **2009**, *74*, 487–498.

[192] Joghee, P.; Malik, J. N. *MRS Energy Sustain.* **2015**, *2*, 1–31.

[193] Bukhtiyarova, M.; Lunkenbein, T.; Kähler, K.; Schlögl, R. *Catal. Lett.* **2017**, *147* (2), 416–427.

[194] Schlçgl, R. *Angew. Chem. Int. Ed.* **2022**, *61*.

[195] Kaithal, A.; Chatterjee, B.; Werle, C.; Leitner, W. *Angew. Chem. Int. Ed.* **2021**, *60*, 26500–26505.

[196] Chatterjee, B.; Chang, W.; Jena, S.; Werle, C. *ACS Catal.* **2020**, *10*, 14024–14055.

[197] Elsby, M. R.; Baker, R. T. *Chem. Soc. Rev.* **2020**, *49*, 8933–8987.

[198] Chatterjee, B.; Chang, W.-C.; Werlé, C. *ChemCatChem* **2021**, *13*, 1659–1682.

[199] Kaithal, A.; Schmitz, M.; Hölscher, M.; Leitner, W. *ChemCatChem* **2019**, *11*, 5287–5291.

[200] Kaithal, A.; Schmitz, M.; Hölscher, M.; Leitner, W. *ChemCatChem* **2020**, *12*, 781–787.

[201] Mar, M. J.; Andersen, J. M.; Kandasamy, V.; Liu, J.; Solem, C.; Jensen, P. R. *Biotechnol. Biofuels* **2020**, *13* (1), 1–10.

[202] Chen, Z.; Wu, Y.; Huang, J.; Liu, D. *Bioresour. Technol.* **2015**, *197*, 260–265.

[203] Sun, D.; Li, Y.; Yang, C.; Su, Y.; Yamada, Y.; Sato, S. *Fuel Process. Technol.* **2020**, *197*, 106193.

[204] Arai, T.; Tamura, M.; Nakagawa, Y.; Tomishige, K. *ChemSusChem* **2016**, *9* (13), 1680–1688.

[205] urk, Mark J.; Pharkya, Priti; Bugard, A. P. 2010.

[206] Jeong, S.; Kim, H.; Bae, J. H.; Kim, D. H.; Peden, C. H. F.; Park, Y. K.; Jeon, J. K. *Catal. Today* **2012**, *185* (1), 191–197.

[207] López Contreras, A. M.; Kuit, W.; Siemerink, M. A. J.; Kengen, S. W. M.; Springer, J.; Claassen, P. A. M. *Bioalcohol Prod.* **2010**, 415–460.

[208] Dürre, P. *Biotechnol. J.* **2007**, *2* (12), 1525–1534.

[209] Prabu, K.; Prabu, M.; Venugopal, A. K.; Venugopalan, A. T.; Sandilya, W. V. Y. S.; Gopinath, C. S.; Raja, T. *Appl. Catal. A Gen.* **2016**, *525*, 237–246.

[210] Dagle, V. L.; Winkelman, A. D.; Jaegers, N. R.; Saavedra-Lopez, J.; Hu, J.; Engelhard, M. H.; Habas, S. E.; Akhade, S. A.; Kovarik, L.; Glezakou, V. A.; Rousseau, R.; Wang, Y.; Dagle, R. A. *ACS Catal.* **2020**, *10* (18), 10602–10613.

[211] Eagan, N. M.; Kumbhalkar, M. D.; Buchanan, J. S.; Dumesic, J. A.; Huber, G. W. 2019, p 223.

[212] Mascal, M. *Biofuels, Bioproducts and Biorefining.* 2012, pp 483–493.

[213] Wang, W.; Tao, L. *Renew. Sust. Energ. Rev.* **2016**, *53*, 801–822.

[214] Mascal, M.; Davis, C. *Biofuels, Bioprod. Bioref.* **2012**, *6* (4), 483–493.

[215] Leimgruber, S.; Trimmel, G. *Monatsh. Chem.* **2015**, *146* (7), 1081–1097.

[216] Li, F.; Dai, X.; Lu, X.; Wang, C.; Qi, W. *Catal. Sci. Technol.* **2021**, *11*, 4500–4508.

[217] Cordon, M. J.; Zhang, J.; Purdy, S. C.; Wegener, E. C.; Unocic, K. A.; Allard, L. F.; Zhou, M.; Assary, R. S.; Miller, J. T.; Krause, T. R.; Lin, F.; Wang, H.; Kropf, A. J.; Yang, C.; Liu, D.; Li, Z. *ACS Catal.* **2021**, *11*, 7193–7209.

[218] Nolan, D. P. In *Handbook of Fire and Explosion Protection Engineering Principles for Oil, Gas, Chemical, and Related Facilities*; 2019; pp 65–88.

[219] Li, C.; Ban, H.; Cai, W.; Zhang, Y.; Li, Z.; Fujimoto, K. *J. Saudi Chem. Soc.* **2017**, *21* (8), 974–982.

[220] Kots, P. A.; Zabilska, A. V.; Grigor'ev, Y. V.; Ivanova, I. I. *Pet. Chem.* **2019**, *59* (8), 925–934.

[221] Kwak, J. H.; Rousseau, R.; Mei, D.; Peden, C. H. F.; Janos Szanyi. *ChemCatChem* **2011**, *3*, 1557–1561.

[222] Piccirilli, L.; Pinheiro, D. L. J.; Nielsen, M. *Catalysts* **2020**, *10* (7), 773.

[223] Kuriyama, W.; Matsumoto, T.; Ogata, O.; Ino, Y.; Aoki, K.; Tanaka, S.; Ishida, K.; Kobayashi, T.; Sayo, N.; Saito, T. *Org. Process Res. Dev.* **2012**, *16* (1), 166–171.

[224] Sordakis, K.; Tang, C.; Vogt, L. K.; Junge, H.; Dyson, P. J.; Beller, M.; Laurenczy, G. *Chem. Rev.* **2018**, *118* (2), 372–433.

[225] Gabriëls, D.; Hernández, W. Y.; Sels, B. F.; Van Der Voort, P.; Verberckmoes, A. *Catal. Sci. Technol.* **2015**, *5* (8), 3876–3902.

[226] Sponholz, P.; Mellmann, D.; Cordes, C.; Alsabeh, P. G.; Li, B.; Li, Y.; Nielsen, M.; Junge, H.; Dixneuf, P.; Beller, M. *ChemSusChem* **2014**, *7* (9), 2419–2422.

[227] Wu, L.; Liu, Q.; Fleischer, I.; Jackstell, R.; Beller, M. *Nat. Commun.* **2014**, *5*, 3091.

[228] Rodriguez, C. J.; Foster, D. F.; Eastham, R.; Cole-hamilton, D. J. *Chem. Commun.* **2004**, 1720–1721.

[229] Li, H.; Dong, K.; Jiao, H.; Neumann, H.; Jackstell, R.; Beller, M. *Nat. Chem.* **2016**, *8*, 1159–1166.

[230] Waiba, S.; Maji, B. *ChemCatChem* **2020**, *12* (7), 1891–1902.

[231] Daw, P.; Ben-david, Y.; Milstein, D. *J. Am. Chem. Soc.* **2018**, *140*, 11931–11934.

[232] Nad, P.; Mukherjee, A. *Asian J. Org. Chem.* **2021**, *10*, 1958–1985.

[233] Zhang, M.; Yu, Y. *Ind. Eng. Chem. Res.* **2013**, *52*, 9505–9514.

[234] Klein, T.; Oliveira, R. De; Rosset, M.; Perez-lopez, O. W. *Catal. Commun.* **2018**, *104*, 32–36.

[235] Pang, J.; Yin, M.; Wu, P.; Li, X.; Li, H. *Green Chem* **2021**, *23*, 7902–7916.

[236] Akkarawatkhoosith, N.; Kaewchada, A.; Jaree, A. *Energy Fuels* **2019**, *33*, 5322–5331 Article.

[237] Zhang, S.; Guo, F.; Yan, W.; Dong, W.; Zhou, J.; Zhang, W.; Xin, F.; Jiang, M. *Appl. Microbiol. Biotechnol.* **2020**, *104* (17), 7239–7245.

[238] Fischer, E.; Speier, A. *Chem. Ges.* **1895**, *28*, 3252–3258.

[239] Khusnutdinova, J. R.; Garg, J. A.; Milstein, D. *ACS Catal.* **2015**, *5* (4), 2416–2422.

[240] Aboo, A. H.; Bennett, E. L.; Deeprose, M.; Robertson, C. M.; Iggo, J. A.; Xiao, J. *Chem. Commun.* **2018**, *54*, 11805–11808.

[241] Garg, N.; Sarkar, A.; Sundararaju, B. *Coord. Chem. Rev.* **2021**, *433*, 213728.

[242] Sklyaruk, J.; Zubar, V.; Borghs, J. C.; Rueping, M. *Org. Lett.* **2020**, *22*, 6067–6071.

[243] Garg, N.; Paira, S.; Sundararaju, B. *ChemCatChem* **2020**, *12*, 3472–3476.

[244] Weingart, P.; Thiel, W. R. *ChemCatChem* **2018**, *10*, 4844–4848.

[245] Wang, Y.; Huang, Z.; Leng, X.; Zhu, H.; Liu, G.; Huang, Z. *J. Am. Chem. Soc.* **2018**, *140*, 4417–4429.

[246] Castellanos-blanco, N.; Arévalo, A.; García, J. J. *Dalt. Trans.* **2016**, *45*, 13604–13614.

[247] Lundberg, H.; Adolfsson, H. *Tetrahedron Lett.* **2011**, *52* (21), 2754–2758.

[248] Liu, W.; Yuan, M.; Yang, X.; Li, K.; Xie, J. *Chem. Commun.* **2015**, *51*, 6123–6125.

[249] Sakaguchi, S.; Yamaga, T.; Ishii, Y. *J. Org. Chem.* **2001**, *66* (6), 4710–4712.

[250] Baratta, W.; Rigo, P. *Eur. J. Inorg. Chem.* **2008**, 4041–4053.

[251] Baratta, W.; Ballico, M.; Esposito, G.; Rigo, P. *Chem. Eur. J.* **2008**, *14*, 5588 – 5595.

Appendix A – Chapter 3.1

A. Supplementary information for Chapter 3.1

Most chemicals were purchased from commercial suppliers and used without further purification unless otherwise stated. Neat ethanol (purity 99.99%), NaOtBu (purity 97%), NaOEt (purity 95%), and precatalysts **Ru-1 - Ru-5** are commercially available and used without further purification. N_2 gas ($H_2O \leq 3$ ppm; $O_2 \leq 2$ ppm) 1-butene (purity 98%), cis-2-butene (purity 99%), and $trans$-2-butene (purity 99%), butane (purity 99.5%) were purchased from a commercial supplier as well. All reactions dealing with air or moisture-sensitive compounds were performed using standard Schlenk techniques or in an argon-filled glovebox. ^{1}H-NMR and ^{13}C-NMR spectra were recorded on a Bruker Avance III 400 MHz spectrometer and were referenced on the deuterated solvent peak. Chemicals handling and loading into the autoclave container were done in a glovebox. After taking the loaded autoclave out of the glovebox, the autoclave was quickly sealed and purged three times with N_2 before carrying out the experiments. All of the starting materials and dehydrogenation products are literature-known compounds, and the experimental data fit with those reported. All chemicals used for calibration curves were analytical standards.

Reactor A (stainless steel, inner diameter 25.0 mm, reactor capacity: 22.8 mL; Teflon cup volume: 13.0 mL). The pressure record is non-electronic and subject to error.

Reactor B (Alloy 600, 2550 flat gasket microvessel, 5.0 mL; reactor capacity: 16.0 mL; Teflon cup volume: 6.0 mL). The electronic dashboard records pressure with accurate data.

General procedure for a catalytic reaction. A 22.8 mL stainless steel container of a high-pressure reactor (reactor A) provided with a Teflon cup and stirrer was loaded with the catalyst (8.3-1000 ppm) and base (10-25 mol%) inside of the glovebox. The sealed container was removed from the glovebox. Then, degassed EtOH (2.5, 3.5, or 5.0 mL) was added with a syringe. The reactor was quickly purged three times with N_2 before carrying out the experiments at the desired temperature (85-115 ^{o}C) for 1-168 h at a stirring rate of 600 rpm.

After the reaction time, the reactor was cooled down to room temperature, using an ice bath. The gas was slowly released into a gas sampling bag to analyze the gas phase. The remnant reaction mixture was neutralized with NH_4Cl (equimolar with the added base, 458 mg-1145 mg). Tridecane (100 uL) was added as the internal standard for the quantification of 2-butanol, 1-butanol, 2-propanol, diethoxymethane, ethyl acetate, 2-pentanol, 3-hexanol, and 4-heptanol. Decane (20 uL) was used as an internal standard for the quantification of ethanol and dimethyl sulfoxide (50 uL) was also added as an internal standard to quantify the amount of sodium acetate. Finally, the resulting solution was diluted with dichloromethane (10-15 mL) and analyzed by NMR, GC-FID, and GC-MS. The gas phase was analyzed by GC-MS, GC-TCD, and Micro-GC. The remnant solid product was analyzed by ^1H and ^{13}C NMR using D_2O as solvent.

Reaction pathways of each product (liquid, gas, solid phase)
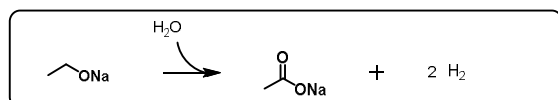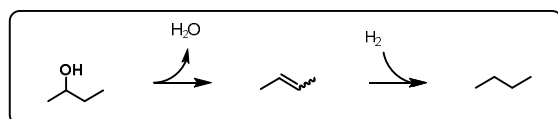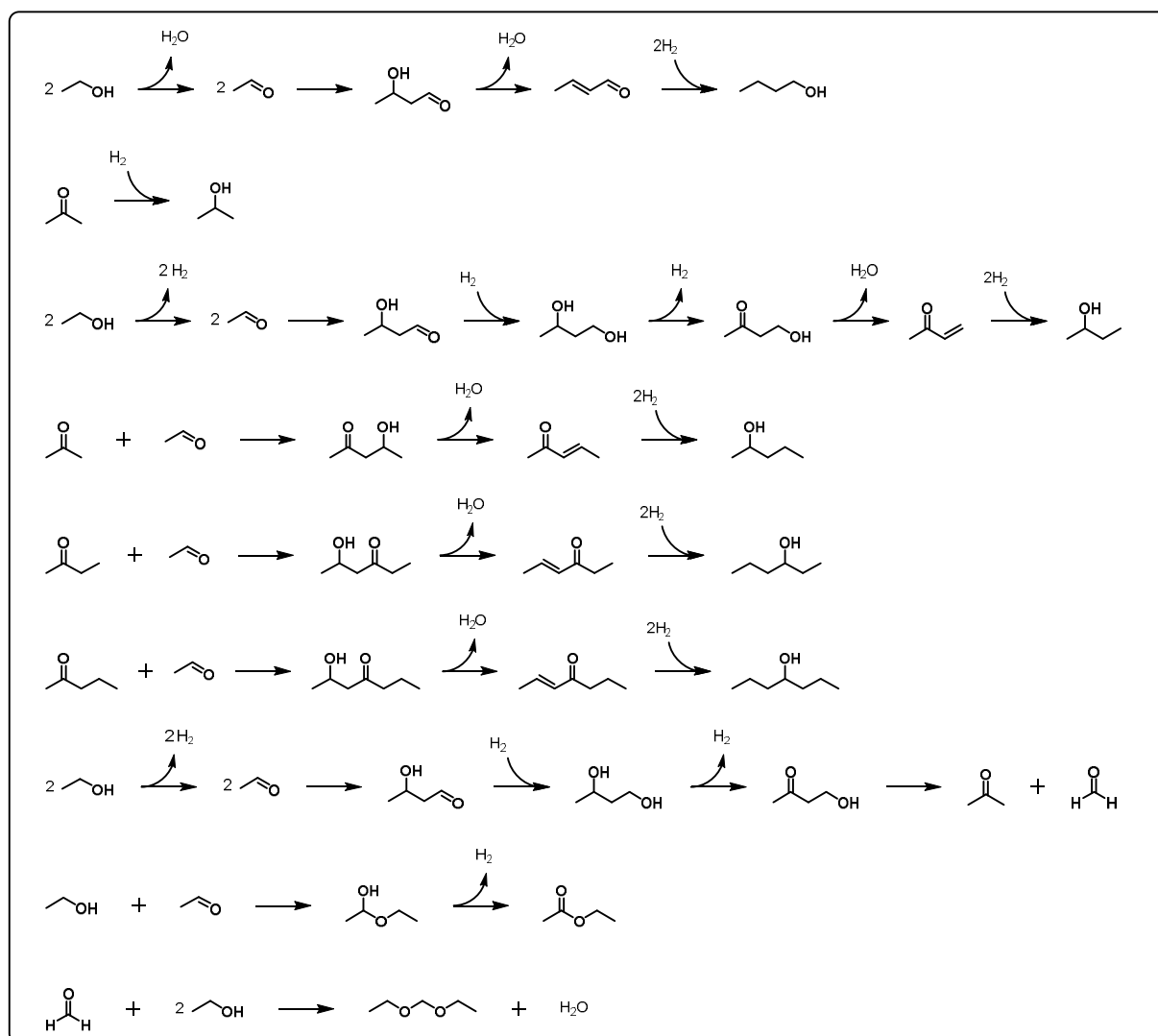
Pressure change studies

Reaction conditions: 2.5 mL ethanol, **Ru-2** (250 ppm), 96 h, 130 ºC, NaOEt (20 mol%) in a 18.4 mL high-pressure Parr reactor and 600 rpm.
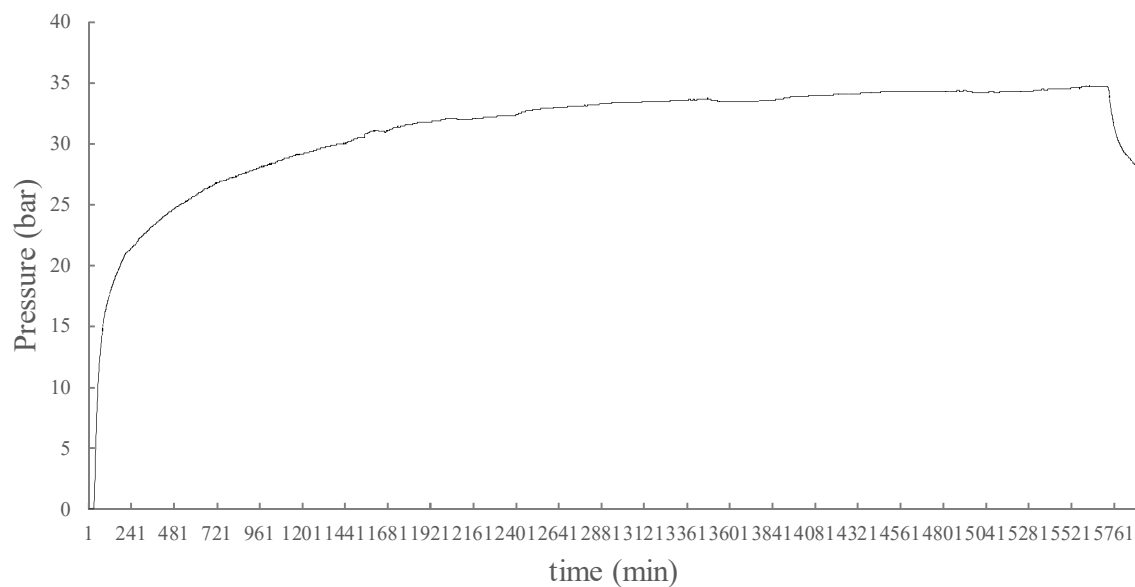
Figure A.1: Pressure changes over time were observed by Parr system digital recording.

GC-MS spectra of liquid products
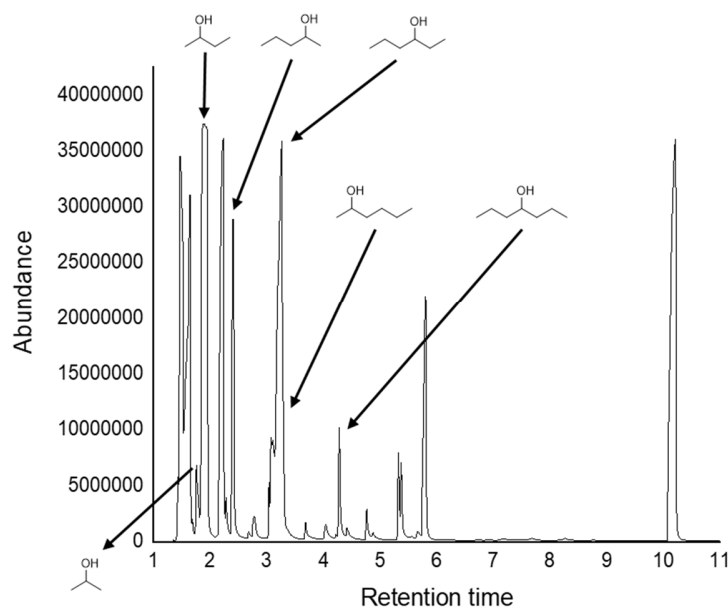
Figure A.2: A typical MS spectrum of a reaction mixture. (Table 3-4, Entry 5)
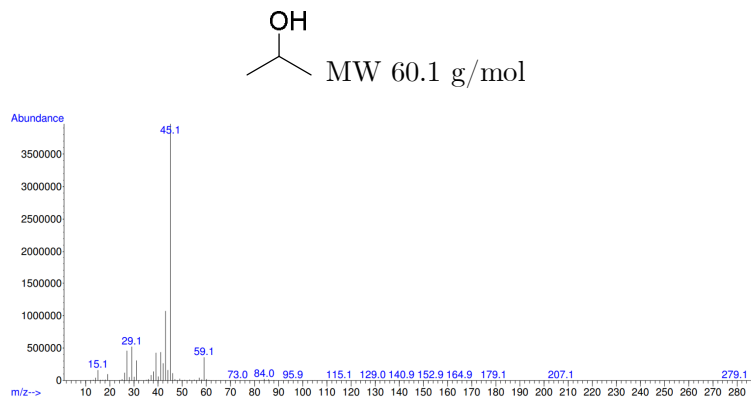
Figure A.3: A MS spectrum of 2-propanol. (Table 3-4, Entry 5)
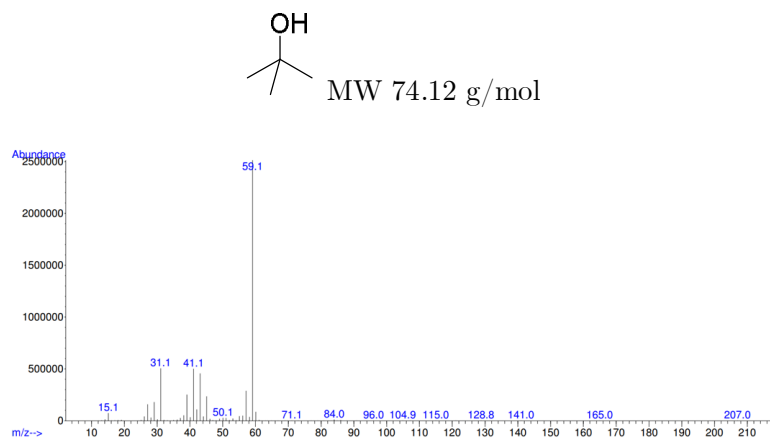
Figure A.4: A MS spectrum of *tert*-butanol. (Table 3-4, Entry 5)
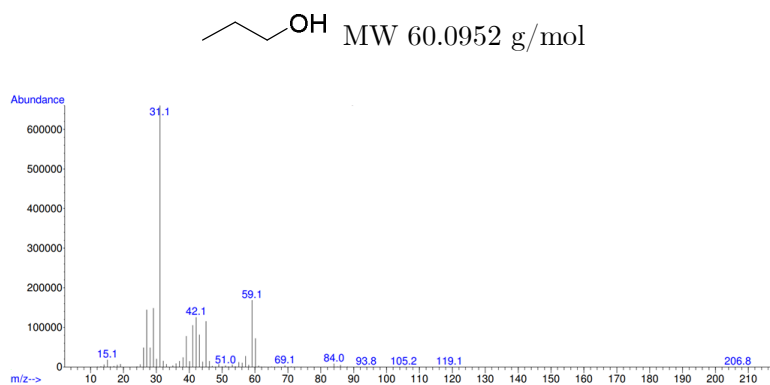
Figure A.5: A MS spectrum of 1-propanol. (Table 3-4, Entry 5)
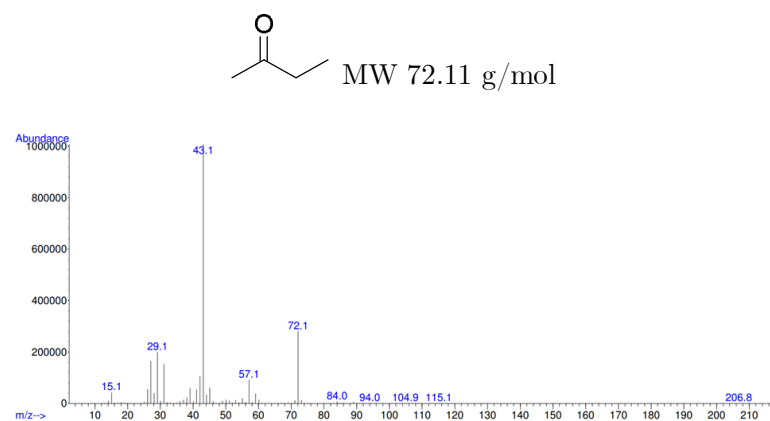
Figure A.6: A MS spectrum of 2-butanone. (Table 3-4, Entry 5)
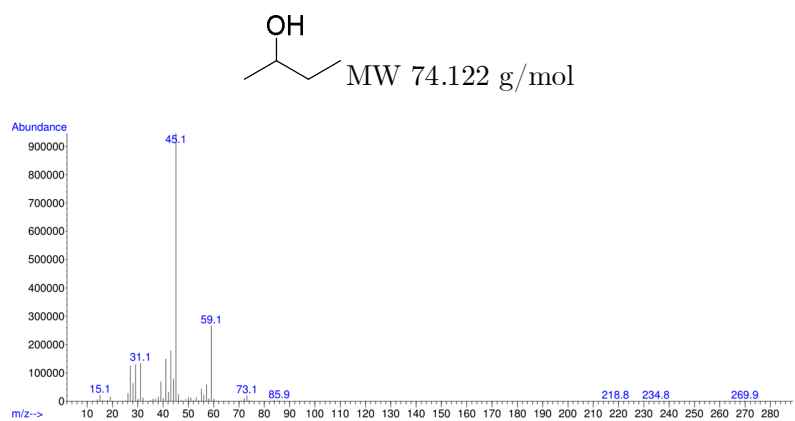
Figure A.7: A MS spectrum of 2-butanol. (Table 3-4, Entry 5)
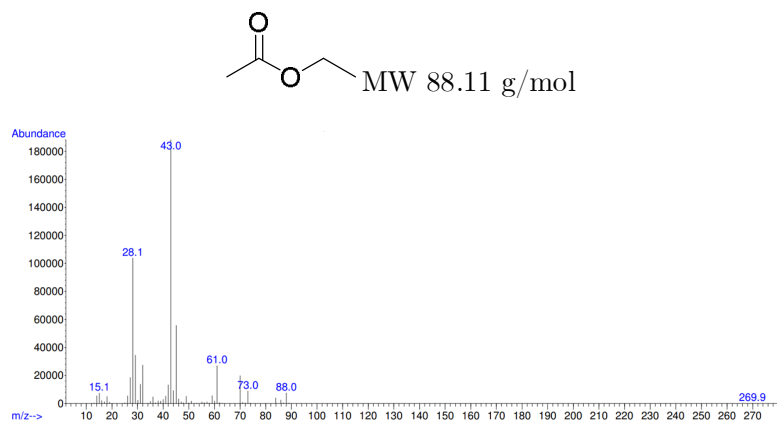
Figure A.8: A MS spectrum of ethyl acetate. (Table 3-4, Entry 5)
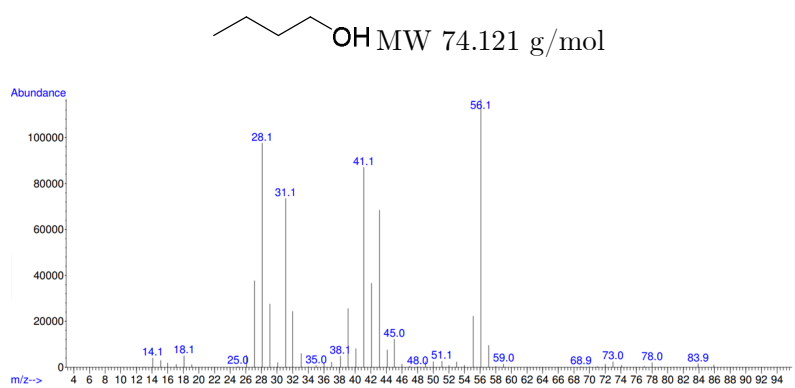
Figure A.9: A MS spectrum of 1-butanol. (Table 3-4, Entry 5)

MW 104.15 g/mol
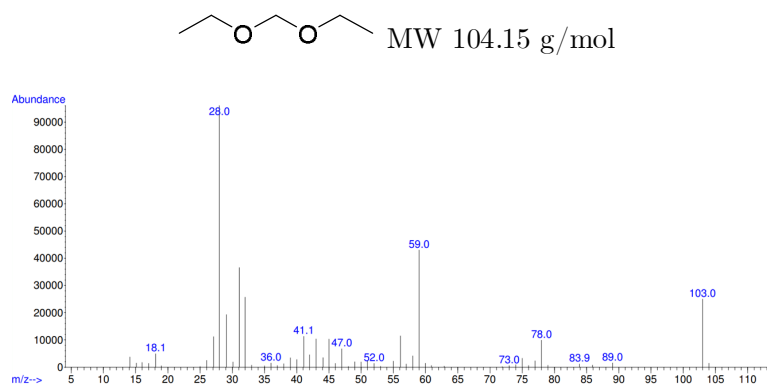
Figure A.10: A MS spectrum of diethoxymethane. (Table 3-4, Entry 5)

MW 88.148 g/mol
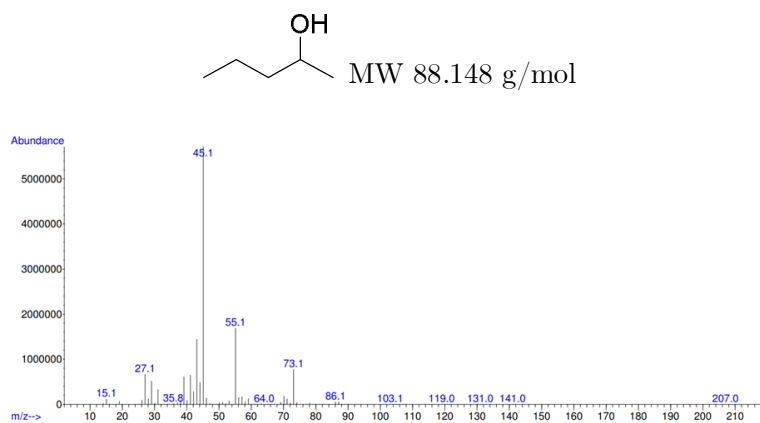
Figure A.11: A MS spectrum of 2-pentanol. (Table 3-4, Entry 5)

MW 100.1589 g/mol
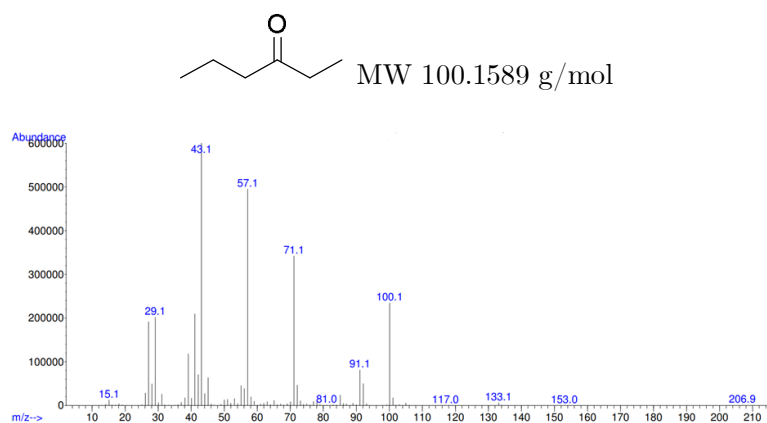
Figure A.12: A MS spectrum of 3-hexanone. (Table 3-4, Entry 5)
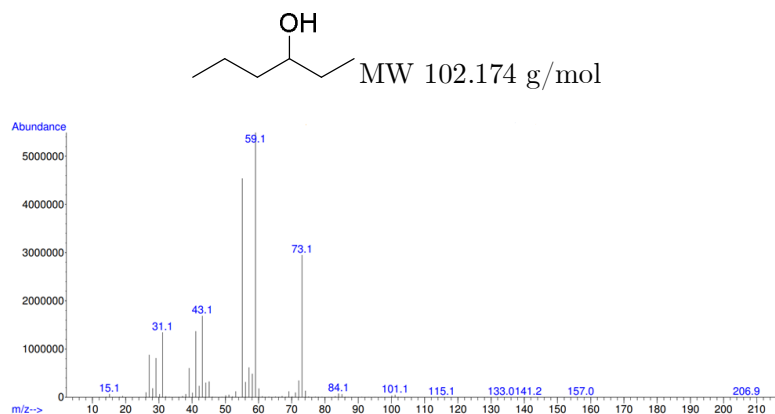
Figure A.13: A MS spectrum of 3-hexanol. (Table 3-4, Entry 5)
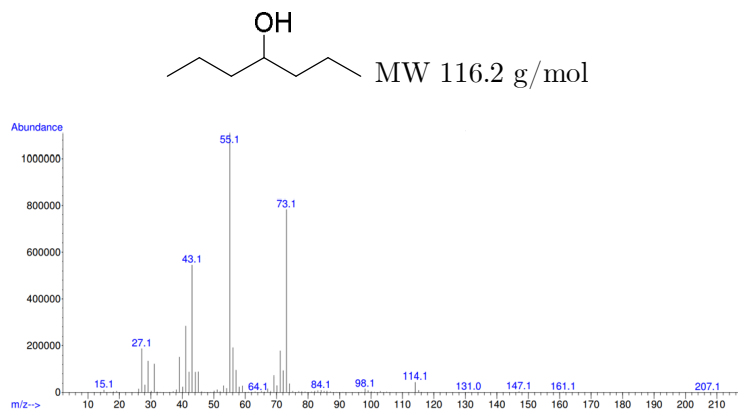
Figure A.14: A MS spectrum of 4-heptanol. (Table 3-4, Entry 5)

GC-TCD reports of inorganic gas

Reaction conditions: 5 mL EtOH, **Ru-2** (500 ppm, 25.1 mg), 48 h, 105 ºC, NaOtBu (10 mol%, 823 mg) in a 25.9 mL high-pressure reactor and 600 rpm.
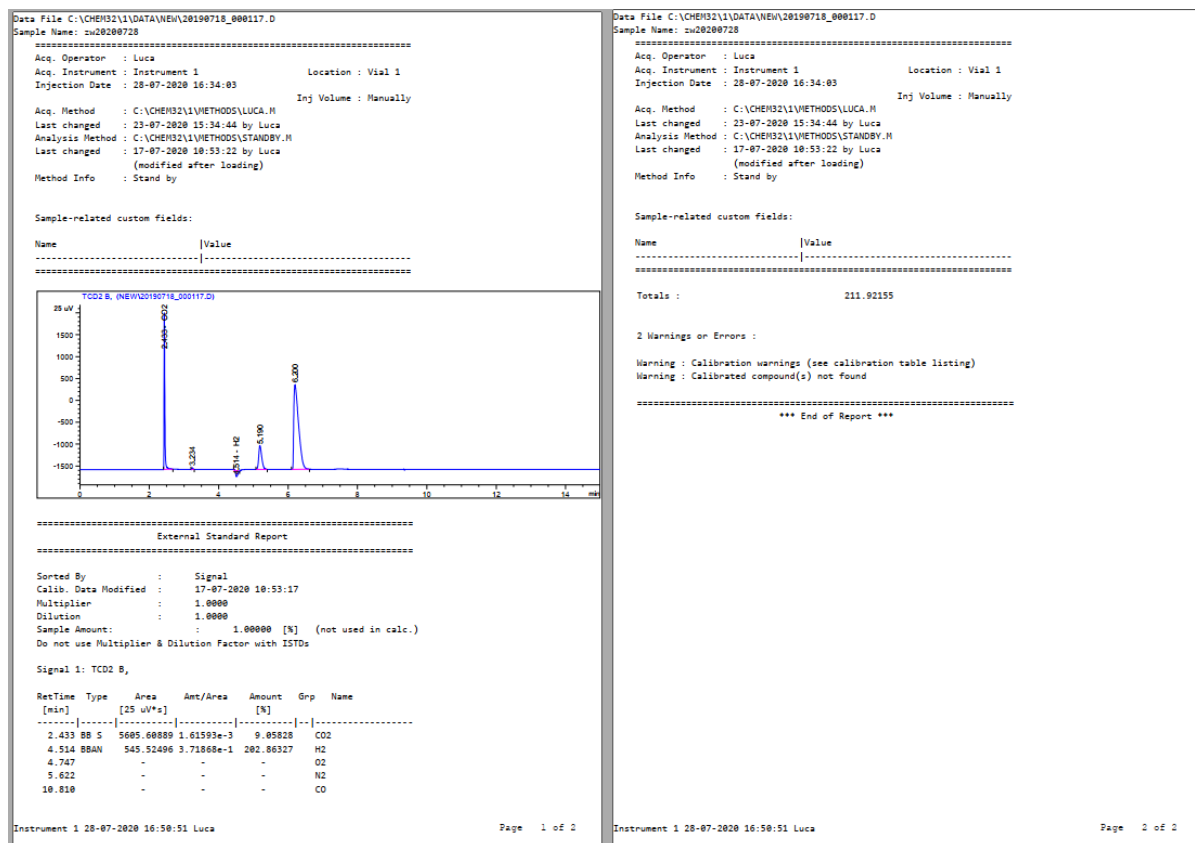
Reaction conditions: 5 mL EtOH, **Ru-4** (250 ppm, 16.2 mg), 41 h, 115 ºC, NaOEt (20 mol%, 1166 mg) in a 25.9 mL high-pressure reactor and 600 rpm.

Reaction conditions: 5 mL EtOH, **Ru-5** (250 ppm, 13.5 mg), 41 h, 115 ºC, NaOEt (20 mol%, 1166 mg) in a 25.9 mL high-pressure reactor and 600 rpm.

GC-FID reports of liquid products

Reaction conditions: 5 mL EtOH, **Ru-1** (830 ppm, 51.8 mg), 96 h, 115 ºC, NaOEt (20 mol%, 1166 mg) in a 25.9 mL high-pressure reactor and 600 rpm.

```
Data File C:\CHEM32\1\DATA\2022\ZWENTRY0405.D
Sample Name: ZWENTRY0405
===============================================================================
Acq. Operator   : MBB                      Seq. Line :    4
Acq. Instrument : GC                        Location : Vial 8
Injection Date  : 2/12/2022 3:33:16 PM           Inj :    1
                                          Inj Volume : 1 µl
Acq. Method     : C:\CHEM32\1\METHODS\GC-FID_WT.M
Last changed    : 11/29/2021 10:07:34 AM by MBB
Analysis Method : C:\CHEM32\1\METHODS\GC-FID_WT.M
Last changed    : 4/25/2022 3:43:45 PM by MBB
                  (modified after loading)
```

FID1 A, (2022\ZWENTRY0405.D)

```
===============================================================================
                         Area Percent Report
===============================================================================
Sorted By           :        Signal
Calib. Data Modified :        12/8/2006 12:33:15 PM
Multiplier          :        1.0000
Dilution            :        1.0000
Use Multiplier & Dilution Factor with ISTDs

Signal 1: FID1 A,

Peak RetTime Type  Width     Area       Area      Name
  #   [min]        [min]    [pA*s]        %
----|-------|----|-------|----------|----------|----------------
  1   1.208 BV    8.72e-3 4.09781e-1  0.00030  ?
  2   1.255 VV S  9.85e-3 6389.10449  4.73584  ?
  3   1.271 VV S   0.0157 5144.05615  3.81297  ?
  4   1.315 VV S   0.0103 7469.47461  5.53665  ?
  5   1.335 VV S   0.0164 8293.04492  6.14711  ?
  6   1.374 BV X   0.0110   99.97847  0.07411  ?
  7   1.393 VV X   0.0148  168.33704  0.12478  ?
  8   1.411 VV X   0.0102   11.68013  0.00866  ?
  9   1.434 VB S   0.0156 1.01745e5 75.41698  ?
 10   1.510 BV X  8.66e-3   18.66752  0.01384  ?
 11   1.525 VB X   0.0161   39.50623  0.02928  ?
 12   1.647 BV     0.0108  964.02954  0.71457  ?
 13   1.662 VV     0.0144 1569.88892  1.16366  ?
 14   1.705 VB     0.0257   17.86863  0.01324  ?
 15   1.980 BV     0.0234  869.32996  0.64438  ?
 16   2.077 VV     0.0310   16.39939  0.01216  ?
 17   2.142 VV     0.0393   13.84229  0.01026  ?
 18   2.217 VH     0.0282  227.67053  0.16876  ?
```

```
Data File C:\CHEM32\1\DATA\2022\ZWENTRY0405.D
Sample Name: ZWENTRY0405
===============================================================================
Acq. Operator   : MBB                      Seq. Line :    4
Acq. Instrument : GC                        Location : Vial 8
Injection Date  : 2/12/2022 3:33:16 PM           Inj :    1
                                          Inj Volume : 1 µl
Acq. Method     : C:\CHEM32\1\METHODS\GC-FID_WT.M
Last changed    : 11/29/2021 10:07:34 AM by MBB
Analysis Method : C:\CHEM32\1\METHODS\GC-FID_WT.M
Last changed    : 4/25/2022 3:43:45 PM by MBB
                  (modified after loading)
===============================================================================
Peak RetTime Type  Width     Area       Area      Name
  #   [min]        [min]    [pA*s]        %
----|-------|----|-------|----------|----------|----------------
 19   2.722 BB     0.0266    6.23966  0.00463  ?
 20   2.859 BB     0.0287   12.15615  0.00901  ?
 21   2.993        0.0000    0.00000  0.00000  C14
 22   3.075 BV     0.0255   99.38644  0.07367  ?
 23   3.116 VV     0.0254   93.43029  0.06925  ?
 24   3.174 VB     0.0301  515.06836  0.38179  ?
 25   3.466        0.0000    0.00000  0.00000  C15
 26   3.926        0.0000    0.00000  0.00000  C16
 27   4.476 BB     0.0491   26.30742  0.01950  ?
 28   5.612 HH     0.0306   11.03261  0.00818  ?
 29   5.657 HH     0.0642   23.07819  0.01711  ?
 30   6.072 HB     0.0362  197.88586  0.14668  ?
 31  10.394 BB     0.0422  866.97992  0.64264  ?

Totals :                            1.34910e5

1 Warnings or Errors :

Warning : Calibrated compound(s) not found
===============================================================================
                         Summed Peaks Report
===============================================================================
Signal 1: FID1 A,
-------------------------------------------------------------------------------
                     Final Summed Peaks Report
===============================================================================
Signal 1: FID1 A,
Name              Total Area    Area
                    [pA*s]       %
----------------|------------|--------|
C14               0.00000     0.0000
C15               0.00000     0.0000
C16               0.00000     0.0000

Totals :                      0.0000

                  *** End of Report ***
```

Reaction conditions: 5 mL EtOH, **Ru-2** (250 ppm, 15.1 mg), 96 h, 115 °C, NaOEt (20 mol%, 1166 mg) in a 25.9 mL high-pressure reactor and 600 rpm.

Data File C:\CHEM32\1\DATA\OLD DATA\2020\ZW2020100901B.D
Sample Name: zw2020100901b

```
Acq. Operator   :                          Seq. Line :   4
Acq. Instrument : GC                       Location : Vial 3
Injection Date  : 10/12/2020 10:32:57 AM       Inj :   1
                                            Inj Volume : 1 µl
Acq. Method     : C:\CHEM32\1\METHODS\GC-FID_WT.M
Last changed    : 1/2/2020 9:38:52 AM
Analysis Method : C:\CHEM32\1\METHODS\GC-FID_WEFA.M
Last changed    : 7/30/2022 1:56:07 PM by MBB
                  (modified after loading)
```



```
                    Area Percent Report

Sorted By           :    Signal
Calib. Data Modified :   12/8/2006 12:33:15 PM
Multiplier          :    1.0000
Dilution            :    1.0000
Use Multiplier & Dilution Factor with ISTDs

Signal 1: FID1 A,

Peak RetTime Type  Width     Area       Area     Name
  #   [min]        [min]    [pA*s]       %
---|-------|------|-------|----------|--------|----------------
  1   1.225 BV    9.32e-3    1.23934  0.00042 ?
  2   1.275 VV    0.0203  1121.09192  0.38115 ?
  3   1.287 VV    0.0124   591.10468  0.20096 ?
  4   1.327 VV S  0.0200 3.45047e4   11.73087 ?
  5   1.381 VV S  0.0446 9.07979e4   30.86938 ?
  6   1.424 VV S  0.0237 2897.57007   0.98511 ?
  7   1.438 VV S  0.0288 9.81318e4   33.36273 ?
  8   1.517 BV T  8.71e-3  100.12383   0.03404 ?
  9   1.558 VB T  0.0299   960.73492   0.32663 ?
 10   1.718 VB S  0.0491 2.94293e4   10.00533 ?
 11   2.029 BV    0.0317 8425.74414   2.86458 ?
 12   2.118 VV    0.0237  134.34705   0.04568 ?
 13   2.169 VB    0.0219   74.00436   0.02516 ?
 14   2.252 BB    0.0255 3115.85864   1.05933 ?
 15   2.591 BB    0.0280   77.04747   0.02619 ?
 16   2.736 BV    0.0287  124.03327   0.04217 ?
 17   2.885 VB    0.0438   30.21939   0.01027 ?
 18   2.993       0.0000    0.00000  0.00000 C14
```

GC 8/11/2022 1:14:49 PM MBB   Page 1 of 3

Data File C:\CHEM32\1\DATA\OLD DATA\2020\ZW2020100901B.D
Sample Name: zw2020100901b

```
Peak RetTime Type  Width     Area       Area     Name
  #   [min]        [min]    [pA*s]       %
---|-------|------|-------|----------|--------|----------------
 19   3.110 BV    0.0465 2150.84644  0.73124 ?
 20   3.234 VV    0.0408 8092.85254  2.75140 ?
 21   3.264 VB    0.0193  466.93616  0.15875 ?
 22   3.436 BB    0.0286    7.08656  0.00241 C15
 23   3.643 BB    0.0300    2.99125  0.00102 ?
 24   3.774 BV    0.0268  134.06415  0.04558 ?
 25   3.838 VB    0.0288   16.02896  0.00545 C16
 26   4.103 BV    0.0277   16.24332  0.00552 ?
 27   4.160 VV    0.0262   98.44160  0.03347 ?
 28   4.210 VB    0.0311   94.59988  0.03216 ?
 29   4.370 BV    0.0291   31.80890  0.01081 ?
 30   4.455 VV    0.0296  660.98340  0.22472 ?
 31   4.538 VV    0.0321   16.23707  0.00552 ?
 32   4.602 VB    0.0311   94.16107  0.03201 ?
 33   4.941 BV    0.0278    6.71564  0.00228 ?
 34   5.004 VB    0.0326  208.44847  0.07087 ?
 35   5.264 BB    0.0375    4.69270  0.00160 ?
 36   5.469 BB    0.0338    3.12300  0.00106 ?
 37   5.598 BV    0.0317  445.77228  0.15155 ?
 38   5.643 VB    0.0288  340.31897  0.11570 ?
 39   5.694 BB    0.0221    4.95860  0.00169 ?
 40   5.759 BV    0.0275   12.09626  0.00411 ?
 41   5.804 VB    0.0304   16.20230  0.00551 ?
 42   5.905 BV    0.0239   26.67260  0.00907 ?
 43   5.943 VB    0.0319   86.11308  0.02928 ?
 44   6.037 BV    0.0304  152.46394  0.05183 ?
 45   6.105 VB    0.0333 2189.15063  0.74427 ?
 46   6.259 BB    0.0353   10.94623  0.00372 ?
 47   6.363 BB    0.0323    3.85348  0.00131 ?
 48   6.963 BB    0.0345   17.95320  0.00610 ?
 49   7.203 BB    0.0408   25.62371  0.00871 ?
 50   7.446 BB    0.0349   45.09594  0.01533 ?
 51   7.795 BB    0.0341    8.18611  0.00278 ?
 52   7.973 BB    0.0403   45.25560  0.01539 ?
 53   8.388 BB    0.0415   10.64935  0.00362 ?
 54   8.541 BV    0.0330   19.48375  0.00662 ?
 55   8.576 VV    0.0320   15.27477  0.00519 ?
 56   8.667 VB    0.0398    5.43259  0.00185 ?
 57   8.892 BV    0.0459   12.45529  0.00423 ?
 58   9.043 VB    0.0456   10.15500  0.00345 ?
 59  10.463 BB    0.0412 7827.92480  2.66133 ?
 60  11.495 BB    0.0413    4.65901  0.00158 ?
 61  11.706 BB    0.0405   10.81459  0.00368 ?
 62  18.239 BB    0.0460   88.63823  0.03014 ?
 63  18.794 BB    0.0414   76.71286  0.02608 ?

Totals :                  2.94136e5


1 Warnings or Errors :

Warning : Calibrated compound(s) not found

====================================================================
                   Summed Peaks Report
====================================================================
```

GC 8/11/2022 1:14:49 PM MBB   Page 2 of 3

Data File C:\CHEM32\1\DATA\OLD DATA\2020\ZW2020100901B.D
Sample Name: zw2020100901b

```
Signal 1: FID1 A,
====================================================================
                   Final Summed Peaks Report
====================================================================

Signal 1: FID1 A,
Name          Total Area   Area
                [pA*s]       %
-------------|-----------|---------|
C14           0.00000     0.0000
C15           7.08656     2.409e-3
C16          16.02896     5.450e-3

Totals :                  7.8588e-3

                   *** End of Report ***
```

GC 8/11/2022 1:14:49 PM MBB   Page 3 of 3

Reaction conditions: 5 mL EtOH, **Ru-3** (250 ppm, 12.1 mg), 96 h, 115 ºC, NaOEt (20 mol%, 583 mg) in reactor A and 600 rpm.

Page 1 of 3

Data File C:\CHEM32\1\DATA\ZW20220404IPR02.D
Sample Name: ZW20220404IPR02

Acq. Operator   : MBB   Seq. Line :   3
Acq. Instrument : GC   Location : Vial 8
Injection Date : 4/9/2022 11:24:33 AM   Inj :   1
                                               Inj Volume : 1 µl
Acq. Method   : C:\CHEM32\1\METHODS\GC-FID_WT.M
Last changed   : 11/29/2021 10:07:34 AM by MBB
Analysis Method : C:\CHEM32\1\METHODS\GC-FID_WEFA.M
Last changed   : 7/30/2022 1:56:07 PM by MBB
                  (modified after loading)

FID1 A, (ZW20220404IPR02.D)

Area Percent Report

Sorted By   :   Signal
Calib. Data Modified :   12/8/2006 12:33:15 PM
Multiplier   :   1.0000
Dilution   :   1.0000
Use Multiplier & Dilution Factor with ISTDs

Signal 1: FID1 A,

Peak #	RetTime [min]	Type	Width [min]	Area [pA*s]	Area %	Name
1	1.209	BV	9.23e-3	3.63889	0.00157	?
2	1.224	VV	9.16e-3	6.27948	0.00271	?
3	1.244	VV	5.76e-3	69.95351	0.03019	?
4	1.257	VV	0.0195	828.55597	0.35754	?
5	1.287	VV	9.39e-3	220.26422	0.09505	?
6	1.369	VV S	0.0480	1.09729e5	47.35016	?
7	1.404	VV S	6.42e-3	724.32721	0.31256	?
8	1.433	VV S	0.0151	8.62456e4	37.21646	?
9	1.522	BB X	0.0130	25.62975	0.01106	?
10	1.623	BV T	9.78e-3	8.94422	0.00386	?
11	1.670	VB S	0.0176	6602.84082	2.84924	?
12	1.708	BV X	0.0113	51.02412	0.02202	?
13	1.747	VB X	0.0119	7.57018	0.00327	?
14	1.850	BV	0.0227	4.42525	0.00191	?
15	1.893	VV	0.0139	2.10827	0.00091	?
16	1.909	VB	0.0189	3.56003	0.00154	?
17	2.027	BV	0.0290	1.43262e4	6.18201	?
18	2.098	VV	0.0151	8.79898	0.00380	?

GC 8/11/2022 4:05:37 PM MBB   Page 1 of 3

Page 2 of 3

Peak #	RetTime [min]	Type	Width [min]	Area [pA*s]	Area %	Name
19	2.126	VB	0.0347	32.28118	0.01393	?
20	2.183	BV	0.0154	4.50564	0.00194	?
21	2.221	VB	0.0163	617.71112	0.26655	?
22	2.472	BB	0.0261	2.39181	0.00103	?
23	2.719	BV	0.0334	13.52132	0.00583	?
24	2.795	VV	0.0282	5.94306	0.00256	?
25	2.831	VB	0.0354	10.97776	0.00474	?
26	2.993		0.0000	0.00000	0.00000	C14
27	3.075	BV	0.0277	399.29022	0.17230	?
28	3.117	VV	0.0245	299.28064	0.12914	?
29	3.186	VB	0.0249	1816.89905	0.78402	?
30	3.418	BB	0.0318	3.81951	0.00165	C15
31	3.620	BB	0.0317	11.43251	0.00493	?
32	3.768	BB	0.0290	195.20767	0.08424	?
33	3.965	BB	0.0240	1.59192	0.00069	C16
34	4.036	BV	0.0331	7.02854	0.00303	?
35	4.158	VB	0.0457	439.27859	0.18956	?
36	4.375	BB	0.0291	4.97975	0.00215	?
37	4.448	BB	0.0322	138.97281	0.05997	?
38	4.636	BB	0.0396	6.79570	0.00293	?
39	4.998	BB	0.0395	76.37727	0.03296	?
40	5.596	BV	0.0304	94.77338	0.04090	?
41	5.640	VB	0.0375	88.80987	0.03832	?
42	5.908	BB	0.0426	10.13351	0.00437	?
43	6.079	BB	0.0341	1456.10242	0.62833	?
44	7.021	BB	0.0445	5.81037	0.00251	?
45	7.263	BB	0.0546	9.34663	0.00403	?
46	7.818	BB	0.0422	5.05652	0.00218	?
47	7.994	BB	0.0557	18.27660	0.00789	?
48	8.816	BB	0.0476	9.94424	0.00429	?
49	9.954	BV	0.1215	79.87674	0.03447	?
50	10.437	VB	0.0429	7004.85645	3.02272	?

Totals :   2.31740e5

1 Warnings or Errors :

Warning : Calibrated compound(s) not found

Summed Peaks Report

Signal 1: FID1 A,

Final Summed Peaks Report

Signal 1: FID1 A,

Name	Total Area [pA*s]	Area %
C14	0.00000	0.0000
C15	3.81951	1.648e-3
C16	1.59192	6.869e-4

GC 8/11/2022 4:05:37 PM MBB   Page 2 of 3

Page 3 of 3

Name	Total Area [pA*s]	Area %
Totals :		2.3351e-3

*** End of Report ***

GC 8/11/2022 4:05:37 PM MBB   Page 3 of 3

Reaction conditions: 5 mL EtOH, **Ru-4** (250 ppm, 16.2 mg), 96 h, 115 ºC, NaOEt (20 mol%, 583 mg) in reactor A and 600 rpm.

Page 1 of 3

Data File C:\CHEM32\1\DATA\ZW20220411CY.D
Sample Name: ZW20220411CY

```
Acq. Operator   : MBB                        Seq. Line :   2
Acq. Instrument : GC                         Location : Vial 5
Injection Date  : 4/15/2022 1:27:25 PM          Inj :   1
                                          Inj Volume : 1 µl
Acq. Method     : C:\CHEM32\1\METHODS\GC-FID_WT.M
Last changed    : 11/29/2021 10:07:34 AM by MBB
Analysis Method : C:\CHEM32\1\METHODS\GC-FID_WEFA.M
Last changed    : 7/30/2022 1:56:07 PM by MBB
                  (modified after loading)
```


FID1 A, (ZW20220411CY.D)

Area Percent Report

```
Sorted By             :      Signal
Calib. Data Modified  :      12/8/2006 12:33:15 PM
Multiplier            :      1.0000
Dilution              :      1.0000
Use Multiplier & Dilution Factor with ISTDs
```

Signal 1: FID1 A,

Peak #	RetTime [min]	Type	Width [min]	Area [pA*s]	Area %	Name
1	0.909	BB	4.40e-3	5.05292e-1	0.00023	?
2	1.225	BV	0.0164	11.79963	0.00543	?
3	1.257	VV	0.0203	769.30280	0.35389	?
4	1.359	VV S	0.0316	8.45103e4	38.87546	?
5	1.400	VV S	7.22e-3	741.91418	0.34129	?
6	1.434	VV S	0.0161	1.01393e5	46.64151	?
7	1.518	BB X	0.0196	40.71590	0.01873	?
8	1.665	VB S	0.0183	6692.29688	3.07851	?
9	1.708	BB X	0.0157	28.06654	0.01291	?
10	1.850	BV	0.0210	4.46128	0.00205	?
11	1.893	VV	0.0130	7.83748e-1	0.00036	?
12	1.912	VB	0.0168	1.49783	0.00069	?
13	2.016	BV	0.0294	1.13096e4	5.20252	?
14	2.092	VV	0.0192	19.78473	0.00910	?
15	2.135	VB	0.0285	38.62411	0.01777	?
16	2.182	BV	0.0139	2.50488	0.00115	?
17	2.215	VB	0.0171	666.55798	0.30662	?
18	2.595	BB	0.0390	5.32872	0.00245	?

GC 8/11/2022 4:06:39 PM MBB   Page   1 of 3

Page 2 of 3

Data File C:\CHEM32\1\DATA\ZW20220411CY.D
Sample Name: ZW20220411CY

Peak #	RetTime [min]	Type	Width [min]	Area [pA*s]	Area %	Name
19	2.719	BB	0.0262	21.85930	0.01006	?
20	2.850	BB	0.0435	17.45679	0.00803	?
21	2.993		0.0000	0.00000	0.00000	C14
22	3.068	BV	0.0340	591.69104	0.27218	?
23	3.114	VV	0.0258	337.33456	0.15518	?
24	3.184	VB	0.0253	2086.07300	0.95961	?
25	3.448	BB	0.0404	6.27957	0.00289	C15
26	3.767	BB	0.0314	215.58574	0.09917	?
27	3.926		0.0000	0.00000	0.00000	C16
28	4.039	BB	0.0299	4.11672	0.00189	?
29	4.159	BV	0.0286	213.89169	0.09839	?
30	4.183	VB	0.0252	134.91428	0.06206	?
31	4.372	BV	0.0316	5.55791	0.00256	?
32	4.444	VV	0.0352	208.58214	0.09595	?
33	4.632	VB	0.0486	16.32118	0.00751	?
34	4.925	BV	0.0269	5.54105	0.00255	?
35	4.988	VV	0.0387	209.18854	0.09623	?
36	5.214	VB	0.0416	5.87237	0.00270	?
37	5.591	BV	0.0314	135.81680	0.06248	?
38	5.636	VB	0.0378	130.80392	0.06017	?
39	5.901	BV	0.0379	45.72844	0.02104	?
40	6.072	VV	0.0352	1088.52576	0.50073	?
41	6.254	VB	0.0491	12.17787	0.00560	?
42	6.424	BB	0.0592	19.38824	0.00892	?
43	7.236	BB	0.0560	38.03513	0.01750	?
44	7.493	BB	0.0533	10.37852	0.00477	?
45	7.800	BB	0.0390	20.03848	0.00922	?
46	7.978	BB	0.0495	56.36426	0.02593	?
47	8.806	BV	0.0530	25.29536	0.01164	?
48	8.908	VB	0.0767	33.43079	0.01538	?
49	10.423	BB	0.0391	5422.88037	2.49457	?
50	18.910	BB	0.0731	31.38426	0.01444	?

Totals :   2.17387e5

1 Warnings or Errors :

Warning : Calibrated compound(s) not found

Summed Peaks Report

Signal 1: FID1 A,

Final Summed Peaks Report

Signal 1: FID1 A,

Name	Total Area [pA*s]	Area %
C14	0.00000	0.0000
C15	6.27957	2.889e-3
C16	0.00000	0.0000

GC 8/11/2022 4:06:39 PM MBB   Page   2 of 3

Page 3 of 3

Data File C:\CHEM32\1\DATA\ZW20220411CY.D
Sample Name: ZW20220411CY

Name	Total Area [pA*s]	Area %
Totals :		2.8887e-3

*** End of Report ***

GC 8/11/2022 4:06:39 PM MBB   Page   3 of 3

Appendix A – Chapter 3.1

Reaction conditions: 2.5 mL EtOH, **Ru-5** (250 ppm, 6.8 mg), 96 h, 130 °C, NaOEt (20 mol%, 583 mg) in a 18.4 mL high-pressure reactor and 600 rpm.

Left report:

```
Data File C:\CHEM32\1\DATA\2022\ZWTBU0610.D
Sample Name: zwtbu0610
================================================
Acq. Operator   : MBB              Seq. Line :   2
Acq. Instrument : GC               Location : Vial 15
Injection Date  : 2/15/2022 12:17:42 PM    Inj :   1
                                   Inj Volume : 1 µl
Acq. Method     : C:\CHEM32\1\METHODS\GC-FID_WT.M
Last changed    : 11/29/2021 10:07:34 AM by MBB
Analysis Method : C:\CHEM32\1\METHODS\GC-FID_WT.M
Last changed    : 4/25/2022 3:43:45 PM by MBB
                  (modified after loading)
================================================

FID1 A, (2022\ZWTBU0610.D)
```

```
=====================================
        Area Percent Report
=====================================
Sorted By            :    Signal
Calib. Data Modified :    12/8/2006 12:33:15 PM
Multiplier           :    1.0000
Dilution             :    1.0000
Use Multiplier & Dilution Factor with ISTDs

Signal 1: FID1 A,

Peak RetTime Type  Width    Area      Area    Name
 #   [min]        [min]    [pA*s]      %
---|-------|----|------|---------|--------|----
  1  1.225 BV   8.33e-3   3.04329  0.00155 ?
  2  1.256 VV S 0.0150 1197.84033  0.60822 ?
  3  1.317 VV S 0.0120 1.20135e4   6.10001 ?
  4  1.336 VV S 0.0206 1.28063e4   6.50258 ?
  5  1.396 BV T 0.0111    6.91694  0.00351 ?
  6  1.413 VV T 0.0121   22.65540  0.01150 ?
  7  1.433 VB S 0.0234 1.47459e5  74.87437 ?
  8  1.522 BB X 0.0197   11.14011  0.00566 ?
  9  1.630 BV   0.0115   14.71358  0.00747 ?
 10  1.649 VV   0.0113   98.60337  0.05007 ?
 11  1.666 VB   0.0193  207.80112  0.10551 ?
 12  1.903 BB   0.0287    9.79536  0.00497 ?
 13  2.024 BV   0.0321 1.49088e4   7.57011 ?
 14  2.225 VH   0.0453   80.65794  0.04096 ?
 15  2.596 HB   0.0346    5.05089  0.00256 ?
 16  2.993       0.0000    0.00000  0.00000 C14
 17  3.090 BV   0.0228   17.05194  0.00866 ?
 18  3.129 VV   0.0252   18.64929  0.00947 ?

GC 4/25/2022 4:39:41 PM MBB                    Page  1 of 2
```

Right report:

```
Data File C:\CHEM32\1\DATA\2022\ZWTBU0610.D
Sample Name: zwtbu0610
================================================
Acq. Operator   : MBB              Seq. Line :   2
Acq. Instrument : GC               Location : Vial 15
Injection Date  : 2/15/2022 12:17:42 PM    Inj :   1
                                   Inj Volume : 1 µl
Acq. Method     : C:\CHEM32\1\METHODS\GC-FID_WT.M
Last changed    : 11/29/2021 10:07:34 AM by MBB
Analysis Method : C:\CHEM32\1\METHODS\GC-FID_WT.M
Last changed    : 4/25/2022 3:43:45 PM by MBB
                  (modified after loading)
================================================

Peak RetTime Type  Width    Area      Area    Name
 #   [min]        [min]    [pA*s]      %
---|-------|----|------|---------|--------|----
 19  3.185 VB   0.0321  149.42226  0.07587 ?
 20  3.466       0.0000    0.00000  0.00000 C15
 21  3.776 BB   0.0273  900.70880  0.45735 ?
 22  3.926       0.0000    0.00000  0.00000 C16
 23  4.033 BB   0.0371    3.76583  0.00191 ?
 24  4.184 BB   0.0319 2093.11304  1.06280 ?
 25  4.466 BV   0.0374   30.36146  0.01542 ?
 26  4.514 VB   0.0357   20.57612  0.01045 ?
 27  5.610 HH   0.0310   20.70299  0.01051 ?
 28  5.655 HB   0.0365   18.72048  0.00951 ?
 29  6.079 HB   0.0334 1097.64246  0.55734 ?
 30  6.558 BB   0.0376  144.53439  0.07339 ?
 31  7.196 BB   0.0585   95.98708  0.04874 ?
 32 10.418 BB   0.0359 3444.03467  1.74875 ?
 33 19.041 BB   0.1083   40.93631  0.02079 ?

Totals :                1.96943e5

1 Warnings or Errors :

Warning : Calibrated compound(s) not found

=====================================
         Summed Peaks Report
=====================================
Signal 1: FID1 A,
=====================================
       Final Summed Peaks Report
=====================================
Signal 1: FID1 A,
Name          Total Area    Area
               [pA*s]        %
----------|-----------|---------|
C14           0.00000    0.0000
C15           0.00000    0.0000
C16           0.00000    0.0000

Totals :                 0.0000

          *** End of Report ***

GC 4/25/2022 4:39:41 PM MBB                    Page  2 of 2
```

GC-MS (liquid phase) reports of products

Reaction conditions: 5 mL EtOH, **Ru-1** (1000 ppm, 52 mg), 96 h, 115 ºC, NaO*t*Bu (20 mol%, 1646 mg) in a 25.9 mL high-pressure reactor and 600 rpm.

```
                            Area Percent Report

Data Path : C:\msdchem\1\DATA\2020\
Data File : ZW2020100403.D
Acq On    :  4 Oct 2020  17:08
Operator  :
Sample    : ZW2020100403
Misc      :
ALS Vial  : 11   Sample Multiplier: 1

Integration Parameters: events.e
Integrator: ChemStation

Method    : C:\msdchem\3\METHODS\Hajar\GC_STANDARD.M
Title     :

Signal    : TIC: ZW2020100403.D\data.ms

peak  R.T. first  max last  PK   peak      corr.    corr.    % of
 #    min   scan scan scan  TY  height      area    % max.  total
---  ----- ----- ---- ---- ---  -------   -------   ------  -------
 1   1.367  110  113  115  BV   109190     1533782   0.06%   0.010%
 2   1.435  115  119  120  VV 2 7331078   92108826   3.47%   0.608%
 3   1.480  120  123  125  VV 2 34478150 863227873  32.50%   5.693%
 4   1.513  125  126  128  VV 2 34137124 635973656  23.94%   4.195%
 5   1.663  128  139  147  VV 4 31203046 2656087416 100.00% 17.518%

 6   1.782  147  149  153  VV    9854592 156399071   5.89%   1.032%
 7   1.917  153  161  176  VV 4 37665611 2227223903 83.85%  14.690%
 8   2.205  176  187  191  VV 2 33481476 1123128824 42.29%   7.408%
 9   2.273  191  193  199  VV    4176761 104970025   3.95%   0.692%
10   2.397  199  204  225  VV   28610180 781939039  29.44%   5.157%

11   2.688  225  229  233  VV 3  600689   25606096   0.96%   0.169%
12   2.763  233  236  244  VV 2 1590134   49592972   1.87%   0.327%
13   2.904  244  248  257  VV 3  476165   32089433   1.21%   0.212%
14   3.068  257  263  264  VV 2 7819336 264120531   9.94%   1.742%
15   3.100  264  266  268  VV   6803889 154290328   5.81%   1.018%

16   3.260  268  280  314  VV 2 37892791 2266166719 85.32% 14.946%
17   3.691  314  318  339  VV    922468   46819909   1.76%   0.309%
18   4.037  339  348  357  VV 2 2027580  78940943   2.97%   0.521%
19   4.164  357  359  362  VV 3  392737   10712855   0.40%   0.071%
20   4.214  362  364  366  VV 2  610238   13157788   0.50%   0.087%

21   4.282  366  370  380  VV   11797057 304316668  11.46%   2.007%
22   4.420  380  382  408  VV 3 1159907   59102677   2.23%   0.390%
23   4.759  408  412  448  VV   4638803 101458099   3.82%   0.669%
24   5.323  455  461  464  BV   7641118 146942689   5.53%   0.969%
25   5.373  464  466  479  VV   7408419 172520352   6.50%   1.138%

26   5.673  487  492  496  VV 4  588961   26369160   0.99%   0.174%
27   5.795  496  503  518  VV 3 20418235 581154003  21.88%   3.833%
28   6.679  571  581  595  BV 3  171209    8686822   0.33%   0.057%
29   7.145  617  622  651  VV 3  312093   24285552   0.91%   0.160%
30   7.673  651  669  696  VB 4  239572   21262150   0.80%   0.140%

31   8.274  715  722  751  VV 5  184062   14755570   0.56%   0.097%
32  10.199  870  891  937  BB   35063113 2103928204 79.21%  13.876%
33  18.813 1646 1651 1664 PV    295723   13004612   0.49%   0.086%


                  Sum of corrected areas: 15161876546
 Signal    : TIC: ZW2020100403.D\datasim.ms

peak  R.T. first  max last  PK   peak      corr.    corr.    % of
 #    min   scan scan scan  TY  height      area    % max.  total
---  ----- ----- ---- ---- ---  -------   -------   ------  -------

   No peaks were detected using the method integration parameters!

GC_STANDARD.M Thu Apr 28 13:32:27 2022
```

```
File       :C:\msdchem\1\DATA\2020\ZW2020100403.D
Operator   :
Acquired   :  4 Oct 2020  17:08   using AcqMethod JIAN-FF-FAOL-2.M
Instrument :    MSD
Sample Name: ZW2020100403
Misc Info  :
Vial Number: 11
```
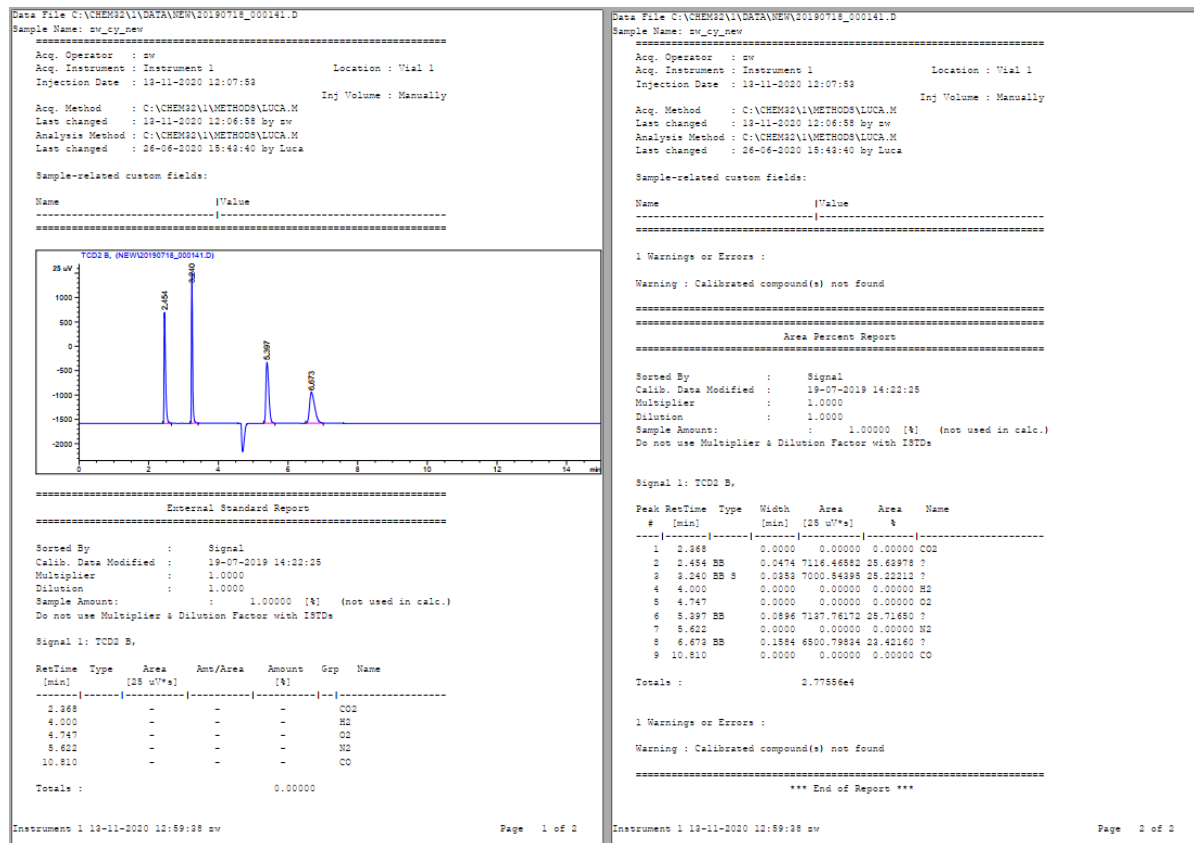
Reaction conditions: 5 mL EtOH, **Ru-2** (250 ppm, 15.1 mg), 96 h, 115 °C, NaOEt (20 mol%, 1166 mg) in a 25.9 mL high-pressure reactor and 600 rpm.
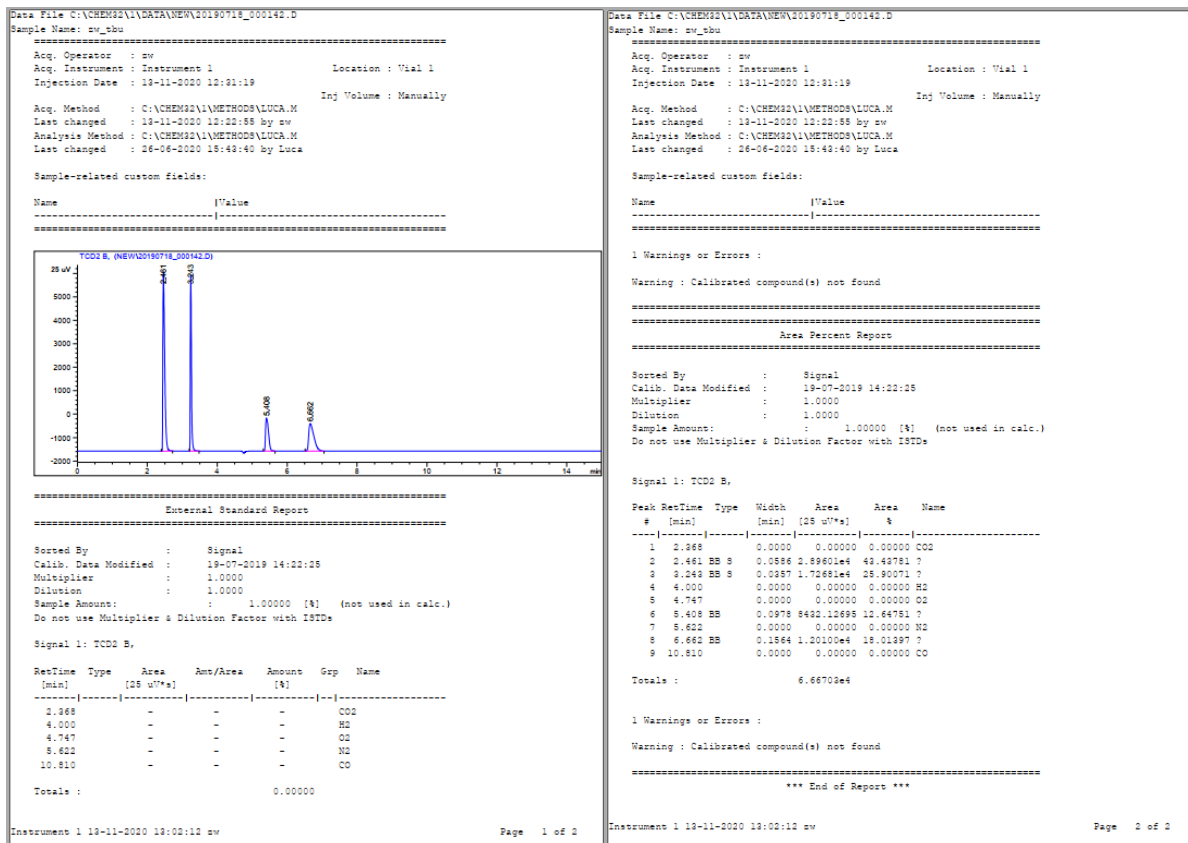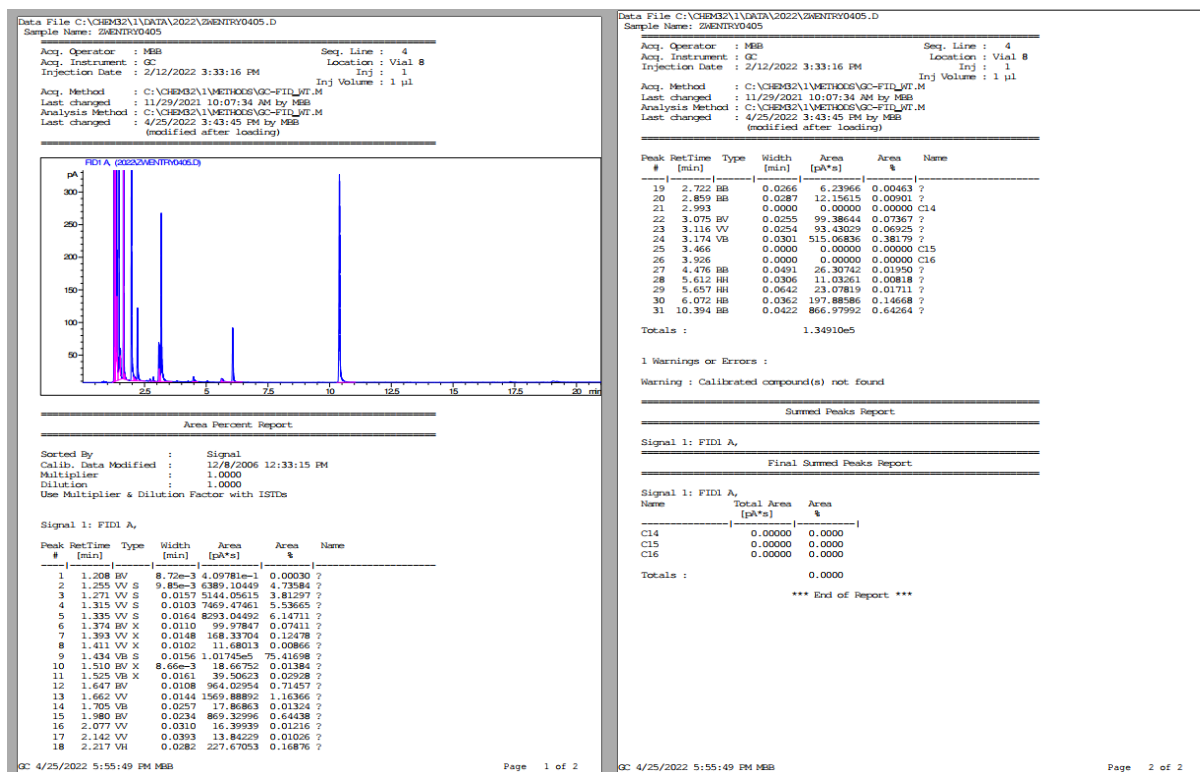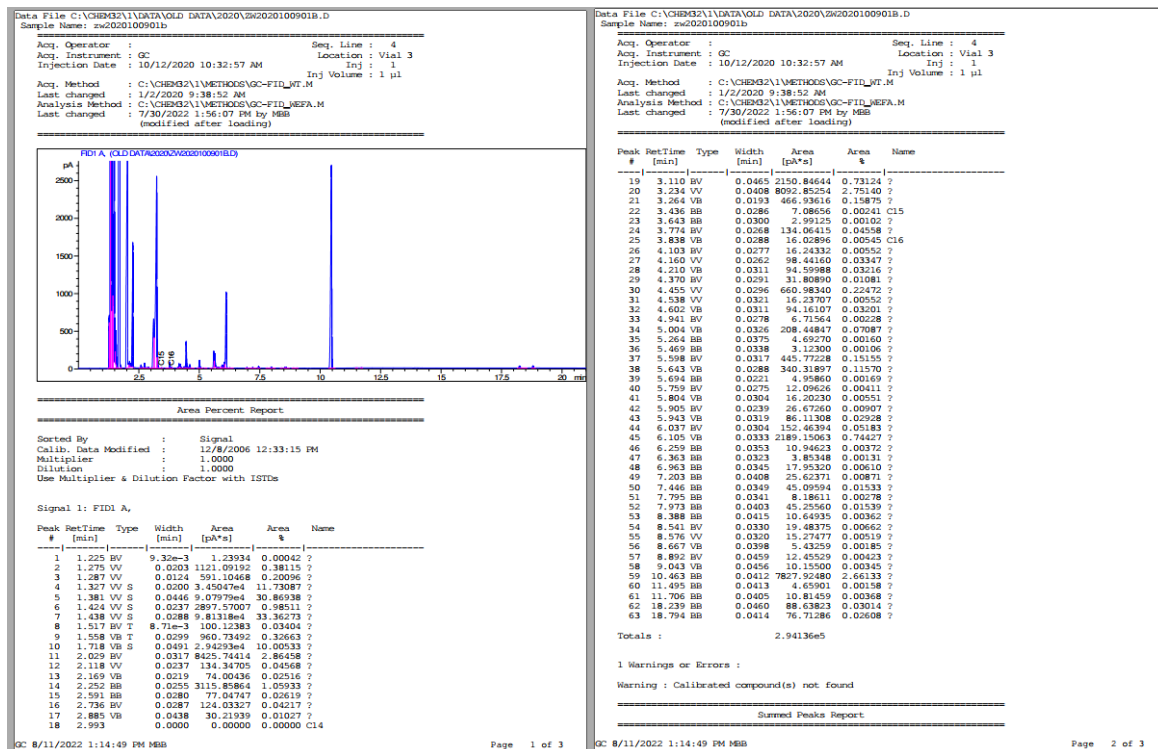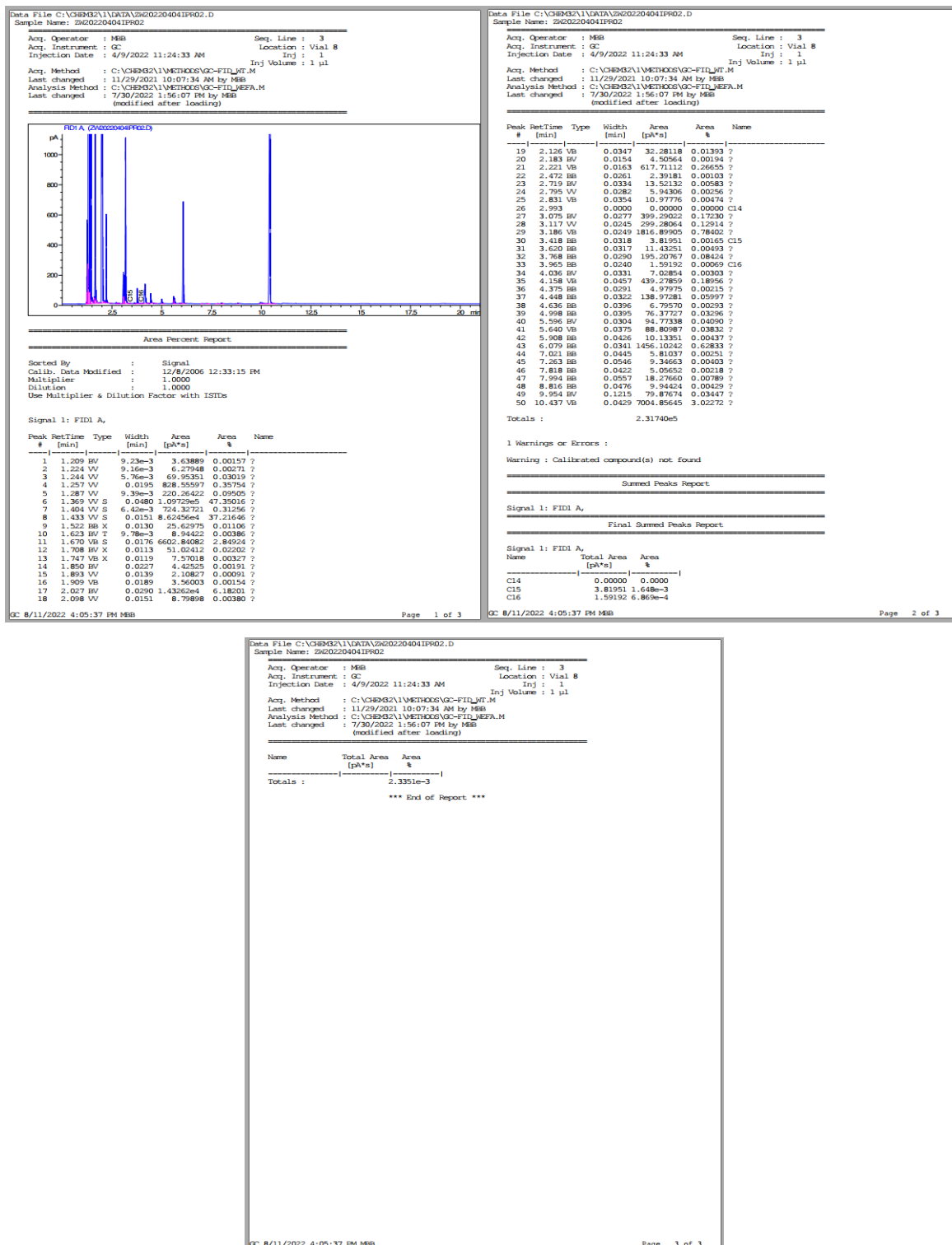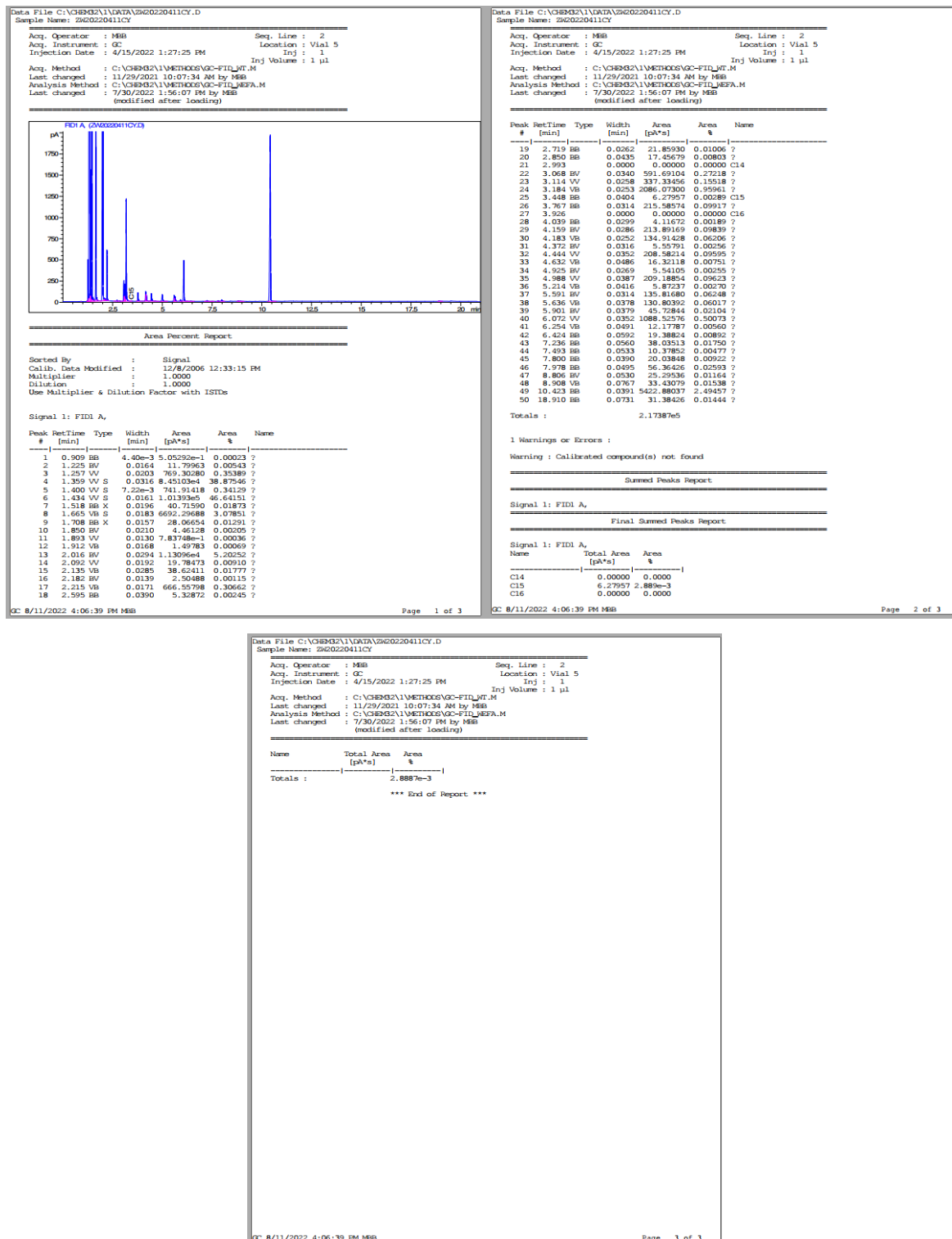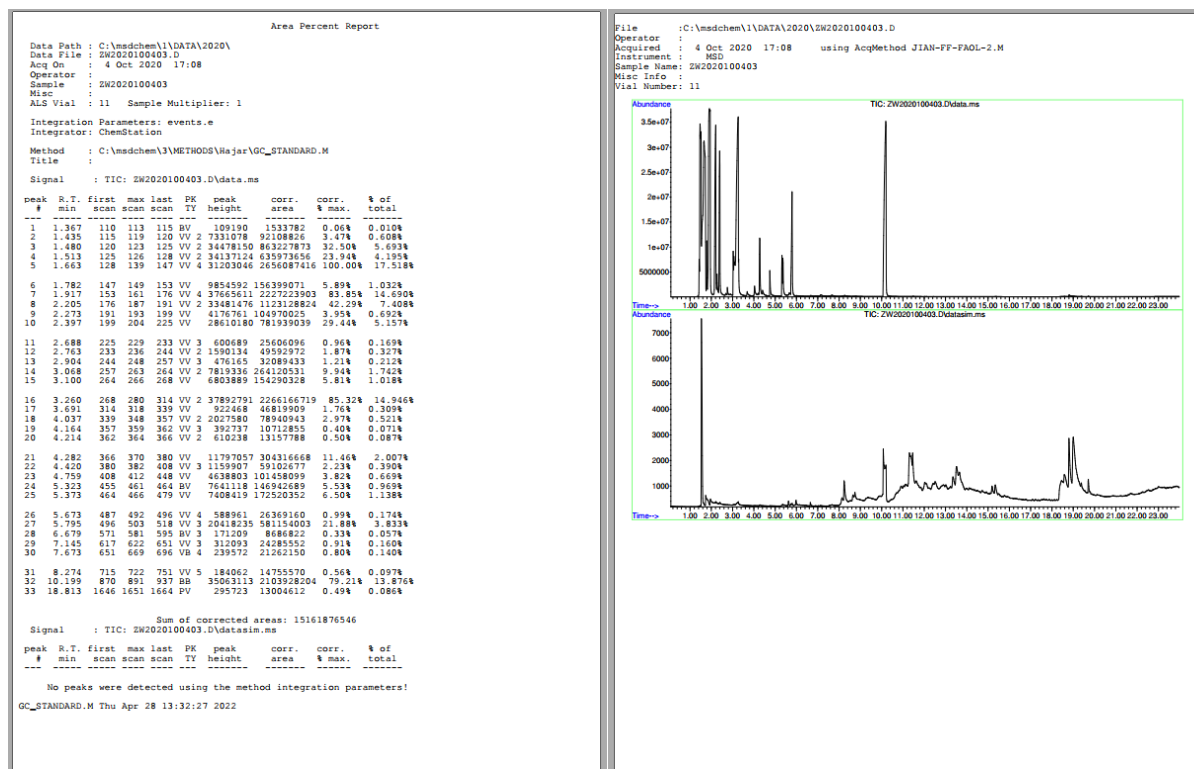
```
                              Area Percent Report

  Data Path : C:\msdchem\1\DATA\2020\
  Data File : zw2020102402.D
  Acq On    : 24 Oct 2020  22:31
  Operator  :
  Sample    : zw2020102402
  Misc      :
  ALS Vial  : 18   Sample Multiplier: 1

  Integration Parameters: events.e
  Integrator: ChemStation

  Method    : C:\msdchem\3\METHODS\Hajar\GC_STANDARD.M
  Title     :

  Signal    : TIC: zw2020102402.D\data.ms

  peak  R.T. first  max last  PK   peak      corr.    corr.   % of
   #    min   scan scan scan  TY  height      area    % max.  total
  ---  ----- ----- ---- ---- ---  -------   -------   ------  ------
   1   1.333  106  110  112  BV    126722   1924754   0.09%   0.022%
   2   1.447  112  120  126  VV 4 39556668 2026304360 100.00% 23.464%
   3   1.582  126  132  143  VV 4 28171134 1086549541  53.62% 12.582%
   4   1.755  143  147  149  VV 3   843537   28252825   1.39%  0.327%
   5   1.846  149  155  175  VV 2 40344493 1196213678  59.03% 13.852%

   6   2.139  175  181  194  VV   35582139 1128952416  55.71% 13.073%
   7   2.319  194  197  232  VV   11190051  244070235  12.05%  2.826%
   8   3.012  252  258  259  VV    4888475   67581835   3.34%  0.783%
   9   3.047  259  261  263  VV    4387645   97878209   4.83%  1.133%
  10   3.121  263  267  306  VV 2 22326260  694041934  34.25%  8.037%

  11   3.615  306  311  336  VV 2   781734   49842970   2.46%  0.577%
  12   3.973  336  342  351  VV 5   260702   20894675   1.03%  0.242%
  13   4.191  358  362  404  VV 2  2295138  110495747   5.45%  1.280%
  14   4.734  404  410  448  VV 5   337263   34311445   1.69%  0.397%
  15   5.267  448  457  488  VV    2321559  112960812   5.57%  1.308%

  16   5.703  488  495  538  VV   18111289  437082455  21.57%  5.061%
  17  10.057  868  879  902  BV   34062401 1298317982  64.07% 15.034%

              Sum of corrected areas:  8635675871
  Signal    : TIC: zw2020102402.D\datasim.ms

  peak  R.T. first  max last  PK   peak      corr.    corr.   % of
   #    min   scan scan scan  TY  height      area    % max.  total
  ---  ----- ----- ---- ---- ---  -------   -------   ------  ------

    No peaks were detected using the method integration parameters!

  GC_STANDARD.M Fri Apr 29 12:02:48 2022
```

```
File        :C:\msdchem\1\DATA\2020\zw2020102401.D
Operator    :
Acquired    : 24 Oct 2020  21:59     using AcqMethod JIAN-FF-FAOL-2.M
Instrument  :     MSD
Sample Name: zw2020102401
Misc Info   :
Vial Number: 17
```
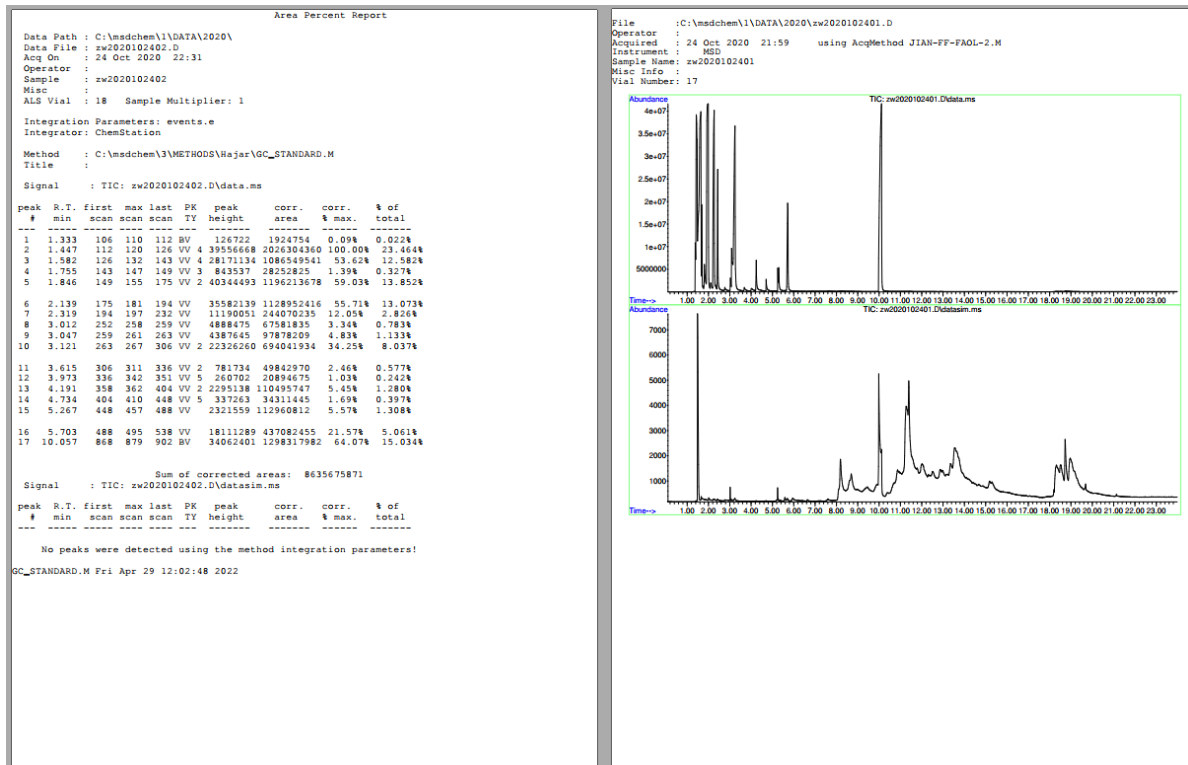
Reaction conditions: 5 mL EtOH, **Ru-3** (250 ppm, 12.1 mg), 67 h, 115 ºC, NaOEt (20 mol%, 1166 mg) in a 25.9 mL high-pressure reactor and 600 rpm.
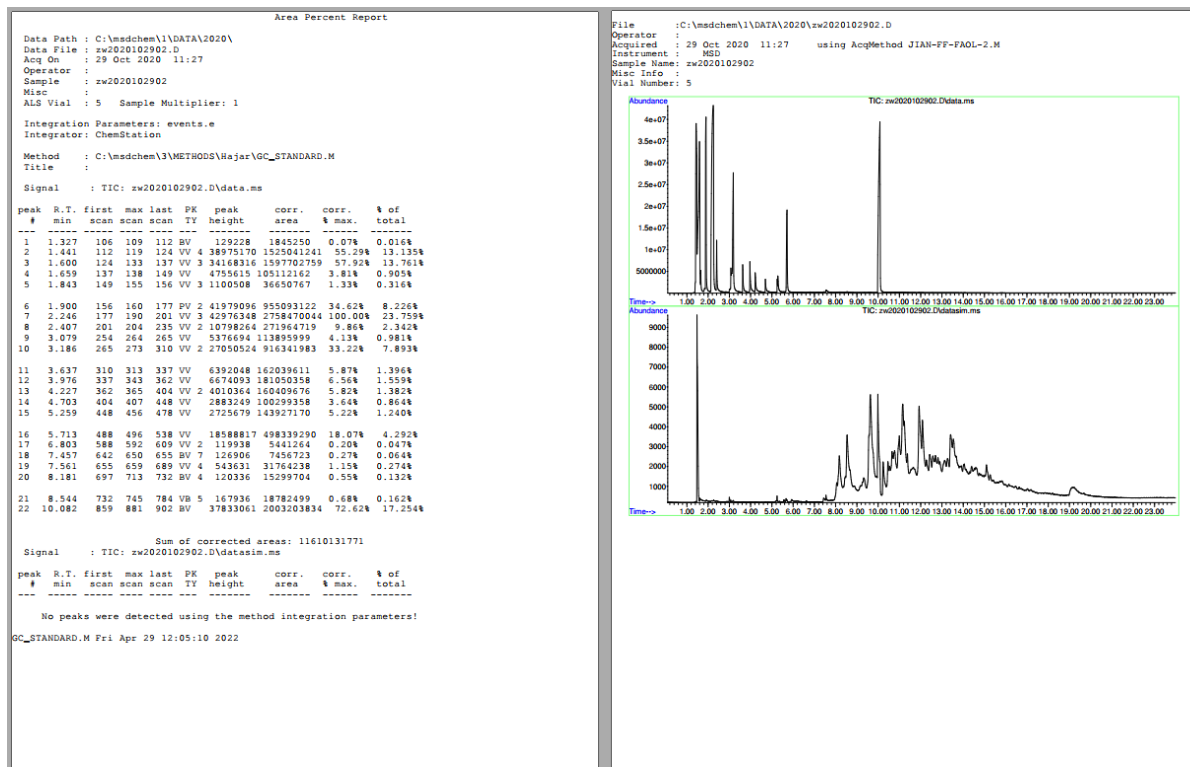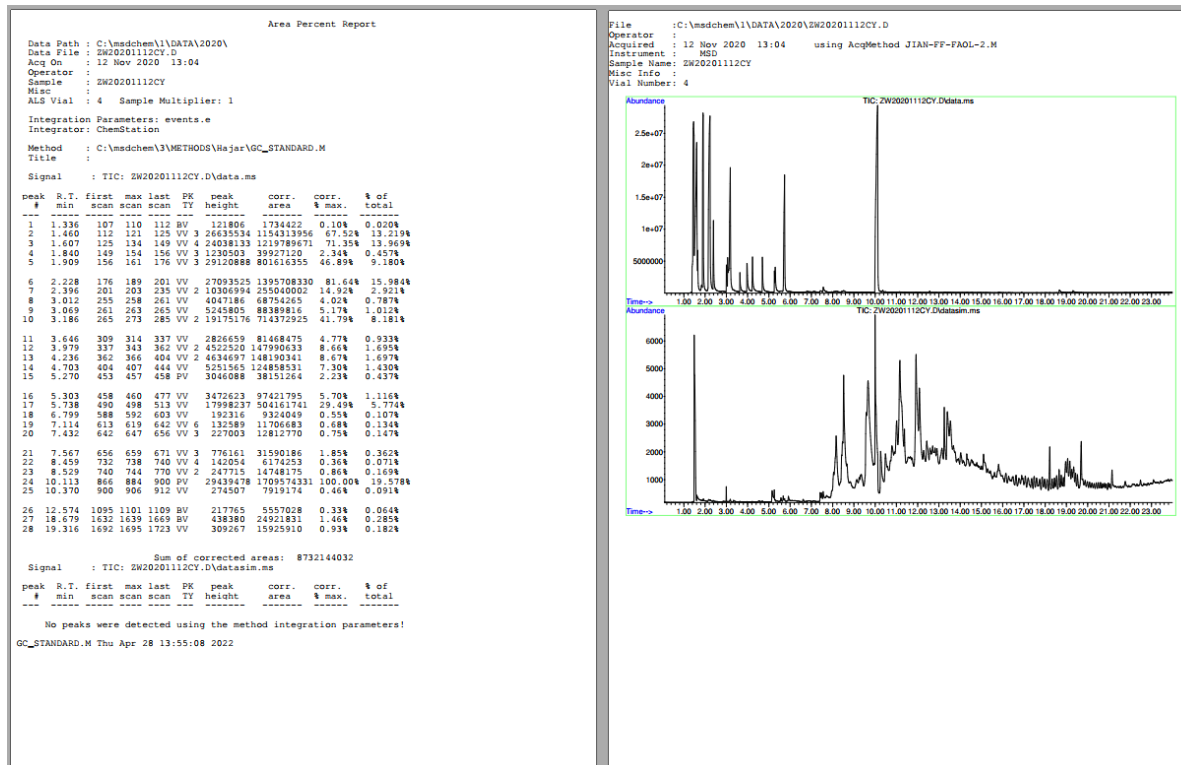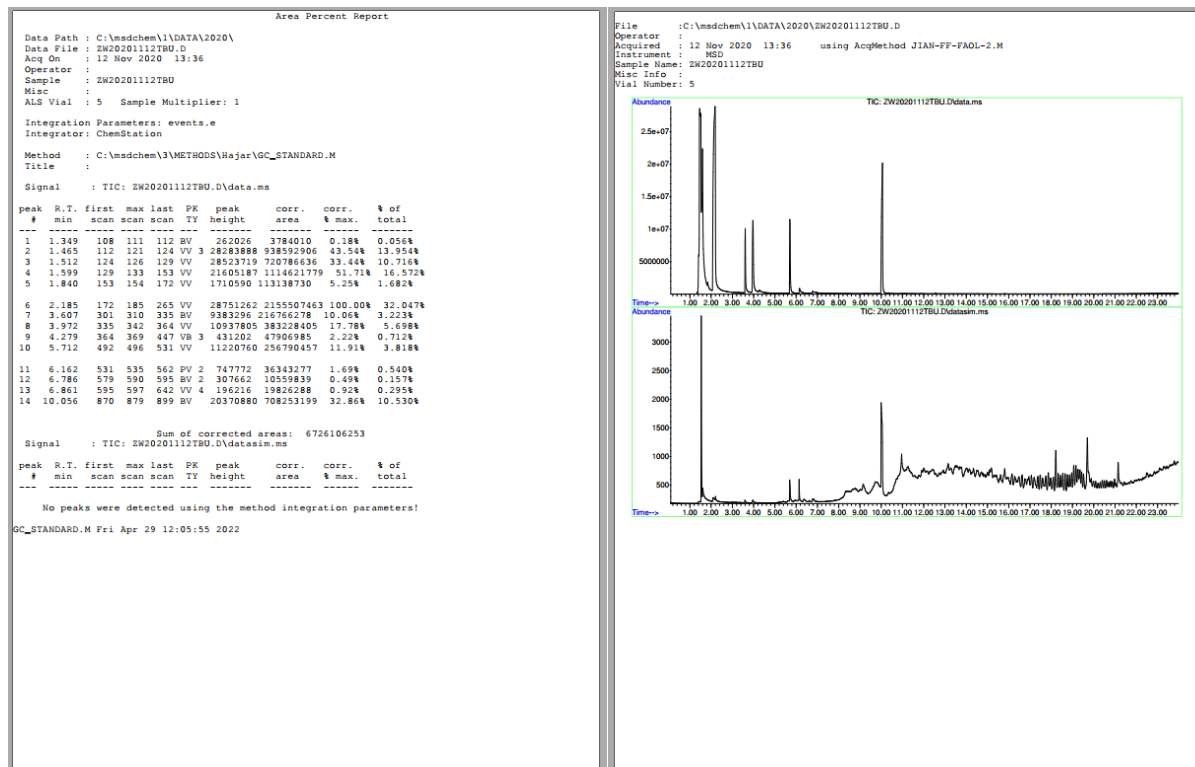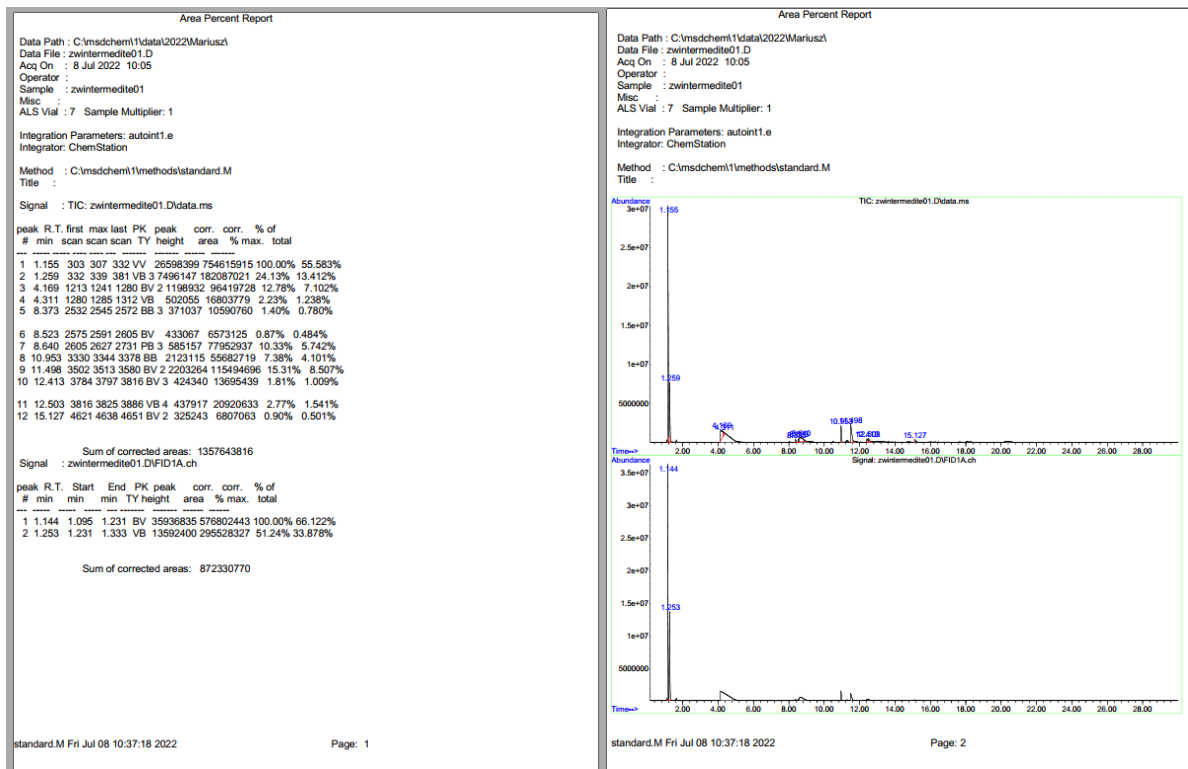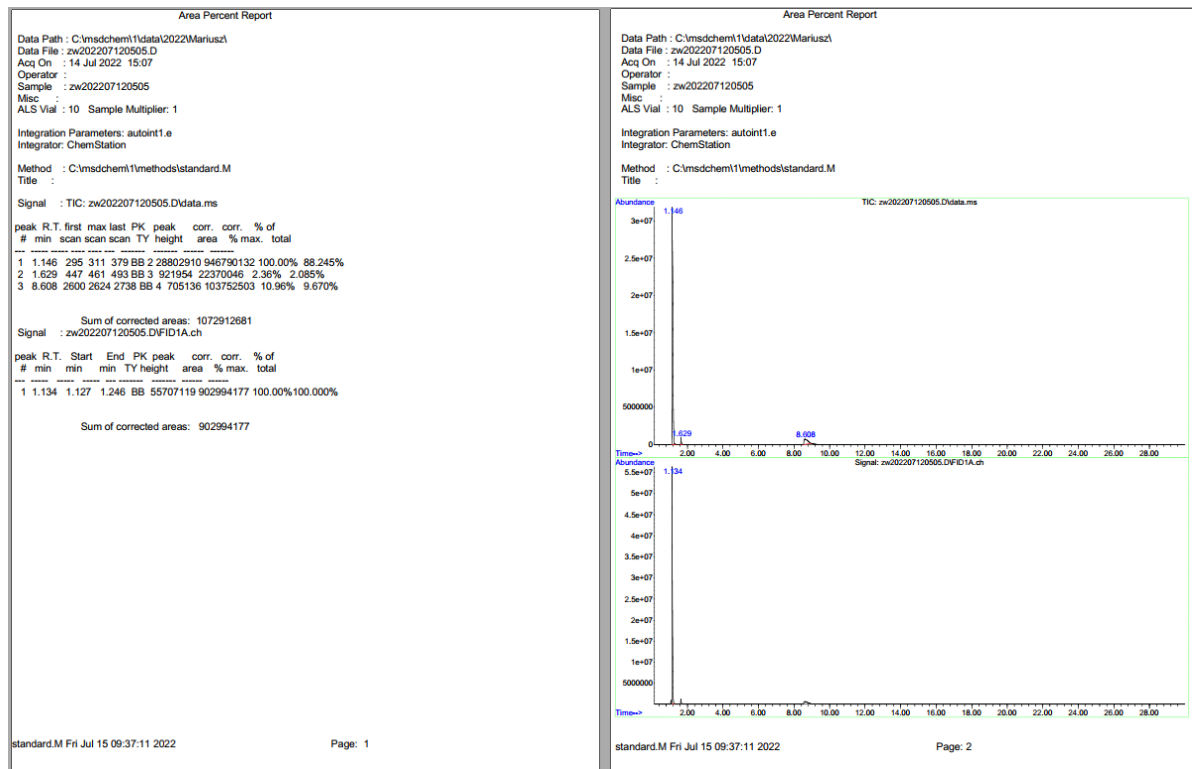
```
                                Area Percent Report

   Data Path : C:\msdchem\1\DATA\2020\
   Data File : zw2020102902.D
   Acq On    : 29 Oct 2020  11:27
   Operator  :
   Sample    : zw2020102902
   Misc      :
   ALS Vial  : 5    Sample Multiplier: 1

   Integration Parameters: events.e
   Integrator: ChemStation

   Method    : C:\msdchem\3\METHODS\Hajar\GC_STANDARD.M
   Title     :

   Signal      : TIC: zw2020102902.D\data.ms

   peak  R.T. first  max last  PK    peak      corr.    corr.    % of
    #    min   scan scan scan  TY   height      area    % max.   total
   ---  ----- ----- ---- ---- ---  -------   -------   ------  -------
    1   1.327  106  109  112 BV     129228    1845250    0.07%   0.016%
    2   1.441  112  119  124 VV 4 38975170 1525041241   55.29%  13.135%
    3   1.600  124  133  137 VV 3 34168316 1597702759   57.92%  13.761%
    4   1.659  137  138  149 VV    4755615  105112162    3.81%   0.905%
    5   1.843  149  155  156 VV 3 1100508    36650767    1.33%   0.316%

    6   1.900  156  160  177 PV 2 41979096  955093122   34.62%   8.226%
    7   2.246  177  190  201 VV 3 42976348 2758470044  100.00%  23.759%
    8   2.407  201  204  235 VV 2 10798264  271964719    9.86%   2.342%
    9   3.079  254  264  265 VV    5376694  113895999    4.13%   0.981%
   10   3.186  265  273  310 VV 2 27050524  916341983   33.22%   7.893%

   11   3.637  310  313  337 VV    6392048  162039611    5.87%   1.396%
   12   3.976  337  343  362 VV    6674093  181050358    6.56%   1.559%
   13   4.227  362  365  404 VV 2 4010364   160409676    5.82%   1.382%
   14   4.703  404  407  448 VV    2883249  100299358    3.64%   0.864%
   15   5.259  448  456  478 VV    2725679  143927170    5.22%   1.240%

   16   5.713  488  496  538 VV   18588817  498339290   18.07%   4.292%
   17   6.803  588  592  609 VV 2  119938     5441264    0.20%   0.047%
   18   7.457  642  650  655 BV 7  126906     7456723    0.27%   0.064%
   19   7.561  655  659  689 VV 4  543631    31764238    1.15%   0.274%
   20   8.181  697  713  732 BV 4  120336    15299704    0.55%   0.132%

   21   8.544  732  745  784 VB 5  167936    18782499    0.68%   0.162%
   22  10.082  859  881  902 BV   37833061 2003203834   72.62%  17.254%


                       Sum of corrected areas: 11610131771
   Signal      : TIC: zw2020102902.D\datasim.ms

   peak  R.T. first  max last  PK    peak      corr.    corr.    % of
    #    min   scan scan scan  TY   height      area    % max.   total
   ---  ----- ----- ---- ---- ---  -------   -------   ------  -------

      No peaks were detected using the method integration parameters!

   GC_STANDARD.M Fri Apr 29 12:05:10 2022
```

```
   File      :C:\msdchem\1\DATA\2020\zw2020102902.D
   Operator  :
   Acquired  : 29 Oct 2020  11:27   using AcqMethod JIAN-FF-FAOL-2.M
   Instrument :    MSD
   Sample Name: zw2020102902
   Misc Info :
   Vial Number: 5
```
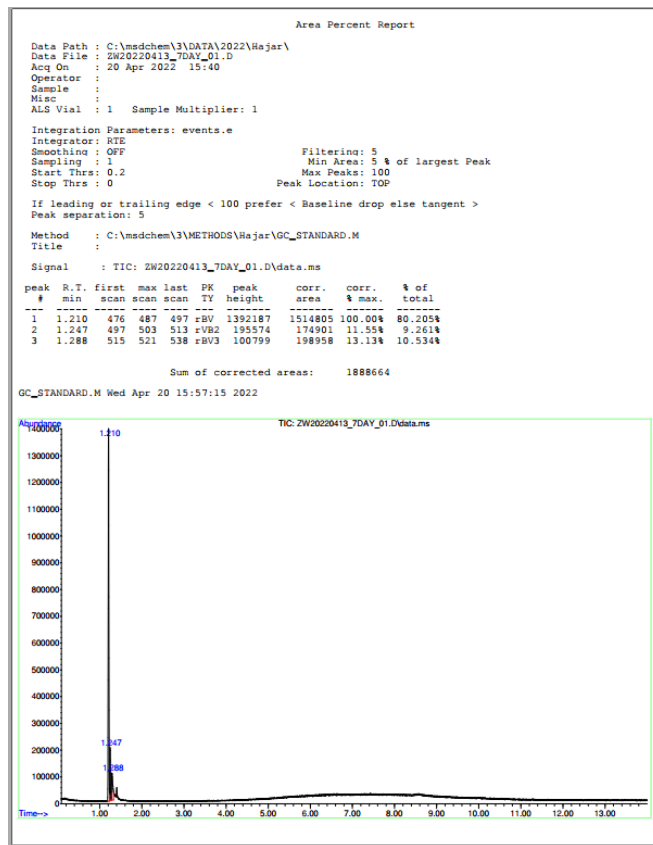
Reaction conditions: 5 mL EtOH, **Ru-4** (250 ppm, 16.2 mg), 41 h, 115 ºC, NaOEt (20 mol%, 1166 mg) in a 25.9 mL high-pressure reactor and 600 rpm.
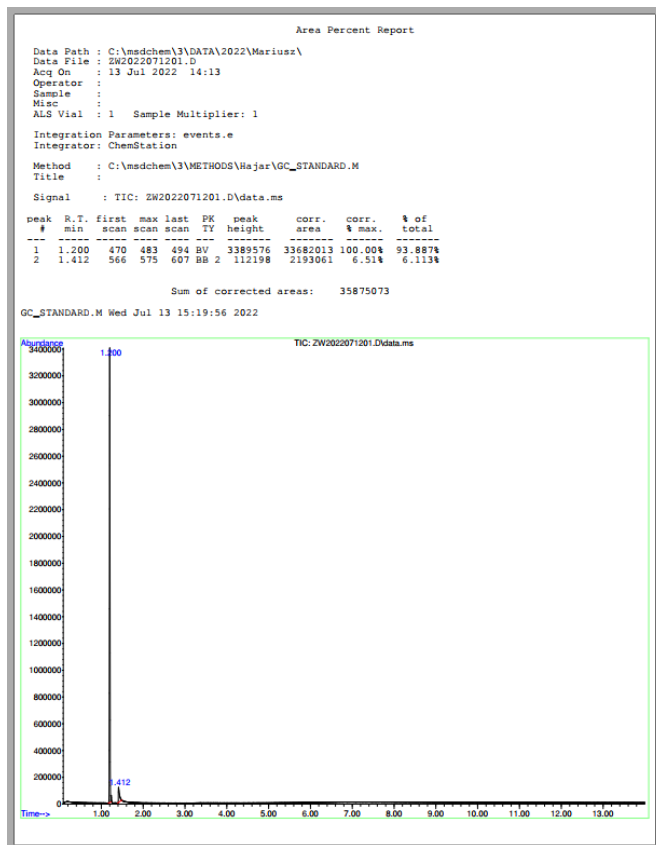


```
                              Area Percent Report

 Data Path : C:\msdchem\1\DATA\2020\
 Data File : ZW20201112CY.D
 Acq On    : 12 Nov 2020  13:04
 Operator  :
 Sample    : ZW20201112CY
 Misc      :
 ALS Vial  : 4   Sample Multiplier: 1

 Integration Parameters: events.e
 Integrator: ChemStation

 Method    : C:\msdchem\3\METHODS\Hajar\GC_STANDARD.M
 Title     :

 Signal    : TIC: ZW20201112CY.D\data.ms

 peak  R.T. first  max last  PK   peak      corr.    corr.    % of
  #    min  scan scan scan   TY  height     area    % max.   total
 ---  ----- ---- ---- ----   --  ------    ------   ------  -------
  1   1.336  107  110  112 BV    121806   1734422   0.10%   0.020%
  2   1.460  112  121  125 VV 3 26635534 1154313956  67.52%  13.219%
  3   1.607  125  134  149 VV 4 24038133 1219789671  71.35%  13.969%
  4   1.840  149  154  156 VV 3 1230503   39927120   2.34%   0.457%
  5   1.909  156  161  176 VV 3 29120888 801616355  46.89%   9.180%

  6   2.228  176  189  201 VV   27093525 1395708330  81.64%  15.984%
  7   2.396  201  203  235 VV 2 10306994 255040002  14.92%   2.921%
  8   3.012  255  258  261 VV    4047186   68754265   4.02%   0.787%
  9   3.069  261  263  265 VV    5245805   88389816   5.17%   1.012%
 10   3.186  265  273  285 VV 2 19175176 714372925  41.79%   8.181%

 11   3.646  309  314  337 VV    2826659   81468475   4.77%   0.933%
 12   3.979  337  343  362 VV 2 4522520 147990633   8.66%   1.695%
 13   4.236  362  366  404 VV 2 4634697 148190341   8.67%   1.697%
 14   4.703  404  407  444 VV   5251565 124858531   7.30%   1.430%
 15   5.270  453  457  458 PV   3046088  38151264   2.23%   0.437%

 16   5.303  458  460  477 VV   3472623  97421795   5.70%   1.116%
 17   5.738  490  498  513 VV  17998237 504161741  29.49%   5.774%
 18   6.799  588  592  603 VV    192316   9324049   0.55%   0.107%
 19   7.114  613  619  642 VV 6  132589  11706683   0.68%   0.134%
 20   7.432  642  647  656 VV 3  227003  12812770   0.75%   0.147%

 21   7.567  656  659  671 VV 3  776161  31590186   1.85%   0.362%
 22   8.459  732  738  740 VV 4  142054   6174253   0.36%   0.071%
 23   8.529  740  744  770 VV 2  247715  14748175   0.86%   0.169%
 24  10.113  866  884  900 PV  29439478 1709574331 100.00%  19.578%
 25  10.370  900  906  912 VV    274507   7919174   0.46%   0.091%

 26  12.574 1095 1101 1109 BV    217765   5557028   0.33%   0.064%
 27  18.679 1632 1639 1669 BV    438380  24921831   1.46%   0.285%
 28  19.316 1692 1695 1723 VV    309267  15925910   0.93%   0.182%

              Sum of corrected areas:  8732144032
 Signal    : TIC: ZW20201112CY.D\datasim.ms

 peak  R.T. first  max last  PK   peak      corr.    corr.    % of
  #    min  scan scan scan   TY  height     area    % max.   total
 ---  ----- ---- ---- ----   --  ------    ------   ------  -------

   No peaks were detected using the method integration parameters!

 GC_STANDARD.M Thu Apr 28 13:55:08 2022
```

```
 File      :C:\msdchem\1\DATA\2020\ZW20201112CY.D
 Operator  :
 Acquired  : 12 Nov 2020  13:04    using AcqMethod JIAN-FF-FAOL-2.M
 Instrument :   MSD
 Sample Name: ZW20201112CY
 Misc Info  :
 Vial Number: 4
```

Reaction conditions: 5 mL EtOH, **Ru-5** (250 ppm, 13.5 mg), 41 h, 115 ℃, NaOEt (20 mol%, 1166 mg) in a 25.9 mL high-pressure reactor and 600 rpm.

Reaction conditions: 5 mL 4-hydroxy-2-butanone, **Ru-2** (250 ppm, 8.5 mg), 24 h, 115 ºC, 22 bar H$_2$, in a 25.9 mL high-pressure reactor and 600 rpm.

Reaction conditions: 2.5 mL 4-hydroxy-2-butanone, **Ru-2** (250 ppm, 4.3 mg), 24 h, 115 $^{\circ}$C, 22 bar H_2, in a 25.9 mL high-pressure reactor and 600 rpm.

Reaction conditions: 2.5 mL 4-hydroxy-2-butanone, **Ru-2** (250 ppm, 4.3 mg), NaOAc (20 mol%, 595 mg), 24 h, 115 °C, 22 bar H$_2$, in a 25.9 mL high-pressure reactor and 600 rpm.

Area Percent Report

Data Path : C:\msdchem\1\data\2022\Mariusz\
Data File : zw202207120605.D
Acq On : 14 Jul 2022 15:40
Operator :
Sample : zw202207120605
Misc :
ALS Vial : 11 Sample Multiplier: 1

Integration Parameters: autoint1.e
Integrator: ChemStation

Method : C:\msdchem\1\methods\standard.M
Title :

Signal : TIC: zw202207120605.D\data.ms

peak R.T. first max last PK peak corr. corr. % of
min scan scan scan TY height area % max. total
--- ----- ---- ---- ---- --- ------- ------- ------ -------
1 1.149 301 321 347 BV 2 28375395 869114795 100.00% 72.115%
2 1.256 347 355 399 VB 2 7877165 180709868 20.79% 14.994%
3 8.629 2629 2640 2662 BB 2 386013 7119700 0.82% 0.591%
4 9.356 2841 2865 2895 VB 2 385005 12016833 1.38% 0.997%
5 11.531 3529 3540 3569 BB 1167279 34332955 3.95% 2.849%

6 12.356 3777 3795 3816 BV 3 1000993 33433224 3.85% 2.774%
7 12.452 3816 3825 3878 VB 2 989035 41403133 4.76% 3.435%
8 16.411 5028 5052 5080 BB 2 734393 18002844 2.07% 1.494%
9 18.097 5563 5575 5588 PV 3 462420 9049972 1.04% 0.751%

Sum of corrected areas: 1205183325
Signal : zw202207120605.D\FID1A.ch

peak R.T. Start End PK peak corr. corr. % of
min min min TY height area % max. total
--- ----- ----- ----- --- ------- ------- ------ -------
1 1.136 1.127 1.226 BV 51405931 816197946 100.00% 74.528%
2 1.250 1.226 1.330 VB 13734147 278959603 34.18% 25.472%

Sum of corrected areas: 1095157550

standard.M Fri Jul 15 09:39:51 2022   Page: 1

Area Percent Report

Data Path : C:\msdchem\1\data\2022\Mariusz\
Data File : zw202207120605.D
Acq On : 14 Jul 2022 15:40
Operator :
Sample : zw202207120605
Misc :
ALS Vial : 11 Sample Multiplier: 1

Integration Parameters: autoint1.e
Integrator: ChemStation

Method : C:\msdchem\1\methods\standard.M
Title :

standard.M Fri Jul 15 09:39:51 2022   Page: 2

GC-MS (gas phase) reports of products

Reaction conditions: 2.5 mL EtOH, **Ru-2** (250 ppm, 7.6 mg), 96 h, 130 ºC, NaOEt (20 mol%, 583 mg) in a 18.4 mL high-pressure reactor and 600 rpm.

Reaction conditions: 2.5 mL EtOH, **Ru-2** (8.3 ppm, 0.0025 mg), 168 h, 130 ºC, NaOEt (20 mol%, 583 mg) in a 18.4 mL high-pressure reactor and 600 rpm.

Reaction conditions: 2.5 mL 4-hydroxy-2-butanone, **Ru-2** (250 ppm, 4.3 mg), 24 h, 115 $^{\circ}$C, 22 bar H$_2$, in a 25.9 mL high-pressure reactor and 600 rpm.

Micro-GC reports of inorganic and organic gas

Reaction conditions: 5 mL EtOH, **Ru-2** (250 ppm, 15.1 mg), 24 h, 115 ºC, NaOEt (20 mol%, 583 mg) in a 25.9 mL high-pressure reactor and 600 rpm.
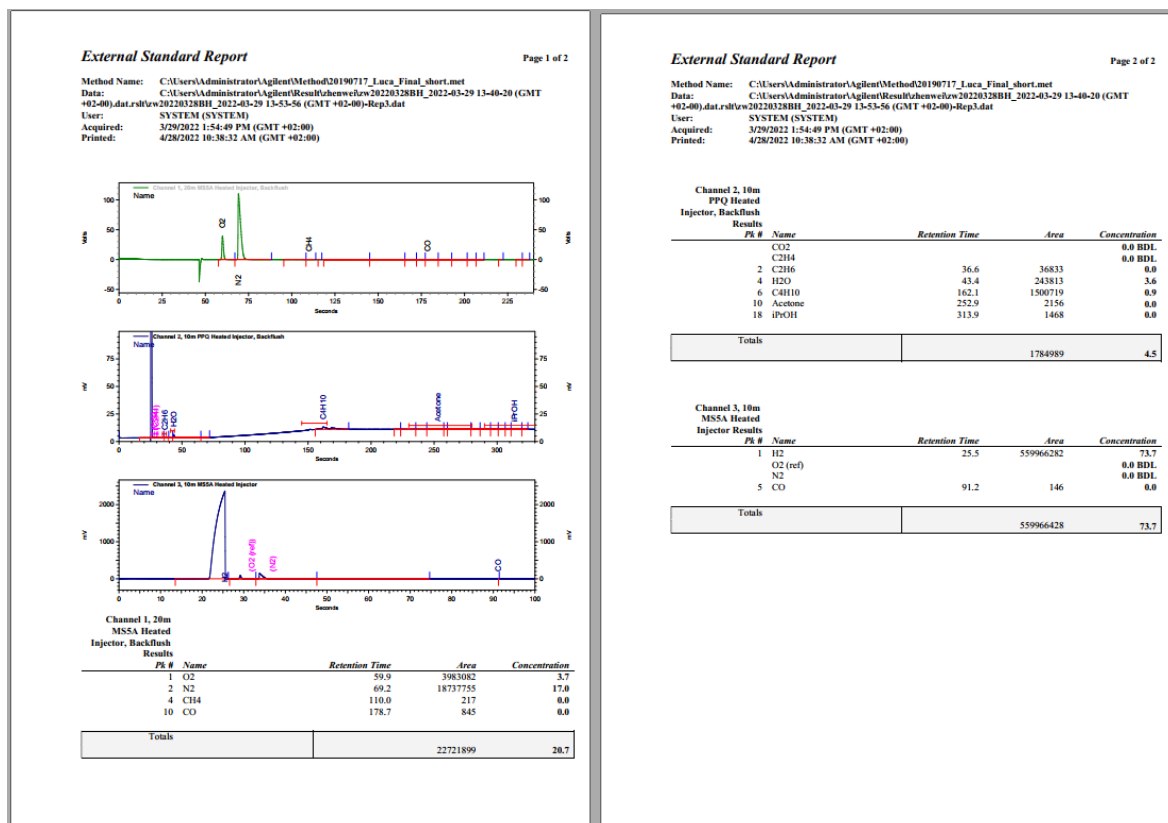
Appendix B – Chapter 3.2

B. Supplementary information for Chapter 3.2

Most chemicals were purchased from commercial suppliers and used without further purification unless otherwise stated. Ethanol absolute (purity 99.98%), toluene (purity 99.99%), o-xylene (purity $\geq$ 98%), m-xylene (purity $\geq$ 99%), p-xylene (purity $\geq$ 99%), ethylbenzene (purity $\geq$ 99.0%), mesitylene (purity 98%), p-cymene (purity $\geq$ 99 %), chlorobenzene (purity $\geq$ 99%), anisole (purity 99.7%), cyclohexane (purity 99.5%), methylcyclohexane (purity $\geq$ 99 %), 1,3-dimethylcyclohexane (purity 99%), tetrahydrofuran (purity 99.99%), 1,4-dioxane (purity 99.8%), cyclopentyl methyl ether (purity $\geq$ 99.9%), γ-valerolactone (purity 99%) were purchased from a commercial supplier as well. All reactions dealing with air or moisture-sensitive compounds were performed using standard Schlenk techniques or in an argon-filled glovebox. Dimethyl sulfoxide (100 uL, purity 99.9%) was added as the internal stand to quantify ethanol conversion and ethyl acetate yield. ^{1}H-NMR and ^{13}C-NMR spectra were recorded on a Bruker Avance III 400 MHz spectrometer and were referenced on the deuterated solvent peak. Catalysts were added in an argon-filled glovebox, substrates and co-solvents were loaded into a 50 mL flask using standard Schlenk techniques.

Table B-1 provided all the ADC reactions using **Ru-1** under different conditions

Table B-1: Screening of ADC of ethanol under different conditions with **Ru-1**.

Entry	Solvent	Ratio	**Ru-1** [mol%]	Time [h]	Conversion [%][a]	Yield [%][a]	Selectivity [%]
1	toluene	5	0.025	72	39	13	33
2	toluene	5	0.05	24	43	25	58
3	toluene	5	0.05	72	72	54	75
4	toluene	1.25	0.05	24	47	43	91
5	toluene	1.25	0.1	18	89	84	94
6	toluene	1.25	0.1	24	98	92	94
7[b]	toluene	1.25	0.1	24	37	34	92
8	toluene	2.5	0.1	24	91	87	96
9	toluene	5	0.1	24	63	46	73
10	toluene	7.5	0.1	24	53	52	98
11	toluene	5	0.1	48	72	52	72
12	toluene	5	0.1	72	92	86	93
13	o-xylene	5	0.05	48	52	33	63
14	o-xylene	5	0.1	24	58	51	88
15	m-xylene	2.5	0.1	24	86	78	91
16	m-xylene	5	0.1	24	87	79	91
17	m-xylene	7.5	0.1	24	69	68	99
18	m-xylene	5	0.1	48	95	76	80
19	p-xylene	5	0.1	24	40	27	68
20	p-xylene	5	0.1	48	45	28	62
21	ethylbenzene	2.5	0.1	24	58	48	83
22	ethylbenzene	5	0.1	24	68	55	81

23	ethylbenzene	7.5	0.1	24	69	50	72
24	ethylbenzene	5	0.1	48	72	55	76
25	mesitylene	5	0.1	24	30	15	50
26	p-cymene	5	0.1	24	66	53	80
27	chlorobenzene	5	0.1	24	10	5	50
28	anisole	5	0.1	24	61	49	80
29	anisole	5	0.1	48	73	57	78
30	cyclohexane	5	0.05	24	25	25	100
31	cyclohexane	5	0.1	24	52	50	96
32	cyclohexane	5	0.1	48	51	34	67
33	methylcyclohexane	5	0.1	24	55	50	91
34	1,3-dimethylcyclohexone	5	0.1	24	51	46	90
35	tetrahydrofuran	5	0.1	24	22	20	91
36	tetrahydrofuran	5	0.1	48	63	58	92
37	tetrahydrofuran	5	0.1	72	65	63	97
38	1,4-dioxane	5	0.1	24	53	41	77
39	1,4-dioxane	5	0.1	48	59	43	73
40	Cyclopentyl methyl ether	5	0.1	24	52	46	88
41	Cyclopentyl methyl ether	5	0.1	48	56	45	80
42	γ-valerolactone	5	0.1	24	12	7	58
43	γ-valerolactone	5	0.1	48	14	8	57

[a] Determined by NMR, dimethyl sulfoxide is an internal standard. [b] temperature, 100 °C.

Table B-2 provided ADC reactions with different catalysts under optimization conditions.

Table B-2: Screening of different catalysts in ADC of ethanol with toluene.

Entry	Catalyst	Conversion [%][a]	Yield [%][a]

1	**Ru-2**	<5	<5
2	**Ru-3**	/	/
3	**Ru-4**	/	/
4	**Ru-5**	/	/
5	**Ru-6**	/	/
6	**Ir-1**	/	/

ª Determined by NMR, dimethyl sulfoxide is an internal standard.
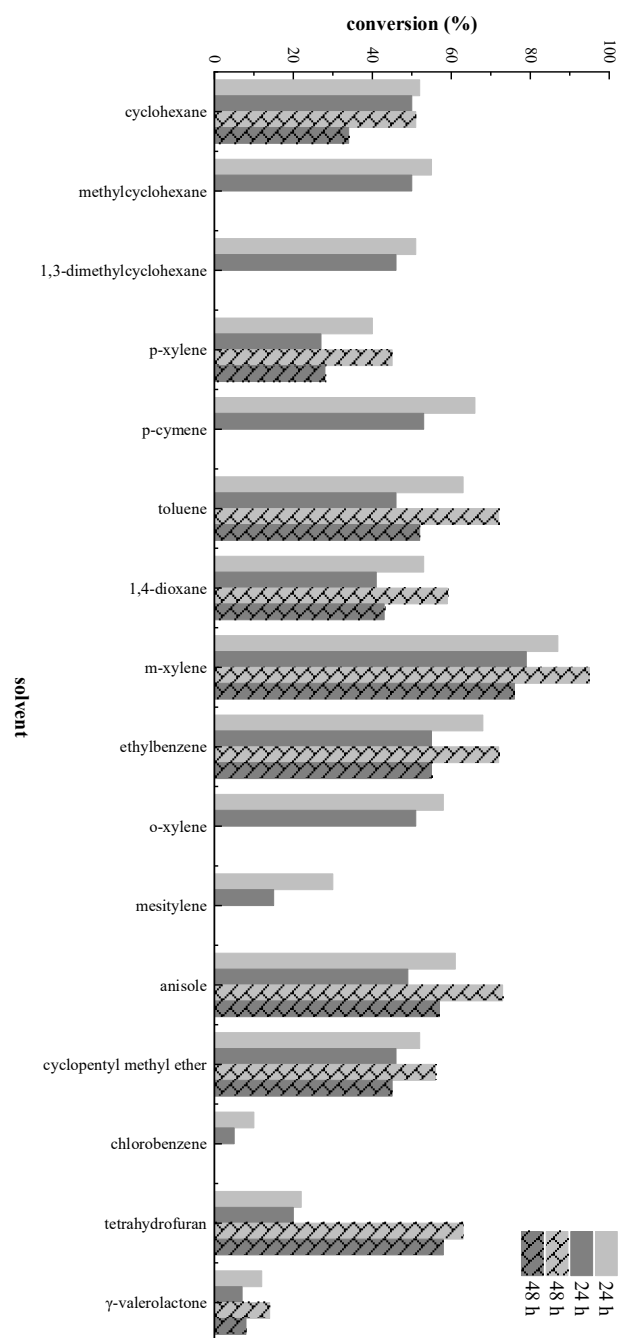
Figure B.1: Co-solvent screening for ADC of ethanol (2 mL EtOH, 10 mL solvent, 0.1 mol% **Ru-1**, 24h or 48 h, 120 ºC)

The following NMR spectra show the ADC of ethanol to ethyl acetate for 24 h, at 120 °C, with

0.1 mol% **Ru-1** or **Ru-2** using 2 mL ethanol and 10 mL co-solvent.
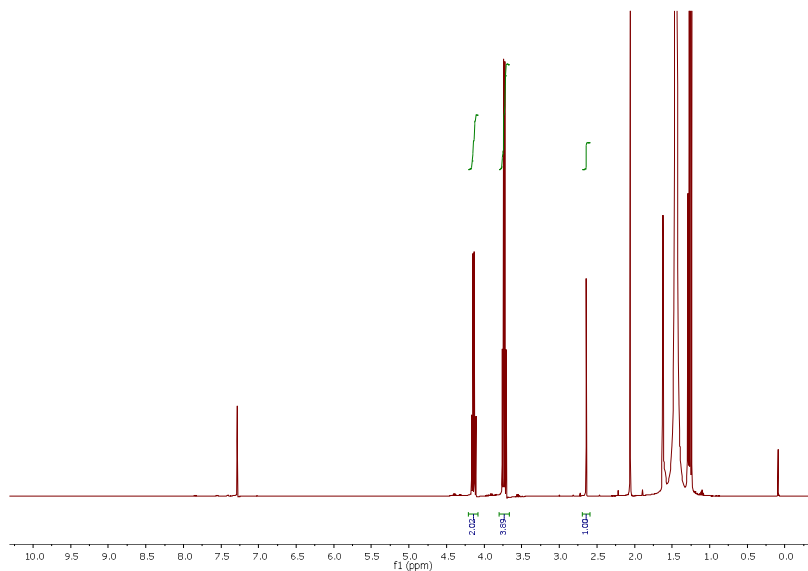
Figure B.2: ^{1}H NMR of ADC of ethanol with cyclohexane (CDCl$_3$, 25 °C, 400 MHz, Table 3-10, Entry 1).
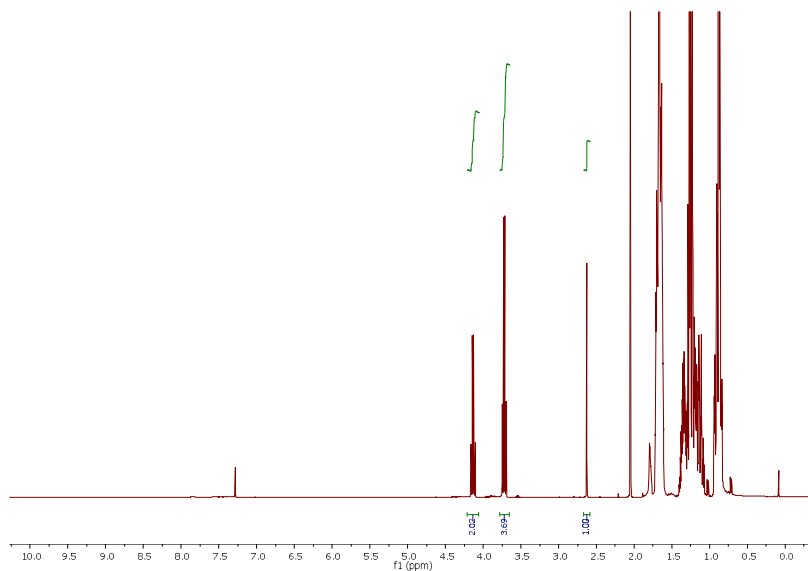
Figure B.3: ^{1}H NMR of ADC of ethanol with methylcyclohexane (CDCl$_3$, 25 °C, 400 MHz, Table 3-10, Entry 2).
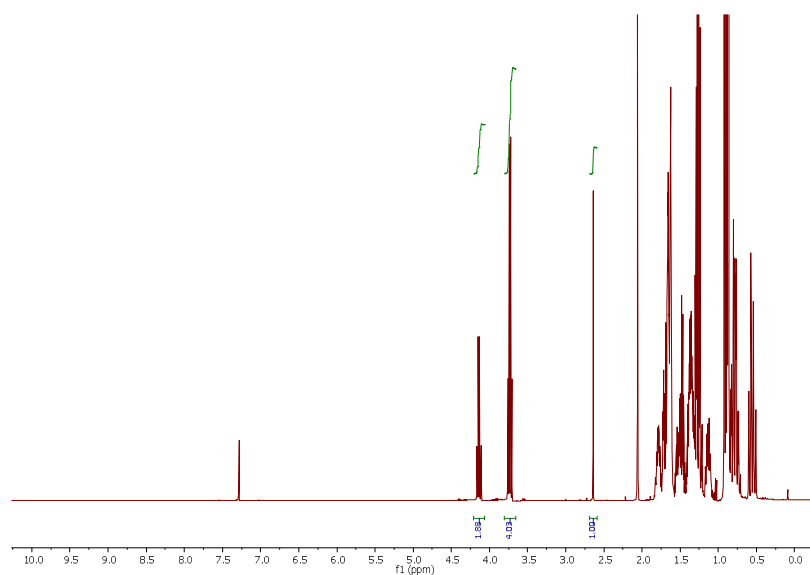
Figure B.4: ^{1}H NMR of ADC of ethanol with 1,3-dimethylcyclohexane (CDCl$_3$, 25 ^{o}C, 400 MHz, Table 3-10, Entry 3).
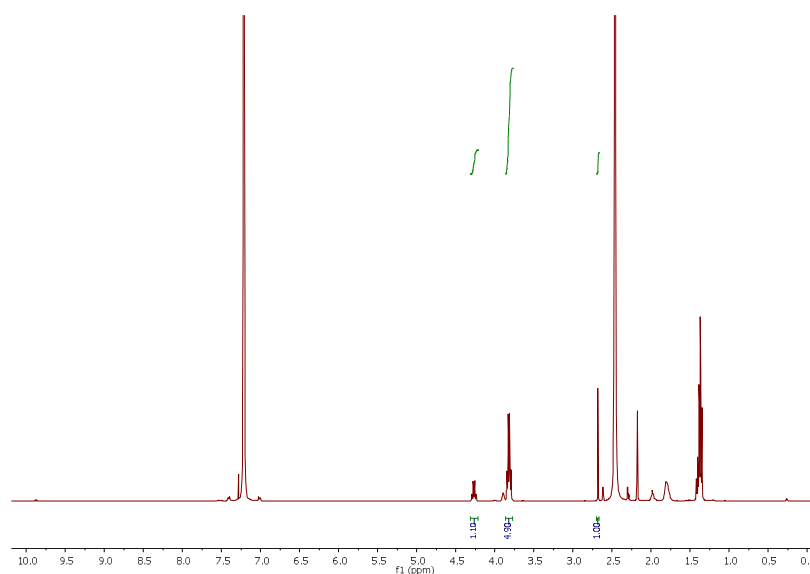
Figure B.5: ^{1}H NMR of ADC of ethanol with p-xylene (CDCl$_3$, 25 ^{o}C, 400 MHz, Table 3-10, Entry 4).
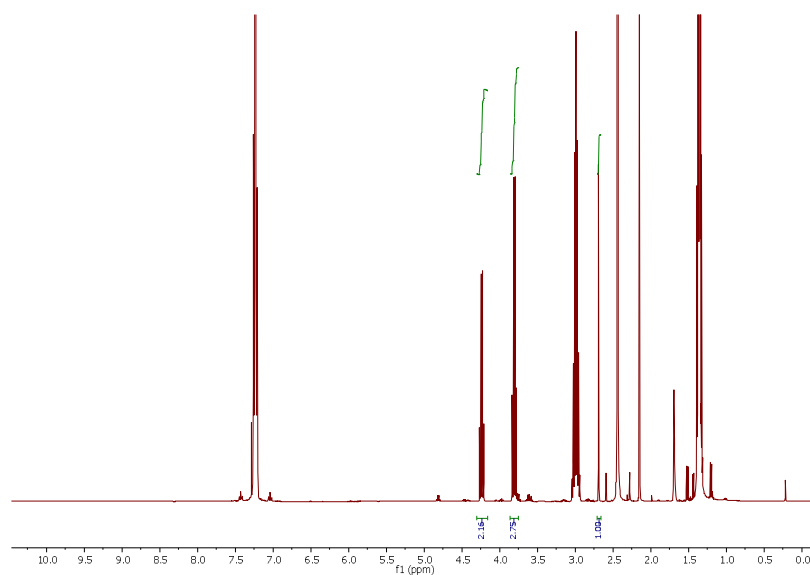
Figure B.6: ^{1}H NMR of ADC of ethanol with *p*-cymene (CDCl$_3$, 25 ^{o}C, 400 MHz, Table 3-10, Entry 5).
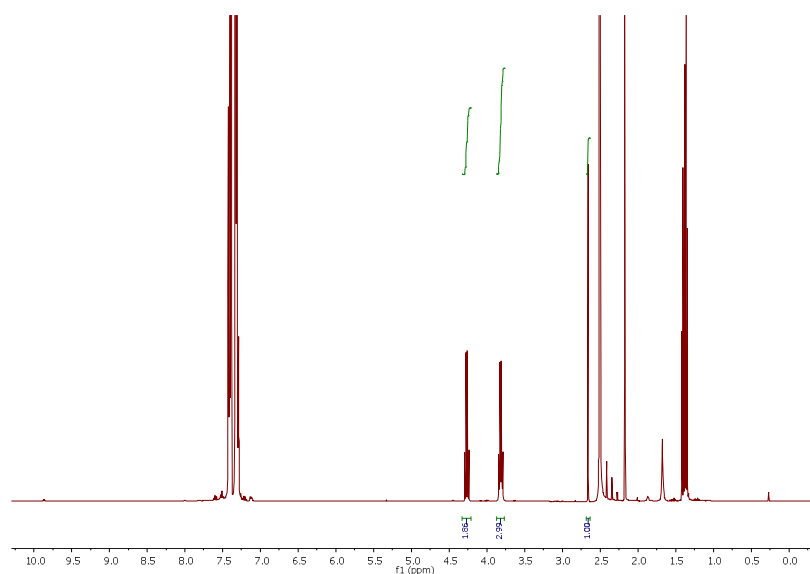
Figure B.7: ^{1}H NMR of ADC of ethanol with toluene (CDCl$_3$, 25 ^{o}C, 400 MHz, Table 3-10, Entry 6).
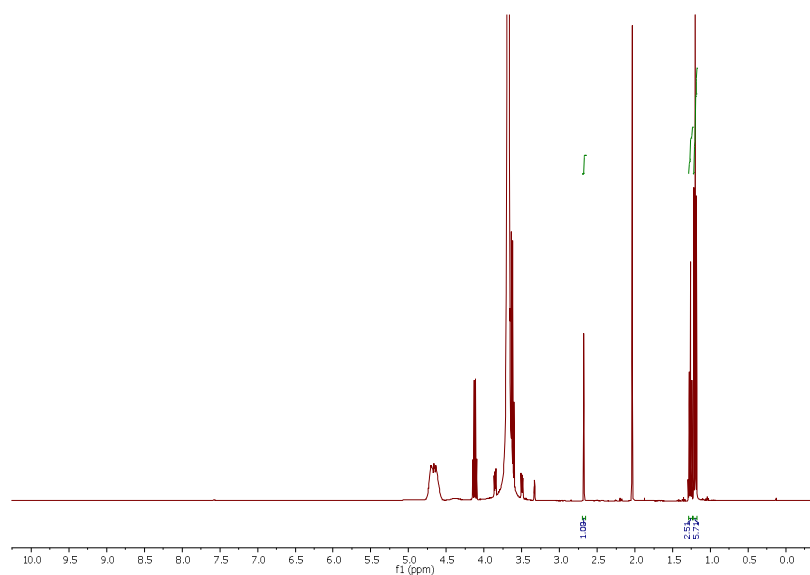
Figure B.8: ^{1}H NMR of ADC of ethanol with 1,4-dioxane (CD$_3$OD, 25 ^{o}C, 400 MHz, Table 3-10, Entry 7).
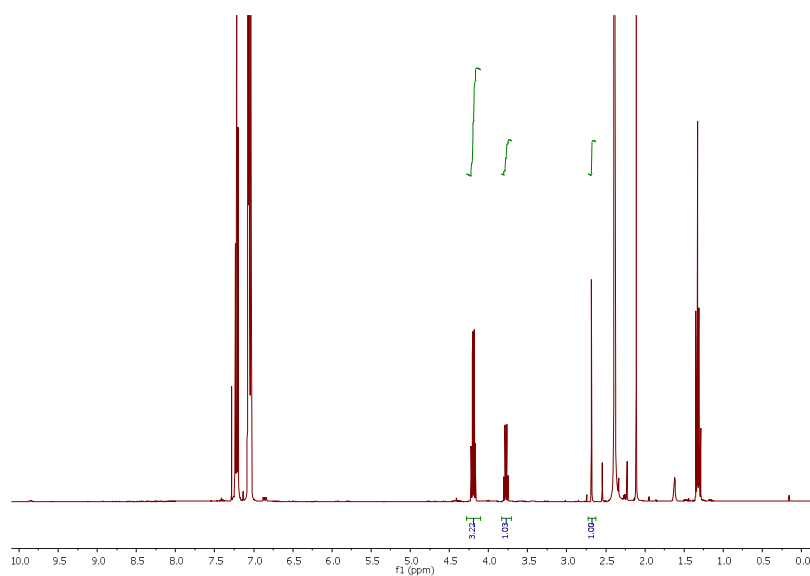
Figure B.9: ^{1}H NMR of ADC of ethanol with *m*-xylene (CDCl$_3$, 25 ^{o}C, 400 MHz, Table 3-10, Entry 8).
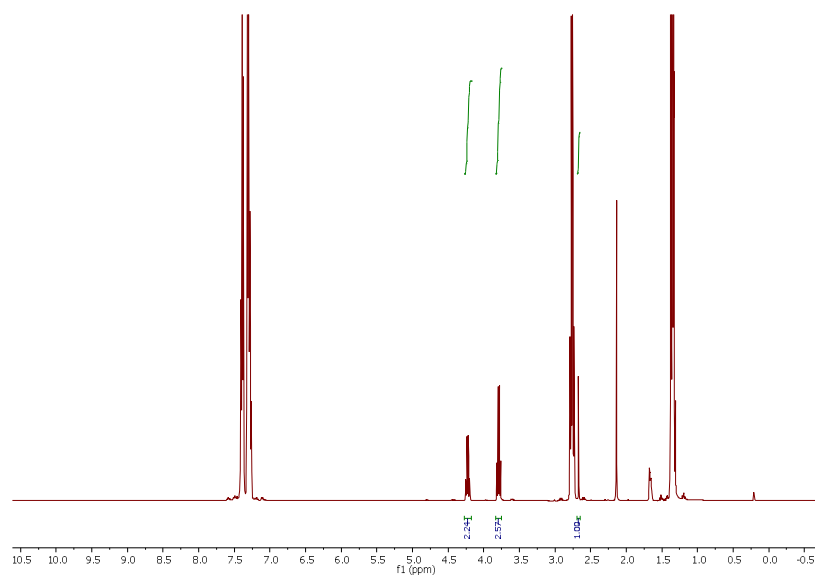
Figure B.10: ^{1}H NMR of ADC of ethanol with ethylbenzene (CDCl$_3$, 25 ºC, 400 MHz, Table 3-10, Entry 9).
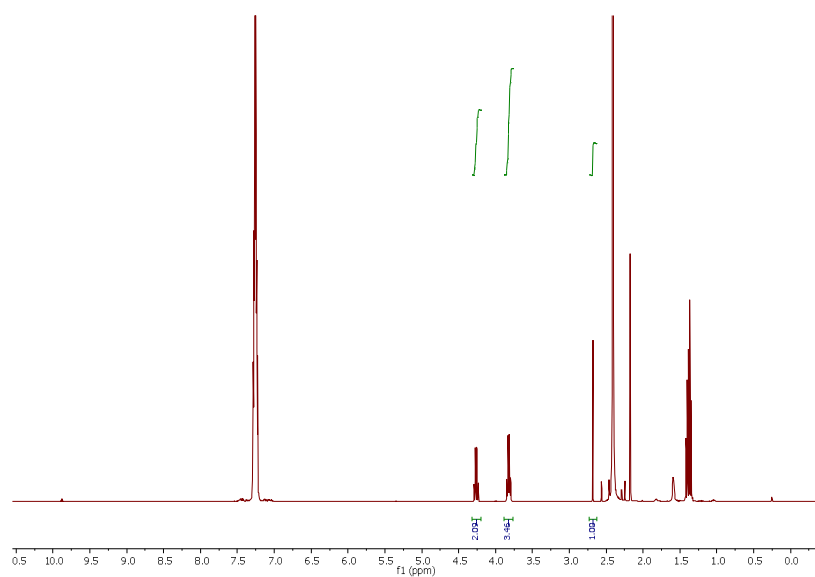
Figure B.11: ^{1}H NMR of ADC of ethanol with *o*-xylene (CDCl$_3$, 25 ºC, 400 MHz, Table 3-10, Entry 10).
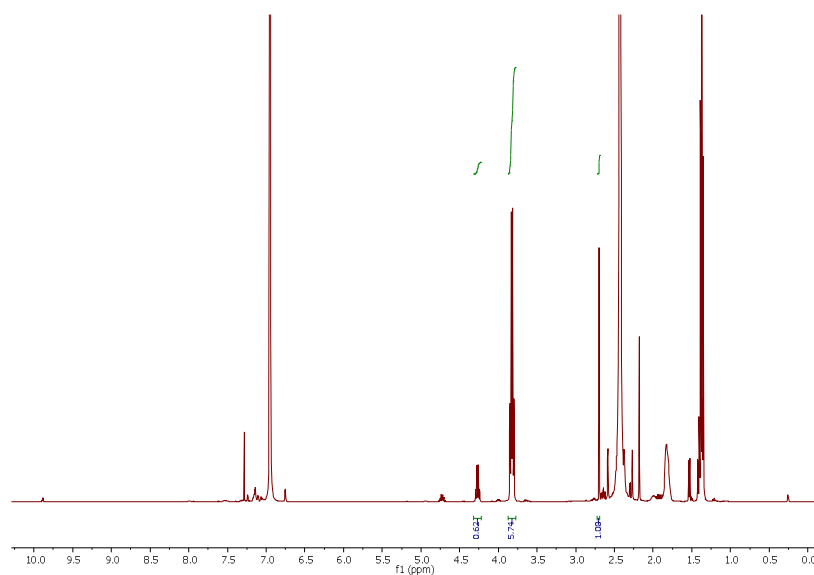
Figure B.12: ^{1}H NMR of ADC of ethanol with mesitylene (CDCl$_3$, 25 ^{o}C, 400 MHz, Table 3-10, Entry 11).
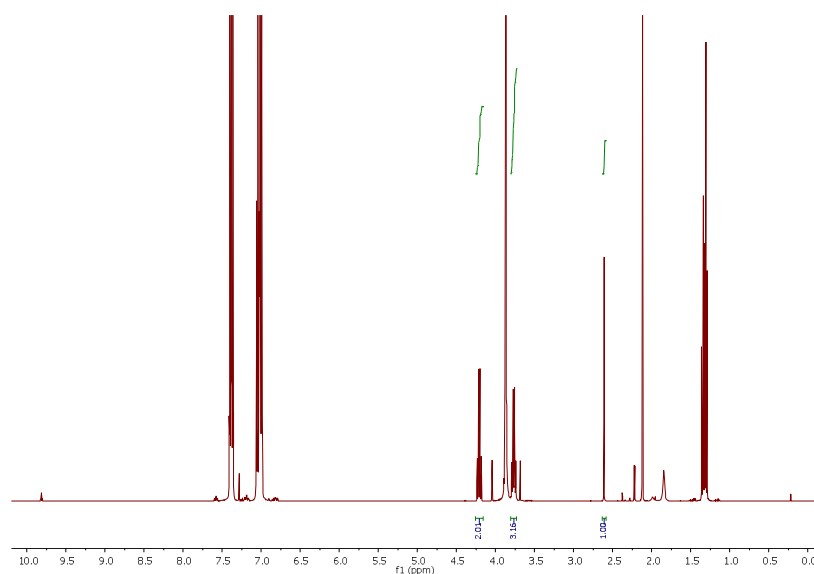
Figure B.13: ^{1}H NMR of ADC of ethanol with anisole (CDCl$_3$, 25 ^{o}C, 400 MHz, Table 3-10, Entry 12).
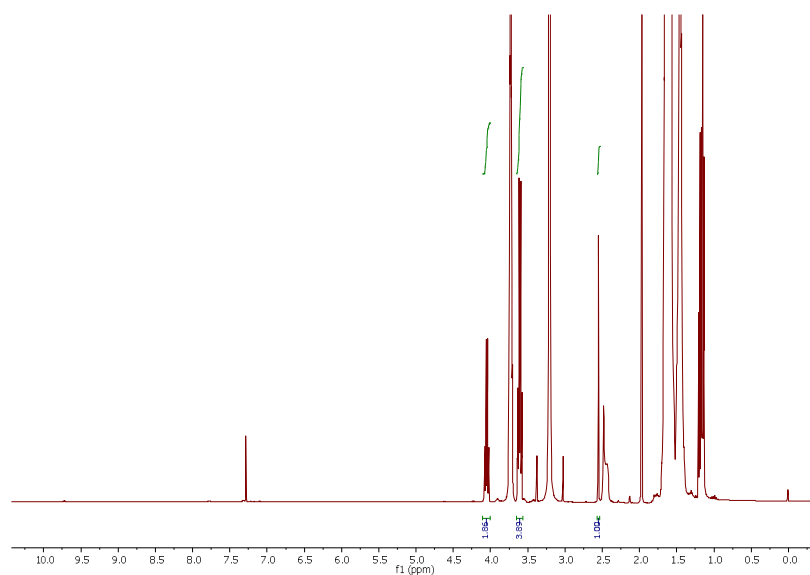
Figure B.14: ^{1}H NMR of ADC of ethanol with cyclopentyl methyl ether (CDCl$_3$, 25 ^{o}C, 400 MHz, Table 3-10, Entry 13).
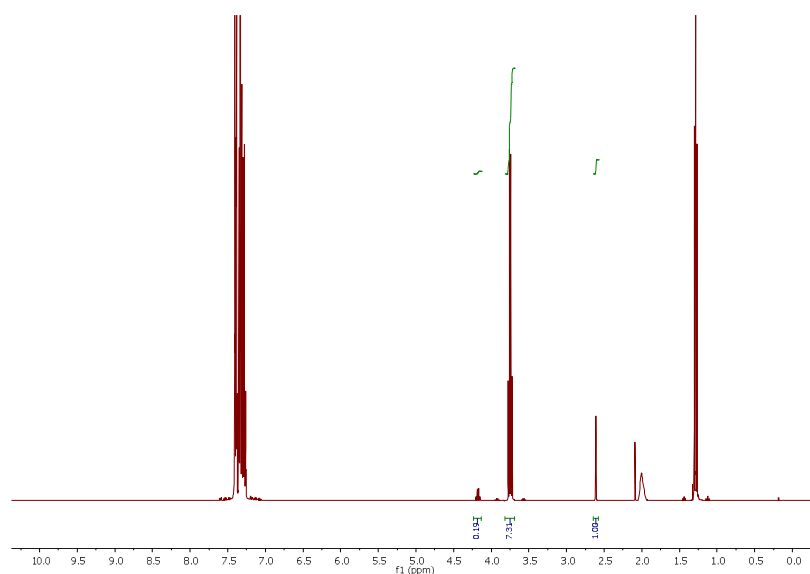
Figure B.15: ^{1}H NMR of ADC of ethanol with chlorobenzene (CDCl$_3$, 25 ^{o}C, 400 MHz, Table 3-10, Entry 14).
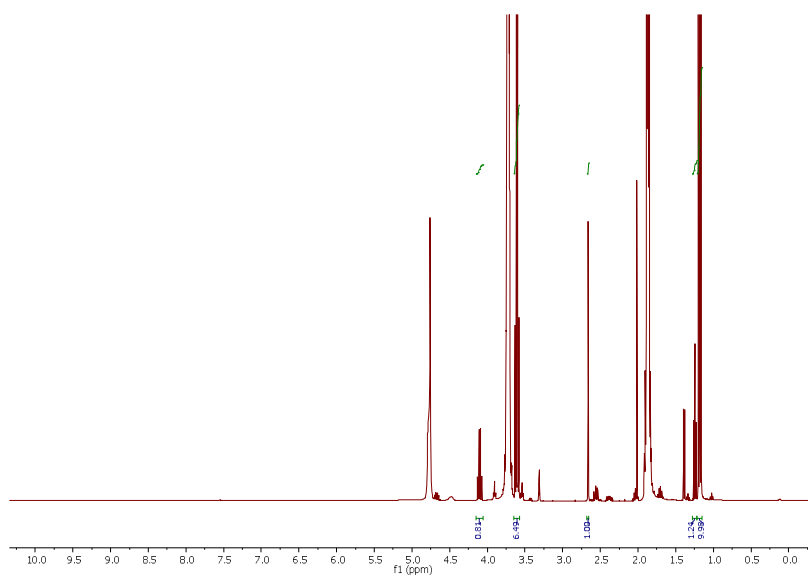
Figure B.16: ^{1}H NMR of ADC of ethanol with tetrahydrofuran (CD$_3$OD, 25 ^{o}C, 400 MHz, Table 3-10, Entry 15).
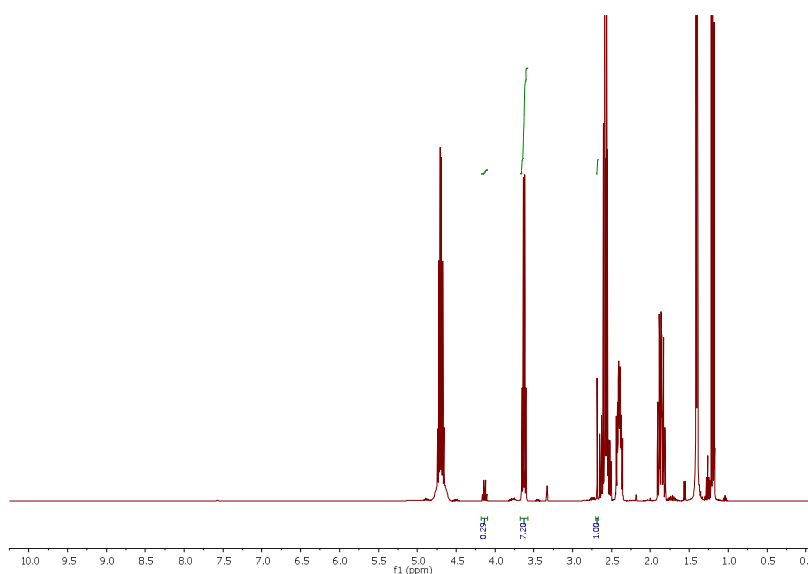
Figure B.17: ^{1}H NMR of ADC of ethanol with γ-valerolactone (CD$_3$OD, 25 ^{o}C, 400 MHz, Table 3-10, Entry 16).
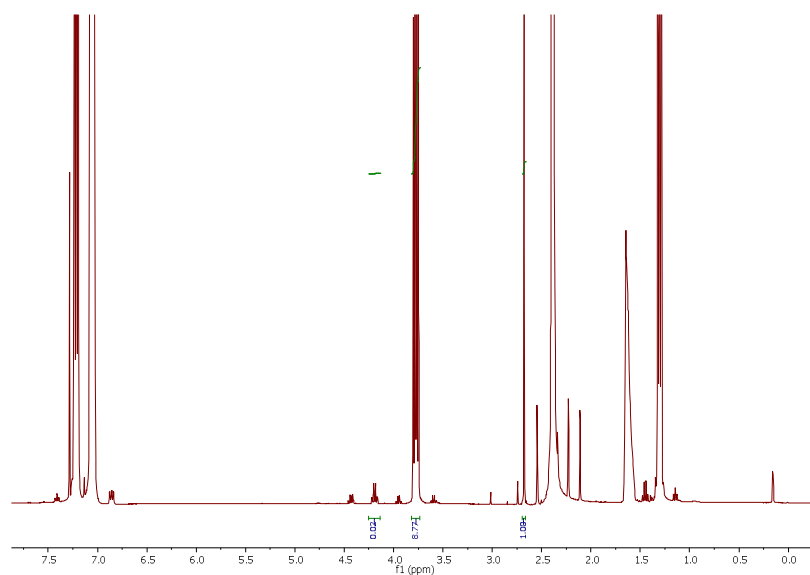
Figure B.18: ^{1}H NMR of ADC of ethanol with *m*-xylene (CDCl$_3$, 25 ^{o}C, 400 MHz, Table B-2, Entry 1).

Appendix C – Chapter 3.3

C. Supplementary information for Chapter 3.3

General information

Most chemicals were purchased from commercial suppliers and used without further purification unless otherwise stated. Ru-MACHO-BH was purchased from StremChemicals and stored in a glove box. Water-d_2 (^{1}H, 4.79 ppm) and methanol-d_4 (^{1}H, 3.31 ppm; ^{13}C, 49.00$\pm$0.01 ppm) for NMR analysis were purchased from Flurochem. Glycerol (purity $\geq$ 99.5%), benzaldehyde (purity > 98%), acetophenone (purity 99%), 2-hexanone (purity 98%), benzophenone (purity > 99%), 2-acetylfuran (purity 99%), 4'-Methylacetophenone (purity 95%) were purchased from a commercial supplier as well.

All reactions dealing with air or moisture-sensitive compounds were performed using standard Schlenk techniques or in an argon-filled glovebox. ^{1}H-NMR and ^{13}C-NMR spectra were recorded on a Bruker Avance III 400 MHz spectrometer and were referenced on the deuterated solvent peak. Catalysts were added in an argon-filled glovebox, substrates and solvents were loaded into a 15 mL pressure tube using standard Schlenk techniques.

Appendix D – Paper I

This paper has been submitted to *Nature Communications* on 17th August 2022, and it is based on the research of Chapter 3.1. There was a small error in the article, which was submitted and therefore not corrected yet. In the abstract, line 11, 20 mol% of NaOEt should be 20 mol% of NaO*t*Bu as well as in Table 1, Entry 1. This work was conducted at DTU Chemistry in collaboration with Rosa Padilla, Lucas dos Santos Mello and Assoc. Prof. Martin Nielsen.

1   **Low-temperature selective ethanol upgrading to primary or secondary alcohols by homogeneous**

2   **catalysis**

3   Zhenwei Ni, Rosa Padilla, Lucas dos Santos Mello & Martin Nielsen*

4   Technical University of Denmark (DTU), Department of Chemistry, 2800 Kgs. Lyngby, Denmark;

5   marnie@kemi.dtu.dk.

6   **ABSTRACT:** Ethanol is one of the most promising renewable resources for the production of key in-

7   dustrial commodities. Herein, we present the first direct and selective conversion of ethanol to either

8   primary or secondary alcohols, or to hydrocarbons, using ruthenium PNP pincer complexes

9   [(^{R}PNP)RuHXCO] (R= iPr, Ph, Cy, tBu; X = Cl, H-BH$_3$) as catalysts. Using phenyl substituted phos-

10   phines leads to the selective production of secondary alcohols. Hence, employing [(^{Ph}PNP)RuH(Cl)CO]

11   (**Ru-1**) as a catalyst in ethanol, containing 20 mol% of NaOEt, at 115 ºC leads to 89% selective produc-

12   tion of secondary alcohols over primary alcohols. A yield of 12% of 2-butanol, and in total 22% of sec-

13   ondary alcohols, was achieved. In addition, minor amounts of 2-butenes/butane (≤5%) were observed in

14   the gas phase. On the contrary, when using bulky phosphine substituents, such as t-butyl, the selectivity

15   completely shifts toward primary alcohols. Thus, using [(^{tBu}PNP)RuH(Cl)CO] (**Ru-5**) leads to >99%

16   selectivity of 1-butanol (13% yield) over secondary alcohols at 115 ºC. In fact, the catalytic system is

17   highly competitive for producing 1-butanol with 22% yield obtained at 130 ºC, a temperature signifi-

18   cantly lower than previously reported systems. Our methodology unveils the potential for using bulk

19   bio-alcohols to selectively produce primary or secondary alcohols and hydrocarbons under mild condi-

20   tions.

21

22

23

24

25 **Introduction**

26 Current research within sustainable chemistry aims for solutions that provide renewable carbon sources

27 as well as clean energy alternatives[1]. The substitution of conventional fossil fuels is necessary to reduce

28 greenhouse gas emissions in the transportation sector[2]. Hence, alternative and benign fuels derived from

29 biomass conversion represent promising sustainable options[3].

30 Despite the promising applications of ethanol as a biofuel additive[4], there are several drawbacks, such as

31 low energy density (70% of that of gasoline)[5], high water solubility[6], and corrosion effects on the

32 engine[7]. Recently, some alternative fuels from renewable resources have been investigated, such as 1-

33 butanol and higher primary alcohols[8]. These biofuels arise not only as more favourable alternatives than

34 ethanol but also as less susceptible to phase separation being more hydrophobic[9].

35 Previous reports of ethanol upgrading (Supplementary Fig. 1) are based on the Guerbet reaction[10] for

36 carbon-chain growth, with selective production of 1-butanol and higher primary alcohols (Fig. 1, upper

37 pathway). Wass[11] reported the use of 0.1 mol% of [RuCl$_2$(η^6-p-cymene)]$_2$ and INDOLPhos[12] ligand for

38 the upgrade of ethanol to 1-butanol in 28% yield (93% selectivity) and TON =314 at 150 ºC in the pres-

39 ence of NaOEt (5 mol%). The same author used Ru-MACHO (**Ru-1**) as the precatalyst for 1-butanol

40 production, leading to only 13% conversion and merely 2% yield of the primary alcohol. In another at-

41 tempt, Milstein[13] reported a highly efficient conversion of ethanol (73%) with [RuHCl(Acr-^{iPr}PNP)(CO)]

42 (200 ppm) and NaOEt (20 mol%) at 150 ºC for 40 h (Supplementary Fig. 1). The desired product 1-

43 butanol was formed in 36% yield. To the best of our knowledge, there are no reports on ethanol upgrad-

44 ing to 2-butanol nor hydrocarbons under mild catalytic conditions (Fig. 1, lower pathway).

45

46
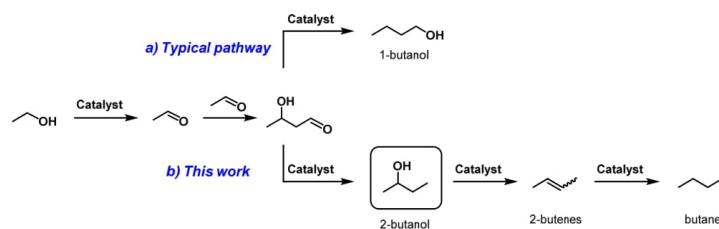
47 **Fig. 1 | Ethanol upgrading pathways.** a) Typical Guerbet reaction sequence for catalytic ethanol up-

48 grading to 1-butanol. b) Reaction pathway in this work for the novel catalytic ethanol upgrading to 2-

49 butanol, 2-butenes, and butane.

50 The industrial production of 2-butanol exceeds 800,000 tons per year[14], and is manufactured from glu-

51 cose by fermentation[15,16]. 2-butanol is widely used as a pharmaceutical standard[17], solvent[18], and fuel

52 additive[19]. Among these applications, it is a crucial intermediate in the chemical production of 1-butene,

53 2-butene[20], butyl acetate[21,22], *sec*-butyl acetate[21], and methyl ethyl ketone (MEK)[23]. Moreover, it has a

54 large market potential as a biofuel and other synthetic applications. Nevertheless, investigations for

55 catalytically upgrading ethanol report the production of 1-butanol with 2-butanol as byproduct[24].

56 The direct production of alkenes/alkanes from ethanol represents a potentially more economic route to

57 jet- and diesel-range hydrocarbon fuels relative to the state-of-the-art technology[25,26], rendering the se-

58 lective production of 2-butenes from renewable feedstock a critical challenge[27]. Moreover, these hydro-

59 carbons are also essential feedstock for the production of high-value-added products, such as rubbers,

60 polymers, and synthetic oils[28]. Indeed, recently the production of butenes from bioethanol has attracted

61 more attention in sustainability research fields, with yields exceeding 60% at reaction temperatures be-

62 tween 300-400 ºC[29,25]. As a significant component of liquefied petroleum gases (LP gases), butane is

63 industrially derived from natural gas and crude oil[30]. It may alternatively be obtained from ethanol using

64 heterogeneous catalysis at reaction temperatures between 200-300 ºC, typically resulting in low yields

65 of linear butane (<5%) and higher yields of the branched isomers (up to 85%)[31,32]. However, the use of

66   homogeneous catalytic systems and mild conditions for all the transformations of ethanol to 2-butanol,

67   2-butenes, or butane remains undisclosed.

68   Herein, we demonstrate the selective catalyzed transformation of ethanol to 2-butanol with the pincer

69   complexes Ru-MACHO (**Ru-1**) and Ru-MACHO-BH (**Ru-2**)[33], as well as the formation of low

70   amounts 2-butenes/butane under mild conditions (Fig. 1, lower pathway). Simply shifting to the analo-

71   gous complex **Ru-5**, with the *P*-substituents changing to *t*-butyls, leads to selective production of

72   1-butanol (Fig. 1, upper pathway).

73

74   **Results**

75   We commenced our studies by studying the ruthenium PNP pincer complexes **Ru-1** to **Ru-5** shown in

76   Table 1 for the catalytic upgrading of ethanol. These complexes are robust catalysts for a wide range of

77   sustainable chemical transformations under mild reaction conditions[33–38]. However, in support of the

78   findings made by Wass[11], Liauw recently suggested that consumption of ethoxide additive, *via* for-

79   mation of NaOAc by ethyl acetate saponification, is a major reason for low yields of ethanol upgrading

80   to 1-butanol catalyzed by **Ru-2**[39]. Indeed, NaOEt is often used for Guerbet reactions promoting the aldol

81   condensation of acetaldehyde and selective formation of 1-butanol and higher primary alcohols[10,11,13].

82   Thus, we set to study the outcome in the solid-, liquid-, and gas phase of the upgrading reaction of etha-

83   nol containing 20 mol% NaOEt using **Ru-1** to **Ru-5** as catalysts.

84   Corroborating the findings by Wass[11], carrying out the upgrading reaction with 1000 ppm of **Ru-1** for

85   96 h led to merely 3% of 1-butanol. In fact, 12% of unprecedented 2-butanol and 22% of total secondary

86   alcohols (C3-C7) were formed instead (Table 1, Entry 1). This corresponds to a unique 89% selectivity

87   towards secondary alcohols over primary ones. Furthermore, in the gas phase, a mixture of 2-butenes

88   and butane was observed. We speculate that 2-butanol dehydrates to the 2-butenes under these reaction

89   conditions[40,20]. A similar outcome is observed with 830 ppm and 250 ppm of **Ru-1** (Entries 2 and 3, re-

149

90   spectively). Interestingly, increasing the reaction temperature to 130 °C led to lower production of the

91   longer-chain alcohols (Entry 4).

92   Likewise, consistent with Liauw's results[39], with **Ru-2** we found poor coupling of ethanol to 1-butanol.

93   On the contrary, 830 ppm of **Ru-2** catalyzed 2-butanol production with a yield of 8% and an 86% selec-

94   tivity towards secondary alcohols (Entry 5). Lowering the catalyst loading to 420 ppm still allowed for

95   producing 7% and 10% of 2-butanol after 48 and 96 h, respectively (Entries 6 and 7). Further lowering

96   the catalyst loading to 250 ppm even provided 12% of 2-butanol (TON = 480) and 18% of total second-

97   ary alcohols (TON of 720) after 96 h (Entry 8). Longer-chain alcohol production decreased at higher

98   temperature (Entry 9). As expected, the ethanol conversion and 2-butanol formation decreased when

99   using only 83 ppm **Ru-2** (24% conversion and 5% yield, Entry 10). Extending the reaction time to 168 h

100   gave 32% conversion, with 8% 1-butanol yield and with the observation of hexane albeit not quantified

101   (Supplementary Table 17). Further increasing the temperature to 160 ºC did not improve the butane

102   yield (5%) (Supplementary Table 3, Entry 13).

103   Using **Ru-3** (250 ppm) for 96 h resulted in a low ethanol conversion (27%) along with the unselective

104   production of 1-butanol (5% yield) and 5% yield of combined secondary alcohols (Entry 11). The com-

105   plex **Ru-4** seemingly also showed a lack of selectivity affording 5% of 1-butanol and 6% of combined

106   secondary alcohols after 96 h (Entry 12). Interestingly, the complex **Ru-5** showed >99% selectivity to-

107   wards primary alcohols, generating 1-butanol in 13% yield while no 2-butanol and higher secondary

108   alcohols were detected after 96 h under optimized conditions (Entry 13). Besides the main primary al-

109   cohol, 2-ethyl-1-butanol (<1%), and 1-hexanol (1%) were also observed (Supplementary Table 5, Entry

110   3). In fact, when heating to 130 °C, 1-butanol production increased to 18% after 24 h and to 22% after

111   96 h (Entries 14 and 15).

112

113

114 **Table 1 | Homogeneous catalytic ethanol upgrading to secondary alcohols and 2-butenes/butane**
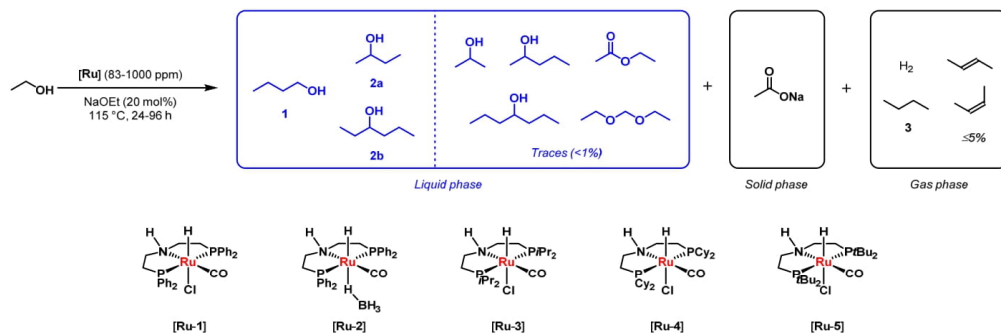
115

116

Entry	Catalyst (ppm)	Time [h]	Conversion [%][a]	Yields from liquid phase [%][a]					
				1° alcohols		2° alcohols			
				1 (TON)	Selectivity [%] (1° vs 2° alcohol)	**2a**	**2b**	Total **2**[b] (TON)	Selectivity [%] (2° vs 1° alcohol)
1	**Ru-1** (1000)	96	57	3 (30)	5 (11)	12	6	22 (220)	39 (89)
2	**Ru-1** (830)	96	61	3 (36)	5 (19)	9	2	13 (157)	21 (81)
3	**Ru-1** (250)	96	57	3 (120)	5 (14)	10	4	17 (680)	30 (86)
4[c]	**Ru-1** (250)	96	60	3 (120)	5 (23)	6	2	10 (400)	17 (77)
5	**Ru-2** (830)	48	38	2 (24)	5 (14)	8	2	12 (145)	32 (86)
6	**Ru-2** (420)	48	42	3 (71)	7 (21)	7	2	11 (262)	26 (79)
7	**Ru-2** (420)	96	50	3 (71)	6 (19)	10	3	15 (357)	26 (81)
8	**Ru-2** (250)	96	55	3 (120)	5 (13)	12	4	18 (720)	33 (87)
9[c]	**Ru-2** (250)	96	68	3 (120)	4 (21)	7	1	10 (400)	15 (79)
10	**Ru-2** (83)	96	24	3 (362)	13 (28)	5	2	8 (964)	33 (72)
11	**Ru-3** (250)	96	27	5 (200)	19 (50)	3	1	5 (200)	19 (50)
12	**Ru-4** (250)	96	26	5 (200)	19 (45)	4	2	6 (240)	23 (55)
13	**Ru-5** (250)	96	42	13 (520)	31 (>99)	<1	<1	<1	<1 (<1)
14[c]	**Ru-5** (250)	24	33	18 (720)	55 (>99)	<1	<1	<1	<1 (<1)
15[c]	**Ru-5** (250)	96	49	22 (880)	45 (96)	1	<1	1 (40)	2 (4)

[a] Only yields from the liquid phase are shown. Determined by NMR (liquid phase products), GC-FID (liquid phase products), and GC-MS (liquid phase products).

[b] Total yield of secondary alcohols (C3-C7).

[c] Reaction at 130 °C.

117

118   The time-dependent conversion of ethanol with 250 ppm of **Ru**-**2** and the production of 2-butanol, com-

119   bined with secondary alcohols is depicted in Fig. 2. The plot displays a steady increase in the formation

120   of secondary alcohols, with 2-butanol as the major product in solution, until it reaches a plateau after

121   approximately 72 h. Likewise, ethanol is steadily converted, and its conversion is at all times higher

122   than the amount of formed liquid-phase products and continues its conversion after 72 h. Apart from the

123   main secondary alcohols produced, small amounts of EtOAc, diethoxymethane, ketones, C5-C7

124   branched alcohols, and C9+ secondary alcohols and even some aromatics were produced. In the gas

125   phase, a trace of methane and/or ethane were also observed, depending on the reaction conditions (Sup-

126   plementary section 10). We speculate that formaldehyde might arise from a retro-aldol reaction of 4-

127   hydroxy-2-butanone, which simultaneously leads to acetone (Fig. 3). Further hydrogenation of acetone

128   leads to the observed 2-propanol. The formation of diethoxymethane might be promoted by an acetali-

129   zation reaction of the formaldehyde with ethanol. Moreover, these observations corroborate the for-

130   mation of carbon compounds in other phases. We therefore also analyzed the solid phase and the gas

131   phase.
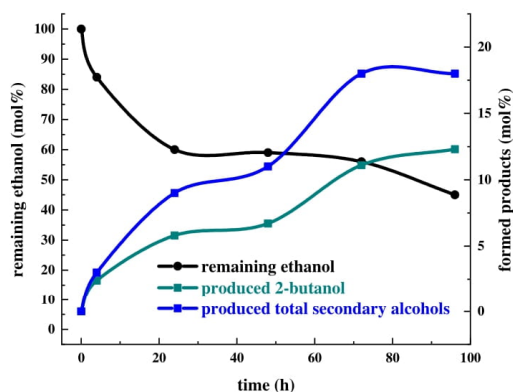
132

133   **Fig. 2 | Ethanol conversion and production of 2-butanol and other secondary alcohols over time.**

134   Reaction conditions: 250 ppm **Ru**-**2** and 20 mol% NaOEt at 115 ºC.

135   Often, NaOAc is observed as a side product in traditional ethanol upgrading[41]. The Cannizzaro or Tish-

136   chenko mechanisms[11] or the dehydrogenative pathway[42] could be responsible for its formation. Indeed,

137   we also detect NaOAc. It precipitates under our reaction conditions, and after 96 h, NaOAc was ob-

138   served with a yield of 11% when using **Ru-2** as a catalyst (Table 2, Entry 3). It is worth mentioning that

139   the formation of NaOAc starts in the early stage of the reaction (Supplementary Table 5, Entry 4), indi-

140   cating that water formation, likely from the Aldol condensation, also occurs rapidly. Moreover, the re-

141   sults in Table 2 suggest a less straightforward relationship between catalyst structure and NaOAc selec-

142   tivity than what was observed for alcohol production.

143   In all the reactions, a drastic pressure increase was observed to 10 bar in the first 30 minutes, which

144   reached a maximum pressure of approximately 30 bar after 24 h (Supplementary Fig. 12). In all the re-

145   actions, a significant amount of H_2 was observed corresponding to around 65 – 95% of the total gas

146   composition. Often, the H_2 yield roughly equals double that of NaOAc (Table 2), suggesting that the

147   formation of NaOAc is the main source of H_2 production. Finally, small amounts of organic products

148   (≤5%) were also detected. Whereas they are mixtures of 2-butenes and butane when the reactions are

149   conducted at 115 °C, only butane is observed at 130 °C, both when using the 2-butanol selective **Ru-1**

150   or the 1-butanol selective **Ru-5** (Entries 2 and 7).

151

152

153

154

155

156

157

158

159 **Table 2 | Homogeneous catalytic ethanol upgrading to secondary alcohols and 2-butenes/butane**

160
161
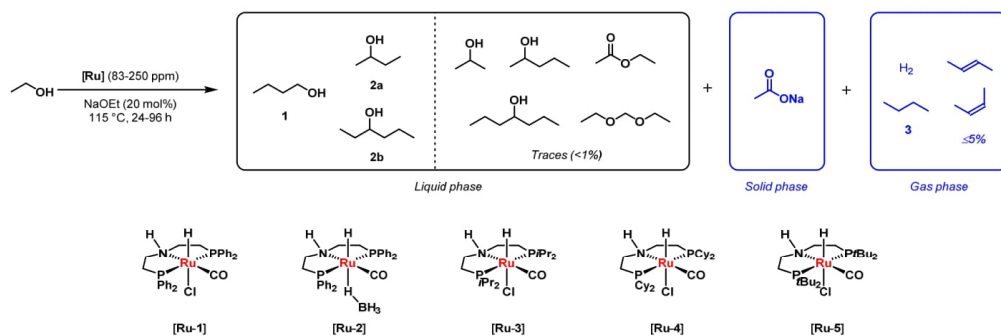
Entry	Catalyst (ppm)	Time [h]	Conversion [%][a]	Yields from solid and gas phases [%][a]				
				Solid phase		Gas phase		
				NaOAc (TON)	Selectivity [%]	H$_2$	3 (TON)	Selectivity [%] (of 3)
1	**Ru-1** (250)	96	57	d	-			-
2[c]	**Ru-2** (250)	96	68	16 (640)	24	26	3 (120)	4
3	**Ru-2** (250)	96	55	11 (440)	20	25		-
4	**Ru-2** (83)	96	24	8 (964)	33	20		-
5	**Ru-3** (250)	96	27	4 (160)	15	18		-
6	**Ru-4** (250)	96	26	9 (360)	35	22		-
7[c]	**Ru-5** (250)	24	33	5 (200)	15	13	2 (80)	6

[a] Only yields from solid and gas phases are shown. Determined by NMR (NaOAc), GC-TCD (H$_2$), GC-MS (organic gases), and Micro-GC (H$_2$ and organic gases).
[b] Total yield of secondary alcohols (C3-C7).
[c] Reaction runs at 130 °C.
[d] Blank refers to not determined.

162

163   We then turned our attention to the reaction mechanism. As Fig. 3 shows, the selectivity between 1° and

164   2° alcohols changes drastically depending on the choice of catalyst. For instance, the catalysts **Ru-1** and

165   **Ru-2** containing less bulky phenyl substituted phosphines afford mainly secondary alcohols, whereas

166   **Ru-3** and **Ru-4** containing semi-bulky *i*-propyl (-*i*Pr) and cyclohexyl (-Cy) *P*-substituents, respectively,

167   provide practically no selectivity. Finally, **Ru-5** containing the bulky *t*-butyl (*-t*Bu) *P*-substituents gives

168   almost exclusively primary alcohols.

169
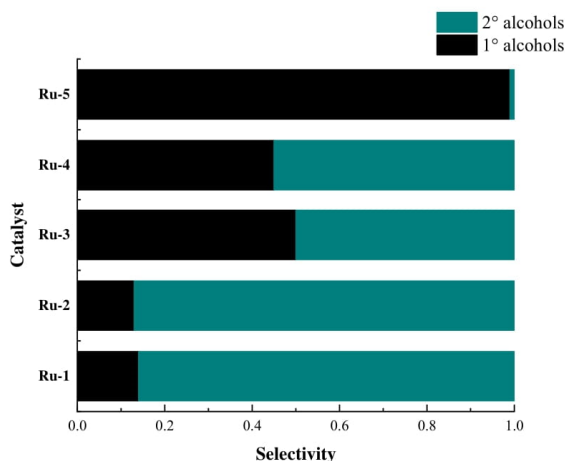
Fig. 3| Distribution of 1° and 2° alcohols using Ru-1 to Ru-5 complexes under optimal conditions in each reaction. Reaction conditions: 250 ppm [**Ru**] and 20 mol% NaOEt at 115 ºC for 96 h.

172

173   As in the typical Guerbet-type ethanol upgrading, our system also relies on generating acetaldol by the

174   Aldol reaction of two acetaldehyde molecules, initially formed by ethanol dehydrogenation (Fig. 4).

175   Typically, acetaldol then proceeds to dehydrate to crotonaldehyde and water followed by hydrogenation

176   to 1-butanol (grey-colored route). However, here we observe a competing reaction that likely involves a

177   dehydrogenation/hydrogenation process to the novel key intermediate 4-hydroxy-2-butanone. This in-

178   termediate then undergoes dehydration to yield methyl vinyl ketone (MVK) and water, and hydrogena-

179   tion of MVK yields 2-butanol. We suggest that the given reaction conditions are, to some extent, capa-

180   ble of inducing dehydration of 2-butanol to 2-butenes, which are then finally hydrogenated to butane.

181   The water is likely responsible for the observation of NaOAc, which also provides the necessary excess

182   of H_2 for hydrogenating the 2-butenes to butane.

155

183 To further validate our hypothesis of 4-hydroxy-2-butanone comprising a novel key intermediate to-

184 wards secondary alcohols and hydrocarbons, some qualitative test reactions were performed with this

185 compound as substrate and **Ru-2** as the catalyst at 115 ºC in the presence of 22 bar of H_2. Using 2.6

186 equivalents of 4-hydroxy-2-butanone to H_2 led to the formation of MVK and a minor amount of

187 2-butanol along with almost complete consumption of H_2 (Supplementary Table 18, Entry 1). There was

188 a large amount of 4-hydroxy-2-butanone remaining, and 2-butanone and acetone were also observed. As

189 a note, several different long-carbon products were observed as well. On the contrary, when

190 4-hydroxy-2-butanone and H_2 are present in lower excess (1.3 equivalent), 2-butanol and 1,3-butanediol

191 were produced as two main products, and trace amounts of butenes/butane were found in the gas phase

192 (Supplementary Table 18, Entry 2). Moreover, there was still H_2 left at the end of the reaction (7 bar

193 pressure). Finally, the addition of 20 mol% NaOAc was also tested while the two substrates were kept in

194 1.3 equivalent of 4-hydroxy-2-butanone (Supplementary Table 18, Entry 3). Acetone, 2-butanone, and

195 2-butanol were produced and almost no H_2 pressure was left while some 4-hydroxy-2-butanone re-

196 mained. These results corroborate the hypothesis that 4-hydroxy-2-butanone is the key intermediate to-

197 wards 2-butanol or butenes/butane.

198
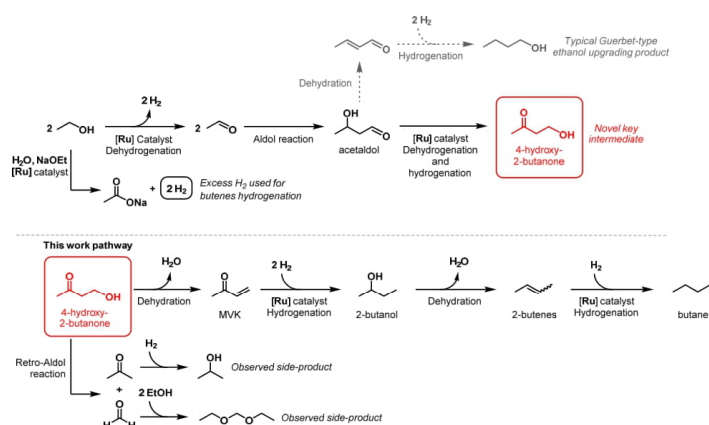
199 **Fig. 4 | Proposed mechanism for the novel transformation of ethanol to 2-butanol, 2-butenes, and**

200 **butane.**

201   In conclusion, we present a previously undisclosed homogeneous catalytic ethanol upgrading pathway

202   to secondary alcohols and hydrocarbons. Using a range of ruthenium pincer catalysts with varying ancil-

203   lary ligand bulkiness, significant differences in the selectivity of the upgrading were achieved, with the

204   less bulky catalyst favouring secondary alcohols and hydrocarbons, and the bulkier catalyst selectively

205   steering the production towards primary alcohols. Hence, we disclose fundamentally new insights into

206   the carbon chain growth of ethanol upgrading, providing a novel pathway leading to highly valuable

207   secondary alcohols and hydrocarbons. We demonstrate that complexes with phenyl substituted phos-

208   phines lead to produce secondary alcohols, low catalyst loading of [(^{Ph}PNP)RuH(HBH$_3$)CO] (250 ppm)

209   with NaOEt (20 mol%) at 115 ºC produced up to 12% of 2-butanol (TON of 480), 4% of 3-hexanol

210   (TON of 160) and a combined 18% of all secondary alcohols (TON of 720). Employing 1000 ppm

211   [(^{Ph}PNP)RuH(Cl)CO] under the same conditions got in total 22% of secondary alcohols. Complex

212   [(^{tBu}PNP)RuH(Cl)CO] primarily follows the traditional Guerbet reaction and produces 22% of 1-butanol

213   already at 115 ºC. This work represents the first example of a homogeneous catalytic system to produce

214   2-butanol as well as higher secondary alcohols and hydrocarbons from ethanol. Finally, a few control

215   experiments support the suggestion of a new mechanism for the selective production of these novel

216   products from ethanol upgrading.

217

218   **Methods**

219   **General procedure for a catalytic reaction**. A 22.8 mL stainless steel container of a high-pressure re-

220   actor (reactor A) or a 16.0 mL Alloy 600 container of a high-pressure reactor (reactor B) provided with a

221   Teflon cup and stirrer was loaded with the catalyst (8.3-1000 ppm) and base (10-25 mol%) inside of a

222   glovebox. The sealed container was removed from the glovebox. Then, degassed EtOH (2.5, 3.5, or 5.0

223   mL) was added with a precise syringe. The reactor was quickly purged three times with N$_2$ before carry-

224   ing out the experiments at the desired temperature (85-130 ºC) for 1-168 h at a stirring rate of 600 rpm.

225   After the reaction time, the reactor was cooled down to room temperature, using an ice bath. The gas

226   was slowly released into a gas sampling bag to analyze the gas phase. The remnant reaction mixture was

227   neutralized with NH_4Cl (equimolar with the added base, 458 mg-1145 mg). Tridecane (100 µL) was

228   added as the internal standard for the quantification of 2-butanol, 1-butanol, 2-propanol, diethox-

229   ymethane, ethyl acetate, 2-pentanol, 3-hexanol, and 4-heptanol. Decane (20 µL) was used as an internal

230   standard for the quantification of ethanol and dimethyl sulfoxide (50 µL) was also added as an internal

231   standard to quantify the amount of sodium acetate. Finally, the resulting solution was diluted with di-

232   chloromethane (10-15 mL) and analyzed by NMR, GC-FID, and GC-MS. The gas phase was analyzed

233   by GC-MS, GC-TCD, and Micro-GC. The remnant solid product was analyzed by ^{1}H and ^{13}C NMR

234   using D_2O as solvent.

235   A control experiment with EtOH and NaO*t*Bu without a catalyst was carried out at 105 ºC for 1 h (Sup-

236   plementary Table 2, Entry 1), and no pressure was detected after this time. The reaction of EtOH with

237   NaO*t*Bu produces NaOEt and *t*BuOH. An additional benchmark reaction of EtOH in presence of **Ru-1**

238   and absence of base was also carried out under similar reaction conditions (Supplementary Table 2, En-

239   try 2). A low pressure (1-2 bar) was observed in the reactor manometer. The control experiment with

240   **Ru-1** (0.05 mol%) and NaO*t*Bu (10 mol%) showed 2-butanol as the main product (Supplementary Table

241   2, Entry 3). If we only use **Ru-2** without base, the reaction liquid product was EtOAc (Supplementary

242   Table 2, Entry 4).

243

249

References

1. Tilman, D., Socolow, R., Foley, J., Hill, J., Larson, E., Lynd, L., Pacala, S., Reilly, J., Searchinger, T., Somerville, C. & Williams, R. Beneficial Biofuels—The Food, Energy, and Environment Trilemma. *Science* **325**, 270-271 (2009).

2. Pasel, J., Häusler, J., Schmitt, D., Valencia, H., Meledina, M., Mayer, J. & Peters, R. Ethanol Dehydrogenation: A Reaction Path Study by Means of Temporal Analysis of Products. *Catalysts* **10**, 1151 (2020).

3. Díaz-Pérez, M. & Serrano-Ruiz, J. Catalytic Production of Jet Fuels from Biomass. *Molecules* **25**, 802 (2020).

4. Naik, S., Goud, V., Rout, P. & Dalai, A. Production of first and second generation biofuels: A comprehensive review. *Renew. Sustain. Energy Rev.* **14**, 578-597 (2010).

5. Veza, I., M. Said, M. & A. Latiff, Z. Improved Performance, Combustion and Emissions of SI Engine Fuelled with Butanol: A Review. *Int. J. Automot. Eng.* **17**, 7648-7666 (2020).

6. Tseng, K., Lin, S., Kampf, J. & Szymczak, N. Upgrading ethanol to 1-butanol with a homogeneous air-stable ruthenium catalyst. *Chem. Commun.* **52**, 2901-2904 (2016).

7. Liu, Q., Xu, G., Wang, X. & Mu, X. Selective upgrading of ethanol with methanol in water for the production of improved biofuel—isobutanol. *Green Chem.* **18**, 2811-2818 (2016).

8. Salvi, B., Subramanian, K. & Panwar, N. Alternative fuels for transportation vehicles: A technical review. *Renew. Sustain. Energy Rev.* **25**, 404–419 (2013).

9. Zuo, C., Hindley, J., Ding, X., Gronnow, M., Xing, W. & Ke, X. Transmission of butanol isomers in pervaporation based on series resistance model. *J. Membr. Sci.* **638**, 119702 (2021).

10. Gabriëls, D., Hernández, W., Sels, B., Van Der Voort, P. & Verberckmoes, A. Review of catalytic systems and thermodynamics for the Guerbet condensation reaction and challenges for biomass valorization. *Catal. Sci. Technol.* **5**, 3876–3902 (2015).

11. Wingad, R., Gates, P., Street, S. & Wass, D. Catalytic Conversion of Ethanol to *n*-Butanol Using

275   Ruthenium P–N Ligand Complexes. *ACS Catal.* **5**, 5822–5826 (2015).

276   12.   Wassenaar, J. & Reek, J. INDOLPhos: novel hybrid phosphine-phosphoramidite ligands for

277   asymmetric hydrogenation and hydroformylation. *Dalt. Trans.* 3750–3753 (2007).

278   13.   Xie, Y., Ben-David, Y., Shimon, L. J. W. & Milstein, D. Highly Efficient Process for Production

279   of Biofuel from Ethanol Catalyzed by Ruthenium Pincer Complexes. *J. Am. Chem. Soc.* **138**,

280   9077–9080 (2016).

281   14.   Mar, M., Andersen, J., Kandasamy, V., Liu, J., Solem, C. & Jensen, P. Synergy at work: linking

282   the metabolism of two lactic acid bacteria to achieve superior production of 2-butanol.

283   *Biotechnol. Biofuels* **13**, 1–10 (2020).

284   15.   Chen, Z., Wu, Y., Huang, J. & Liu, D. Metabolic engineering of Klebsiella pneumoniae for the de

285   novo production of 2-butanol as a potential biofuel. *Bioresour. Technol.* **197**, 260–265 (2015).

286   16.   Sun, D., Li, Y., Yang, C., Su, Y., Yamada, Y. & Sato, S. Production of 1,3-butadiene from

287   biomass-derived C4 alcohols. *Fuel Process. Technol.* **197**, 106193 (2020).

288   17.   Arai, T., Tamura, M., Nakagawa, Y. & Tomishige, K. Synthesis of 2-Butanol by Selective

289   Hydrogenolysis of 1,4-Anhydroerythritol over Molybdenum Oxide-Modified Rhodium-

290   Supported Silica. *ChemSusChem* **9**, 1680–1688 (2016).

291   18.   Burk, J., Pharkya, Priti. & Bugard, P. Mcroorganısmıs For The Productıon Of Methyl Ethyl

292   Ketone And 2-Butanol. (US 2010/0184173 A1). (2010).

293   19.   Pereira, J., Overbeek, W., Gudiño-Reyes, N., Andrés-García, E., Kapteijn, F., van der Wielen, L.

294   & Straathof, A. Integrated Vacuum Stripping and Adsorption for the Efficient Recovery of

295   (Biobased) 2-Butanol. *Ind. Eng. Chem. Res.* **58**, 296–305 (2019).

296   20.   Jeong, S., Kim, H., Bae, J., Kim, D., Peden, C., Park, Y. & Jeon, J. Synthesis of butenes through

297   2-butanol dehydration over mesoporous materials produced from ferrierite. *Catal. Today.* **185**,

298   191–197 (2012).

299   21.   Lopez-Contreras, A., Kuit, W., Siemerink, N., Kengen, S., Springer, J. & Claasen, P. Production

300   of longer-chain alcohols from lignocellulosic biomass: Butanol, isopropanol and 2,3-butanediol.

301   *Bioalcohol Prod.* 415–460 (2010).

302 22. Dürre, P. Biobutanol: An attractive biofuel. *Biotechnol. J.* **2**, 1525–1534 (2007).

303 23. Prabu, K., Prabu, M., Venugopal, A., Venugopalan, A., Sandilya, W., Gopinath, C. & Raja, T.

304   Effective and selective oxidation of 2-butanol over Mn supported catalyst systems. *Appl. Catal. A*

305   *Gen.* **525**, 237–246 (2016).

306 24. Wang, D., Liu, Z. & Liu, Q. Efficient conversion of ethanol to 1-butanol and C5-C9 alcohols

307   over calcium carbide. *RSC Adv.* **9**, 18941–18948 (2019).

308 25. Dagle, V., Winkelman, A., Jaegers, N., Saavedra-Lopez, J., Hu, J., Engelhard, M., Habas, S.,

309   Akhade, S., Kovarik, L., Glezakou, V., Rousseau, R., Wang, Y. & Dagle, R. Single-Step

310   Conversion of Ethanol to *n*-Butene over Ag-ZrO$_2$/SiO$_2$ Catalysts. *ACS Catal.* **10**, 10602–10613

311   (2020).

312 26. Eagan, N., Kumbhalkar, M., Buchanan, J., Dumesic, J. & Huber, G. Chemistries and processes

313   for the conversion of ethanol into middle-distillate fuels. *Nat Rev Chem.* **3**, 223-249 (2019).

314 27. Mascal, M. Chemicals from biobutanol: technologies and markets. *Biofuel Bioprod Biorefin* **6**,

315   483-493 (2012).

316 28. Li, F., Dai, X., Lu, X., Wang, C. & Qi, W. Dehydration of *n*-butanol on phosphate-modified

317   carbon nanotubes: active site and intrinsic catalytic activity. *Catal. Sci. Technol.* **11**, 4500–4508

318   (2021).

319 29. Cordon, M., Zhang, J., Purdy, S., Wegener, E., Unocic, K., Allard, L., Zhou, M., Assary, R.,

320   Miller, J., Krause, T., Lin, F., Wang, H., Kropf, A., Yang, C., Liu, D. & Li, Z. Selective Butene

321   Formation in Direct Ethanol-to-C3+-Olefin Valorization over Zn–Y/Beta and Single-Atom Alloy

322   Composite Catalysts Using In *Situ*-Generated Hydrogen. *ACS Catal.* **11**, 7193–7209 (2021).

323 30. Nolan, D. P. Physical Properties of Hydrocarbons and Petrochemicals. *Handbook of Fire and*

324   *Explosion Protection Engineering Principles for Oil, Gas, Chemical, and Related Facilities* 65–

325   88 (2019).

326   31.   Li, C., Ban, H., Cai, W., Zhang, Y., Li, Z. & Fujimoto, K. Direct synthesis of *iso*-butane from

327   synthesis gas or CO_2 over CuZnZrAl/Pd-β hybrid catalyst. *J. Saudi Chem. Soc.* **21**, 974–982

328   (2017).

329   32.   Kots, P. A., Zabilska, A. V., Grigor'ev, Y. V. & Ivanova, I. I. Ethanol to Butanol Conversion

330   over Bifunctional Zeotype Catalysts Containing Palladium and Zirconium. *Pet. Chem.* **59**, 925–

331   934 (2019).

332   33.   Piccirilli, L., Pinheiro, D. L. J. & Nielsen, M. Recent progress with pincer transition metal

333   catalysts for sustainability. *Catalysts* **10**, 773 (2020).

334   34.   Kuriyama, W., Matsumoto, T., Ogata, O., Ino, Y., Aoki, K., Tanaka, S., Ishida, K., Kobayashi,

335   T., Sayo, N. & Saito, T. Catalytic Hydrogenation of Esters. Development of an Efficient Catalyst

336   and Processes for Synthesising (R)-1,2-Propanediol and 2-(l-Menthoxy)ethanol. *Org. Process*

337   *Res. Dev.* **16**, 166–171 (2012).

338   35.   Sordakis, K., Tang, C., Vogt, L., Junge, H., Dyson, P., Beller, M. & Laurenczy, G. Homogeneous

339   Catalysis for Sustainable Hydrogen Storage in Formic Acid and Alcohols. *Chem. Rev.* **118**, 372–

340   433 (2018).

341   36.   Nielsen, M., Junge, H., Kammer, A. & Beller, M. Towards a green process for bulk-scale

342   synthesis of ethyl acetate: Efficient acceptorless dehydrogenation of ethanol. *Angew. Chem. Int.*

343   *Ed.* **51**, 5711–5713 (2012).

344   37.   Nielsen, M., Alberico, E., Baumann, W., Drexler, H., Junge, H., Gladiali, S. & Beller, M. Low-

345   temperature aqueous-phase methanol dehydrogenation to hydrogen and carbon dioxide. *Nature*

346   **495**, 85–89 (2013).

347   38.   Li, Y., Nielsen, M., Li, B., Dixneuf, P., Junge, H. & Beller, M. Ruthenium-catalyzed hydrogen

348   generation from glycerol and selective synthesis of lactic acid. *Green Chem.* **17**, 193–198 (2015).

349   39.   Ohligschläger, A., Staalduinen, N., Cormann, C., Mühlhans, J., Wurm, J. & Liauw, M. The

350   Guerbet Reaction Network – a Ball-in-a-Maze-Game or: Why Ru-MACHO-BH is Poor in

351   Coupling two Ethanol to *n*-Butanol. *Chemistry—Methods* **1**, 181–191 (2021).

352 40. Kwak, J. H., Rousseau, R., Mei, D., Peden, C. H. F. & Janos Szanyi. The Origin of

353   Regioselectivity in 2-Butanol Dehydration on Solid Acid Catalysts. *ChemCatChem* **3**, 1557–1561

354   (2011).

355 41. O'Lenick, A. J. Guerbet Chemistry. *J. Surfactants Deterg.* **4**, 311–315 (2001).

356 42. Sponholz, P., Mellmann, D., Cordes, C., Alsabeh, P., Li, B., Li, Y., Nielsen, M., Junge, H.,

357   Dixneuf, P. & Beller, M. Efficient and Selective Hydrogen Generation from Bioethanol using

358   Ruthenium Pincer-type Complexes. *ChemSusChem* **7**, 2419–2422 (2014).

359

360

361

362

363

364

365

366

367

368

369

1   **Supporting Information**

2

3   **Low-temperature selective ethanol upgrading to primary or secondary alcohols by**
4   **homogeneous catalysis**

5   Zhenwei Ni, Rosa Padilla, Lucas dos Santos Mello & Martin Nielsen*

6   Technical University of Denmark (DTU), Department of Chemistry, 2800 Kgs. Lyngby, Denmark;
7   marnie@kemi.dtu.dk.

8

9

10   **Table of contents**

11

27

28

29

1

30 **1**. **General information**

31 Neat ethanol (purity 99.99%), NaO*t*Bu (purity 97%), NaOEt (purity 95%), and precatalysts **Ru-1**
32 to **Ru-5** are commercially available and used without further purification. N_2 gas ($H_2O \leqslant 3$ ppm;
33 $O_2 \leqslant 2$ ppm) 1-butene (purity 98%), *cis*-2-butene (purity 99%), and *trans*-2-butene (purity 99%),
34 butane (purity 99.5%), NH_4Cl (purity ≥99.5%), 4-hydroxy-2-butanone (purity 95%), tridecane
35 (100 uL, purity ≥99.0%), decane (purity 99.0%), dimethyl sulfoxide (purity 99.9%),
36 dichloromethane (purity 100%) were purchased from a commercial supplier as well. All chemicals
37 used for calibration curves were analytical standards. All reactions dealing with air or moisture-
38 sensitive compounds were performed using standard Schlenk techniques or in an argon-filled
39 glovebox. ^{1}H NMR and ^{13}C NMR spectra were recorded on a Bruker Avance III 400 MHz
40 spectrometer and were referenced on the deuterated solvent peak.

41 All of the starting materials and dehydrogenation products are literature-known compounds, and
42 the experimental data fit with those reported.

43

44 **Supplementary Table S1 | Properties of gasoline, ethanol, 1-butanol, and 2-butanol**[1]

Properties	gasoline	ethanol	1-butanol	2-butanol
Boiling point	200	78	117	100
Flashpoint	-43	13	34	31
Research octane number (RON)	91 - 99	120 - 135	94 - 96	101
Motor octane number (MON)	81 - 89	100 - 106	78 - 81	91
Energy Density [MJ/L]	32	21	29.2	32
Self-ignition temperature [°C]	247 - 280	365 - 423	343	380 - 406
Explosive limits [%]	1.4 - 7.6	4 - 19	1.4 - 11.2	1.7 - 9.8
Solubility in water [wt%]	Not soluble	Fully miscible	7.7	12.5

45

2

46

Supplementary Figure 1 | Reported catalytic systems for ethanol upgrading to 1-butanol and/or other longer-chain primary alcohols based on the Guerbet reaction[2].

49

50
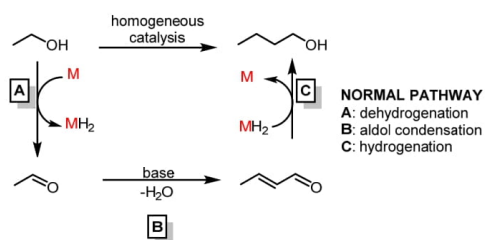
Supplementary Figure 2 | Typical Guerbet reaction sequence for ethanol upgrading.

52

53

3

54 **2**. **Experimental section**

55 **General instrumentation.**

56 NMR (Bruker Avance III 400 MHz spectrometer), GC-MS (Agilent Technologies 6890 Network
57 GC System and Agilent Technologies 7890A Network GC System), GC-FID (Agilent
58 Technologies 6890N Network GC System), GC-TCD (Agilent Technologies 6890N Network GC
59 System), Micro-GC (Agilent Technologies 490 Network GC System).

60 **General information of the two reactors.**

61 Reactor A (stainless steel, inner diameter 25.0 mm, reactor capacity: 22.8 mL; Teflon cup volume:
62 13.0 mL). The pressure record is non-electronic and subject to error.

63 Reactor B (2550 flat gasket microvessel, Alloy 600, 5.0 mL; reactor capacity: 16.0 mL; Teflon
64 cup volume: 6.0 mL). The electronic dashboard records pressure with accurate data.

65

66

67

68 **Supplementary Table 2 | Control experiments and model reaction for the ethanol upgrading**

69
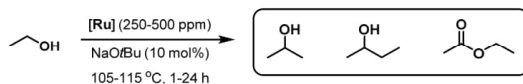
Entry	Catalyst (ppm)	NaOtBu [mol%]	EtOH [mL]	T [ºC]	Time [h]	Conversion [%]	Yield [%][a]			
							2-propanol	2-butanol	EtOAc	H$_2$
1	-	10	2.5	105	1	0	-	-	-	-
2	**Ru-1** (500)	/	2.5	105	1	0	-	-	-	-
3	**Ru-1** (500)	10	5	105	1	3	0.2	0.9	-	-
4	**Ru-2** (250)	/	5	115	24	16	-	-	5.4	1.6

Reaction conditions: 2.5-5.0 mL EtOH, 250-500 ppm catalyst, 10 mol% NaOtBu, 105-115 ºC, 1-24 h, in reactor A
and 600 rpm.

[a] Determined by GC-FID (liquid phase products), GC-MS (liquid phase products), and Micro-GC (H$_2$).

70

71

72

4

73 **3**. **Butenes, butane, and nitrogen calibration curves, and reactor standard curve**

74 Commercially available butenes (*cis*- and *trans*-2-butene) and butane standards were used for the
75 analysis of the gas phase by GC-MS. Gas/air sampling bags were evacuated with the vacuum/N_2
76 before use and different volumes of the standard gases were loaded at 2, 4, 6, 8, 10, 20, and 30 µL,
77 respectively. A calibration curve was performed employing the mentioned gas volumes against the
78 observed area (abundance).

79 The gas volume contained in the headspace of the reactor was determined with a collection of
80 blank tests with the same reaction mixture in the pressure reactor, loading 5.0, 7.5, and 10 bar N_2,
81 respectively. The released gas volume was quantified using the water displacement method.

82 To experimentally determine the composition of the gas produced in the upgrading experiments,
83 a sampling bag was attached to the pressure reactor at 25 °C. The product identification was
84 performed using GC-MS analysis and the above standard curves by direct injection of 20 µL (three
85 times) of the gas mixture using a high-precision syringe (100 µL) and known standards.

86 **4. Scope of the reactions for the ethanol upgrading**

87 Supplementary Tables 3–5 provided the information on all the detected products. Among them,
88 NaOAc was quantified by NMR, liquid products were quantified by GC-FID, organic gases were
89 quantified by GC-MS, and H_2 was quantified by Micro-GC.

5

90 **Supplementary Table 3 | Experiments for the ethanol upgrading with Ru-1**
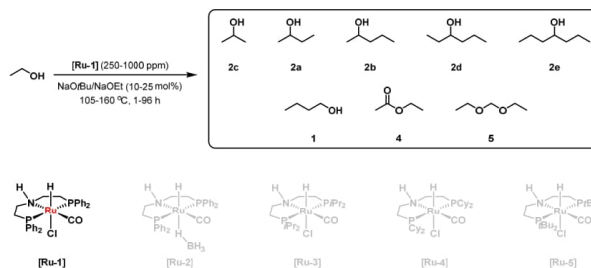
91

Entry	Ru-1 [ppm]	Base (%)	T [°C]	Time [h]	Conversion [(%)ᵃ]	Yield [%]ᵃ										Pressure (bar)ᵉ
						2c	2a	2d	2b	2e	Total 2	1	4	5	H₂	
1	500	NaOrBu (10)	105	1	3	0.2	0.9	0	0	0	1.1	0.3	0.7	0.16	ᵇ	5
2	1000	NaOrBu (20)	115	4	23	1.3	5.3	0.4	1.2	traceᶜ	8.2	1.9	trace	0.25		15
3	1000	NaOrBu (20)	115	19	40	0.8	7.5	0.4	3.0	0.1	11.8	2.7	trace	trace		36
4	1000	NaOrBu (20)	115	48	43	1.6	7.5	0.9	2.6	trace	12.6	1.9	trace	0.09		32
5	1000	NaOrBu (20)	115	72	57	2.3	10.3	1.5	4.6	0.2	18.9	2.4	trace	0.08		21
6	1000	NaOrBu (20)	115	96	57	2.7	11.5	2.0	5.8	0.3	22.3	3.0	trace	0.16		18
7	910	NaOEt (10)	105	72	50	1.0	5.3	0.2	0.6	trace	7.1	1.1	0.2	0.09		12
8	420	NaOEt (20)	105	72	36	1.4	7.5	0.6	2.0	trace	11.5	2.3	trace	trace		18
9	830	NaOEt (20)	105	72	27	0.6	5.4	0.3	1.0	trace	7.3	1.4	trace	0.21		27
10ᵈ	830	NaOEt (20)	115	96	61	1.5	8.6	0.8	2.4	trace	13.3	2.6	trace	trace	21.5	37
11	250	NaOEt (20)	115	96	57	2.0	9.6	1.3	3.6	0.1	16.6	3.0	0.8	trace		12
12	1000	NaOrBu (25)	115	24	53	0.9	5.4	0.7	2.3	trace	9.3	1.6	trace	trace		23
13	250	NaOEt (20)	160	96	60	1.2	5.8	0.7	2.0	trace	9.7	3.0	trace	trace	22.2	34.9 (27.7)

Reaction conditions: 5.0 mL EtOH in reactor A at 105 and 115 °C and 2.5 mL EtOH in reactor B at 160 °C, 250-1000 ppm **Ru-1**, 10-25 mol% base, 1-96 h, 600 rpm.
ᵃ Determined by NMR (NaOAc), GC-TCD (H₂), GC-FID (liquid phase products), GC-MS (liquid phase products, organic gases), and Micro-GC (H₂ and organic gases).
ᵇ Blank entry refers to not determined.
ᶜ Trace refers to yield < 0.1%.
ᵈ Mixture of *trans*, *cis*-2-butene and butane, ≤ 5% in the gas phase.
ᵉ The pressure outside the brackets indicates the reaction pressure before cooling. The pressure in parentheses is after cooling down.

92

93

94

95

96

97

98

6

99 **Supplementary Table 4 | Experiments for the ethanol upgrading with Ru-2.**
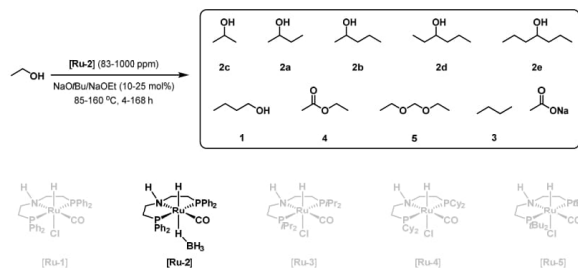
100

Entry	Ru-2 [ppm]	Base (%)	T [°C]	Time [h]	Conv. [%]a	Yield [%]a												Pressure (bar)f
						2c	2a	2d	2b	2e	Total 2	1	4	5	H₂	NaOAc	3	
1	250	NaOEt (20)	115	4	16	trace^b	2.4	0.2	0.5	trace	3.1	1.2	trace	trace	c			18
2d	250	NaOEt (20)	115	24	40	1.2	5.8	0.5	1.5	trace	9	2.1	trace	0.15	15.6			33 (27)
3d	250	NaOEt (20)	115	48	41	1.3	6.7	0.5	1.7	trace	10.2	1.9	trace	0.12	18.7			33 (28)
4d	420	NaOEt (20)	115	48	42	1.3	7.2	0.7	1.8	trace	11	2.5	trace	trace	17.2			31 (26)
5d	420	NaOEt (20)	115	96	50	1.8	9.6	1.0	2.8	trace	15.2	2.7	trace	trace	19.1			33 (27)
6d	830	NaOEt (20)	115	48	38	1.3	7.7	0.7	2.2	trace	11.9	2.3	trace	trace	14.9			31 (26)
7	250	NaOEt (20)	115	72	44	2.0	11.1	1.3	4.2	0.1	18.7	2.8	trace	trace				15
8d	250	NaOEt (20)	115	96	55	0.6	12.3	1.4	3.9	trace	18.2	2.5	trace	trace	25.1	10.6		41 (35)
9	270	NaOEt (10)	115	72	28	1.2	8.0	0.4	1.1	trace	10.7	1.8	trace	trace				16
10	250	NaOEt (20)	85	72	29	0.4	2.0	0.1	0.2	trace	2.7	0.8	trace	trace				9
11d	83	NaOEt (20)	115	96	24	0.9	4.6	0.4	1.6	trace	7.5	3.1	trace	trace	20.1	8.4		37 (30)
12	500	NaOrBu (10)	105	48	22	1.1	5.8	0.2	0.5	trace	7.6	0.9	0.2	0.13				11
13	500	NaOrBu (20)	115	4	26	0.6	4.6	0.3	0.8	trace	6.3	1.3	trace	0.26				16
14	500	NaOrBu (20)	105	96	37	1.5	8.5	0.9	2.9	trace	13.8	2.0	trace	0.19				30
15	1000	NaOrBu (20)	115	48	50	1.7	8.0	1.1	3.4	0.1	14.3	2.3	trace	0.10				23
16	1000	NaOrBu (25)	105	18	59	1.2	5.4	0.7	2.7	0.1	10.1	2.1	trace	0.19				16
17	1000	NaOrBu (25)	105	48	66	0.9	5.7	1.0	4.1	0.3	12	2.1	trace	0.11				20
18d,e	250	NaOEt (20)	115	96	73	1.9	9.7	0.9	2.8	trace	15.3	3.2	trace	trace	15.2			26 (21)
19	250	NaOEt (20)	160	96	86	0.9	4.1	0.8	2.3	trace	8.1	4.1	trace	trace	31.1		4.7	37.4 (28.7)
20	250	NaOEt (20)	130	96	68	1.4	7.1	0.3	1.2	trace	10.0	2.6	trace	trace	26.0	15.9	2.7	35.9 (29.4)
21	8.3	NaOEt (20)	130	168	32	0.3	0.8	0.2	0.4	trace	1.7	7.8	trace	trace	11.5	4.6		20.1 (15.7)

Reaction conditions: 5 mL EtOH in a reactor A at 85, 105, 115 °C and 2.5 mL EtOH in reactor B at 130 and 160 °C, 83-1000 ppm **Ru-2**, 10-25 mol% base, 4-168 h, 600 rpm.
a Determined by NMR (NaOAc), GC-TCD (H₂), GC-FID (liquid phase products), GC-MS (liquid phase products, organic gases), and Micro-GC (H₂ and organic gases).
b Trace refers to yield < 0.1%.
c Blank entry refers to not determined.
d Mixture of *trans*, *cis*-2-butene and butane, ≤ 5% in the gas phase.
e 3.5 mL ethanol.
f The pressure outside the brackets indicates the reaction pressure before cooling. The pressure in parentheses is after cooling down.

7

101 **Supplementary Table 5 | Experiments for ethanol conversion with Ru-3 - Ru-5.**
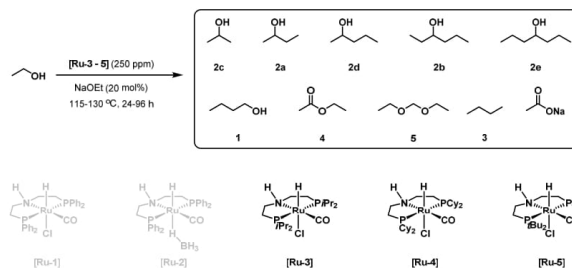
102

Entry	Catalyst (250 ppm)	T [°C]	t [h]	Conv. [%][a]	Yield [%][a]												Pressure (bar)[g]
					2c	2a	2d	2b	2e	Total 2	1	4	5	H$_2$	NaOAc	3	
1	**Ru-3**	115	96	27	0.6	3.0	0.3	1.0	trace[b]	4.9	5.2	trace	trace	17.5	4.0	[c]	31 (26)
2	**Ru-4**	115	96	26	0.7	3.8	0.4	1.5	trace	6.4	5.3	trace	trace	22.3	8.9		37 (30)
3[d]	**Ru-5**	115	96	42	trace	trace	trace	trace	trace	trace	12.9	trace	trace	12.8			24 (20)
4[e]	**Ru-5**	130	24	33	trace	0.9	trace	trace	trace	0.9	17.6	trace	trace	12.5	5.2	2.4	17.4 (14.3)
5[f]	**Ru-5**	130	96	49	trace	1.0	trace	trace	trace	1	22.1	trace	trace	20.4			27.4 (21.5)

Reaction conditions: 5 mL EtOH in reactor A at 115 °C and 2.5 mL EtOH in reactor B at 130 °C, 250 ppm catalyst, 20 mol% NaOEt, 24-96 h, 600 rpm.
[a] Determined by NMR (NaOAc), GC-TCD (H$_2$), GC-FID (liquid phase products), GC-MS (liquid phase products, organic gases), and Micro-GC (H$_2$ and organic gases).
[c] Blank entry refers to not determined.
[b] Trace refers to yield < 0.1%.
[d] 0.4 % of 2-ethyl-1-butanol and 0.9 % of 1-hexanol were also determined.
[e] 0.6 % of 2-ethyl-1-butanol and 2.2 % of 1-hexanol were also determined.
[f] 0.9 % of 2-ethyl-1-butanol and 3.0 % of 1-hexanol were also determined.
[g] The pressure outside the brackets indicates the reaction pressure before cooling. The pressure in parentheses is after cooling down.

103

8

104   **5. Reaction pathways of each product**

105

106   **Supplementary Figure 3 | Reaction pathways of liquid- gas- and solid products.**

107

108

109

110

9

111   **6. GC-TCD reports of inorganic gas**

112   a) Example: Supplementary Table 4, Entry 12.

113   Reaction conditions: 5.0 mL EtOH, **Ru**-**2** (500 ppm, 25.1 mg), 48 h, 105 ºC, NaO*t*Bu (10 mol%,
114   823 mg) in reactor A and 600 rpm.
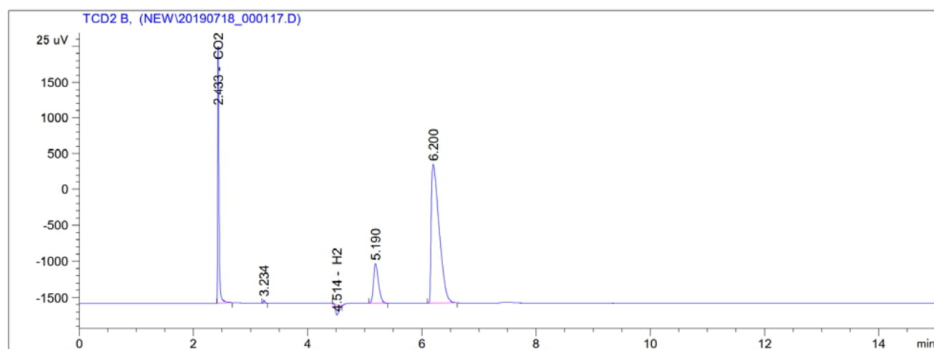
116   **Supplementary Table 6 | Information of products from GC-TCD**[a]

Retention time	Compound
2.433	CO_2
4.514	H_2
5.190	O_2
6.200	N_2

117   [a] GC-TCD is responsible for qualitative studies only, and the area is not positively correlated with
118   the concentration.

119

120

121

122

123

124

125

126

127

128

129

130 b) Reaction conditions: 5.0 mL EtOH, **Ru-4** (250 ppm, 16.2 mg), 41 h, 115 ºC, NaOEt (20 mol%,
131 1166 mg) in reactor A and 600 rpm.

132
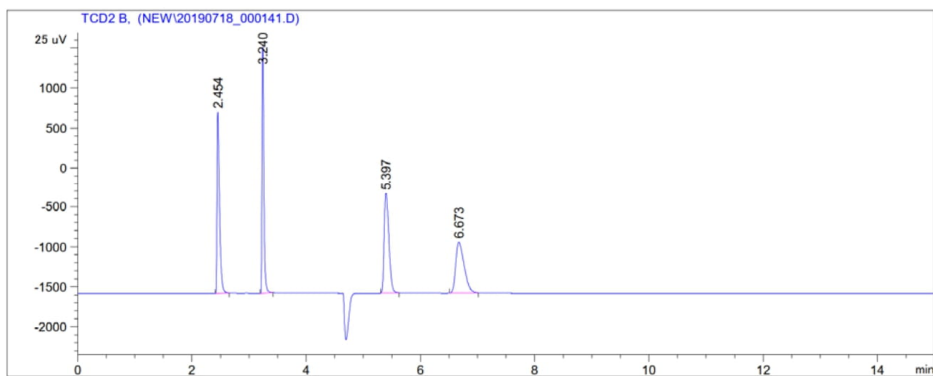
133 **Supplementary Table 7 | Information of products from GC-TCD[a]**

Retention time	Compound
2.454	CO_2
4.747	H_2
5.397	O_2
6.673	N_2

134 [a] GC-TCD is responsible for qualitative studies only, and the area is not positively correlated with
135 the concentration.

136

137

138

139

140

141

142

143

144

145

146

147

11

148   c) Reaction conditions: 5.0 mL EtOH, **Ru-5** (250 ppm, 13.5 mg), 41 h, 115 ºC, NaOEt (20 mol%,
149   1166 mg) in reactor A and 600 rpm.
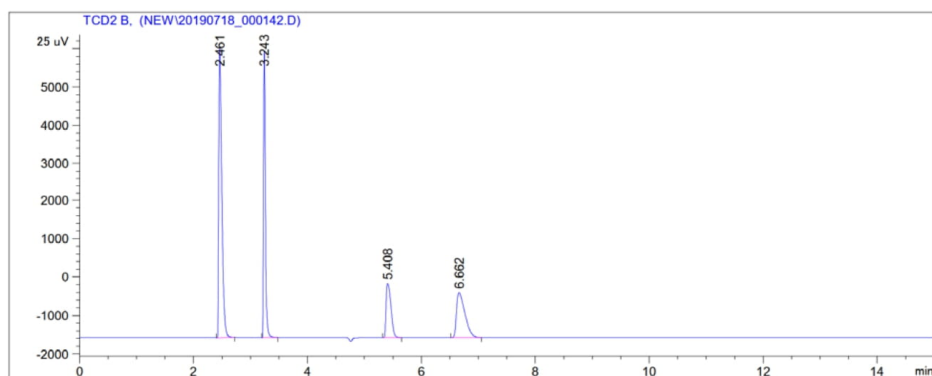
151   **Supplementary Table 8 | Information of products from GC-TCD**[a]

Retention time	Compound
2.461	CO_2
4.747	H_2
5.408	O_2
6.662	N_2

152   [a] GC-TCD is responsible for qualitative studies only, and the area is not positively correlated with the
153   concentration.

154

155

156

157

158

159

160

161

162

163

164

165

166

12

167 **7. GC-FID reports of liquid products**

168 a) Example: Supplementary Table 3, Entry 10.

169 Reaction conditions: 5.0 mL EtOH, **Ru-1** (830 ppm, 51.8 mg), 96 h, 115 ºC, NaOEt (20 mol%,
170 1166 mg) in reactor A and 600 rpm.

171
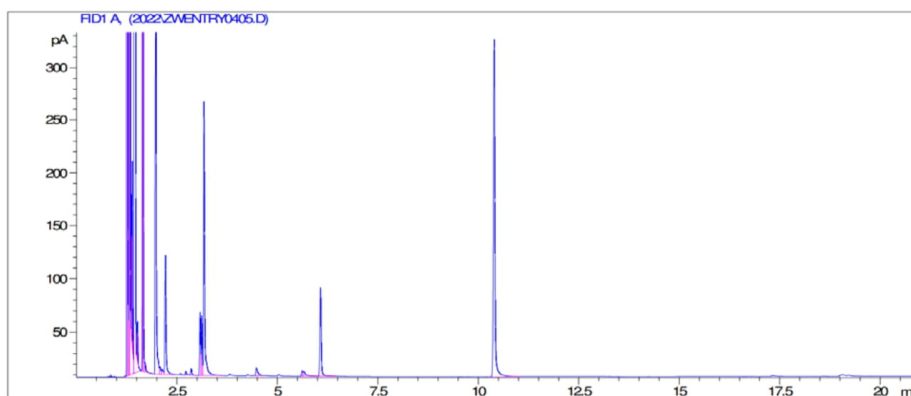
172 **Supplementary Table 9 | Information of products from GC-FID**

Retention time	Compound	Area	Area [%]	Conversion / Yield [%]ᵃ
1.335	ethanol	8293.04492	6.14711	61
1.393	2-propanol	168.33704	0.12478	1.5
1.434	dichloromethane	10174.5	75.41698	/
1.647	ethyl acetate	964.02954	0.71457	trace
1.662	2-butanol	1569.88892	1.16366	8.6
1.980	1-butanol	869.32996	0.64438	2.6
2.077	diethoxymethane	16.39939	0.01216	trace
2.217	2-pentanol	227.67053	0.16876	0.8
3.174	3-hexanol	515.06836	0.38179	2.4
6. 072	decane	197.88586	0.14668	/
10.394	tridecane	866.97992	0.64264	/

173 ᵃ mol% conversion and yield.

174

175

176

177

178

179

180

13

181   b) Example: Supplementary Table 4, Entry 8.

182   Reaction conditions: 5.0 mL EtOH, **Ru-2** (250 ppm, 15.1 mg), 96 h, 115 °C, NaOEt (20 mol%,
183   1166 mg) in reactor A and 600 rpm.

184
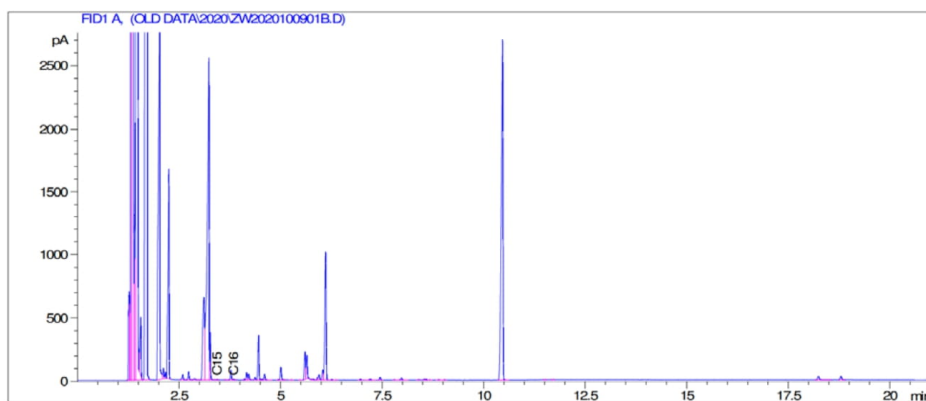
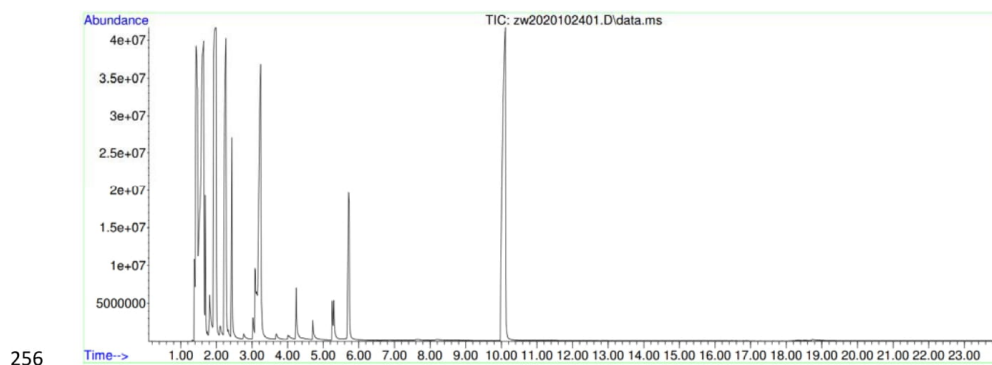185   **Supplementary Table 10 | Information of products from GC-FID**

Retention time	Compound	Area	Area [%]	Conversion / Yield [%][a]
1.381	ethanol	90797.9	30.86938	55
1.424	2-propanol	2897.57007	0.98511	0.6
1.438	dichloromethane	98131.8	33.36273	/
1.718	2-butanol	29429.3	10.00533	12.3
2.029	1-butanol	8425.74414	2.86458	2.5
2.118	diethoxymethane	134.34705	0.04568	trace
2.252	2-pentanol	3115.85864	1.05933	1.4
3.234	3-hexanol	8092.85254	2.75140	3.9
4.455	4-heptanol	660.98340	0.22472	trace
6.105	decane	2189.15063	0.74427	/
10.463	tridecane	7827.92480	2.66133	/

186   [a] mol% conversion and yield.

187

188

189

190

191

192

193

194

14

195   c) Example: Supplementary Table 5, Entry 1.

196   Reaction conditions: 5 mL EtOH, **Ru-3** (250 ppm, 12.1 mg), 96 h, 115 ºC, NaOEt (20 mol%, 583
197   mg) in reactor A and 600 rpm.

198
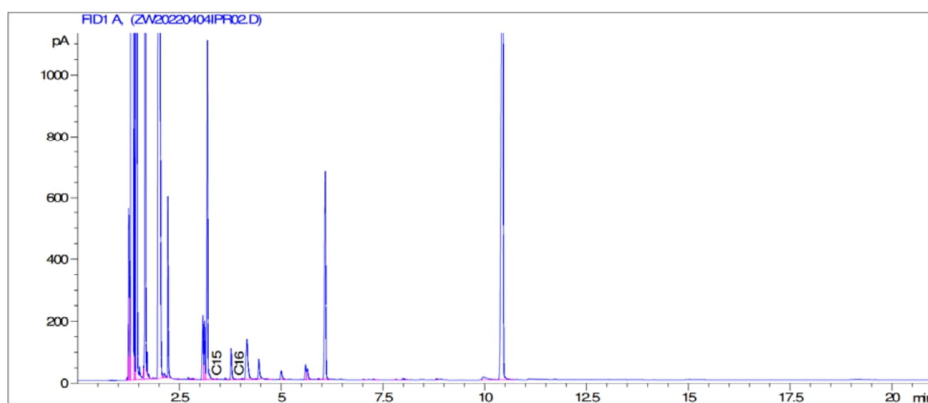
199   **Supplementary Table 11 | Information of products from GC-FID**

Retention time	Compound	Area	Area [%]	Conversion / Yield [%][a]
1.369	ethanol	109729.5	47.35016	27
1.404	2-propanol	724.32721	0.31256	0.6
1.433	dichloromethane	86245.6	37.21646	/
1.623	ethyl acetate	8.94422	0.00386	trace
1.670	2-butanol	6602.84082	2.84924	3.0
2.027	1-butanol	14326.2	6.18201	5.2
2.098	diethoxymethane	8.79898	0.00380	trace
2.221	2-pentanol	617.71112	0.26655	0.3
3.186	3-hexanol	1816.89905	0.78402	1.0
4.448	4-heptanol	138.97281	0.05997	trace
6.079	decane	1456.10242	0.62833	/
10.437	tridecane	7004.85645	3.02272	/

200   [a] mol% conversion and yield.

201

202

203

204

205

206

207

15

208   d) Example: Supplementary Table 5, Entry 2.

209   Reaction conditions: 5 mL EtOH, **Ru**-**4** (250 ppm, 16.2 mg), 96 h, 115 ºC, NaOEt (20 mol%, 583
210   mg) in reactor A and 600 rpm.
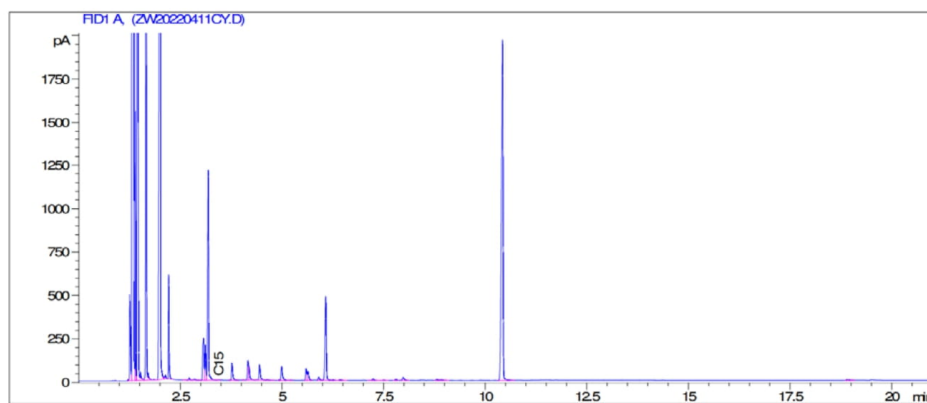
211

212   **Supplementary Table 12 | Information of products from GC-FID**

Retention time	Compound	Area	Area [%]	Conversion / Yield [%][a]
1.359	ethanol	84510.3	38.87546	26
1.400	2-propanol	741.91418	0.34129	0.7
1.434	dichloromethane	101392.7	46.64151	/
1.665	2-butanol	6692.29688	3.07851	3.8
2.016	1-butanol	11309.6	5.20252	6.4
2.092	diethoxymethane	19.78473	0.00910	trace
2.215	2-pentanol	666.55798	0.30662	0.4
3.184	3-hexanol	2086.07300	0.95961	1.5
4.444	4-heptanol	208.58214	0.09595	trace
6.072	decane	1088.52576	0.50073	/
10.423	tridecane	5422.88037	2.49457	/

213   [a] mol% conversion and yield.

214

215

216

217

218

219

220

221

16

222   e) Example: Supplementary Table 5, Entry 5.

223   Reaction conditions: 2.5 mL EtOH, **Ru-5** (250 ppm, 6.8 mg), 96 h, 130 ºC, NaOEt (20 mol%, 583
224   mg) in reactor B and 600 rpm.

225
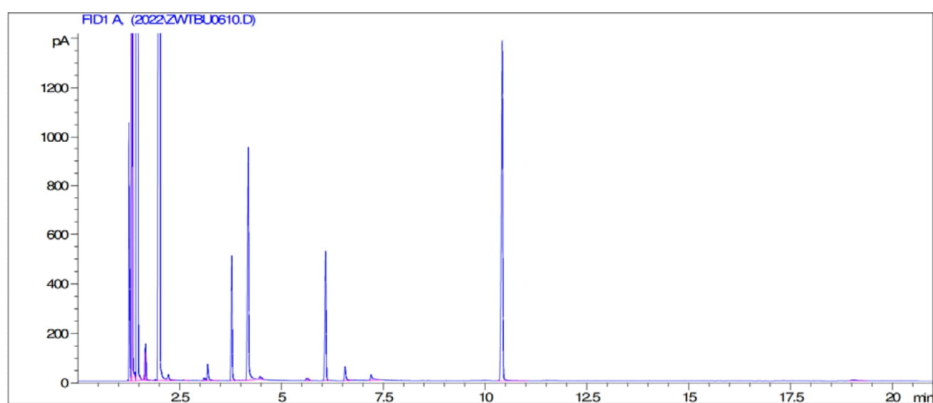
226   **Supplementary Table 13 | Information of products from GC-FID**

Retention time	Compound	Area	Area [%]	Conversion / Yield [%][a]
1.317	ethanol	12013.5	6.10001	49
1.433	dichloromethane	14745.9	74.87437	/
1.666	2-butanol	207.80112	0.10551	1.0
2.024	1-butanol	14908.8	7.57001	22.1
3.776	2-ethyl-1-butanol	900.70880	0.45735	0.9
4.184	1-hexanol	2093.11304	1.06280	3.0
6.558	decane	144.53439	0.07339	/
10.418	tridecane	3444.03467	1.74875	/

227   [a] mol% conversion and yield.

228

229

230

231

232

233

234

235

236

237

17

180

238   **8. GC-MS (liquid phase) reports of products**

239   a) Example: Supplementary Table 3, Entry 6.

240   Reaction conditions: 5.0 mL EtOH, **Ru-1** (1000 ppm, 52 mg), 96 h, 115 ºC, NaO*t*Bu (20 mol%,
241   1646 mg) in reactor A and 600 rpm.

242
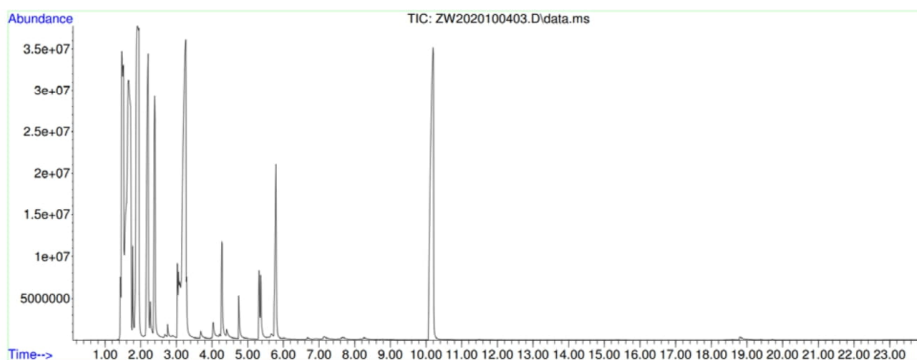
243   **Supplementary Table 14 | Information of products from GC-MS**

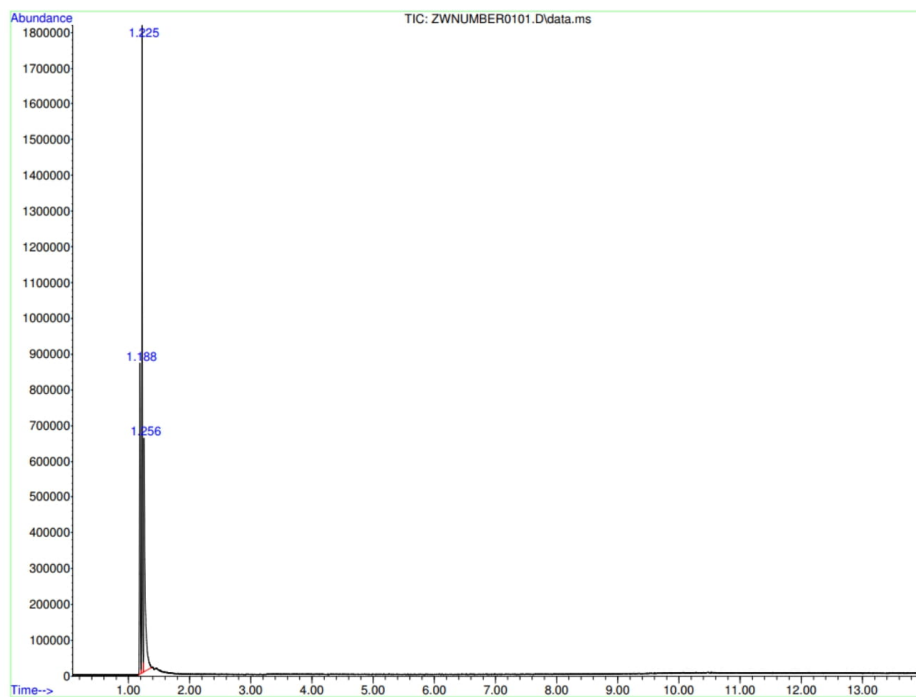| Retention time	Compound	Corr.area	Corr. % max.	% of total (mol%)	Conversion / Yield [%]ᵃ
1.480	ethanol	863227873	32.50	5.693	57
1.513	ethanol	635973656	23.94	4.195	57
1.663	dichloromethane	2656087416	100	17.518	/
1.917	2-butanol	2227223903	83.85	14.690	11.5
2.205	1-butanol	1123128824	42.29	7.408	3.0
2.397	2-pentanol	781939039	29.44	5.157	2.0
3.260	3-hexanol	2266166719	85.32	14.946	5.8
4.282	4-heptanol	304316668	11.46	2.007	0.3
5.795	decane	581154003	21.88	3.833	/
10.199	tridecane	2103928204	79.21	13.876	/

244   ᵃ mol% conversion and yield.

245

246

247

248

249

250

251

252

18

181

253   b) Example: Supplementary Table 4, Entry 8.

254   Reaction conditions: 5.0 mL EtOH, **Ru-2** (250 ppm, 15.1 mg), 96 h, 115 °C, NaOEt (20 mol%,
255   1166 mg) in reactor A and 600 rpm.

256

257   **Supplementary Table 15 | Information of products from GC-MS**

Retention time	Compound	Corr.area	Corr. % max.	% of total (mol%)	Conversion / Yield [%][a]
1.447	ethanol	2026304360	100.00	23.464	55
1.582	dichloromethane	1086549541	53.62	12.582	/
1.846	2-butanol	1196213678	59.03	13.852	12.3
2.139	1-butanol	1128952416	55.71	13.073	2.5
2.319	2-pentanol	244070235	12.05	2.826	1.4
3.121	3-hexanol	694041934	34.25	8.037	3.9
4.191	4-heptanol	110495747	5.45	1.280	trace
5.703	decane	437082455	21.57	5.061	/
10.057	tridecane	1298317982	64.07	15.034	/

258   [a] mol% conversion and yield.

19

259
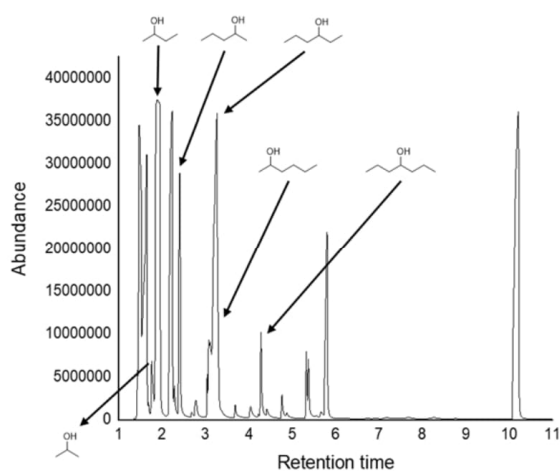
Supplementary Figure 4 | **A typical MS spectrum of a reaction mixture**. (Supplementary Table
4, Entry 8.)

262

263

OH

MW 60.1 g/mol

264
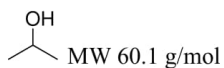
Supplementary Figure 4.1 | **A MS spectrum of 2-propanol**. (Supplementary Table 4, Entry 8.)

266

267

268

269

270

271

20

OH

MW 74.12 g/mol

272

273
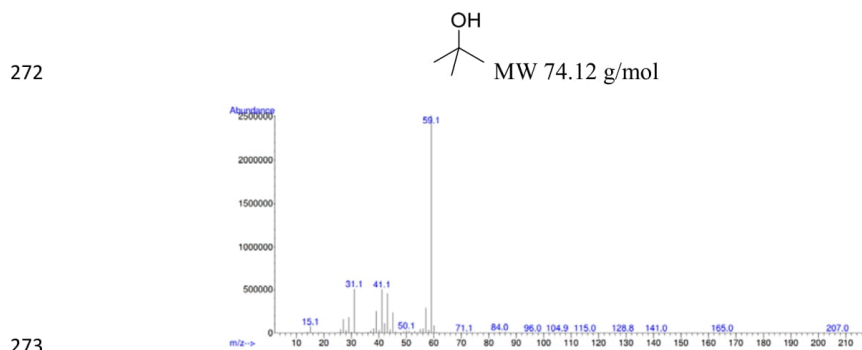
274 **Supplementary Figure 4.2 | A MS spectrum of *tert*-butanol**. (Supplementary Table 4, Entry
275 8.)

276

277 OH MW 60.0952 g/mol

278
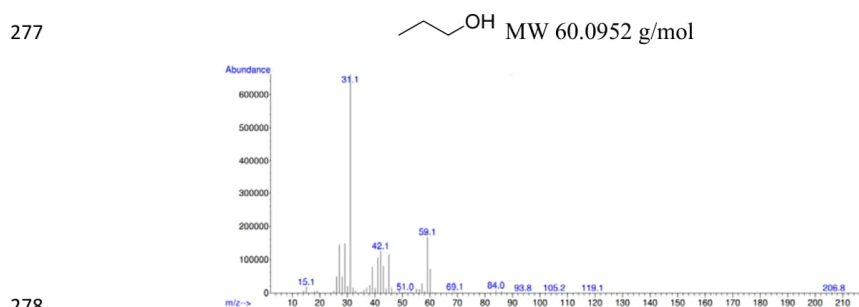
279 **Supplementary Figure 4.3 | A MS spectrum of 1-propanol**. (Supplementary Table 4, Entry 8.)

280

O

281 MW 72.11 g/mol

282
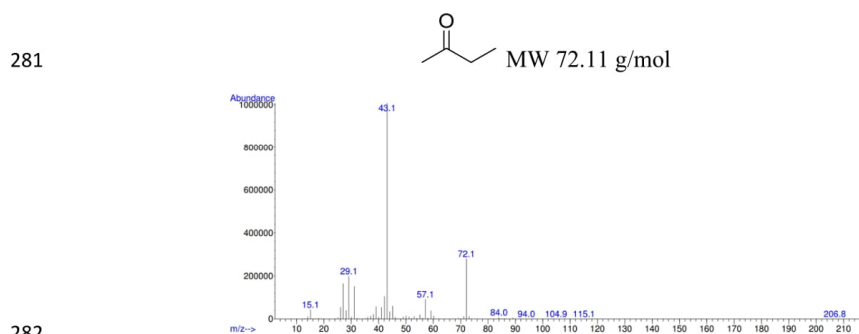
283 **Supplementary Figure 4.4 | A MS spectrum of 2-butanone**. (Supplementary Table 4, Entry 8.)

21

OH

MW 74.122 g/mol
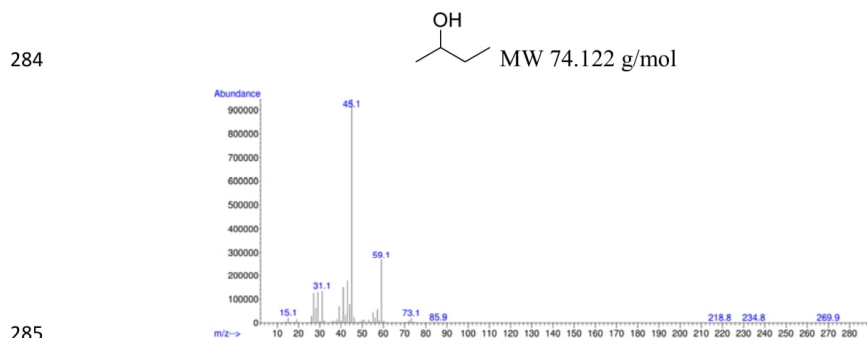
Supplementary Figure 4.5 | A MS spectrum of 2-butanol. (Supplementary Table 4, Entry 8.)

MW 88.11 g/mol
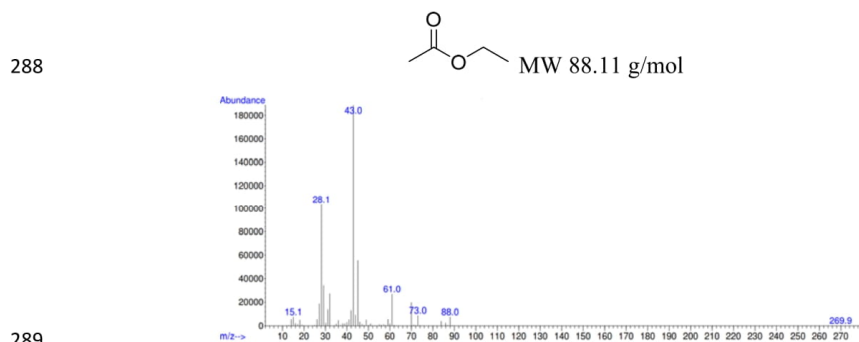
Supplementary Figure 4.6 | A MS spectrum of ethyl acetate. (Supplementary Table 4, Entry 8.)

OH MW 74.121 g/mol

Supplementary Figure 4.7 | A MS spectrum of 1-butanol. (Supplementary Table 4, Entry 8.)

22

296   MW 104.15 g/mol

297
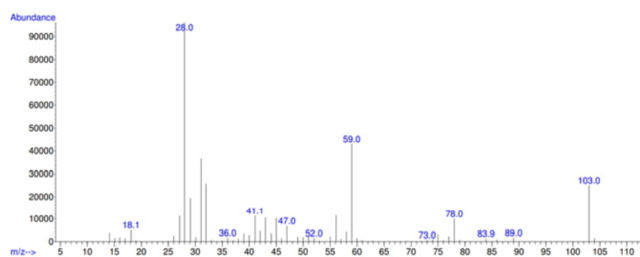
Supplementary Figure 4.8 | A MS spectrum of diethoxymethane. (Supplementary Table 4, Entry 8.)

300

301   MW 88.148 g/mol

302
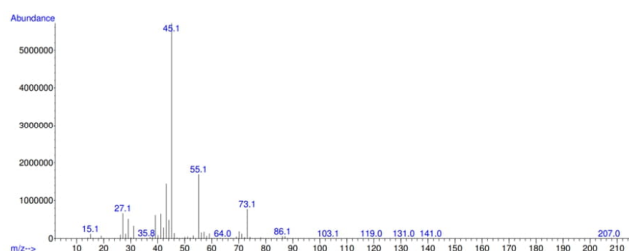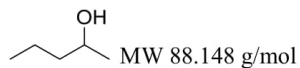
Supplementary Figure 4.9 | A MS spectrum of 2-pentanol. (Supplementary Table 4, Entry 8.)

304

305   MW 100.1589 g/mol

306
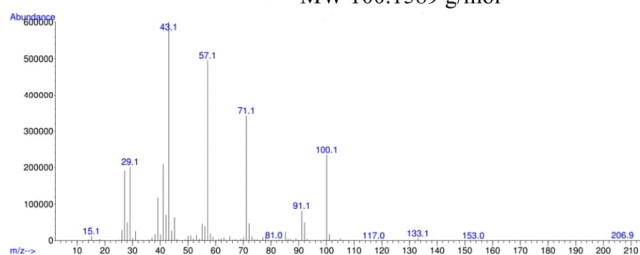
Supplementary Figure 4.10 | A MS spectrum of 3-hexanone. (Supplementary Table 4, Entry 8.)

23

309

OH

MW 102.174 g/mol

310
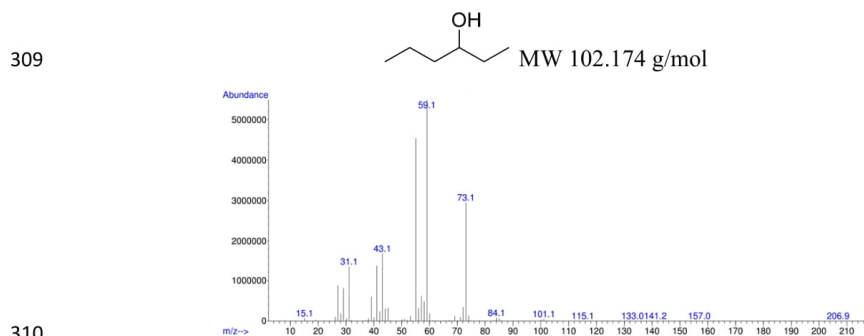
311   **Supplementary Figure 4.11 | A MS spectrum of 3-hexanol**. (Supplementary Table 4, Entry 8.)

312

313

OH

MW 116.2 g/mol

314
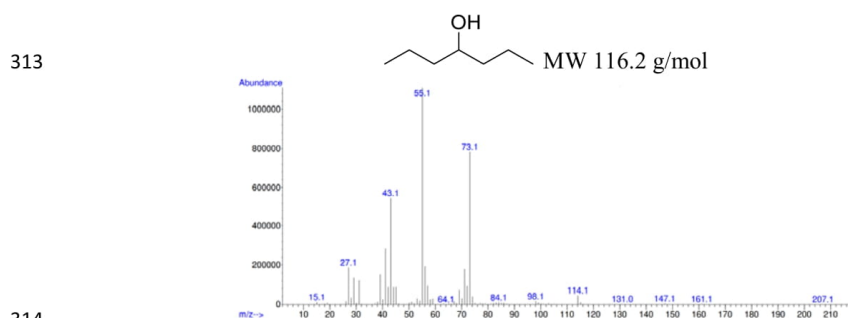
315   **Supplementary Figure 4.12 | A MS spectrum of 4-heptanol**. (Supplementary Table 4, Entry
316   8.)

317

318

319

320

321

322

323

324

325

24

9. GC-MS (gas phase) reports of products

a) Example: Supplementary Table 4, Entry 20.

Reaction conditions: 2.5 mL EtOH, **Ru-2** (250 ppm, 7.6 mg), 96 h, 130 °C, NaOEt (20 mol%, 583 mg) in reactor B and 600 rpm.

Supplementary Table 16 | Information of products from GC-MS

Retention time	Compound	Corr.area	Corr. % max.	% of total	Yield [%][a]
1.188	N_2	7614491	61.75	25.817	/
1.225	butane	12331117	100.00	41.809	2.7
1.256	ethanol	9548633	77.44	32.375	/

[a] mol% yield.

337   MW 56.11 g/mol

338
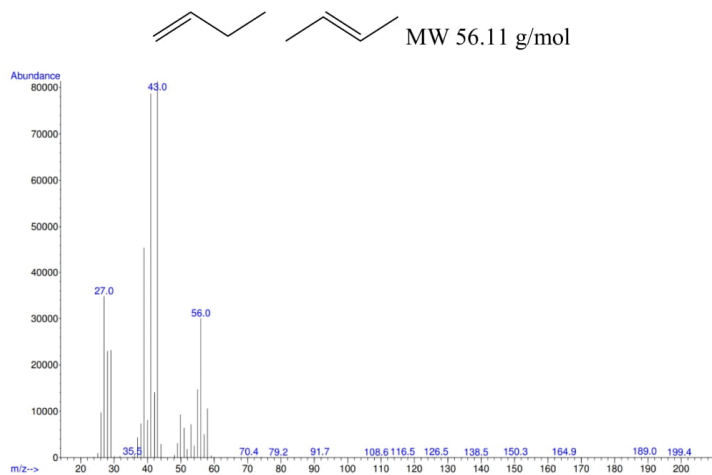
339   **Supplementary Figure 5** | **A MS spectrum of 2-butenes**. (Supplementary Table 4, Entry 8.)

340

341   MW 58.12 g/mol

342
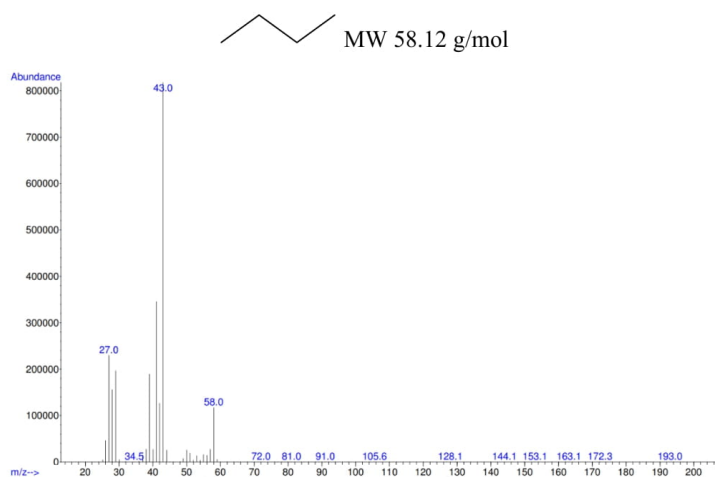
343   **Supplementary Figure 6** | **A MS spectrum of butane**. (Supplementary Table 4, Entry 20.)

344

345

346

347

26

348   b) Example: Supplementary Table 4, Entry 21.

349   Reaction conditions: 2.5 mL EtOH, **Ru-2** (8.3 ppm, 0.0025 mg), 168 h, 130 ºC, NaOEt (20 mol%,
350   583 mg) in reactor B and 600 rpm.
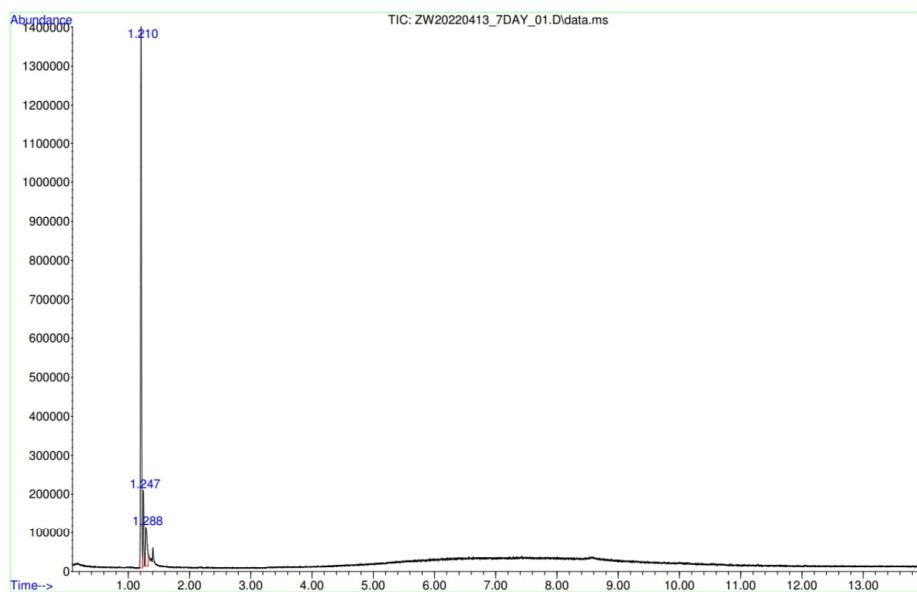
351

352   **Supplementary Table 17 | Information of products from GC-MS**

Retention time	Compound	Corr.area	Corr. % max.	% of total
1.210	N_2	1514805	100.00	80.205
1.247	hexane (partially stays in the gas phase)	174901	11.55	9.261
1.288	ethanol	198958	13.13	10.534

353

354

355

356

357

358

359

360

361

362 MW: 86.18 g/mol

363
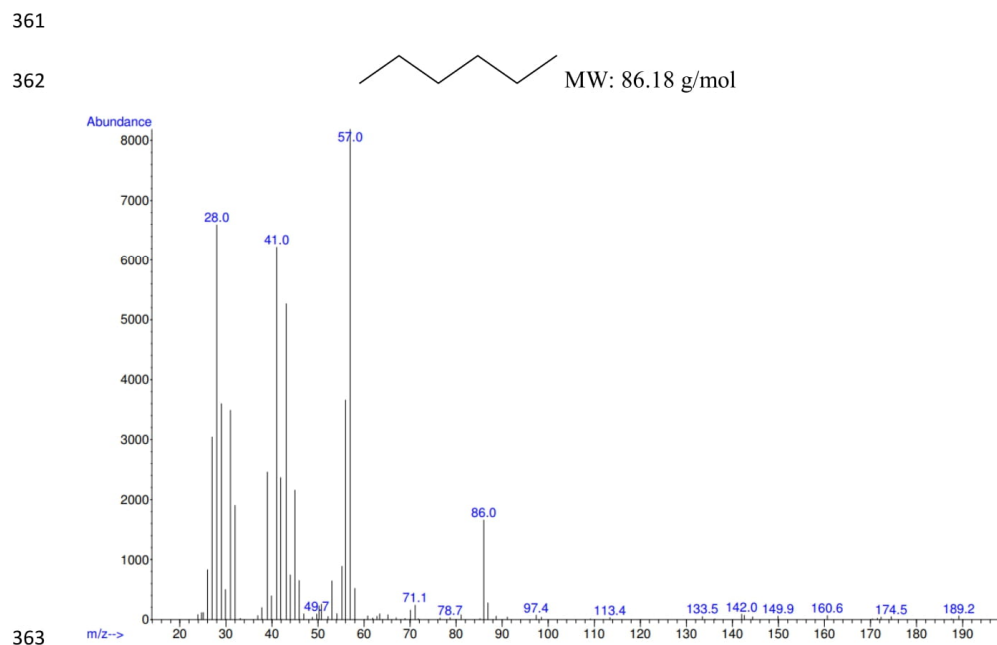
Supplementary Figure 7 | A MS spectrum of hexane. (Supplementary Table 4, Entry 21.)

365

366

367

368

369

370

371

372

373

374

375

376

377

28

378 **10. Micro-GC reports of inorganic and organic gas**

379 Example: Supplementary Table 4, Entry 2.

380 Reaction conditions: 5.0 mL EtOH, **Ru-2** (250 ppm, 15.1 mg), 24 h, 115 °C, NaOEt (20 mol%,
381 1166 mg) in reactor A and 600 rpm.

382

29
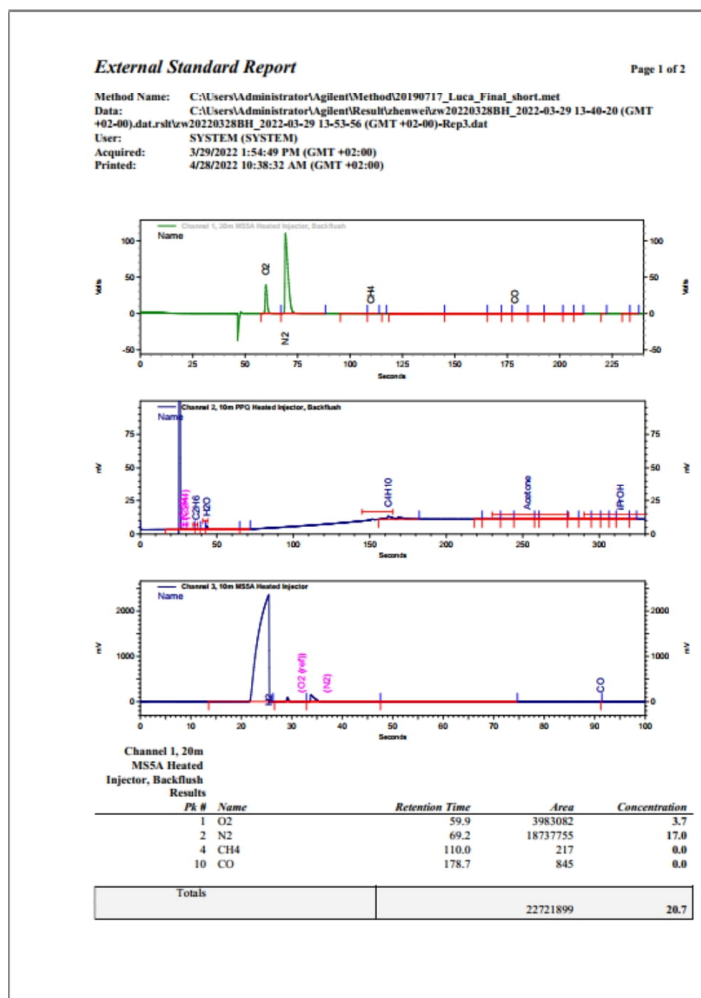
192

External Standard Report   Page 2 of 2

Method Name: C:\Users\Administrator\Agilent\Method\20190717_Luca_Final_short.met
Data: C:\Users\Administrator\Agilent\Result\zhenwei\zw20220328BH_2022-03-29 13-40-20 (GMT
+02-00).dat.rslt\zw20220328BH_2022-03-29 13-53-56 (GMT +02-00)-Rep3.dat
User: SYSTEM (SYSTEM)
Acquired: 3/29/2022 1:54:49 PM (GMT +02:00)
Printed: 4/28/2022 10:38:32 AM (GMT +02:00)

Channel 2, 10m
PPQ Heated
Injector, Backflush
Results

Pk #	Name	Retention Time	Area	Concentration
	CO2			0.0 BDL
	C2H4			0.0 BDL
2	C2H6	36.6	36833	0.0
4	H2O	43.4	243813	3.6
6	C4H10	162.1	1500719	0.9
10	Acetone	252.9	2156	0.0
18	iPrOH	313.9	1468	0.0

Totals				
			1784989	4.5

Channel 3, 10m
MS5A Heated
Injector Results

Pk #	Name	Retention Time	Area	Concentration
1	H2	25.5	559966282	73.7
	O2 (ref)			0.0 BDL
	N2			0.0 BDL
5	CO	91.2	146	0.0

Totals				
			559966428	73.7

383

384

385

386

387

388

389

30

390 **11. A typical NMR spectrum of 2-butanol**

391
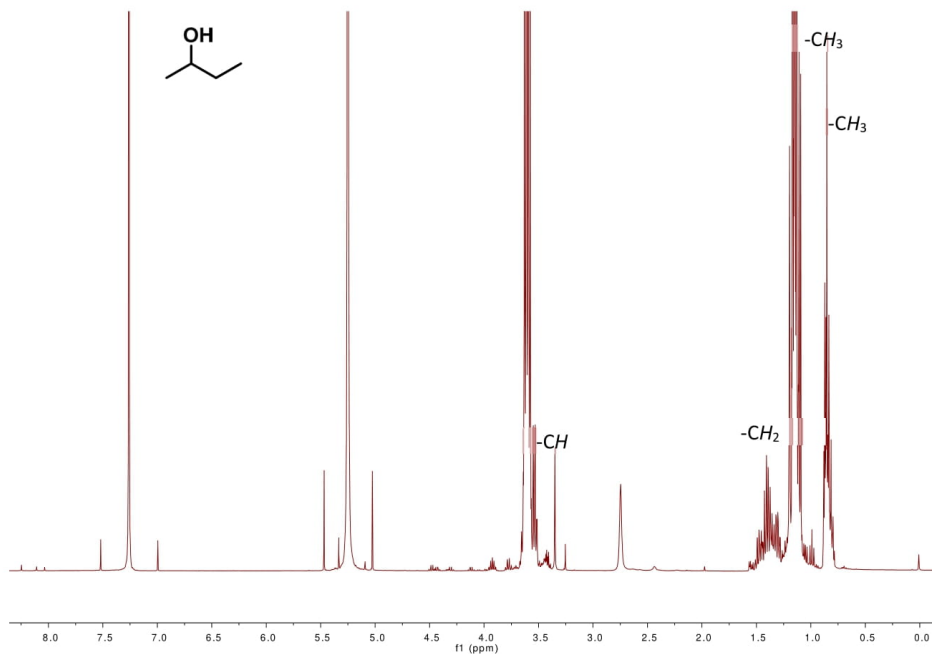
392 **Supplementary Figure 8** | **^{1}H NMR of the reaction mixture (400 MHz, CDCl$_3$ at 25 °C)**.
393 Reaction conditions: 5.0 mL ethanol, **Ru-2** (250 ppm), 96 h, 115 °C, NaOEt (20 mol%) in reactor
394 A and 600 rpm. (Supplementary Table 4, Entry 8.)

395 .

31

Supplementary Figure 9 | ¹³C NMR of the reaction mixture (**100.62 MHz, CDCl₃ at 25 ⁰C**).
Reaction conditions: 5.0 mL ethanol, **Ru-2** (250 ppm), 96 h, 115 ⁰C, NaOEt (20 mol%) in reactor
A and 600 rpm. (Supplementary Table 4, Entry 8.)

32

411   **12. A typical NMR spectrum of sodium acetate quantification**

412
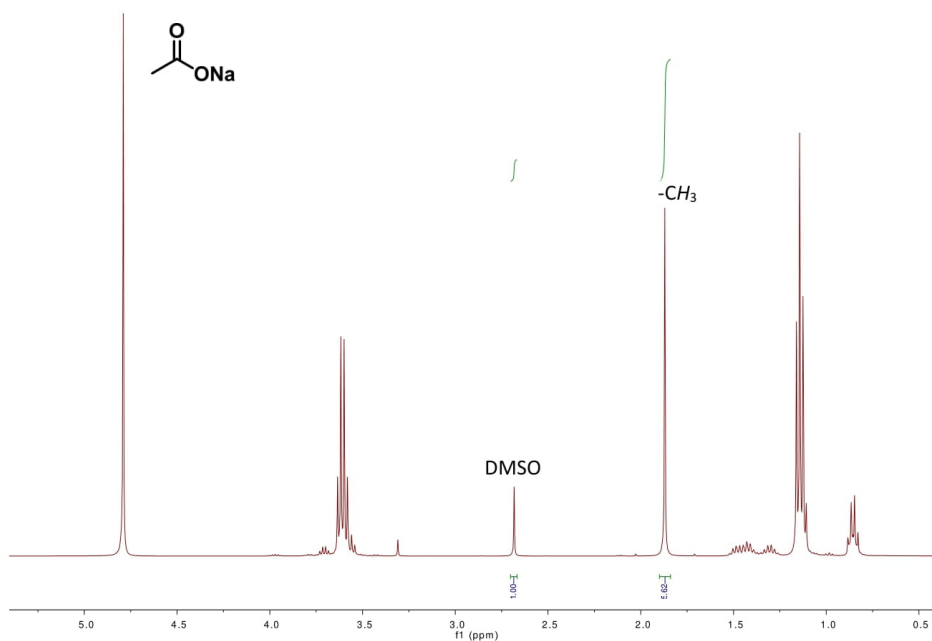
413   **Supplementary Figure 10 | ¹H NMR of sodium acetate quantification (DMSO as internal**
414   **standard, 400 MHz, D₂O at 25 ºC).** Reaction conditions: 2.5 mL ethanol, **Ru-2** (250 ppm), 96 h,
415   130 ºC, NaOEt (20 mol%), in reactor B and 600 rpm. (Supplementary Table 4, Entry 20.)

416

33

417
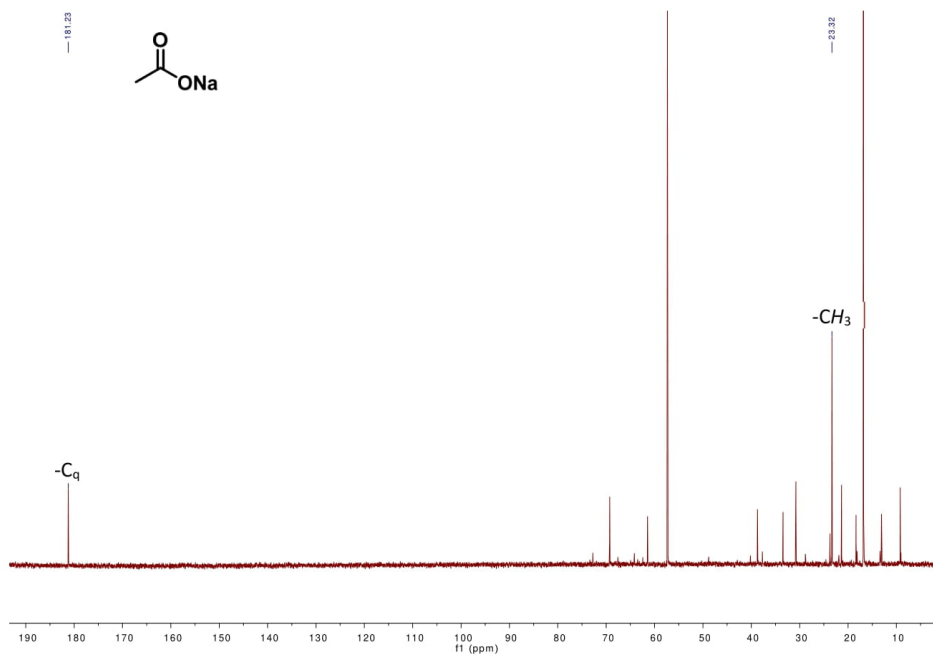
Supplementary Figure 11 | ^{13}**C NMR of sodium acetate quantification (100.62 MHz, D$_2$O at**
25 ^{o}C). Reaction conditions: 2.5 mL ethanol, **Ru-2** (250 ppm), 96 h, 130 ^{o}C, NaOEt (20 mol%) in
reactor B and 600 rpm. (Supplementary Table 4, Entry 20.)

.

432   **13. Pressure change studies**

433
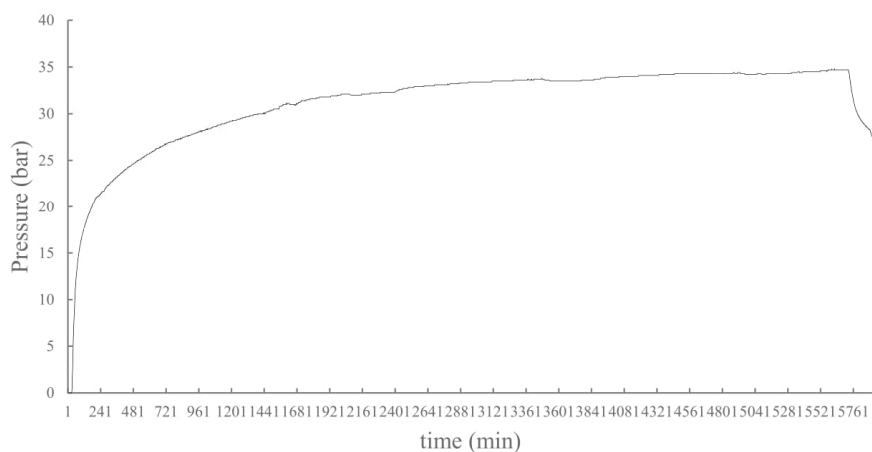
434   **Supplementary Figure 12 | Pressure changes over time observed by Parr system digital**
435   **recording**. Reaction conditions: 2.5 mL ethanol, **Ru-2** (250 ppm), 96 h, 130 ºC, NaOEt (20 mol%)
436   in reactor B and 600 rpm. (Supplementary Table 4, Entry 20.)

437

438

439

440

441

442

443

444

445

446

447

448

449

450

35

451 **14. Mechanistic study**

452 **Supplementary Table 18 | Mechanistic tests with 4-hydroxy-2-butanone as substrate**

453
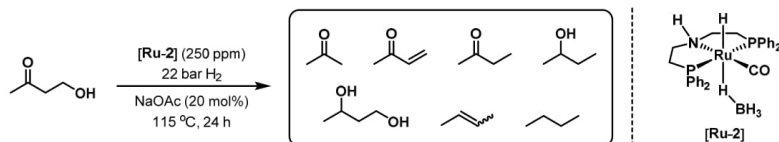
Entry	Additive (mol%)	4-hydroxy-2-butanone [mL / mmol]	H$_2$ [mmol]	GC-MS observed products[a]					
				acetone	methyl vinyl ketone	2-butanone	2-butanol	1,3-butanediol	Butenes
1	/	5.0 / 58	22	√	√	√	√	×	×
2	/	2.5 / 29	22	×	×	×	√	√	√
3	NaOAc (20)	2.5 / 29	22	√	×	√	√	×	×

Reaction conditions: 2.5-5.0 mL 4-hydroxy-2-butanone (29-58 mmol), 22 bar H$_2$ (22 mmol) 250 ppm **Ru-2**, with or without 20 mol% NaOAc, 115 °C, 24 h in reactor A and 600 rpm.
[a] Determined by GC-MS. See the reports for more products.

454

455

456

457

458

459

460

461

462

463

464

465

466

467

36

468   Example: Supplementary Table 18, Entry 1.

469   Reaction conditions: 5.0 mL 4-hydroxy-2-butanone, **Ru**-**2** (250 ppm, 8.5 mg), 24 h, 115 $^{\circ}$C, 22 bar
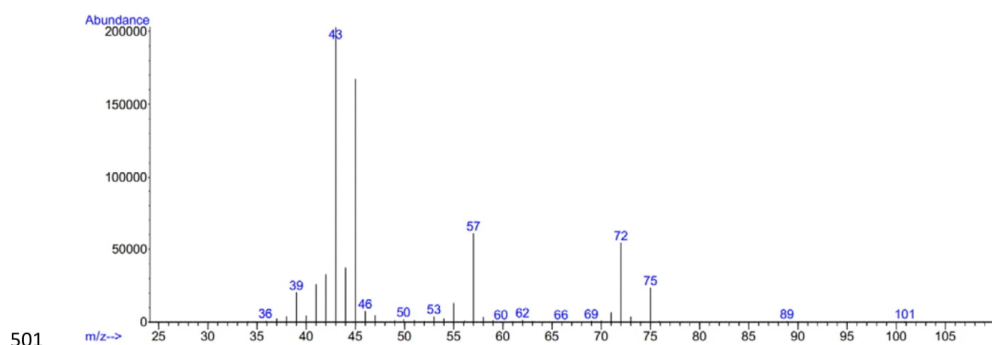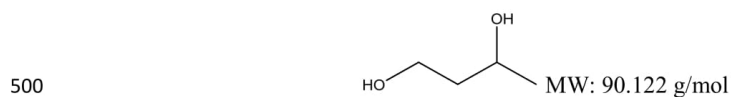470   H$_2$ in reactor A and 600 rpm.

471
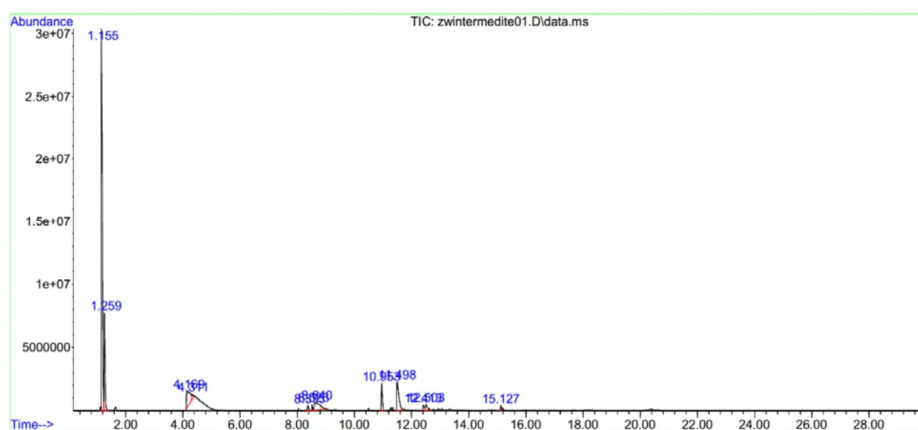
472   **Supplementary Table 19 | Information of products from GC-MS**

Retention time	Compound	Corr.area	Corr. % max.	% of total (mol%)
1.113	acetone	-	-	-
1.155	dichloromethane	754615915	100.00	55.583
1.259	methyl vinyl ketone	182087021	24.13	13.412
1.281	2-butanone	-	-	-
1.655	2-butanol	-	-	-
4.169	4-hydroxyl-2-butanone	96419728	12.78	7.102
4.311	4-hydroxyl-2-butanone	16803779	2.23	1.238

473

474

475

476

477

478

479

480

481

MW: 58.08 g/mol
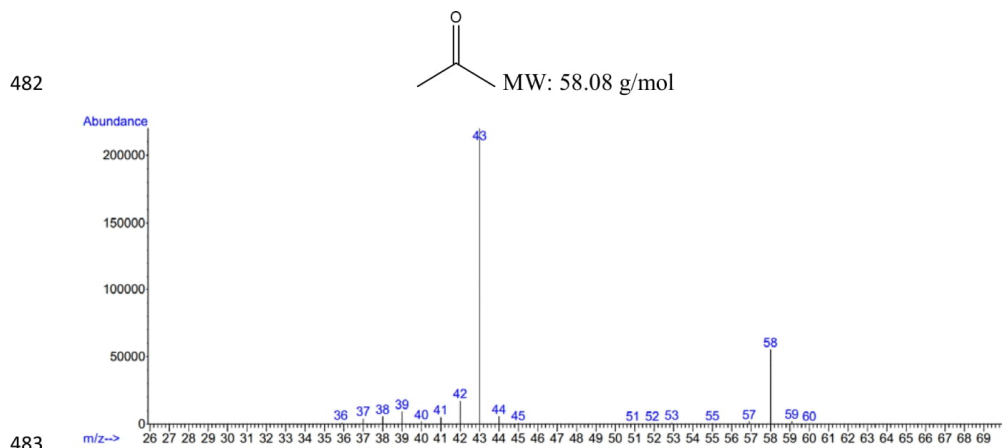
Supplementary Figure 13 | A MS spectrum of acetone. (Supplementary Table 18, Entry 1.)

MW: 70.09 g/mol
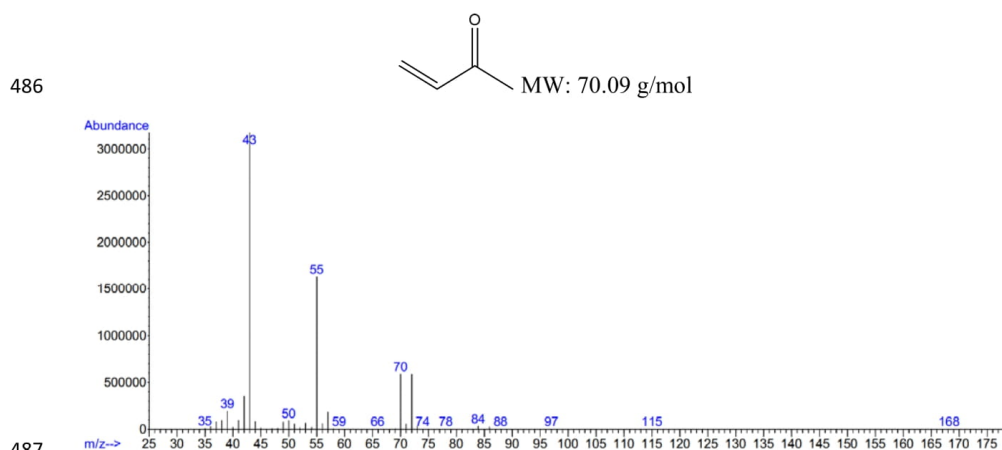
Supplementary Figure 14 | A MS spectrum of methyl vinyl ketone. (Table Supplementary Table 18, Entry 1.)

38

494   Example: Supplementary Table 18, Entry 2. (liquid phase)

495   Reaction conditions: 2.5 mL 4-hydroxy-2-butanone, **Ru-2** (250 ppm, 4.3 mg), 24 h, 115 ºC, 22 bar
496   H_2, in reactor A and 600 rpm.
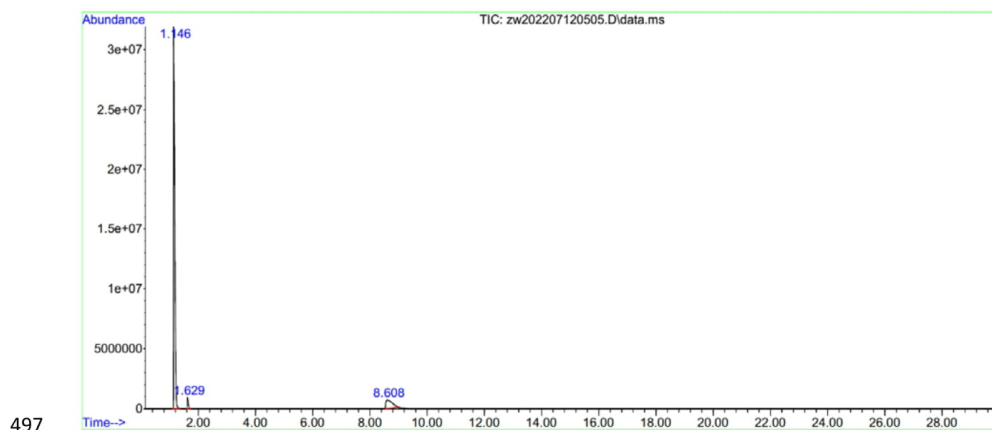
498   **Supplementary Table 20 | Information of products from GC-MS**

Retention time	Compound	Corr.area	Corr. % max.	% of total (mol%)
1.146	dichloromethane	946790132	100.00	88.245
1.629	2-butanol	22370046	2.36	2.085
8.608	1,3-butanediol	103752503	10.96	9.670

MW: 90.122 g/mol

502   **Supplementary Figure 15 | A MS spectrum of 1,3-butanediol.** (Supplementary Table S18,
503   Entry 2.)

39

202

504   Example: Supplementary Table 18, Entry 2. (gas phase)

505   Reaction conditions: 2.5 mL 4-hydroxy-2-butanone, **Ru-2** (250 ppm, 4,3 mg), 24 h, 115 °C, 22 bar
506   H_2, in reactor A and 600 rpm.

507
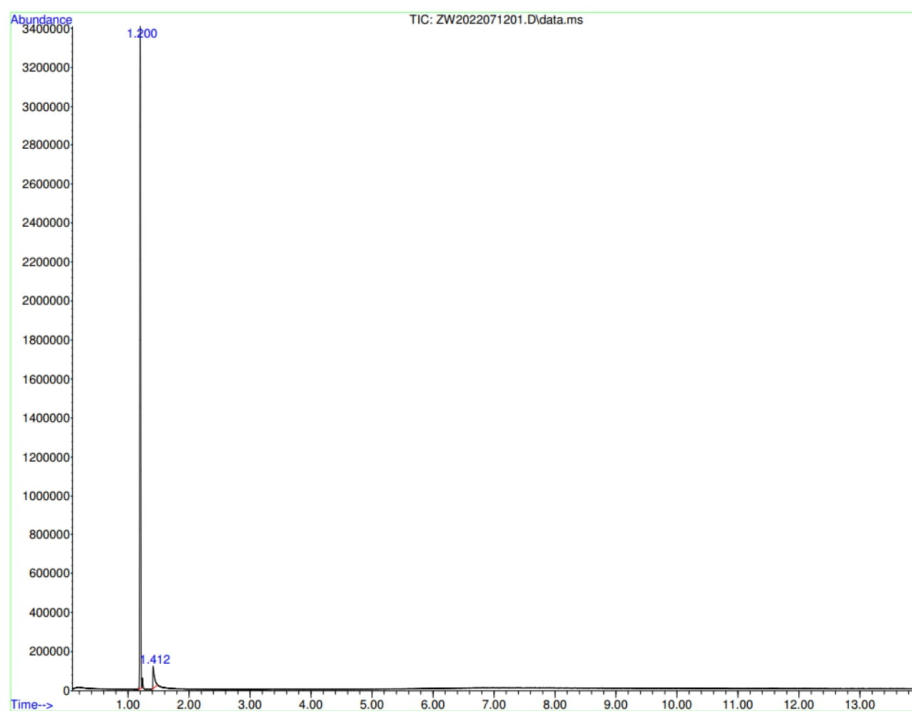
508   **Supplementary Table 21 | Information of products from GC-MS**

Retention time	Compound	Corr.area	Corr. % max.	% of total (mol%)
1.200	N_2	33682013	100.00	93.887
1.412	butenes	2193061	6.51	6.113

509

510

511

512

513

514

515

40

516   Example: Supplementary Table 18, Entry 3.

517   Reaction conditions: 2.5 mL 4-hydroxy-2-butanone, **Ru-2** (250 ppm, 4.3 mg), NaOAc (20 mol%,
518   595 mg), 24 h, 115 ºC, 22 bar H$_2$, in reactor A and 600 rpm.

519
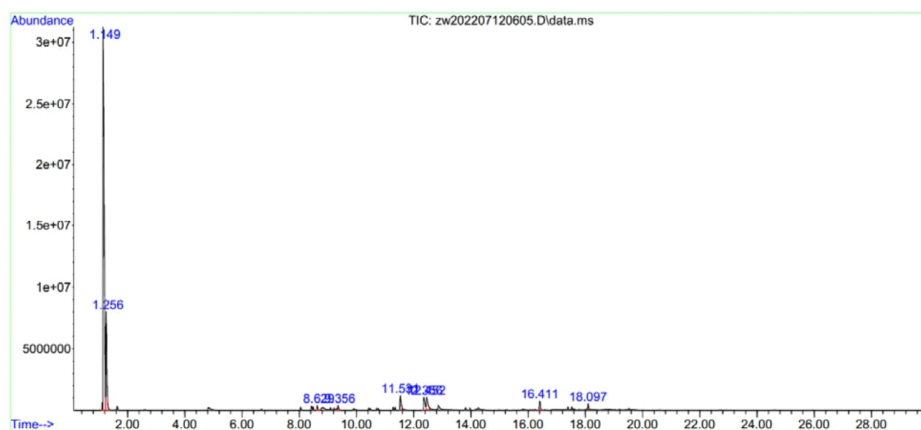
520   **Supplementary Table 22 | Information of products from GC-MS**

Retention time	Compound	Corr.area	Corr. % max.	% of total (mol%)
1.109	acetone	-	-	-
1.149	dichloromethane	869114795	100.00	72.115
1.261	2-butanone	-	-	-
1.635	2-butanol	-	-	-

521

522

523

524

525

526

527

528

529

530

531

41

532

533
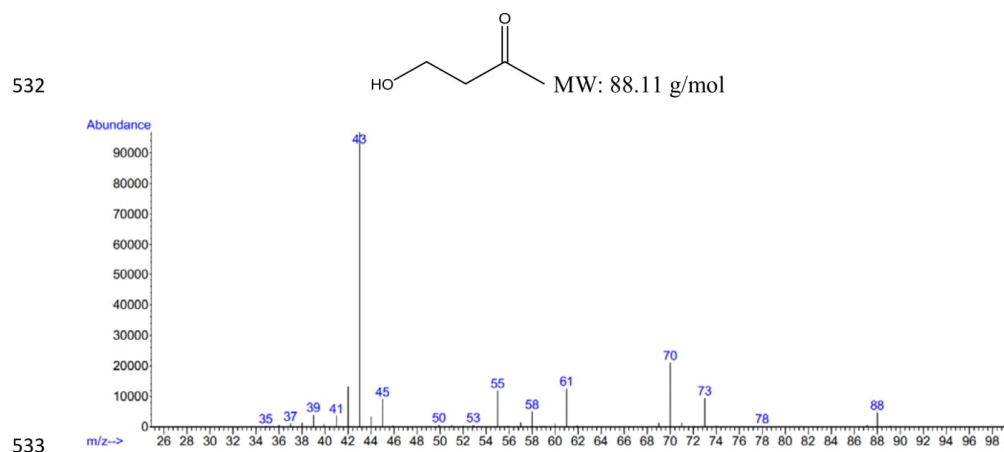
534 **Supplementary Figure 16 | A MS spectrum of 4-hydroxy-2-butanone.** (Supplementary Table
535 18, Entry 3.)

536

537

538

539

540

541

542

543

544

545

546

547

548

549

550

551

15. References

552

553   1. AMF. *Iea-amf.org* (2022). at <https://iea-amf.org/content/fuel_information/butanol/properties>

554   2. O'Lenick, A. J. Guerbet Chemistry. *J. Surfactants Deterg.* **4**, 311–315 (2001).

555

556

557

558

559

560

561

562

563

564

565

Appendix E – Paper II

This paper is under preparation and it is based on the partial research of Chapter 3.2. This work was conducted at DTU Chemistry in collaboration with Rosa Padilla, and Assoc. Prof. Martin Nielsen.

Effect of organic solvents on ethanol dehydrogenation to ethyl acetate with PNP complexes

Zhenwei Ni, Rosa Padilla, and Martin Nielsen*

Technical University of Denmark (DTU), Department of Chemistry, 2800 Kgs. Lyngby, Denmark; marnie@kemi.dtu.dk.

Abstract

The catalytic dehydrogenation of ethanol (EtOH) to ethyl acetate (AcOEt) represents an alternative approach for future applications as hydrogen storage systems and clean synthesis of fine chemicals. In this study, we describe the effect of organic solvents on the EtOH acceptorless dehydrogenation to AcOEt with different Ru-PNP pincer complexes. The catalytic process improves by adding a suitable volume ratio of toluene: ethanol (1.25:1) in presence of **Ru-1** [(^{Ph}PNPRuH)(BH$_4$)CO)] complex (0.1 mol%) affording 98% conversion after 24 h at 120 ^{o}C.

Keywords: Acceptorless dehydrogenation, Pincer complexes, Ethanol, Ethyl acetate, Organic solvents.

Introduction

Solvents are a major class of commodity chemicals widely used in industrial processes. Therefore, world demand for solvents is constantly growing and there is an urgent need for commonly used solvents to have a lower environmental impact.[1–3] For instance, one of the main solvents ethyl acetate (AcOEt) is currently produced from fossil carbon resources. As an alternative to non-sustainable resources, renewable AcOEt could reduce greenhouse gas emissions.[4]

In this sense, the production of AcOEt is highly relevant in the industry with an estimated annual 1.7 million tons produced worldwide in 2013.[5] This basic short-chain ester is widely used in the synthesis of biodiesel, paints, adhesives, herbicides, and resins.[6] Conventionally, AcOEt is produced by Fischer–Speier esterification, refluxing acetic acid and ethanol in presence of concentrated sulfuric acid.[5] However, the addition of concentrated sulfuric acid generates toxic waste, representing an environmental issue. In addition, this process is thermodynamically reversible with slow reaction rates, diminishing the conversion and yield.[7] In fact, the optimization of this technology is necessary to minimize the losses of raw materials and low productivity.

Attempts for the production of esters by homogeneous catalysis are described in the literature. For example, Beller and Hamilton reported the alkoxycarbonylation of various alkenes to give the branched esters under CO pressure.[8–10] However, considering environmentally benign, low cost

and safe production, acceptorless dehydrogenation (AD) of alcohols is attracting huge interest both in industry and academia. In fact, AD-based reactions involve a dehydrogenative process, with the generation of hydrogen gas and water[11] followed by coupling of the dehydrogenated intermediate with another substrate to generate value-added products.[12] This kind of reaction is the foundation for efficient, atom economic, sustainable, and environmentally benign synthetic methodology to construct carbon-carbon and carbon-heteroatom bonds.[13] The low cost of EtOH, its non-toxicity, and its availability offer the opportunity to develop useful chemical processes for the production of different chemicals such as ethylene (ET),[14] diethyl ether (Et$_2$O),[15] acetaldehyde (MeCHO)[16] and ethyl acetate (AcOEt). Overall, the dehydrogenation of biomass-related alcohols, such as bioethanol represents a viable and sustainable alternative to overcome the excessive consumption of fossil fuels.

Up to now, the synthesis of AcOEt by homogeneously catalyzed AD methodology has been broadly studied (Scheme 1). For instance, Beller and co-workers reported the use of Ru-MACHO-BH (**Ru-1**) (0.05 mol%) in presence of NaOEt (1.3 mol%) affording 81% yield of AcOEt at 90 ºC for 6 h.[17] Likewise, Gauvin developed a base-free acceptorless dehydrogenative coupling (ADC) catalytic system [(^{R}PNP)MnH(CO)$_2$] (0.6 mol%) yielding a moderate amount of AcOEt (3%) under refluxing conditions.[18] Szymczak studied the conversion of primary alcohols and diols with a Ru(II) hydride complex [HRu(bmpi)(PPh$_3$)$_2$] (1 mol%) bearing a bmpi ligand (bmpi=1,3-bis(6'-methyl-2'-pyridylimino)-isoindoline) at 110 ºC for 24 h. Interestingly, the dehydrogenation of EtOH in presence of toluene as a co-solvent afforded only 9% yield.[19]
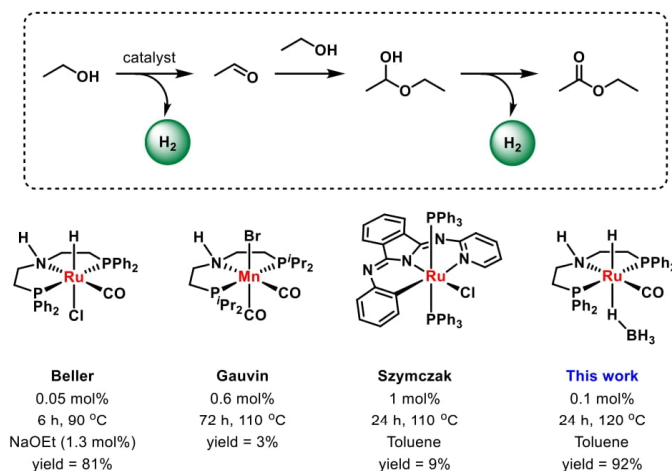
Scheme 1. Examples of ADC catalytic systems for the conversion of EtOH to AcOEt.

To the best of our knowledge, no effective homogeneous catalytic systems have been reported yet for the base-free AD of EtOH. The main issue with the systems described above for producing AcOEt is the gradual loss of the key intermediate acetaldehyde, due to the low boiling point (20 ºC). Conventionally, alcohol dehydrogenation is an endothermic process.[18,19] Some studies with

heterogeneous and homogeneous systems revealed that the first dehydrogenation step of ethanol to acetaldehyde is an uphill process with high energy demand.[18,20–22] These problems make the additive-free, ADC of ethanol extremely difficult.

Herein, we described the base-free, one-step, AD of EtOH to AcOEt, using different commercially available **Ru** and **Ir**-based catalysts (Scheme 2). The reaction was carried out under reflux at 100 - 120 °C in presence of different organic solvents. The effects of temperature, solvent characteristics, catalyst loading on both conversion and selectivity to AcOEt have been investigated. Moreover, the precatalyst **Ru**-1 showed high stability and catalytic performance under the actual reaction conditions.

Scheme 2. Screening of precatalyst for the dehydrogenation of EtOH.

Results and discussion

Our studies commenced with a benchmark reaction for the AD of EtOH to AcOEt with **Ru**-1 (0.05 mol%) complex without any co-solvent. After 24 h at 120 °C, the reaction afforded moderate conversion (43%) and 34% yield (SI, Table S2, Entry 1). Interestingly, the conversion remained similar when extending the reaction time to 48 h (SI, Table S2, Entry 2). In order to improve the catalytic productivity of the system, a series of different co-solvent were added. Firstly, we introduced a co-solvent with suitable boiling point characteristics. For instance, the addition of 10 mL of toluene (b.p. 110 °C) led to 43% conversion at 120 °C and 24 h (Table S3, Entry 2). Next, a screening of different complexes for the dehydrogenation of EtOH was investigated (Table 1). Unfortunately, these complexes were not active under base-free reaction conditions. Likewise, the

complex **Ru**-2 gave limited conversion (≤5%) which is probably due to low activation under mild conditions. In fact, Milstein and coworkers suggested the use of higher reaction temperatures to promote hydrogenation reactions.[23] However, the dearomatized complex **Ru**-2 can react with H_2O to form a hydroxy-H_2O complex that may result to be detrimental to the dehydrogenation of EtOH.

Table 1. Screening of different catalysts in ethanol conversion with toluene

Entry	Catalyst	Conversion [%][a]	Yield [%][a]
1	**Ru-1**	43	25
2	**Ru-2**	<5	<5
3	**Ru-3**	/	/
4	**Ru-4**	/	/
5	**Ru-5**	/	/
6	**Ru-6**	/	/
7	**Ir-1**	/	/

[a] Determined by NMR, dimethyl sulfoxide (DMSO) is the internal standard.

Hence, **Ru**-1 was chosen as the ideal catalyst for the following AD optimization experiments. To further understand the rate of the AD reaction, we studied the influence of different auxiliary solvents. Then, a series of aromatics, haloaromatics, cycloalkanes, ethers, and heterocyclic solvents were tested (Table 2). These experiments were conducted at 120 ºC for 24 h employing slightly higher catalyst loading of **Ru**-1 (0.1 mol%) and 10 mL (volume ratio between co-solvent and ethanol = 5: 1) of the corresponding co-solvent. Our observations suggest that the polarity and boiling point of the co-solvent could affect the EtOH dehydrogenation process and the conversion rate is partially dependent on the polarity of the solvent.

Toluene was tested first under these reaction conditions providing 63% conversion and 46% yield (Table 2, Entry 1). The non-polar *m*-xylene showed significantly better conversion (87%) and 79% yield (Entry 2), while its congener solvent *o*-xylene led to 58% conversion and 51% yield (Entry 3). The conversion decreased to 40% conversion when using *p*-xylene (Entry 4). Among non-polar solvents, the solutions with mesitylene, ethylbenzene, and *p*-cymene showed 30, 68, and 66% conversion respectively (Entries 5-7).

Next, we turned out our attention toward haloaromatic solvents, which have a very high polarity. The ADC reaction of EtOH with **Ru**-1 (0.1 mol%) in presence of chlorobenzene seems to be extremely unfavorable, leading to only 10% conversion and 5% yield at 120 ºC and 24 h (Entry 8).

For cycloalkanes and their derivatives, with non-polar characteristics and different grades of substitution did not affect the conversion according to our investigations. For example, cyclohexane yielded 52% conversion and 50% yield. Furthermore, the use of methylcyclohexane showed similar conversion (55%) and yield (50%), while 1,3-dimethylcyclohexane allowed 51%

conversion and 46% yield under the actual reaction conditions (Entries 9-11). The moderate selectivity of the ADC reaction in presence of **Ru**-1 (0.1 mol%) is attributed to the lower solubility observed during the experiments with the described solvents.

Next, oxygenated solvents such as tetrahydrofuran showed 22% conversion and 20% yield (Entry 12). A more polar solvent, 1,4-dioxane provided similar results with a conversion of 53% and 41% yield (Entry 13). Interestingly, cyclopentyl methyl ether increased the conversion to 52% and 46% yield (Entry 14). Moreover, extending the reaction time to 48 h did not result in significant catalyst productivity in presence of most of these oxygenated solvents (SI, Table S3). During the course of the reaction, the solubilities of the intermediates such as acetaldehyde and 1-ethoxyethanol differ dramatically in the different polarities of the solvents.

Further evaluation of aromatic ethers continues with methoxybenzene (anisole). Then the conversion for the ADC reaction of EtOH with **Ru**-1 (0,1 mol%) improved the conversion to 61% and 49% yield (Entry 15). Among these examples, we also evaluated oxygenated compounds derived from biomass as green solvents.[24–26] The solvent γ-valerolactone (GVL) has the lowest vapor pressure (3.5 kPa at 80 °C) which is a significant parameter of fuel in terms of controlling the emission of volatile organic compounds.[4] However, the ADC reaction of EtOH in presence of GVL achieved only 12% conversion to AcOEt with 7% yield, under standard reaction conditions (Entry 16).

Table 2. Screening of different organic solvents in EtOH conversion with **Ru**-1.

Entry	Solvent	Conversion [%][a]	Yield [%][a]	Selectivity [%]
1	toluene	63	46	73
2	*m*-xylene	87	79	91
3	*o*-xylene	58	51	88
4	*p*-xylene	40	27	68
5	mesitylene	30	15	50
6	ethylbenzene	68	55	81
7	*p*-cymene	66	53	80
8	chlorobenzene	10	5	50
9	cyclohexane	52	50	96
10	methylcyclohexane	55	50	91
11	1,3-dimethylcyclohexane	51	46	90
12	anisole	61	49	80
13	tetrahydrofuran	22	20	91
14	1,4-dioxane	53	41	77
15	cyclopentyl methyl ether	52	46	88
16	γ-valerolactone	12	7	58

[a] Determined by NMR, dimethyl sulfoxide as internal standard.

Based on the experimental results, we hypothesized that the ADC reaction of EtOH occurs in a dual organic phase system where the precatalyst (**Ru-1**) could efficiently interact with the substrate in presence of a co-solvent. Numerous **Ru-1** will stay in the solid phase and will not contact the substrate since the limited solubility in pure ethanol. More **Ru-1** can enter the liquid phase when solvents with less polarity are added to the catalytic system due to the increasing solubility. Even if ethanol is more polarized and solvents are less polar, the exchange rating of **Ru-1** is faster than that of **Ru-1** in the solid phase to pure ethanol. Hence, more **Ru-1** will react with ethanol. If solvents with high polarity are added to the system, the more polar, the more difficult it is for **Ru-1** to enter the liquid phase (first step), and the less contact between **Ru-1** and ethanol.

Having the optimal reaction conditions in hand, we continued our optimization studies by employing the best solvents, toluene, and cyclohexane. By changing the volume of the co-solvent, catalyst loading, and the reaction temperature we could determine if the presence of the co-solvent plays a relevant role in the activation of the precatalyst **Ru-1**.

For the analysis of the results of toluene volume addition, it can be seen that at 24 h, the best volume ratio between ethanol and toluene was 1.25 (98% conversion, 92% yield. **Table 3**, Entry 1), compared to other ratios (Entries 2 - 4). This occurs because less toluene is added, which helps the reflux rate and speeds up the reaction of the catalyst with ethanol, even if the catalyst could not completely be dissolved under 1.25 ratio conditions. Considering this point as well as the reaction intensity, it is not suitable for a further decreading of toluene volume. Keeping the same volume of toluene, a low-temperature reaction (100 °C) was performed (Entry 5), but it turned out that only 37% conversion was achieved, likely since the solubility also decreased with the temperature. In addition, lowering **Ru-1** to 0.05 mol% (still not fully dissolved) caused a halving of conversion and yield (Entry 6). Continually decreasing reaction time to 18 h with 0.1 mol% **Ru-1**, the conversion and yield showed a downtrend to 89% and 84% (Entry 7).

In the optimization with cyclohexane series compounds, 0.1 mol% **Ru-1** could not fully be soluble in the reaction, but they can provide decent results as mentioned above. Hence, it is necessary to further study low catalyst loading with this co-solvent. We decreased **Ru-1** loading to 0.05 mol% (Entry 8), unfortunately, the corresponding conversion and yield fell in equal proportion compared to 0.1 mol% (Entry 9). While extending the reaction time to 48 h (Entry 10), like most other co-solvents, the results remained the same. This result again demonstrated the critical importance of the amount of catalyst introduction in this system. Once the catalyst amount was not sufficient or the catalytic cycle was off then the reaction just stopped.

Table 3. Optimization of ethanol conversion in toluene and cyclohexane.
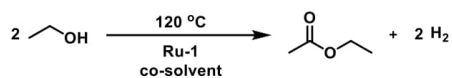
Entry	Catalyst (mol%)	Solvent	ratio	Time [h]	Conversion [%][a]	Yield [%][a]	Selectivity [%]
1	0.1	Toluene	1.25	24	98	92	94
2	0.1	Toluene	2.5	24	91	87	96
3	0.1	Toluene	5	24	63	46	73
4	0.1	Toluene	7.5	24	53	52	98
5[b]	0.1	Toluene	1.25	24	37	34	92
6	0.05	Toluene	1.25	24	47	43	91
7	0.1	Toluene	1.25	18	89	84	94
8	0.05	Cyclohexane	5	24	25	25	100
9	0.1	Cyclohexane	5	24	52	50	96
10	0.1	Cyclohexane	5	48	51	34	67

[a] Determined by NMR, dimethyl sulfoxide as internal standard.
[b] temperature, 100 ºC

Conclusions

In conclusion, we showed the additive-free EtOH dehydrogenation to AcOEt in different co-solvents. The polarity of the co-solvent has a direct effect on the conversion rate of EtOH under dehydrogenative conditions to AcOEt. The reaction of **Ru**-1 (0.1 mol%) with EtOH adding 1.25 times the volume of toluene afforded 98% conversion and 92% yield after 24 h at 120 ºC. This work firstly demonstrated the AD reaction of ethanol in presence of different co-solvents with various boiling points and polarities. Experimental guidelines were given for the selection of such dual-organic phase catalytic systems in acceptorless dehydrogenation.

References

[1]   Kerton, F. M.; Marriott, R. *Alternative Solvents for Green Chemistry (2nd Edition)*; Royal Society of Chemistry (RSC), 2013.

[2]   Gorgojo, P.; Gonzalez-miquel, M.; Lo, P. *ACS Sustain. Chem. Eng.* **2020**, *8*, 8958–8969.

[3]   Green, G.; Market, B. S. *Ind. Biotechnol.* **2020**, *12*, 216–218.

[4]   Zirahi, A.; Sadeghi, H.; Ali, Y.; Mohsen, H. *AIChE J.* **2020**, *66* (2), 1–11.

[5]   Löser, C.; Urit, T.; Bley, T. *Appl. Microbiol. Biotechnol.* **2014**, *98* (12), 5397–5415.

[6]   Zhang, S.; Guo, F.; Yan, W.; Dong, W.; Zhou, J.; Zhang, W.; Xin, F.; Jiang, M. *Appl. Microbiol. Biotechnol.* **2020**, *104* (17), 7239–7245.

[7]   Fischer, E.; Speier, A. *Chem. Ges.* **1895**, *28*, 3252–3258.

[8]   Wu, L.; Liu, Q.; Fleischer, I.; Jackstell, R.; Beller, M. *Nat. Commun.* **2014**, *5*, 3091.

[9]   Rodriguez, C. J.; Foster, D. F.; Eastham, R.; Cole-hamilton, D. J. *Chem. Commun.* **2004**, 1720–1721.

[10] Li, H.; Dong, K.; Jiao, H.; Neumann, H.; Jackstell, R.; Beller, M. *Nat. Chem.* **2016**, *8*, 1159–1166.

[11] Waiba, S.; Maji, B. *ChemCatChem* **2020**, *12* (7), 1891–1902.

[12] Daw, P.; Ben-david, Y.; Milstein, D. *J. Am. Chem. Soc.* **2018**, *140*, 11931–11934.

[13] Nad, P.; Mukherjee, A. *Asian J. Org. Chem.* **2021**, *10*, 1958–1985.

[14] Zhang, M.; Yu, Y. *Ind. Eng. Chem. Res.* **2013**, *52*, 9505–9514.

[15] Klein, T.; Oliveira, R. De; Rosset, M.; Perez-lopez, O. W. *Catal. Commun.* **2018**, *104*, 32–36.

[16] Pang, J.; Yin, M.; Wu, P.; Li, X.; Li, H. *Green Chem* **2021**, *23*, 7902–7916.

[17] Nielsen, M.; Junge, H.; Kammer, A.; Beller, M. *Angew. Chemie* **2012**, *124* (23), 5809–5811.

[18] Nguyen, D. H.; Trivelli, X.; Capet, F.; Paul, J. F.; Dumeignil, F.; Gauvin, R. M. *ACS Catal.* **2017**, *7* (3), 2022–2032.

[19] Tseng, K. N. T.; Kampf, J. W.; Szymczak, N. K. *Organometallics* **2013**, *32* (7), 2046–2049.

[20] Carotenuto, G.; Tesser, R.; Di Serio, M.; Santacesaria, E. *Catal. Today* **2013**, *203*, 202–210.

[21] Men'Shchikov, V. A.; Gol'Dshtein, L. K.; Semenov, I. P. *Kinet. Catal.* **2014**, *55* (1), 12–17.

[22] Li, R.; Zhang, M.; Yu, Y. *Appl. Surf. Sci.* **2012**, *258* (18), 6777–6784.

[23] Khusnutdinova, J. R.; Garg, J. A.; Milstein, D. *ACS Catal.* **2015**, *5* (4), 2416–2422.

[24] Winterton, N. *Clean Technol. Environ. Policy.* **2021**, *23* (9), 2499–2522.

[25] Lomba, L.; Zuriaga, E.; Giner, B. *Curr. Opin. Green Sustain.* **2019**, *18*, 51–56.

[26] Nomura, K.; Terwilliger, P. *e-Polymers* **2019**, *19*, 323–329.

Effect of organic solvents on ethanol dehydrogenation to ethyl acetate with PNP complexes

Zhenwei Ni, Rosa Padilla, and Martin Nielsen*

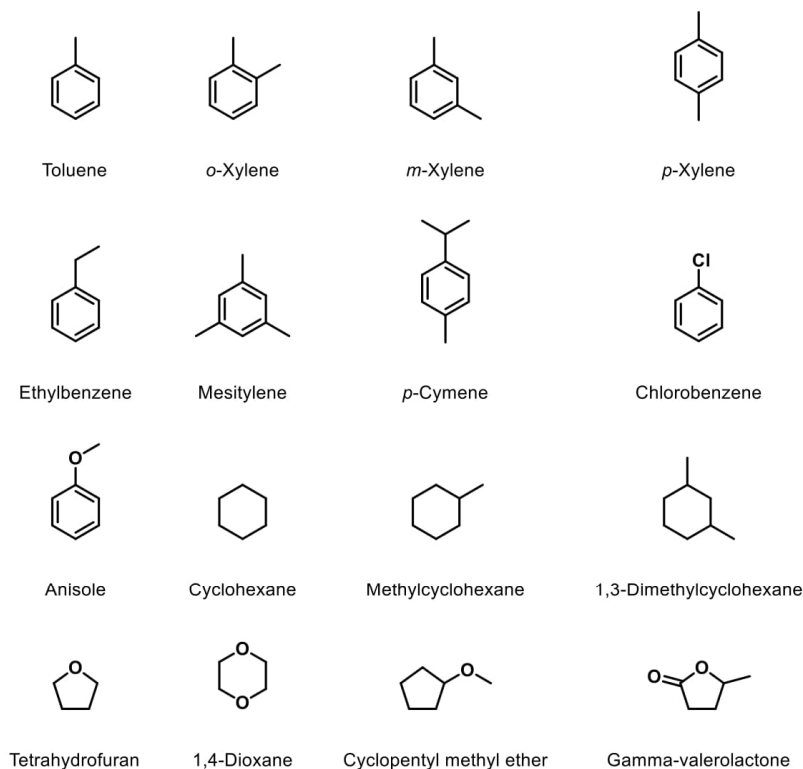Technical University of Denmark (DTU), Department of Chemistry, 2800 Kgs. Lyngby, Denmark; marnie@kemi.dtu.dk.

Table of contents

1. General information

Ethanol absolute (purity 99.98 %), toluene (purity 99.99 %), *o*-xylene (purity >= 98 %), *m*-xylene (purity >= 99 %), *p*-xylene (purity >= 99 %), ethylbenzene (purity ⩾99.0 %), mesitylene (purity 98 %), *p*-cymene (purity >= 99 %), chlorobenzene (purity ⩾99 %), anisole (purity 99.7 %), cyclohexane (purity 99.5 %), methylcyclohexane (purity ⩾ 99 %), 1,3-dimethylcyclohexane (purity 99 %), tetrahydrofuran (purity 99.99 %), 1,4-dioxane (purity 99.8 %), cyclopentyl methyl ether (purity >= 99.9 %), γ-valerolactone (purity 99 %), commercially available catalyst **Ru**-**1**, **Ru**-**3** – **6**. **Ir**-**1** and synthesized catalysts **Ru**-**2** is used without further purification. All reactions dealing with air or moisture-sensitive compounds were performed using standard Schlenk techniques or in an argon-filled glovebox. Dimethyl sulfoxide (100 uL, purity 99.9 %) was added as the internal stand to quantify ethanol conversion and ethyl acetate yield. ^{1}H-NMR and ^{13}C-NMR spectra were recorded on a Bruker Avance III 400 MHz spectrometer and were referenced on the deuterated solvent peak. Catalysts were added in an argon-filled glovebox, substrates and co-solvents (**Scheme S1**) were loaded into a 50 mL flask using standard Schlenk techniques.

Toluene	*o*-Xylene	*m*-Xylene	*p*-Xylene
Ethylbenzene	Mesitylene	*p*-Cymene	Chlorobenzene
Anisole	Cyclohexane	Methylcyclohexane	1,3-Dimethylcyclohexane
Tetrahydrofuran	1,4-Dioxane	Cyclopentyl methyl ether	Gamma-valerolactone

Scheme S1. Used cyclic compounds as co-solvents in this work

Table S1 concluded the properties of different solvents, including boiling point and dielectric constant. The table was arranged according to the dielectric constant from smallest to largest, which means that the polarity of the solvent gets stronger as you go down the list.

Table S1. Properties of different solvents. [1, 2]

Solvent	Boiling point (ºC)	Dielectric constant (20 ºC)
cyclohexane	80.8	2.02
methylcyclohexane	101	2.02
1,3-dimethylcyclohexane	120-125	/
p-xylene	138.4	2.27
p-cymene	177	2.3
toluene	110.6	2.4
1,4-dioxane	101	2.2 (25 ºC)
m-xylene	139	2.36
ethylbenzene	136	2.5
o-xylene	144	2.56
mesitylene	164.7	2.4-3.4
anisole	153.8	4.3
cyclopentyl methyl ether	106	4.76 (25 ºC)
chlorobenzene	132	5.6 (25 ºC)
tetrahydrofuran	66	7.58 (25 ºC)
acetaldehyde	20.2	21.8 (18 ºC)
ethanol	78.4	24.5
γ-valerolactone	207	36.47 (25 ºC)

2. Experimental section

Unless otherwise specified, the volumes of ethanol and solvents used in the catalytic system are 2 mL and 10 mL respectively, the volume of the glass flask is 50 mL and the stirring rate is 600 rpm.

Table S2. Initial attempts for ethanol conversion to ethyl acetate with **Ru-1**.

Entry	Catalyst loading (mol%)	Solvent	Time (h)	Conversion (%)[a]	Yield (%)[a]	Selectivity (%)
1	0.05	/	24	43	34	61
2	0.05	/	48	42	31	74

a: Determined by NMR, dimethyl sulfoxide is an internal standard.

Table S3. Screening of ethanol conversion under different conditions with **Ru-1**

Entry	Ru-1 [mol%]	Solvent	Volume ratio	Time [h]	Conversion [%][a]	Yield [%][a]	Selectivity [%]
1	0.025	Toluene	5	72	39	13	33
2	0.05	Toluene	5	24	43	25	58
3	0.05	Toluene	5	72	72	54	75
4	0.05	Toluene	1.25	24	47	43	91
5	0.1	Toluene	1.25	18	89	84	94
6	0.1	Toluene	1.25	24	98	92	94
7[b]	0.1	Toluene	1.25	24	37	34	92
8	0.1	Toluene	2.5	24	91	87	96
9	0.1	Toluene	5	24	63	46	73
10	0.1	Toluene	7.5	24	53	52	98
11	0.1	Toluene	5	48	72	52	72
12	0.1	Toluene	5	72	92	86	93
13	0.05	o-xylene	5	48	52	33	63
14	0.1	o-xylene	5	24	58	51	88
15	0.1	m-xylene	2.5	24	86	78	91
16	0.1	m-xylene	5	24	87	79	91
17	0.1	m-xylene	7.5	24	69	68	99
18	0.1	m-xylene	5	48	95	76	80
19	0.1	p-xylene	5	24	40	27	68
20	0.1	p-xylene	5	48	45	28	62
21	0.1	Ethylbenzene	2.5	24	58	48	83
22	0.1	Ethylbenzene	5	24	68	55	81
23	0.1	Ethylbenzene	7.5	24	69	50	72
24	0.1	Ethylbenzene	5	48	72	55	76
25	0.1	Mesitylene	5	24	30	15	50
26	0.1	p-cymene	5	24	66	53	80
27	0.1	Chlorobenzene	5	24	10	5	50
28	0.1	Anisole	5	24	61	49	80
29	0.1	Anisole	5	48	73	57	78
30	0.05	Cyclohexane	5	24	25	25	100
31	0.1	Cyclohexane	5	24	52	50	96
32	0.1	Cyclohexane	5	48	51	34	67
33	0.1	Methylcyclohexane	5	24	55	50	91
34	0.1	1,3-Dimethylcyclohexane	5	24	51	46	90
35	0.1	Tetrahydrofuran	5	24	22	20	91
36	0.1	Tetrahydrofuran	5	48	63	58	92
37	0.1	Tetrahydrofuran	5	72	65	63	97
38	0.1	1,4-dioxane	5	24	53	41	77
39	0.1	1,4-dioxane	5	48	59	43	73
40	0.1	Cyclopentyl methyl ether	5	24	52	46	88
41	0.1	Cyclopentyl methyl ether	5	48	56	45	80
42	0.1	γ-Valerolactone	5	24	12	7	58
43	0.1	γ-Valerolactone	5	48	14	8	57

a: Determined by NMR, dimethyl sulfoxide is an internal standard. b: temperature, 100 ºC
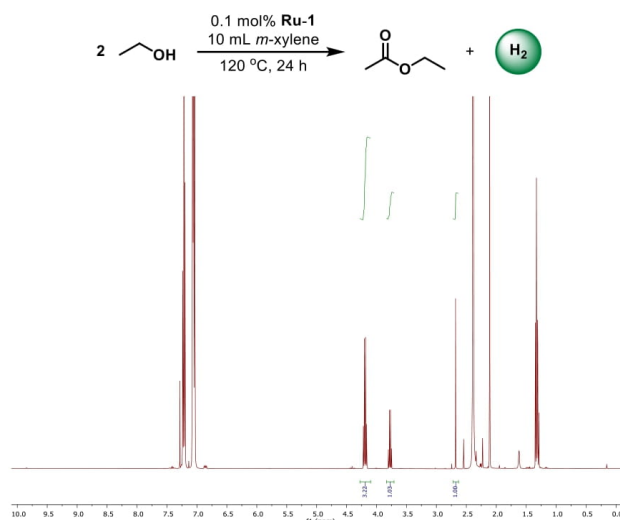
3. Typical NMR spectra of products
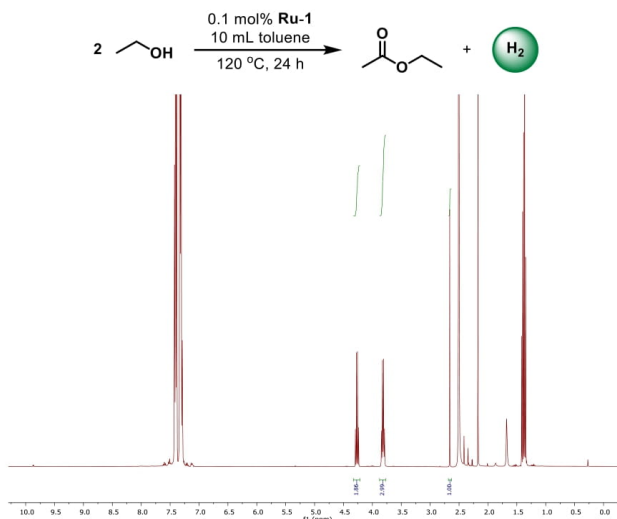
Figure S1. ^{1}H NMR of acceptorless dehydrogenation of ethanol to ethyl acetate (CDCl$_3$, 25 ^{o}C, 400 MHz, 2 mL ethanol, 10 mL toluene, 0.1 mol% **Ru-1**, 24 h, 120 ^{o}C).
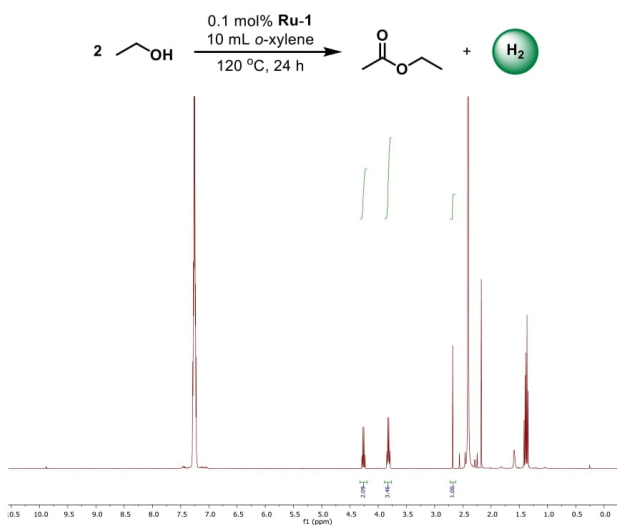
Figure S2. ^{1}H NMR of acceptorless dehydrogenation of ethanol to ethyl acetate (CDCl$_3$, 25 ^{o}C, 400 MHz, 2 mL ethanol, 10 mL o-xylene, 0.1 mol% **Ru-1**, 24 h, 120 ^{o}C).
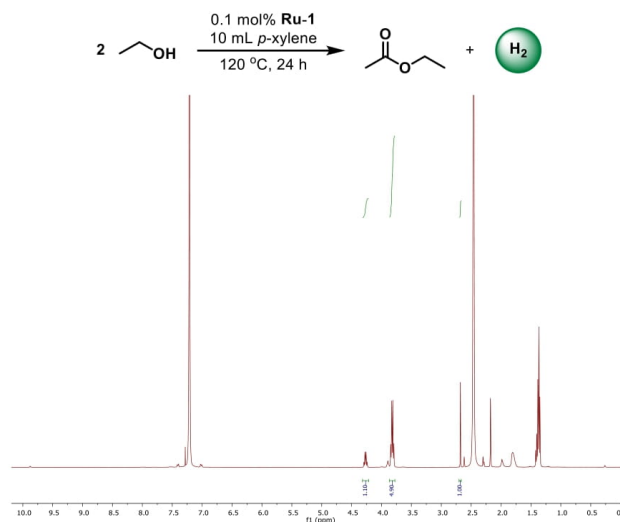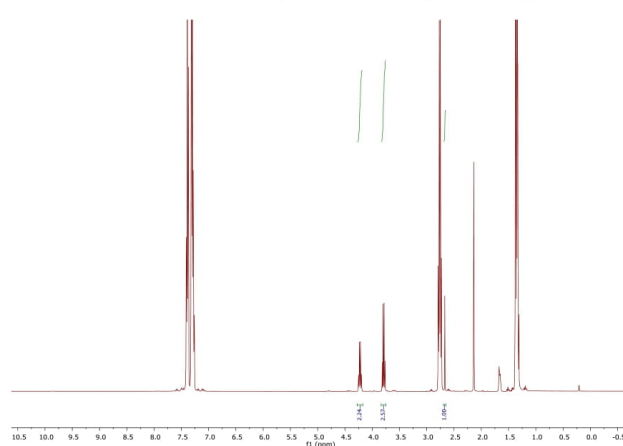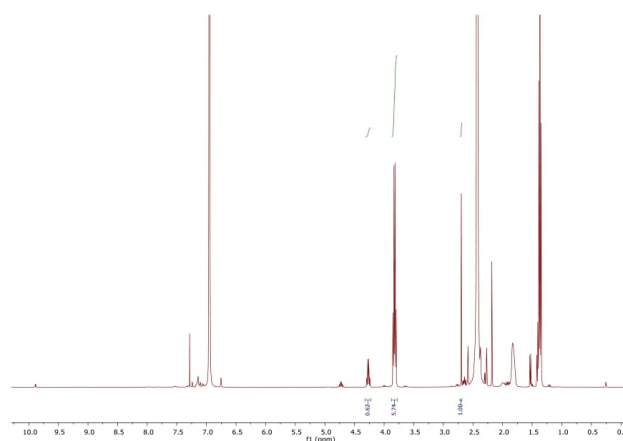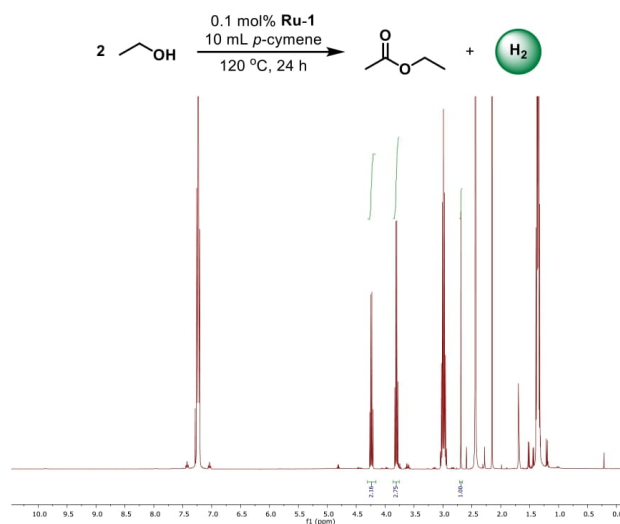
Figure S3. ^{1}H NMR of acceptorless dehydrogenation of ethanol to ethyl acetate (CDCl$_3$, 25 ºC, 400 MHz, 2 mL ethanol, 10 mL m-xylene, 0.1 mol% **Ru-1**, 24 h, 120 ºC).

Figure S4. ^{1}H NMR of acceptorless dehydrogenation of ethanol to ethyl acetate (CDCl$_3$, 25 ºC, 400 MHz, 2 mL ethanol, 10 mL p-xylene, 0.1 mol% **Ru-1**, 24 h, 120 ºC).
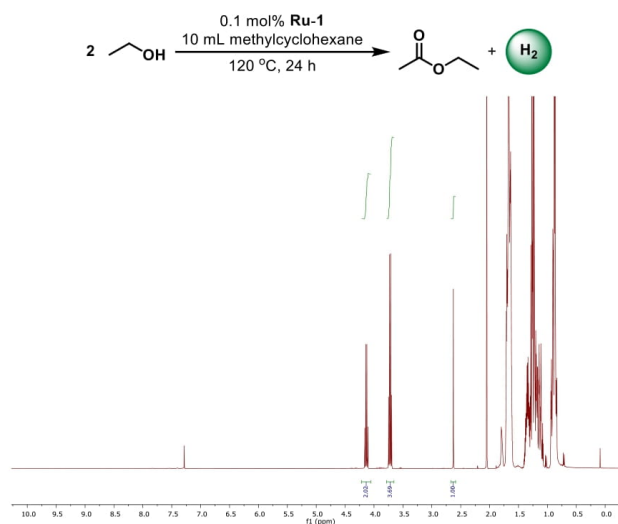
Figure S5. ^{1}H NMR of acceptorless dehydrogenation of ethanol to ethyl acetate (CDCl$_3$, 25 ^{o}C, 400 MHz, 2 mL ethanol, 10 mL ethylbenzene, 0.1 mol% **Ru-1**, 24 h, 120 ^{o}C).

Figure S6. ^{1}H NMR of acceptorless dehydrogenation of ethanol to ethyl acetate (CDCl$_3$, 25 ^{o}C, 400 MHz, 2 mL ethanol, 10 mL mesitylene, 0.1 mol% **Ru-1**, 24 h, 120 ^{o}C).
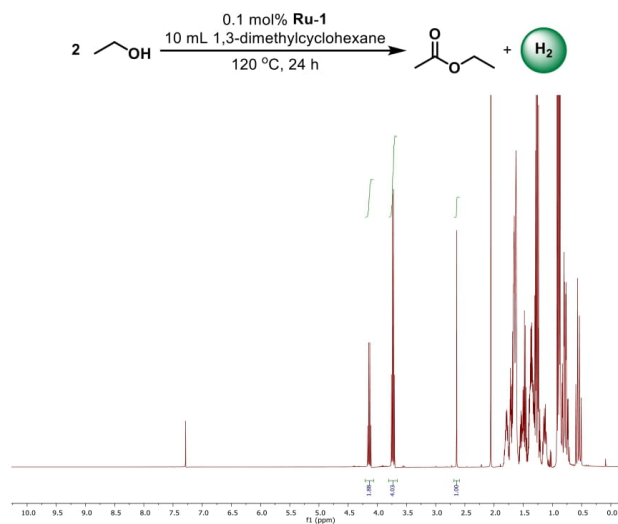
Figure S7. ^{1}H NMR of acceptorless dehydrogenation of ethanol to ethyl acetate (CDCl$_3$, 25 ºC, 400 MHz, 2 mL ethanol, 10 mL p-cymene, 0.1 mol% **Ru-1**, 24 h, 120 ºC).
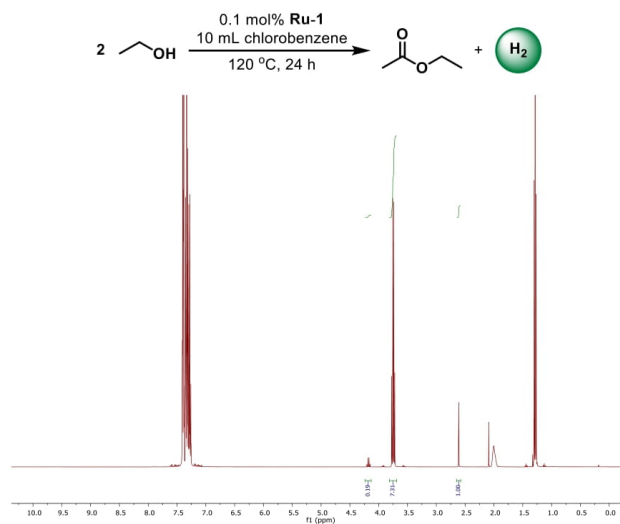
Figure S8. ^{1}H NMR of acceptorless dehydrogenation of ethanol to ethyl acetate (CDCl$_3$, 25 ºC, 400 MHz, 2 mL ethanol, 10 mL chlorobenzene, 0.1 mol% **Ru-1**, 24 h, 120 ºC).
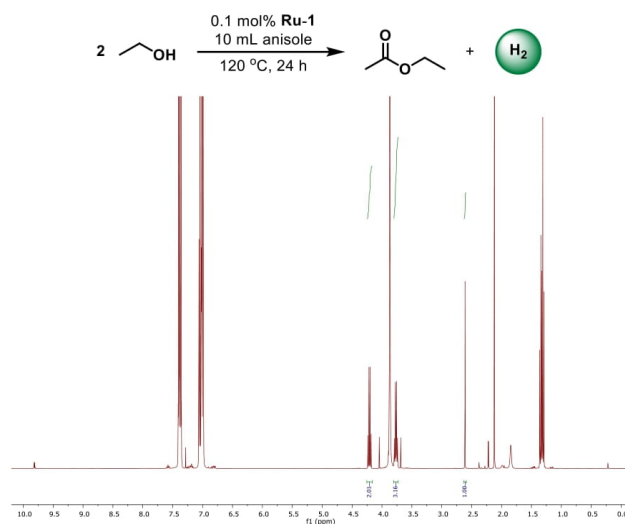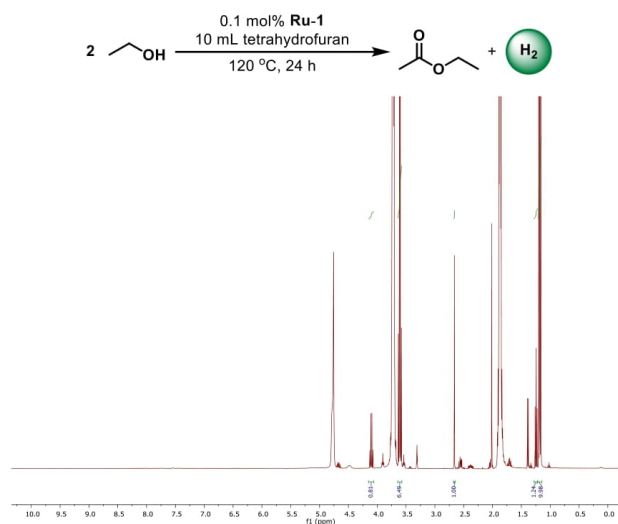
Figure S9. ^{1}H NMR of acceptorless dehydrogenation of ethanol to ethyl acetate (CDCl$_3$, 25 ^{o}C, 400 MHz, 2 mL ethanol, 10 mL anisole, 0.1 mol% **Ru**-**1**, 24 h, 120 ^{o}C).
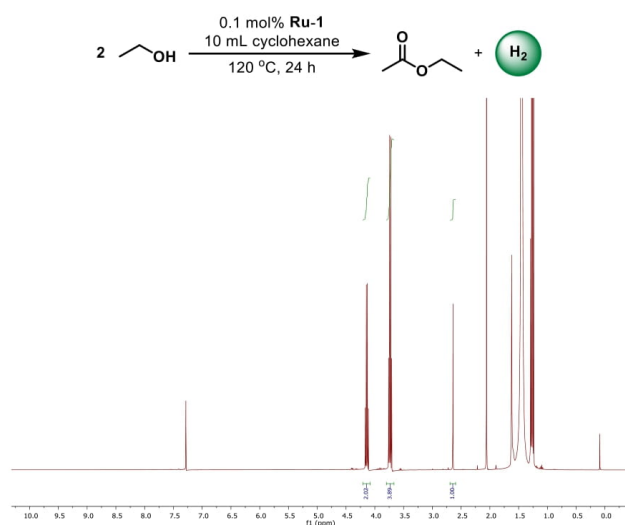
Figure S10. ^{1}H NMR of acceptorless dehydrogenation of ethanol to ethyl acetate (CDCl$_3$, 25 ^{o}C, 400 MHz, 2 mL ethanol, 10 mL cyclohexane, 0.1 mol% **Ru**-**1**, 24 h, 120 ^{o}C).

Figure S11. ^{1}H NMR of acceptorless dehydrogenation of ethanol to ethyl acetate (CDCl$_3$, 25 ^{o}C, 400 MHz, 2 mL ethanol, 10 mL methylcyclohexane, 0.1 mol% **Ru-1**, 24 h, 120 ^{o}C).

Figure S12. ^{1}H NMR of acceptorless dehydrogenation of ethanol to ethyl acetate (CDCl$_3$, 25 ^{o}C, 400 MHz, 2 mL ethanol, 10 mL 1,3-dimethylcyclohexane, 0.1 mol% **Ru-1**, 24 h, 120 ^{o}C).

Figure S13. ^{1}H NMR of acceptorless dehydrogenation of ethanol to ethyl acetate (CD$_3$OD, 25 ºC, 400 MHz, 2 mL ethanol, 10 mL tetrahydrofuran, 0.1 mol% **Ru-1**, 24 h, 120 ºC).
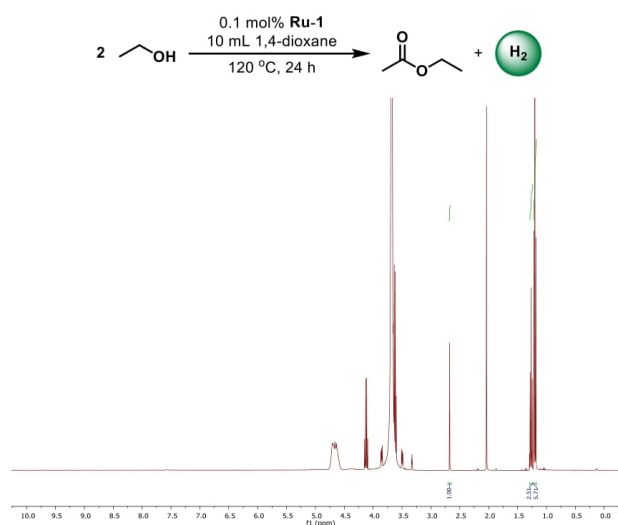
Figure S14. ^{1}H NMR of acceptorless dehydrogenation of ethanol to ethyl acetate (CD$_3$OD, 25 ºC, 400 MHz, 2 mL ethanol, 10 mL 1,4-dioxane, 0.1 mol% **Ru-1**, 24 h, 120 ºC).
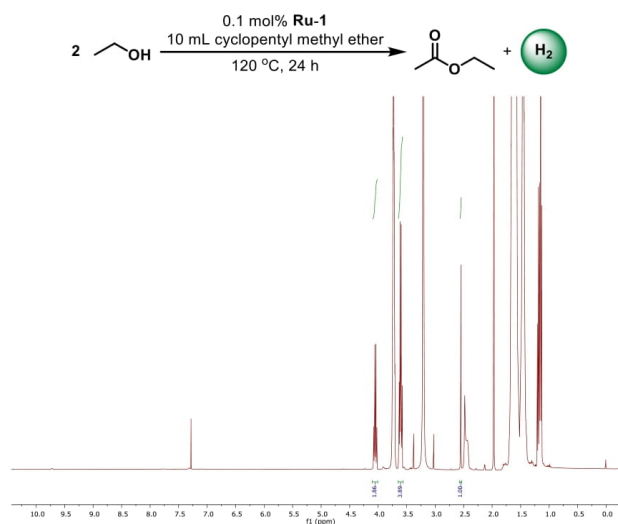
Figure S15. ^{1}H NMR of acceptorless dehydrogenation of ethanol to ethyl acetate (CDCl$_3$, 25 ^{o}C, 400 MHz, 2 mL ethanol, 10 mL cyclopentyl methyl ether, 0.1 mol% **Ru-1**, 24 h, 120 ^{o}C).
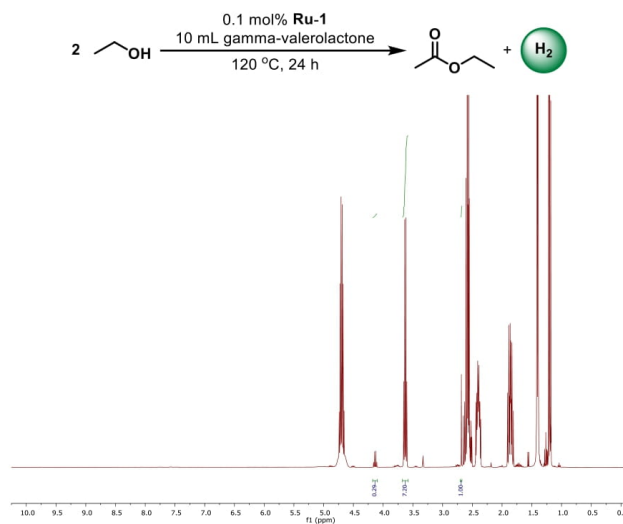
Figure S16. ^{1}H NMR of acceptorless dehydrogenation of ethanol to ethyl acetate (CD$_3$OD, 25 ^{o}C, 400 MHz, 2 mL ethanol, 10 mL γ-valerolactone, 0.1 mol% **Ru-1**, 24 h, 120 ^{o}C).

4. References

1 https://www.engineeringtoolbox.com/liquid-dielectric-constants-d_1263.html

2 http://www.chem.rochester.edu/notvoodoo/pages/reagents.php?page=solvent_polarity